NUREG-XXXX
ORNL/TM-2005/553

The Effect of Elevated Temperature on Concrete Materials and Structures— A Literature Review

Manuscript Completed: November 2005
Date Published:

Prepared by:
D. J. Naus

Oak Ridge National Laboratory
Managed by UT-Battelle, LLC
P.O. Box 2008
Oak Ridge, TN 37831-6283

(Milestone 2.4)

Prepared for the
U.S. Nuclear Regulatory Commission
Office of Nuclear Regulatory Research
Under Interagency Agreement No. 1886-N674-1Y
NRC FIN No. Y6741

NUREG-XXXX

THE EFFECT OF ELEVATED TEMPERATURE ON CONCRETE MATERIALS AND STRUCTURES—A LITERATURE REVIEW

D. J. Naus

(Milestone 2.4)

Prepared for the
U.S. Nuclear Regulatory Commission
Office of Nuclear Regulatory Research
Under Interagency Agreement No. 1886-N674-1Y

NRC FIN No. Y6741

Prepared by the
OAK RIDGE NATIONAL LABORATORY
Oak Ridge, Tennessee 37831-6283
managed by
UT-BATTELLE, LLC
for the
U.S. DEPARTMENT OF ENERGY
under Contract No. DE-AC05-00OR2275

ABSTRACT

The objective of this limited study was to provide an overview of the effects of elevated temperature on the behavior of concrete materials and structures. In meeting this objective the effects of elevated temperatures on the properties of ordinary Portland cement concrete constituent materials and concretes are summarized. The effects of elevated temperature on high-strength concrete materials are noted and their performance compared to normal strength concretes. A review of concrete materials for elevated-temperature service is presented. Nuclear power plant and general civil engineering design codes are described. Design considerations and analytical techniques for evaluating the response of reinforced concrete structures to elevated-temperature conditions are presented. Pertinent studies in which reinforced concrete structural elements were subjected to elevated temperatures are described.

CONTENTS

LIST OF FIGURES

LIST OF TABLES

ACKNOWLEDGMENT

The author would like to acknowledge the significant contribution of Dr. Jy-An Wang who reviewed several of the references presented in this report. The author would also like to acknowledge the continuing support and guidance throughout the program provided by the U.S. Nuclear Regulatory Commission Technical Monitor, Mr. Herman L. Graves III.

1 INTRODUCTION

Under normal conditions, most concrete structures are subjected to a range of temperature no more severe than that imposed by ambient environmental conditions. However, there are important cases where these structures may be exposed to much higher temperatures (e.g., jet aircraft engine blasts, building fires, chemical and metallurgical industrial applications in which the concrete is in close proximity to furnaces, and some nuclear power-related postulated accident conditions). Of primary interest in the present study is the behavior of reinforced concrete elements in designs of new-generation reactor concepts in which the concrete may be exposed to long-term steady-state temperatures in excess of the present *American Society of Mechanical Engineers Pressure Vessel and Piping Code (ASME Code)* limit of 65°C (Ref. 1). Secondary interests include performance of concrete associated with radioactive waste storage and disposal facilities and postulated design-basis accident conditions involving unscheduled thermal excursions. Under such applications the effect of elevated temperature on certain mechanical and physical properties may determine whether the concrete will maintain its structural integrity.

Concrete's thermal properties are more complex than for most materials because not only is the concrete a composite material whose constituents have different properties, but its properties also depend on moisture and porosity. Exposure of concrete to elevated temperature affects its mechanical and physical properties. Elements could distort and displace, and, under certain conditions, the concrete surfaces could spall due to the buildup of steam pressure. Because thermally induced dimensional changes, loss of structural integrity, and release of moisture and gases resulting from the migration of free water could adversely affect plant operations and safety, a complete understanding of the behavior of concrete under long-term elevated-temperature exposure as well as both during and after a thermal excursion resulting from a postulated design-basis accident condition is essential for reliable design evaluations and assessments. Because the properties of concrete change with respect to time and the environment to which it is exposed, an assessment of the effects of concrete aging is also important in performing safety evaluations. Presented in the following sections of this report is a review of the effects of elevated temperature on concrete materials, concrete materials for elevated-temperature service, code and design considerations for reinforced concrete structures exposed to elevated temperature, and the performance of selected structural members subjected to elevated temperature.

2 EFFECTS OF ELEVATED TEMPERATURE ON ORDINARY PORTLAND CEMENT CONCRETE MATERIALS

Portland cements are manufactured by mixing finely divided calcareous materials (i.e., lime containing) and argillaceous materials (i.e., clay). The four compounds that make up more than 90% of the dry weight of the cement are tricalcium silicate ($3CaO•SiO_2$), dicalcium silicate ($2CaO•SiO_2$), tricalcium aluminate ($3CaO•A1_20_3$), and tetracalcium aluminoferrite ($4CaO•A1_20_3•Fe_20_3$). When water is added to Portland cement, an exothermic reaction occurs, and new compounds are formed (i.e., hydrated cement paste): tobermorite gel [$(Ca_5Si_60_{16}(OH)_2•4H_20)$], calcium hydroxide, calcium aluminoferrite hydrate, tetracalcium aluminate hydrate, and calcium monosulfoaliminate. Mature cement paste is normally composed of 70–80% layered calcium-silicate-hydrate (C-S-H) gel, 20% $Ca(OH)_2$, and other chemical compounds.[2] The C-S-H gel structure is made up of three types of groups that contribute to bonds across surfaces or in the interlayer of partly crystallized tobermorite material: calcium ions, siloxanes, and water molecules. Bonding of the water within the layers (gel water) with other groups via hydrogen bonds determines the strength, stiffness, and creep properties of the cement paste. Tobermorite gel is the primary contributor to the cement paste structural properties. Under elevated-temperature exposure, the Portland cement paste experiences physical and chemical changes that contribute to development of shrinkage, transient creep, and changes in strength. Key material features of hydrated Portland cement paste affecting the properties of concrete at elevated temperature are its moisture state (i.e., sealed or unsealed), chemical structure (i.e., loss of chemically bound water from the C-S-H in the unsealed condition, CaO/SiO_2 ratio of the hydrate in the sealed condition, and amount of $Ca(OH)_2$ crystals in sealed or unsealed conditions), and physical structure (i.e., total pore volume including cracks, average pore size, and amorphous/crystalline structure of solid).[3]

Concrete is a heterogeneous multiphase material with relatively inert aggregates that is held together by the hydrated Portland cement paste. When concretes are exposed to high temperatures, changes in mechanical properties and durability occur. Nonlinearities in material properties, variation of mechanical and physical properties with temperature, tensile cracking, and creep effects affect the buildup of thermal forces, the load-carrying capacity, and the deformation capability (i.e., ductility) of the structural members. The property variations result largely because of changes in the moisture condition of the concrete constituents and the progressive deterioration of the cement paste-aggregate bond, which is especially critical where thermal expansion values for the cement paste and aggregate differ significantly. The bond region is affected by the surface roughness of the aggregate and its chemical/physical interactions.[3] Chemical interaction relates to the chemical reactions between the aggregate and cement paste that can be either beneficial or detrimental. Physical interaction relates to dimensional compatibility between aggregate materials and cement paste. Behavior of concrete at high temperature depends on exposure conditions (i.e., temperature-moisture-load-time regime). Curing influences the degree of hydration, while the temperature and load history prior to exposure to elevated temperature could have a significant effect on the behavior of the Portland cement paste and therefore the concrete. Concrete at elevated temperature is sensitive to the temperature level, heating rate, thermal cycling, and temperature duration (as long as chemical and physical transformations occur). Table 1 presents a summary of environmental factors that affect heated concrete and provides an indication of their relative influence.[3]

Research has been conducted on the thermal behavior of concrete in connection with the development of prestressed concrete pressure vessels for nuclear power plants (i.e., 20°C to 200°C) and to study the behavior of reinforced concrete members under fire conditions (i.e., 20°C to 1000°C) (Ref. 4). Interpretation of these results can be difficult however because (1) test materials and curing conditions

Table 1 Influence of Environmental Factors on Heated Concrete

Factor	Influence	Comment
Temperature Level	***	• Chemical-physical structure (see Chapter 2) & most properties (see Chapters 6-14).
	**	• The properties of some concrete (e.g. compressive strength and modulus of elastcicity) when heated under 20-30% load can vary less with temperature - up to about 500°C - than if heated without load (see Chapters 6 & 14).
Heating Rate	**	• *< 2°C/min:* Second order influence.
	***	• *> about 5°C/min:* Becomes significant ⇒ explosive spalling.
Cooling Rate	*	• *< 2°C/minute:* Negligible influence.
	**	• *> 2°C/minute:* Cracking could occur.
	***	• *Quenching*: Very significant influence.
Thermal Cycling	**	• *Unsealed Concrete:* Significant influence mainly during first cycle to given temperature.
	**	• *Sealed concrete*: Influence in so far as it allows longer duration at temperature for hydrothermal transformations to develop.
Duration at Temperature	**	• *Unsealed concrete*: Only significant at early stages while transformations decay.
	***	• *Sealed concrete*: Duration at temperature above 100°C ⇒ Continuing hydrothermal transformations.
Load-Temp. Sequence	***	• Very important - not usually appreciated
Load Level	***	• < 30%: Linear influence on Transient Creep (Chapter 9) at least in range up to 30% cold strength.
	***	• >50%: Failure could occur during heating at high load levels.
Moisture Level	**	• *Unsealed*: Small influence on thermal strain and transient creep particularly above 100°C.
	***	• *Sealed*: Very significant influence on the structure of cement paste and properties of concrete above 100°C.

*** First order influence. ** Second order influence. * First order influence.

Source: G. A. Khoury, "Performance of Heated Concrete—Mechanical Properties," Contract NUC/56/3604A with Nuclear Installations Inspectorate, Imperial College, London, United Kingdom, August 1996.

were different, (2) descriptions of materials are incomplete, (3) different test procedures were utilized (e.g., heating rates and exposure times), (4) test conditions are not comparable (e.g., tested at temperature or permitted to cool to room temperature prior to testing, and loaded or unloaded while heating), and (5) shape and size of the test articles were different (e.g., cube and cylindrical). Contained in the following sections of this chapter is a summary of literature that has been identified addressing the general behavior and pertinent mechanical and physical properties of concrete materials under elevated-temperature conditions.

2.1 General Behavior

2.1.1 Concrete Materials

If concrete made with Portland cement or blast furnace slag cement is subjected to heat, a number of transformations and reactions occur, even if there is only a moderate increase in temperature.[5,6] As aggregate materials normally occupy 65 to 75% of the concrete volume, the behavior of concrete at elevated temperature is strongly influenced by the aggregate type. Commonly used aggregate materials are thermally stable up to 300°C–350°C. Aggregate characteristics of importance to behavior of concrete at elevated temperature include physical properties (e.g., thermal conductivity and thermal expansion), chemical properties (e.g., chemical stability at temperature), and thermal stability/integrity. Aggregate materials may undergo crystal transformations leading to significant increases in volume [e.g., crystalline transformation of α-quartz (trigonal) to β-quartz (hexagonal) between 500 and 650°C with an accompanying increase in volume of ~5.7%]. Some siliceous or calcareous aggregates with some water of constitution exhibit moderate dehydration with increasing temperature that is accompanied by shrinkage (i.e., opal at 373°C exhibits shrinkage of ~13% by volume).[7] Most nonsiliceous aggregates are stable up to about 600°C. At higher temperatures, calcareous aggregates (calcite – $CaCO_3$), magnesite ($MgCO_3$), and dolomite ($MgCO_3/CaCO_3$) dissociate into an oxide and CO_2 ($CaO + CO_2$). Calcium carbonate dissociates completely at 1 atm pressure at 898°C with partial dissociation occurring at temperatures as low as 700°C (Ref. 8). Above 1200°C and up to 1300°C some aggregates, such as igneous rocks (e.g., basalt), show degassing and expansion. Refractory aggregates can be utilized to produce significant improvements in the heat resistance of Portland cement concretes. It has been noted that the thermal stability of aggregates increases in order of gravel, limestone, basalt, and lightweight.[9]

Apart from the crystalline transformations occurring mainly in the aggregate materials during heating, a number of degradation reactions occur, primarily in the cement paste, that result in a progressive breakdown in the structure of the concrete. An increase in temperature produces significant changes in the chemical composition and microstructure of the hardened Portland cement paste. At low temperatures these reactions mainly take the form of dehydration and water expulsion reactions. Changes in the chemical composition and microstructure of the hardened Portland cement paste occur gradually and continuously over a temperature range from room temperature to 1000°C. At room temperature, between 30 and 60% of the volume of saturated cement paste and between 2 and 10% of the volume of saturated structural concrete are occupied by evaporable water. As the temperature to which the cement paste is subjected increases, evaporable water is driven off until at a temperature of about 105°C all evaporable water will be lost, given a sufficient exposure period. At temperatures above 105°C, the strongly absorbed and chemically combined water (i.e., water of hydration) are gradually lost from the cement paste hydrates, with the dehydration essentially complete at 850°C. Dehydration of the calcium hydroxide is essentially zero up to about 400°C, increases most rapidly around 535°C, and becomes complete at about 600°C (Ref. 10). Figures 1 and 2 indicate the influence of temperature on the ultimate compressive strength and modulus of elasticity of a Portland cement paste (Type I Portland cement; water/cement = 0.33) (Ref. 11).

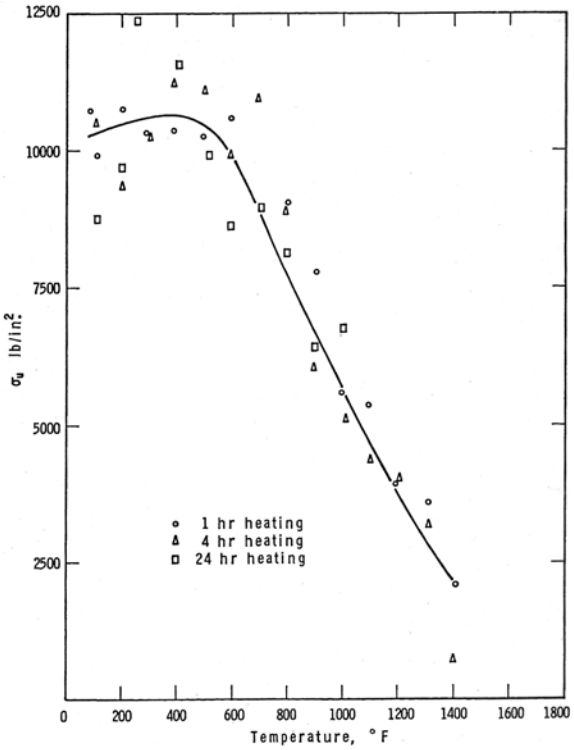

Figure 1 Ultimate strength in compression of hydrated Portland cement (w/c = 0.33) at elevated temperature

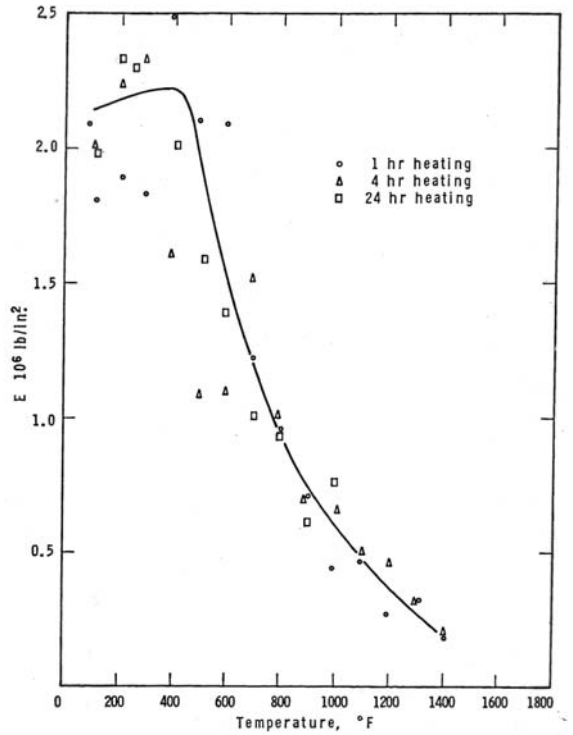

Figure 2 Modulus of elasticity in compression of hydrated Portland cement (w/c = 0.33) at elevated temperature

Source: T. Z. Harmathy and J. E. Berndt, "Hydrated Portland Cement and Lightweight Concrete at Elevated Temperatures," *J. American Concrete Institute* **63**, 93–112 (1966).

A good summary of the degradation reactions that occur in Portland cement concrete is provided in Ref. 4. Upon first heating, substantial water evaporation occurs from the larger pores close to the concrete surface. Then, from 100°C onward, the evaporation proceeds at a faster rate with water being expelled from concrete near the surface as a result of above-atmospheric vapor pressure (i.e., steam flow). At 120°C the expulsion of water physically bound in the smaller pores, or chemically combined, initiates and continues up to about 500°C where the process is essentially complete. From 30°C to 300°C, in conjunction with evaporation, dehydration of the hardened cement paste occurs (first stage) with the maximum rate of dehydration occurring at about 180°C [Tobermorite gel is stable up to a temperature of 150°C (Ref. 12)]. In the temperature range from 450°C to 550°C there is decomposition of the portlandite [i.e., $Ca(OH)_2 \rightarrow CaO + H_2O$) (Ref. 12)]. At 570°C the $\alpha \rightarrow \beta$ inversion of quartz takes place with the transformation being endothermic and reversible. A further process of decomposition of the hardened cement paste takes place between 600°C and 700°C with the decomposition of the calcium-silicate-hydrate phases and formation of β-C_2S. Between 600°C and 900°C the limestone begins to undergo decarbonation (i.e., $CaCO_3 \rightarrow CaO + CO_2$). The rate of decomposition and the temperature at which it occurs are not only dependent on temperature and pressure, but also by the content of SiO_2 present in the limestone. Above 1200°C and up to 1300°C, some components of the concrete begin to melt. Above 1300°C to 1400°C concrete exists in the form of a melt. Apparently liquifaction of the concrete commences with melting of the hardened cement paste followed by melting of the aggregates.[13–15] The melting points of aggregates vary greatly. At 1060°C basalt is at the lower limit of all types of rock, with quartzite not melting below 1700°C (Ref. 5).

2.1.2 Steel Reinforcing Materials

Bonded reinforcement (i.e., deformed bars) is provided to control the extent and width of cracks at operating temperatures, resist tensile stresses and computed compressive stresses for elastic design, and provide structural reinforcement where required by limit condition design procedures. Bonded reinforcement in nuclear power plant structures is often used in conjunction with prestressed steel. The prestressed steel provides the structural rigidity and the major part of the strength while the bonded reinforcement distributes cracks, increases ultimate strength and reinforces those areas not adequately strengthened by the prestressed steel, and provides additional safety for unexpected conditions of loading.

Structural elements fabricated from reinforced concrete, because of their typical size, have a high thermal inertia that results in relatively slow rates of temperature increase through the cross section. As a result, the steel reinforcement temperatures are kept sufficiently low to avoid significant softening. In addition, due to the monolithic nature of construction, the existence of alternate load paths, and compartmentation of fires (i.e., conventional civil engineering construction), reinforced concrete structures generally perform well under elevated-temperature conditions that could result from a fire. However, under certain scenarios (e.g., rapid heat buildup), spalling of the concrete could occur to expose the steel reinforcement to the effects of elevated temperature. Such conditions at a nuclear power plant would occur only in the unlikely event of an accident. For completeness, limited information is provided below on effects of elevated temperature on steel reinforcing bars.

During heating of steels, crystalline transformations occur depending on the temperature (e.g., perlite at 721°C and Curie point at 768°C). Information on the density, mean specific heat, thermal conductivity, thermal diffusivity, and coefficient of thermal expansion of different steels is presented in Figs. 3–7, respectively.[5] Strength characteristics and mechanical properties of steels depend on several factors: amount and type of alloying constituents, heat treatment during manufacture, and retreatment in cold state (e.g., cold drawing). Figures 8–10 present stress-strain relationships, Young's modulus/elongation, and yield/ultimate tensile strength data as a function of temperature for 3500 kgf/cm^2 specified minimum

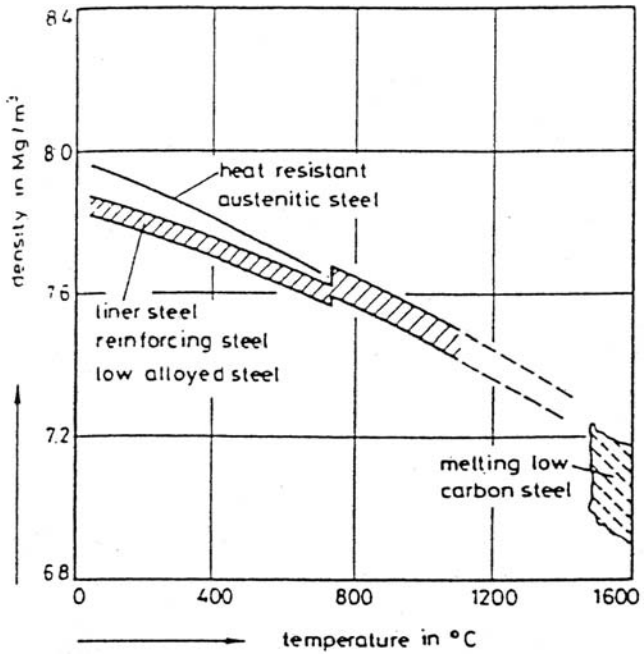

Figure 3 Density of different steels

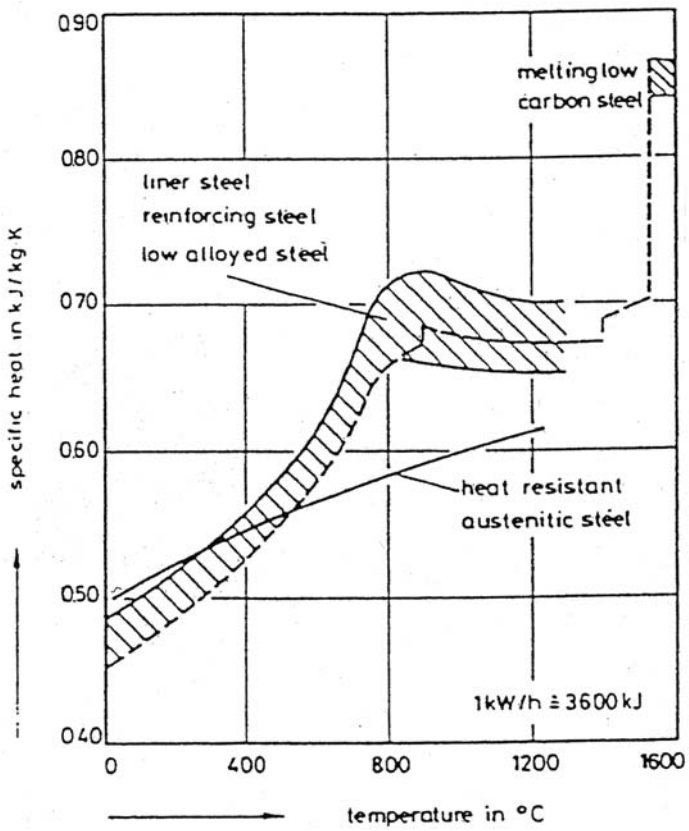

Figure 4 Mean specific heat of different steels

Source: U. Schneider, C. Diererichs, and C. Ehm, "Effect of Temperature on Steel and Concrete for PCRV's," *Nuclear Engineering and Design* **67**, 245–258 (1981).

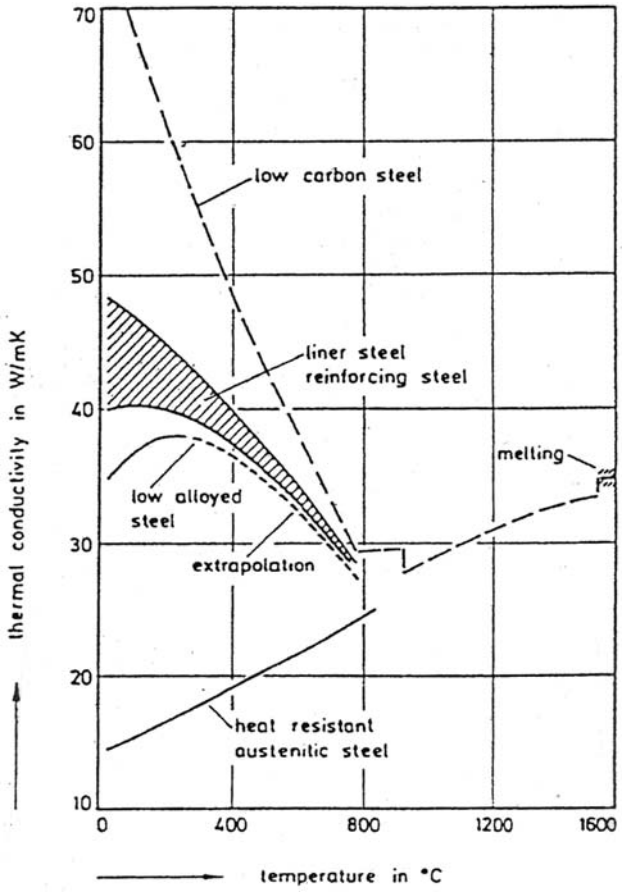

Figure 5 Thermal conductivity of different steels

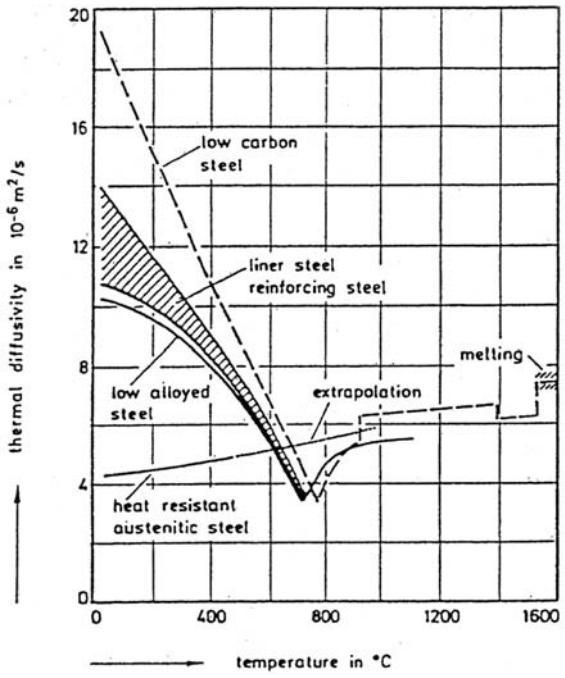

Figure 6 Thermal diffusivity of different steels

Source: U. Schneider, C. Diererichs, and C. Ehm, "Effect of Temperature on Steel and Concrete for PCRV's," *Nuclear Engineering and Design* **67**, 245–258 (1981).

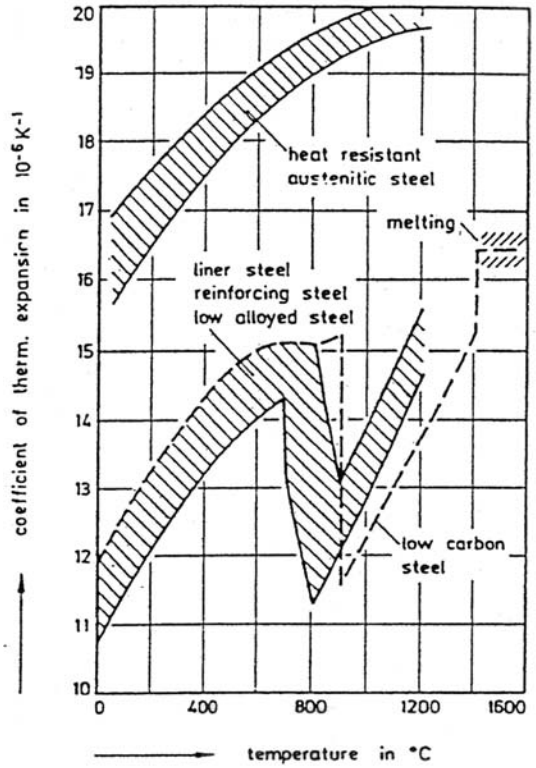

Figure 7 **Coefficient of expansion of different steels.** *Source*: U. Schneider, C. Diererichs, and C. Ehm, "Effect of Temperature on Steel and Concrete for PCRV's," *Nuclear Engineering and Design* **67**, 245–258 (1981).

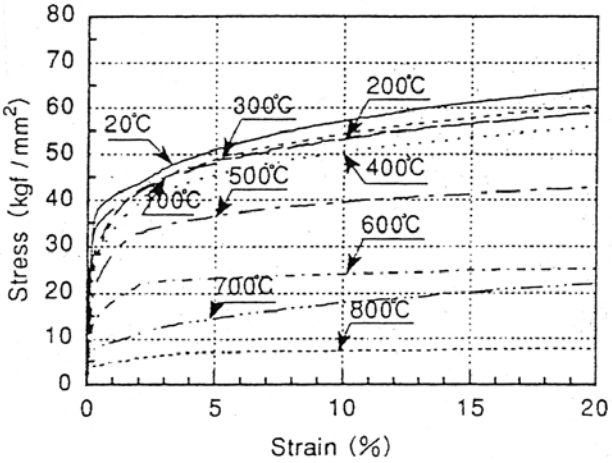

Figure 8 **Stress-strain relationships of reinforcing bars at elevated temperature.** *Source*: M. Takeuchi et al., "Material Properties of Concrete and Steel Bars at Elevated Temperatures," *12th International Conference on Structural Mechanics in Reactor Technology*, Paper H04/4, pp. 133–138, Elsevier Science Publishers, North-Holland, The Netherlands, 1993.

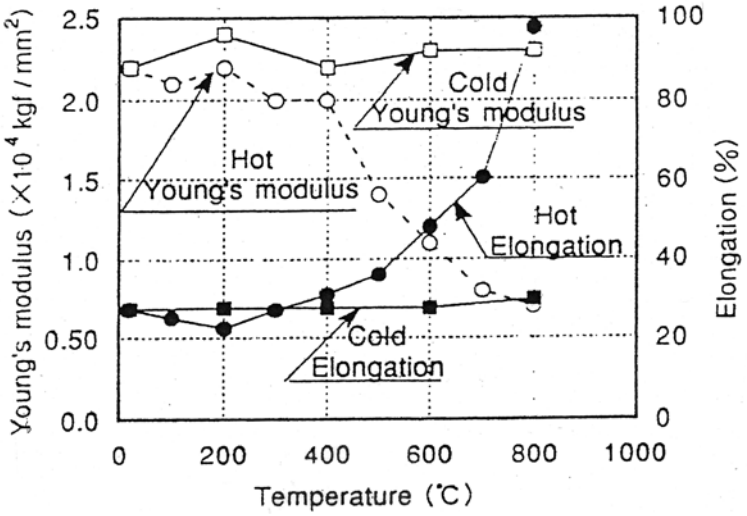

Figure 9 Influence of temperature on Young's modulus and elongation of reinforcing bars. *Source*: M. Takeuchi et al., "Material Properties of Concrete and Steel Bars at Elevated Temperatures," *12th International Conference on Structural Mechanics in Reactor Technology*, Paper H04/4, pp. 133–138, Elsevier Science Publishers, North-Holland, The Netherlands, 1993.

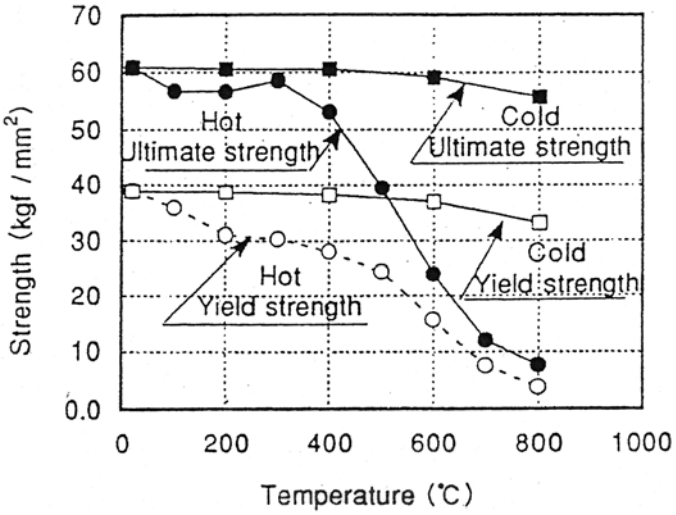

Figure 10 Yield strength and ultimate tensile strength of reinforcing bars at elevated temperature. *Source*: M. Takeuchi et al., "Material Properties of Concrete and Steel Bars at Elevated Temperatures," *12th International Conference on Structural Mechanics in Reactor Technology*, Paper H04/4, pp. 133–138, Elsevier Science Publishers, North-Holland, The Netherlands, 1993.

yield strength 51-mm-diameter steel bars.[16] Information on the effect of elevated-temperature exposure on tensile strength of prestressing steels is available.[5]

2.2 Mechanical and Physical Properties

Material properties are closely related to the specific test method employed. The properties of concrete at elevated temperature can be defined from a number of viewpoints (e.g., ranging from transient such as representing fire conditions to steady-state such as a structure operating at elevated temperature). To interpret results, knowledge of the test condition(s) employed is required. Three main test parameters are involved in the development of data: heating, application of load, and control of strain.[17] These parameters can be fixed at constant values or be varied during testing to provide transient conditions. Six regimes have been identified for determining properties of concrete.[4,17]

1. Stress-strain relationships (stress-rate controlled): data provide stress-strain relationships that can be used to establish tensile strength, modulus of elasticity, and ultimate strain at collapse.
2. Stress-strain relationships (strain-rate controlled): data also provide stress-strain relationships to establish properties noted above as well as mechanical dissipation energy.
3. Creep: steady-state creep tests in which the specimens are heated to a specified temperature and then loaded to provide a relationship between strain and time at different temperatures.
4. Relaxation: specimen heated to a specified temperature, loaded, strain held constant, load monitored as function of time.
5. Total deformation: data provide a relationship between total strain and time and enable failure temperature values and transient creep values for different stress levels to be established.
6. Total forces: data provide a relationship between stress and time for different initial stress or strain levels and can be expressed as a relationship between restraint forces and temperature developed as a consequence of heating.

Each of these methods or regimes determines a specific feature of material behavior. Regimes 1 through 4 are related to steady-state tests and regimes 5 and 6 transient tests. For the current study, the steady-state regimes are of most interest because the transient regimes are primarily related to fire. For example, unstressed tests can simulate conditions of concrete under no initial stress and exposed to high temperature, stressed tests simulate concrete in columns or compressive zones of flexural members subjected to heat, and unstressed residual yields information on strength of unstressed concrete that has been exposed to a thermal excursion. More detailed descriptions of these regimes are available.[4,17]

2.2.1 Mechanical Properties

It has been established that the mechanical properties of concrete can be adversely affected by elevated-temperature exposure.[18–22] Quantitative interpretation of available data is difficult, however, because (1) samples were either tested hot or cold, (2) moisture migration was either free or restricted, (3) concrete was either loaded or unloaded while heated, (4) mix constituents and proportions varied, (5) test specimen size and shape were not consistent, (6) specimens were tested at different degrees of hydration, and (7) heat-soak duration varied from test to test. To provide a consistent basis for evaluation of data, it is recommended that several factors be taken into account:[23] (1) concrete strength class; (2) test specimen size; (3) thermal compatibility of aggregate and cement paste matrix; (4) cement and concrete composition; (5) level of temperature; (6) degree of hydration; (7) moisture content; (8) moisture gradients, rate of drying or wetting; (9) temperature gradient, rate of heating or cooling; (10) duration of temperature exposure; (11) loading during temperature exposure; (12) temperature-activated

transformations in microstructure and chemical composition of cement; (13) state of specimens tested—hot or cold; (14) strength testing procedure; and (15) reference strength selected—wet, moist, or dry.

A review of methods used by various investigators for elevated-temperature testing of concrete indicates that, generally, the tests can be categorized according to cold or hot testing. In cold testing, specimens are gradually heated to a specified temperature, permitted to thermally stabilize at that temperature for a prescribed period of time, permitted to slowly cool to ambient, and then tested to determine residual mechanical properties. In hot testing, specimens are gradually heated to a specified temperature, permitted to thermally stabilize at the temperature for a prescribed period of time, and then tested at temperature to determine mechanical properties. During testing, specimens are maintained in either an open environment where water vapor can escape (unsealed) or a closed environment where the moisture is contained (sealed). The closed environment represents conditions for mass concrete where moisture does not have ready access to the atmosphere, and the open environment represents conditions where the element is either vented or has free atmospheric communication. During heating and cooling, the specimens may be either loaded or unloaded. Mechanical properties in which the specimens have been permitted to return to room temperature prior to testing are referred to as residual properties.

The performance of concrete can be measured by the change of its stiffness, strength, or some other property that would affect its main function in service. Because concrete has a relatively low tensile strength, it is normally relied upon to take compressive forces, with tensile forces taken by steel reinforcement. As a consequence, much of the research conducted on concrete at elevated temperature has concentrated on compressive strength as the fundamental property in examining its deterioration. However, it has been noted that the compressive strength may not be as good an indicator of deterioration at elevated temperature as tensile or flexural strength under short-term loading.[24]

Stress and Strain Characteristics

Evaluation of structures for small strain conditions involves elastic analysis procedures for which knowledge of the concrete modulus of elasticity and strength is sufficient. When large strains are involved, such as could occur when a structure is subjected to elevated temperature, elastic-plastic analysis procedures are required that involve use of the load-deformation or stress-strain relations developed for concrete at the temperature level of interest. A number of relationships have been proposed by various authors to describe concrete's stress-strain behavior.[25,26] These expressions generally provide good agreement with the ascending portion of the stress-strain curve but differ significantly beyond the point of maximum stress. Reference 27 notes that the stress-strain relationships at elevated temperature may be derived from the room-temperature relationships if the variation of maximum stress and corresponding strain with temperature are known.

The majority of stress-strain data reported in the literature are for concrete heated to test conditions without load or loaded under stress-controlled conditions. Stress-strain diagrams for sealed and unsealed limestone aggregate concretes tested at temperature are presented in Figs. 11 and 12, respectively.[28] These results indicate that the unsealed specimens are stiffer than the sealed specimens, but strains at ultimate load were reduced. Figure 13 presents the influence of test temperature on the stress-strain relationship of a quartz aggregate concrete in a stress-rate controlled test.[29] These data show a significant increase in ultimate strain and a loss of stiffness with increasing temperature. Figure 14 shows specimens made from quartz aggregate concrete that are tested at temperature are stiffer and stronger than identical companion specimens heated to the same temperatures and then permitted to cool to room temperature before testing (i.e., up to 450°C the stress-strain curves of specimens tested at temperature do not change appreciably).[30] It was also concluded from this study that the type of cement and the duration of thermal

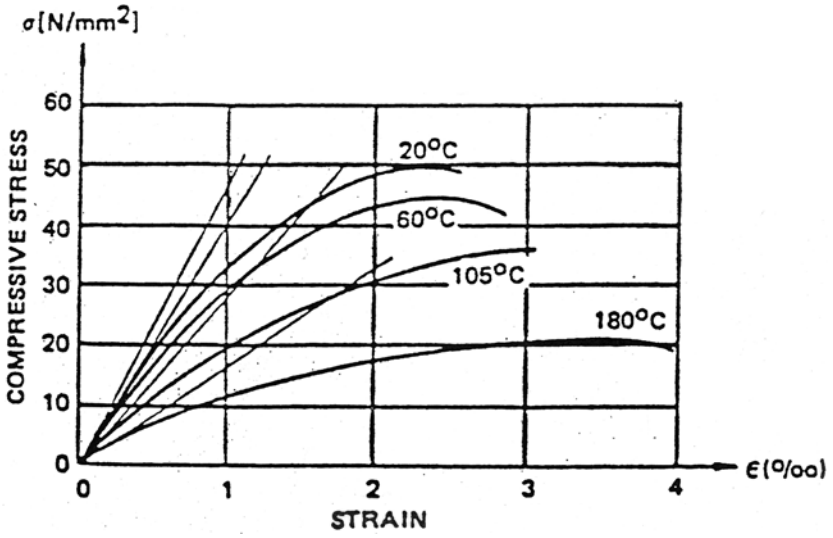

Figure 11 Stress-strain diagrams of sealed limestone concrete specimens. *Source*: R. Kottas, J. Seeberger, and H. K. Hilsdorf, "Strength Characteristics of Concrete in the Temperature Range of 20° to 200°C," Paper HO1/4 in *5th International Conference on Structural Mechanics in Reactor Technology*, p. 8, Elsevier Science Publishers, North-Holland, The Netherlands, August 1979.

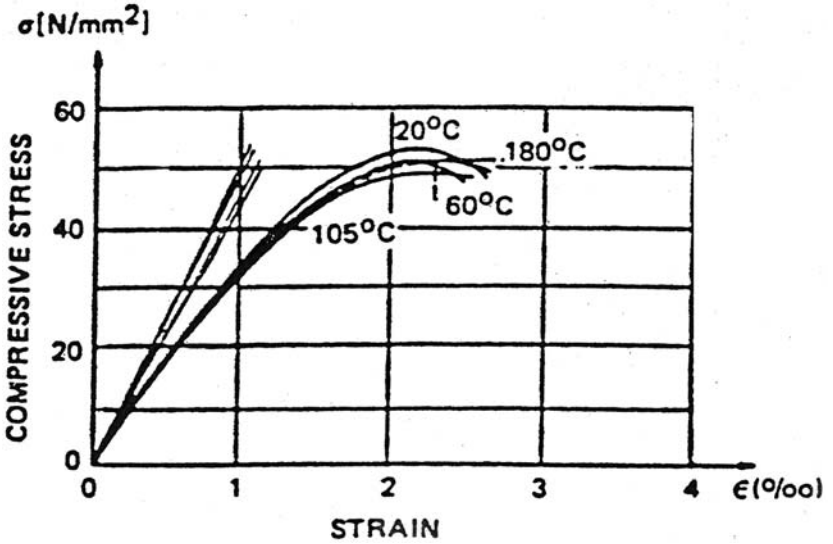

Figure 12 Stress-strain diagrams of unsealed limestone concrete specimens. *Source*: R. Kottas, J. Seeberger, and H. K. Hilsdorf, "Strength Characteristics of Concrete in the Temperature Range of 20° to 200°C," Paper HOI/4 in *5th International Conference on Structural Mechanics in Reactor Technology*, p. 8, Elsevier Science Publishers, North-Holland, The Netherlands, August 1979.

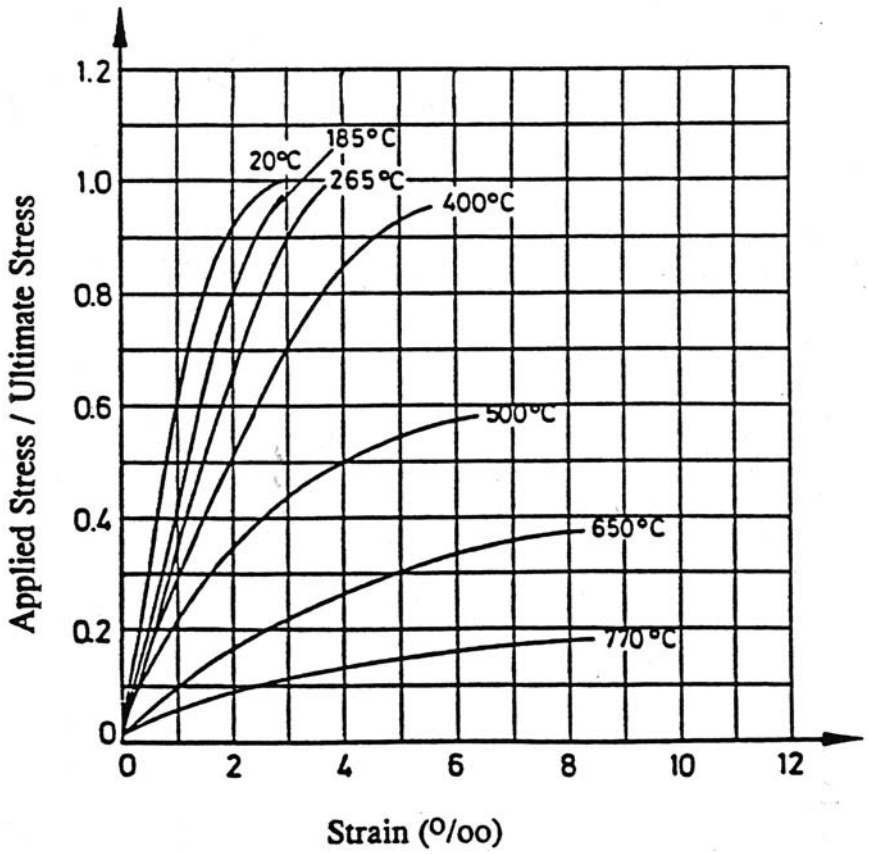

Figure 13 Influence of temperature on the stress-strain relation of unsealed quartz aggregate concrete. *Source*: Y. Anderberg and S. Thelanderson, "Stress and Deformation Characteristics of Concrete at High Temperatures, 2-Experimental Investigation and Material Behaviour Model," Bulletin 54, Lund Institute of Technology, Lund, Sweden, 1976.

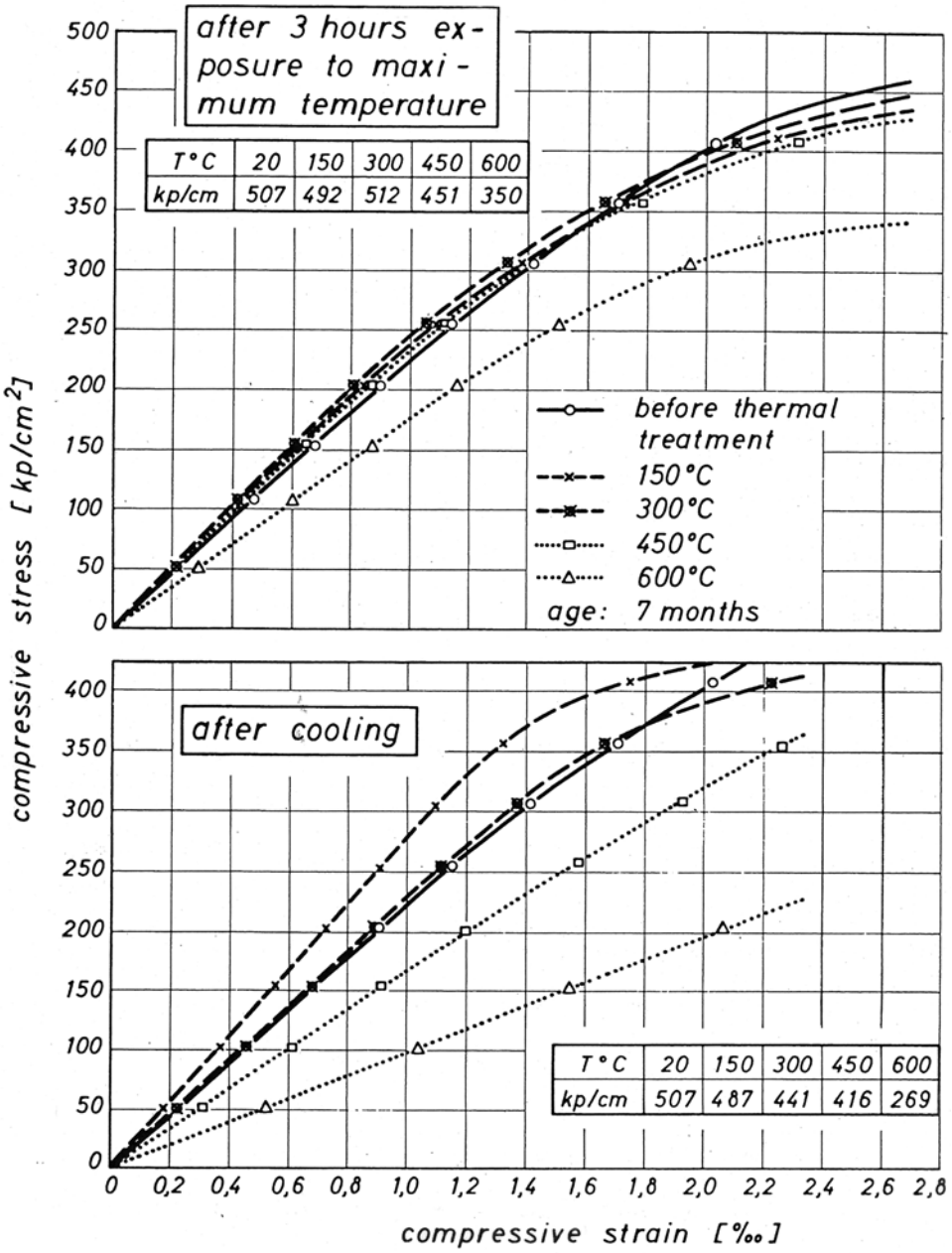

Figure 14 Effect of elevated temperature on stress-strain behavior of a quartz concrete. *Source*: H. Weigler and R. Fischer, "Influence of High Temperatures on Strength and Deformations of Concrete," Paper Sp 34-26 in Special Publication SP-34, Vol. I–III, American Concrete Institute, Farmington Hills, Michigan, 1972.

treatment had a minor affect on the slope of the stress-strain curve. Many nuclear power plant structures, such as prestressed concrete pressure vessels, will be under a compressive load prior to heating. The beneficial effect of applied preload load (0, 10, or 30% the reference strength) during exposure to temperatures of either 250°C or 450°C on strength and stiffness is demonstrated by results presented in Fig. 15.[4]

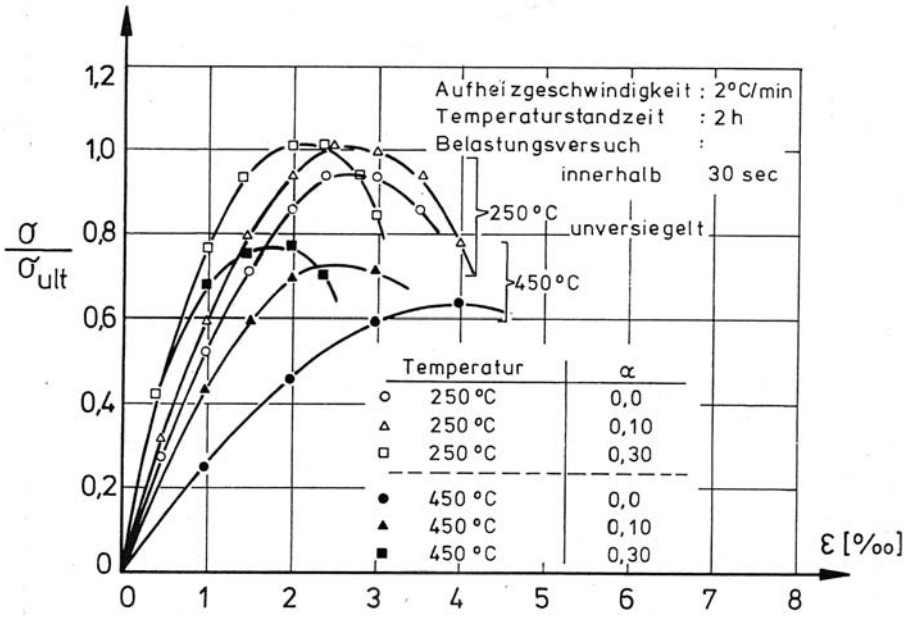

Figure 15 Stress-strain relationship of normal concrete with specimens loaded during the heating period. *Source*: U. Schneider, "Behaviour of Concrete at High Temperature," HEFT 337, Deutscher Ausschuss fur Stahlbeton, Wilhelm Ernst & Sohn, Munich, Germany, 1982.

Relative to temperature effects on concrete's stress-strain curve, several general observations can be made. Under steady-state conditions, the original concrete strength, water-cement ratio, heating rate, and type of cement have minor influence on the stress-strain behavior. Aggregate-cement ratio and aggregate type are the main factors affecting the shape of the stress-strain curve. Concretes made with hard aggregates (e.g., siliceous or basalt) generally have a steeper decrease of the initial slope at high temperature (e.g., >550°C) than softer aggregates (e.g., lightweight). Curing conditions influence the stress-strain behavior only at relatively low temperatures (<300°C) (Ref. 17).

Poisson's Ratio

Poisson's ratio is needed for conducting structural analyses of flat slabs, arch dams, tunnels, tanks, and other statically indeterminate members. At normal ambient conditions, Poisson's ratio for concrete can vary from 0.11 to 0.32, but is generally in the range from 0.15 to 0.20. Available data do not indicate a consistent trend for variation of Poisson's ratio with age, strength, or other concrete properties. However, some test results indicate that the ratio increases with age of concrete up to about 2 years and is lower for higher strength concretes.[31,32]

Data on the effect of elevated temperature on Poisson's ratio are somewhat limited and tend to be inconsistent. Some data indicate that the Poisson's ratio decreases with increasing temperature,[33] whereas elsewhere it has been reported that it ranged from 0.11 to 0.25 at 20°C to 400°C, while above 400°C it increased.[34] Additional data for higher strength concrete indicated that when the stress did not exceed

50% of peak value, the Poisson's ratio decreased with an increase in temperature.[35] Figure 16 presents Poisson's ratio results for a hard sandstone aggregate concrete after various heating periods (i.e., 1, 7, 28, and 91 d) at 175°C for specimens that were either sealed or unsealed during heating.[36] Poisson's ratio ranged from 0.14 to 0.22 with the trend for it to increase with increasing moisture content of the concrete.

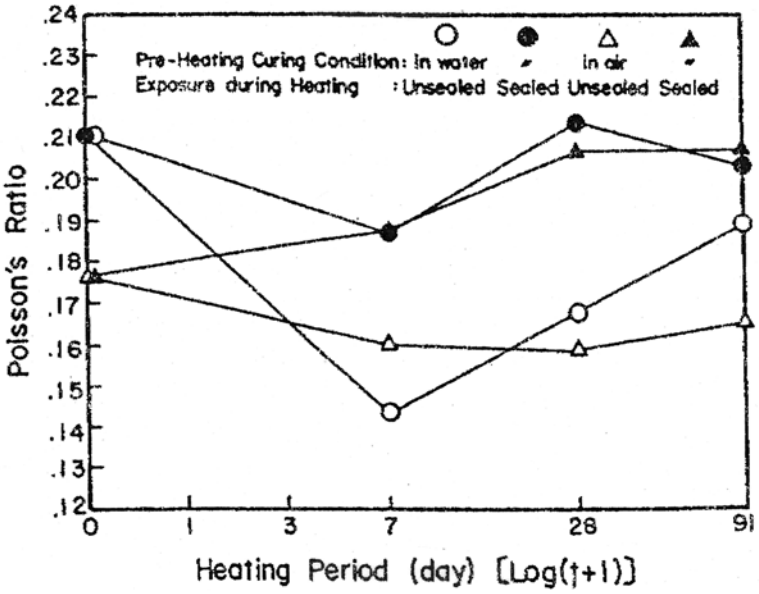

Figure 16 Poisson's ratio results. *Source*: K. Hirano et al., "Physical Properties of Concrete Subjected to High Temperature for MONJU," Paper P2-25, Power Reactor and Nuclear Fuel Development Corporation, Tokyo, Japan.

Modulus of Elasticity

Concrete's modulus of elasticity—a measure of its stiffness or resistance to deformation—is used extensively in the analysis of reinforced concrete structures to determine the stresses developed in simple elements and the stresses, moments, and deflections in more complicated structures. Because concrete's stress-strain curve is nonlinear, the modulus of elasticity is determined either by the initial tangent modulus, secant modulus, or tangent modulus method. Principal variables affecting the modulus include (1) richness of the mix (richer the mix, the greater the modulus increase with age); (2) water/cement ratio (higher values reduce modulus); (3) age (modulus increases rapidly during first few months and shows continual increase up to ~3 years); (4) kind and gradation of aggregate (stiffer aggregates produce higher modulus concretes, and the modulus increases with aggregate fineness modulus as long as the mix is workable); and (5) moisture content at time of test (wet specimens produce higher modulus values than dry specimens). Temperature can significantly affect the modulus values.

Figure 17 summarizes results from several researchers on the temperature dependence of the concrete modulus of elasticity (normalized to reference room temperature modulus.[25] Results for normal strength concrete (NSC) and high-strength concrete (HSC) from researchers in China is presented in Fig. 18.[37] Results show that the elastic modulus for the NSC decreased monotonically with increasing temperature. From the NSC and HSC elastic modulus results obtained at temperature or after thermal exposure (residual), Ref. 37 notes that the elastic modulus after high-temperature exposure (residual) was lower than that obtained at temperature and was influenced by type aggregate, the elastic modulus decreased much more for concrete cured in water than for concrete cured in air, and the deterioration in elastic modulus was more related to the maximum temperature during heating than to the heating-cooling cycle.

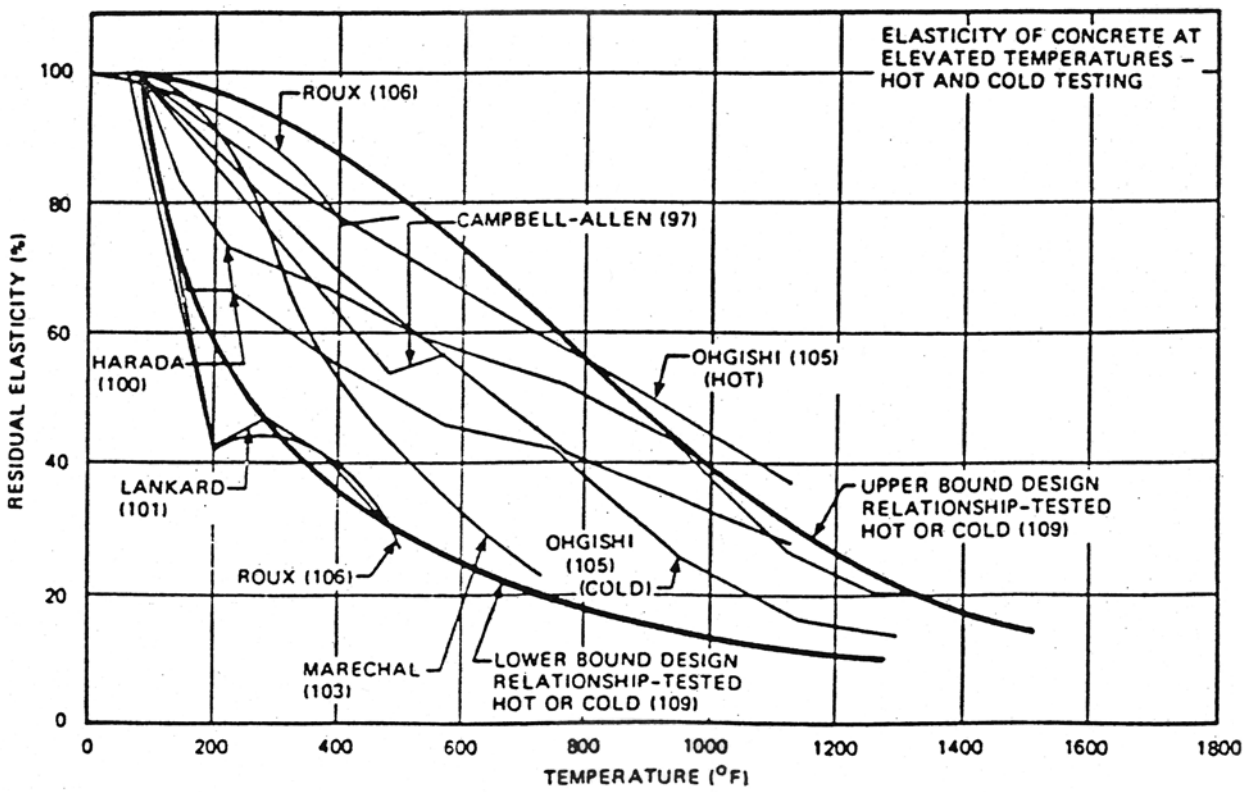

Figure 17 Effect of temperature on the modulus of elasticity of concrete: hot and cold test results. *Source*: G. N. Freskakis, "Behavior of Reinforced Concrete at Elevated Temperature," Paper 3-4, *Source: ASCE Conf. on Civ. Eng. and Nuclear Power* **1**, Paper 3-5, pp. 3-5-1 to 3-5-21, Knoxville, Tennessee, Sept. 15–17, 1980.

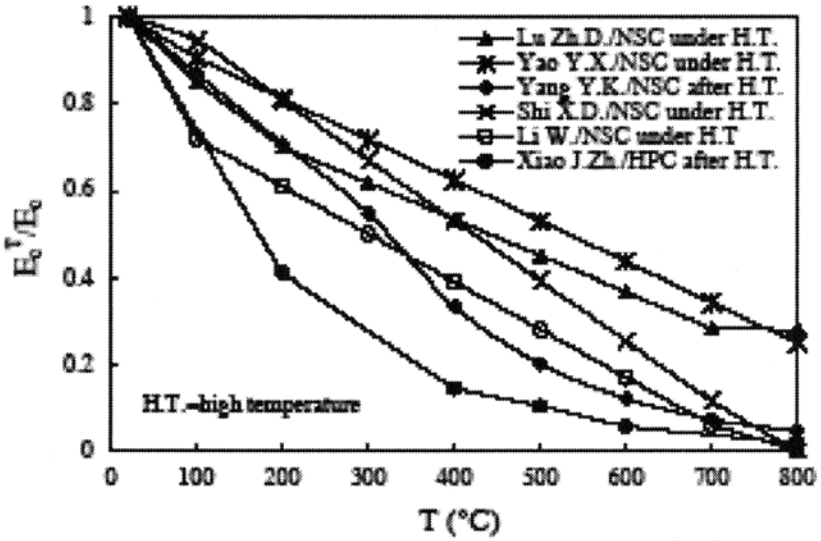

Figure 18 Temperature dependence of the concrete modulus of elasticity (normalized). *Source*: J. Xiao and G. König, "Study of Concrete at High Temperature in China—An Overview," *Fire Safety Journal* **39**, 89–103 (2004).

The strong influence of aggregate type on modulus is presented in Fig. 19.[5] Other conclusions from this study were that a sustained stress during heating affects the modulus significantly and the type of cement had little affect. The influence of water/cement ratio on static and dynamic modulus is illustrated in Fig. 20.[4] Results presented in Fig. 21 for a 31-MPa and a 63-MPa limestone concrete tested at temperature indicate that, when normalized with respect to the room temperature modulus of elasticity, the strength of the concrete does not have a significant effect on the modulus-temperature response.[38]

Results in the literature indicate that the primary factors affecting the modulus of elasticity at high temperature are the type of aggregate (limestone concrete has less loss than quartz concrete) and the presence of sustained stress during heating (sustained stress results in lower decreases in modulus with increasing temperature). Duration of temperature exposure, sealing, type of cement, water/cement ratio and original concrete strength have little effect on modulus results. The age at test apparently also does not affect the residual modulus as noted for a flint/beach gravel concrete for which results were obtained to 150°C at concrete ages of 3 months and 1 year.[39]

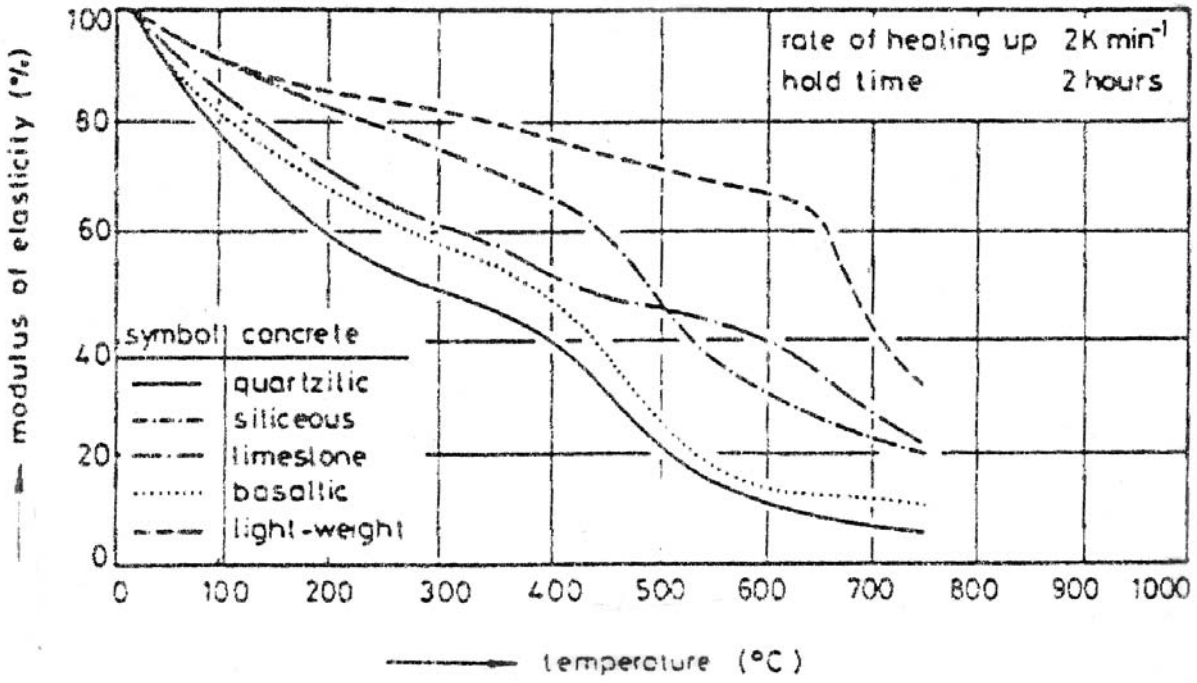

Figure 19 Modulus of elasticity of different concretes at elevated temperature. *Source*: U. Schneider, C. Diererichs, and C. Ehm, "Effect of Temperature on Steel and Concrete for PCRV's," *Nuclear Engineering and Design* **67**, 245–258 (1981).

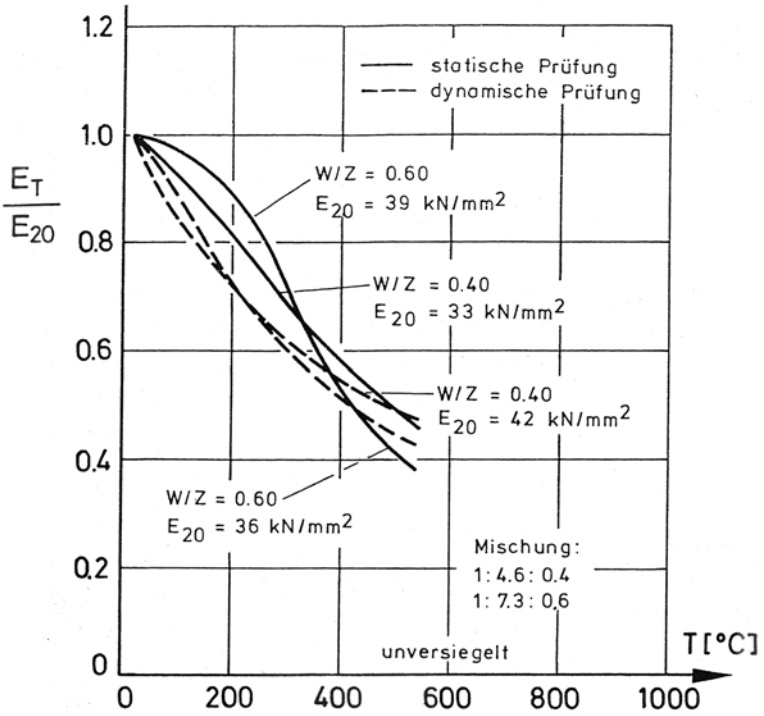

Figure 20 Influence of water/cement ratio on modulus of elasticity of concrete at elevated temperature. *Source*: U. Schneider, "Behaviour of Concrete at High Temperature," HEFT 337, Deutscher Ausschuss für Stahlbeton, Wilhelm Ernst & Sohn, Munich, Germany, 1982.

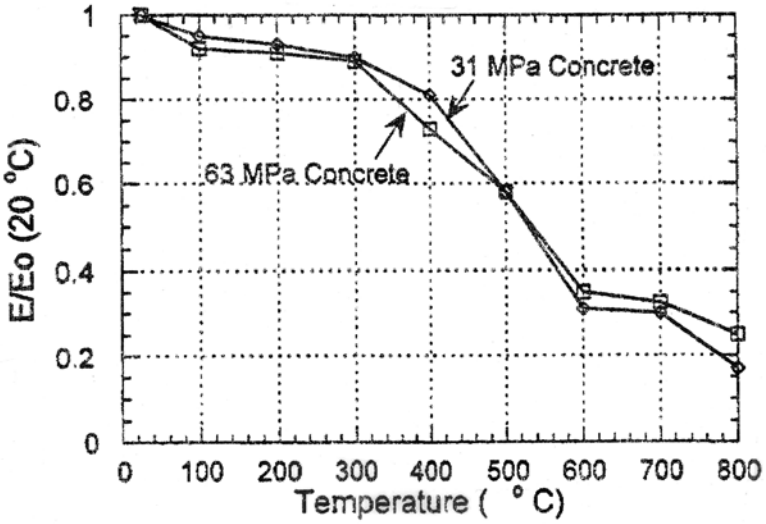

Figure 21 Normalized modulus of elasticity versus temperature relationships NSC and HSC. *Source*: C. Castillo and A. J. Durani, "Effect of Transient High Temperature on High-Strength Concrete," *J. American Concrete Institute*, **87**(1) (1990).

Compressive Strength

The compressive strength influences the load-carrying capacity of a structure. Compressive strength of concrete is generally considered to be its most valuable property.

Thermal gradients affect the concrete strength as well as its stiffness. Figures 22 and 23 present normalized compressive strength results for unstressed specimens tested cold (residual) and at temperature (hot), respectively, that are based on results from several investigators.[25,33,40–51] Additional information is presented in Fig. 24 on the effect of elevated-temperature exposure on the compressive strength of unsealed nuclear power plant PCPV-type concretes (limestone, basalt, or gravel aggregate materials) tested either hot (H) or cold (C) (Ref. 3). These figures indicate the influence of the concrete and the test condition on the residual compressive strength after thermal exposure. The general trend for a strength loss with increasing temperature reflects the influence of the cement paste and the increasing role of the aggregate materials at higher temperatures. Factors have been identified that may contribute to the general trend for loss of compressive strength with increasing temperature:[3] aggregate damage; weakening of the cement paste-aggregate bond; and weakening of the cement paste due to an increase in porosity on dehydration, partial breakdown of the C-S-H, chemical transformation on hydrothermal reactions, and development of cracking. A number of material and environmental-related factors affect the response of concrete materials to elevated-temperature conditions. As many of the aggregate materials are thermally stable up to temperatures of 300°C to 350°C, which includes the temperature range considered for most applications, the compressive strength of concrete at elevated temperature is dependent in large measure on the interaction between the cement paste and aggregate.

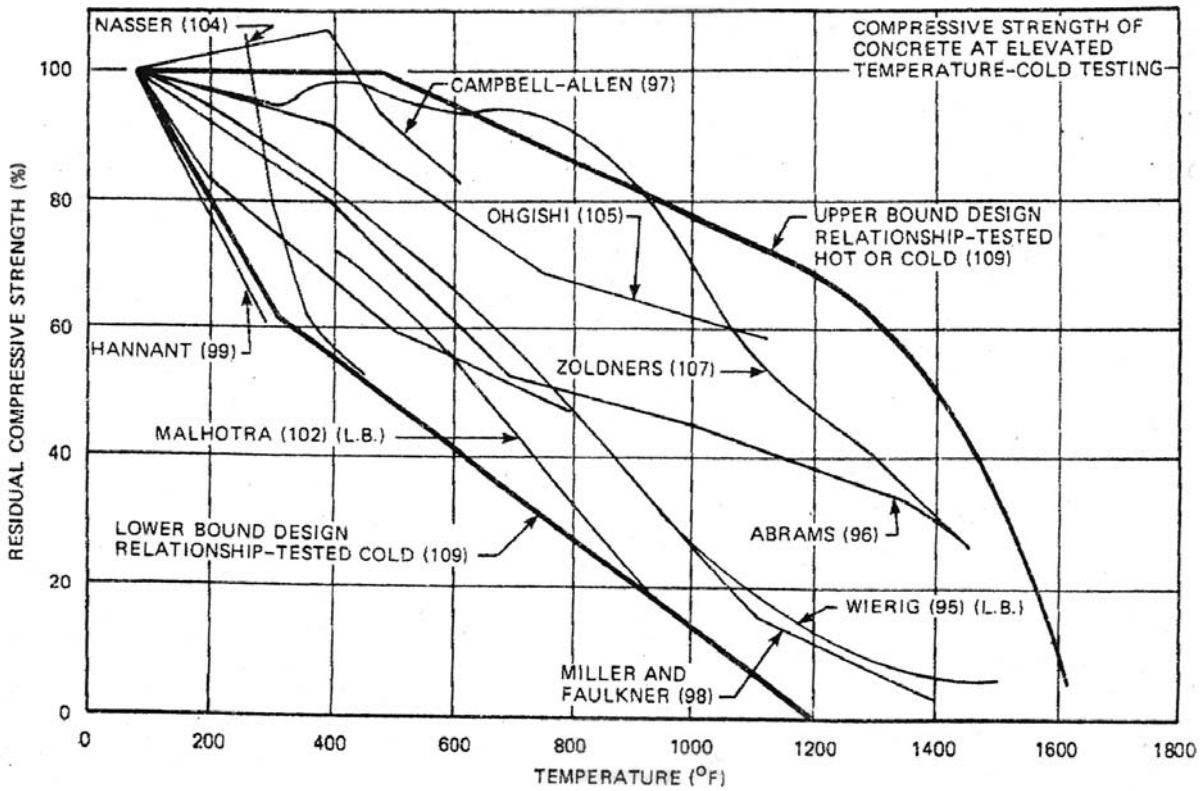

Figure 22 Effect of temperature exposure on compressive strength of concrete: tested cold. *Source*: G. N. Freskakis et al., "Strength Properties of Concrete at Elevated Temperature," *Civil Engineering Nuclear Power*, Vol. 1, ASCE National Convention, American Society of Civil Engineers, Boston, Massachusetts, April 1979.

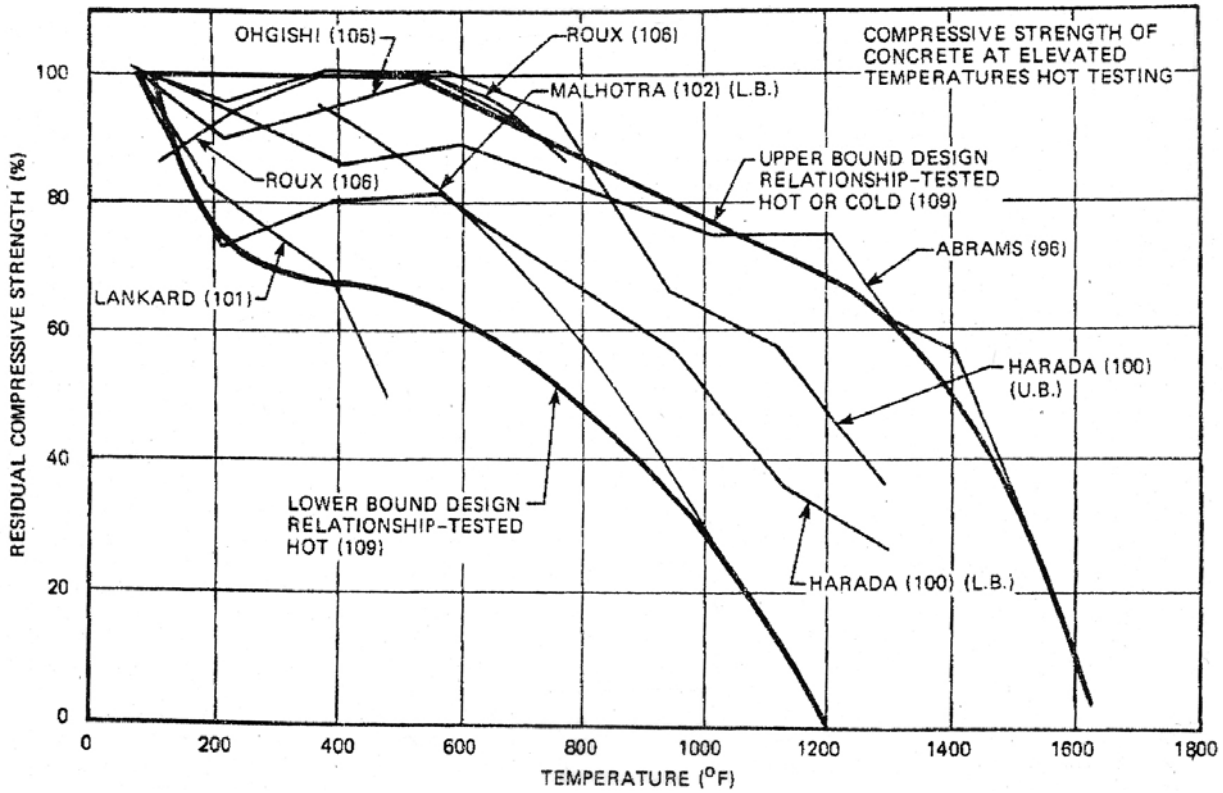

Figure 23 Effect of temperature exposure on compressive strength of concrete: tested hot. *Source*: G. N. Freskakis et al., "Strength Properties of Concrete at Elevated Temperature," *Civil Engineering Nuclear Power*, Vol. 1, ASCE National Convention, American Society of Civil Engineers, Boston, Massachusetts, April 1979.

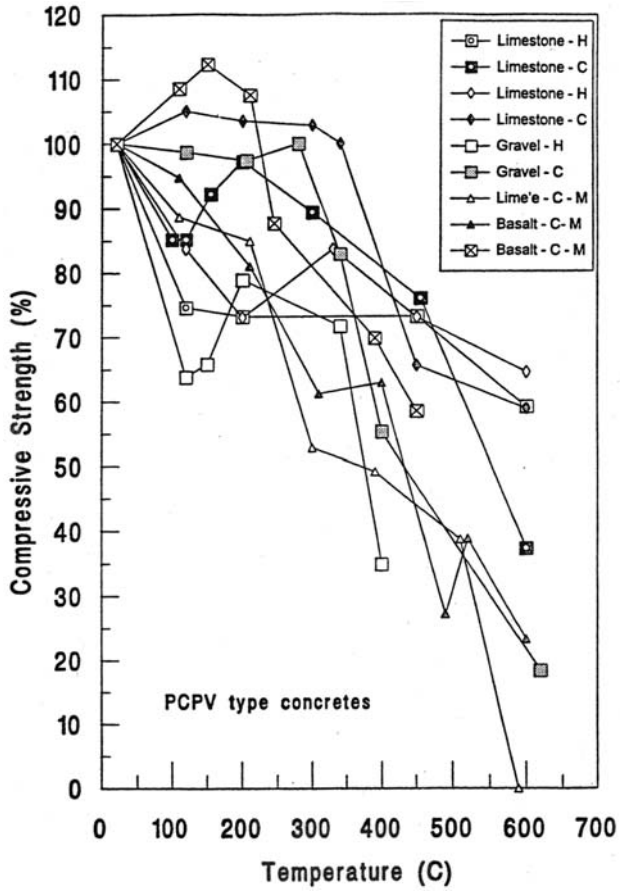

Figure 24 Effect of temperature on uniaxial compressive strength of PCPV unsealed concretes (H = hot, C = cold). *Source*: G. A. Khoury, "Performance of Heated Concrete—Mechanical Properties," Contract NUC/56/3604A with Nuclear Installations Inspectorate, Imperial College, London, United Kingdom, August 1996.

Figure 25, which presents results for unsealed mortars fabricated from ordinary Portland cement, blast furnace slag cement, and truss cement, indicates little difference in strength-temperature characteristics, except the ordinary Portland cement mortar exhibited a sharper decrease in strength at temperatures greater than 500°C (Ref. 4). Another study utilizing a number of cement types (e.g., ordinary Portland cement, fly ash, and blast furnace slag cement) also noted that up to 600°C there was little effect of the cement type.[52] Results presented in Fig. 26 indicate that partial replacement of ordinary Portland cement with pulverized fly ash improves the residual strength and may even produce an increase in strength at higher temperatures.[3,53,*] Water/cement ratio does not appear to have a significant influence on the residual compressive strength of unsealed cement paste as noted by similar trends for three different w/c ratios shown in Fig. 27.[3] These results indicate a peak strength at about 150°C where the residual

*A similar effect was achieved through partial replacement of the ordinary Portland cement with ground granulated blast furnace slag. Partial replacement with silica fume was not beneficial and in some cases produced detrimental residual strength results for unsealed specimens.

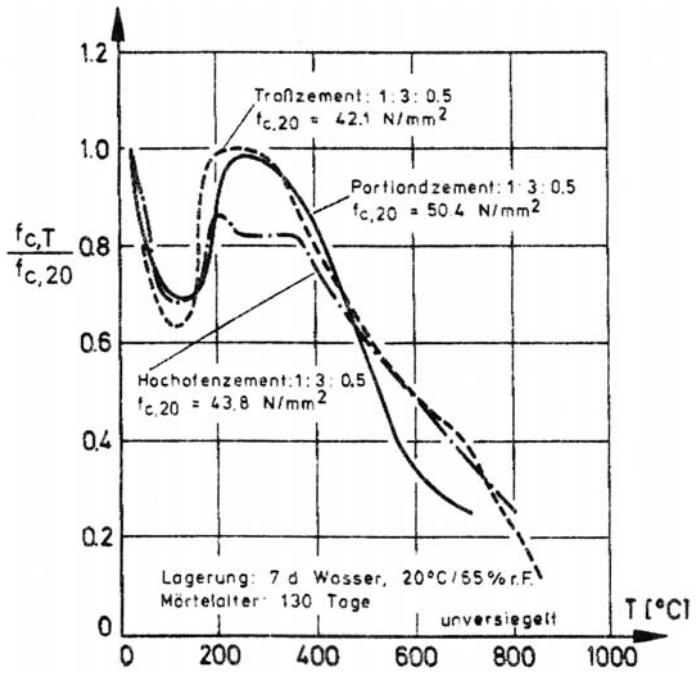

Figure 25 Influence of type of cement on strength loss of mortars. *Source*: U. Schneider, "Behaviour of Concrete at High Temperature," HEFT 337, Deutscher Ausschuss fiir Stahlbeton, Wilhelm Ernst & Sohn, Munich, Germany, 1982.

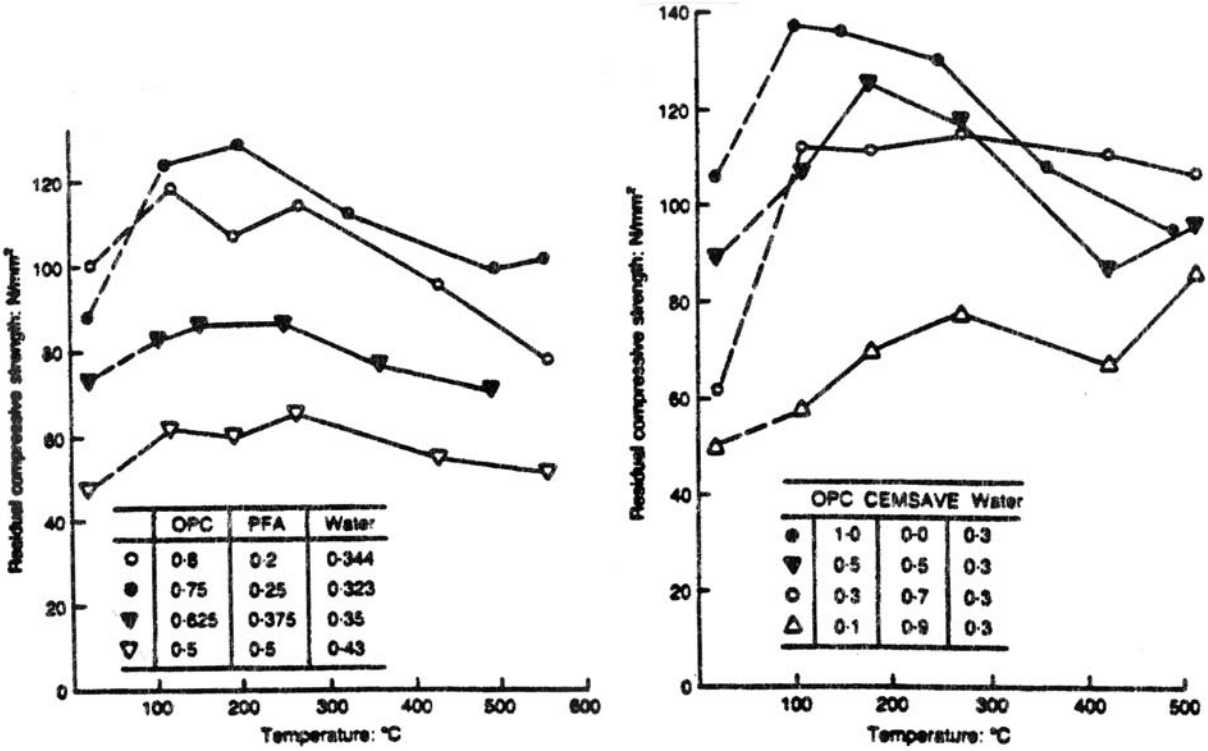

Figure 26 Influence of partial replacement of (a) OPC and (b) slag on residual compressive strength. *Source*: G. A. Khoury, "Performance of Heated Concrete—Mechanical Properties," Contract NUC/56/3604A with Nuclear Installations Inspectorate, Imperial College, London, United Kingdom, August 1996.

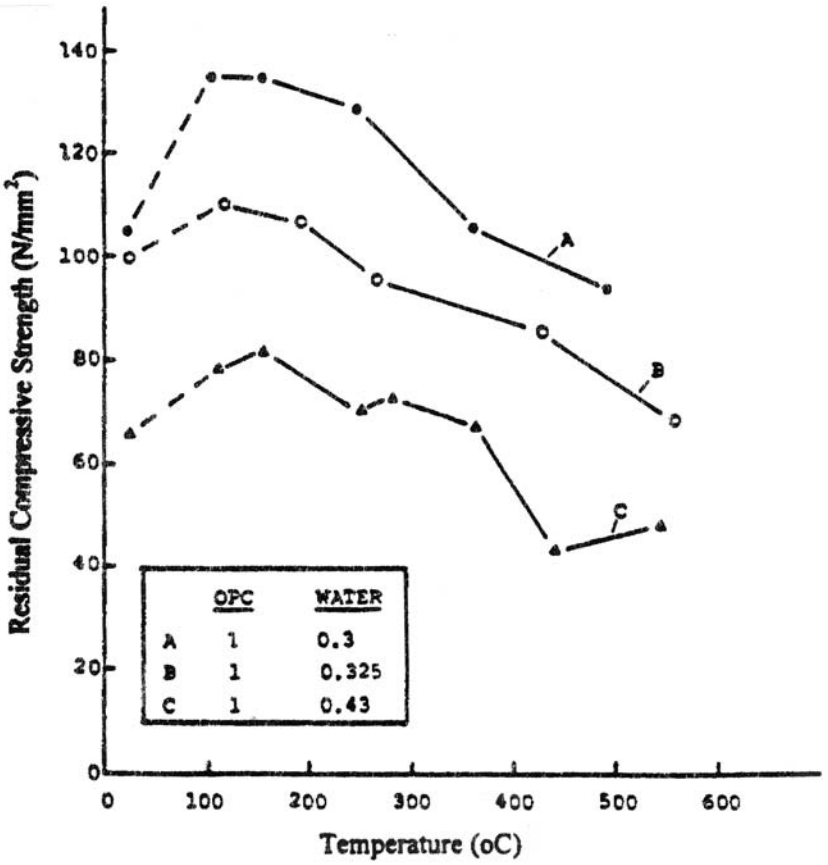

Figure 27 Effect of water/cement ratio on residual compressive strength of OPC. *Source*: G. A. Khoury, "Performance of Heated Concrete—Mechanical Properties," Contract NUC/56/3604A with Nuclear Installations Inspectorate, Imperial College, London, United Kingdom, August 1996.

strengths were 10 to 30% higher than the reference room temperature strength. Although the strength declined at temperatures higher than 300°C to 350°C, at temperatures of 300°C to 350°C it was still higher than the reference strength. Research presented elsewhere involving several aggregate types indicates that the effects of water/cement (w/c) ratio had little influence on the residual compressive strength up to 600°C (Ref. 52). For normal strength Portland cement concretes, the concrete strength has a secondary effect on strength-temperature characteristics. Residual compressive strength results are presented in Fig. 28 for concretes having compressive strengths ranging from 19.6 to 74 MPa (Ref. 54). This study concluded that a HSC has a higher rate of reduction in residual compressive strength (and modulus) than a NSC. Results of unstressed tests for ordinary Portland cement concretes having reference compressive strengths either of 21, 42, or 60 MPa are presented in Fig. 29.[55] Results obtained for each of the concretes was similar in that the compressive strength decreased at 100°C, recovered to the room temperature strength at 200°C, and then decreased monotonically with increasing temperature beyond 200°C. The effect of curing conditions (e.g., in water unsealed, sealed, in-air unsealed) prior to elevated-temperature exposure is presented in Fig. 30.[36] After at least 91 d cure, the specimens, either in a sealed or unsealed condition, were subjected to 175°C for up to 91 d. Unstressed and residual compressive strengths were determined periodically over the exposure period. Although differences in compressive strengths occurred at smaller exposure ages, after 91 d exposure to 175°C, similar results were provided under all test conditions.

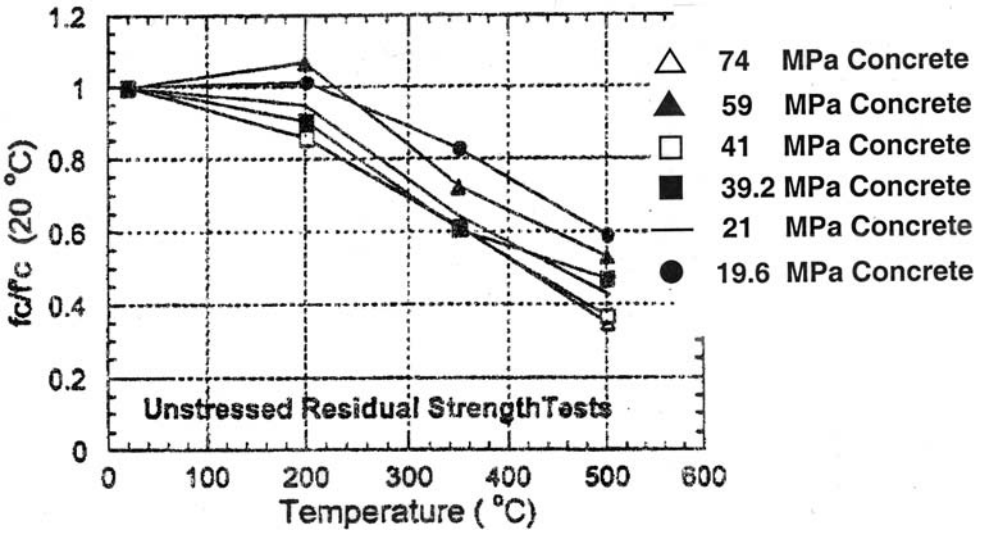

Figure 28 Residual normalized strength vs temperature. *Source*: T. Morita et al., "Residual Mechanical Properties of High Strength Concrete Members Exposed to High Temperature—Part 1. Test on Material Properties," *Summaries of Technical Papers of Annual Meeting*, Architectural Institute of Japan, Naiigata, August 1992.

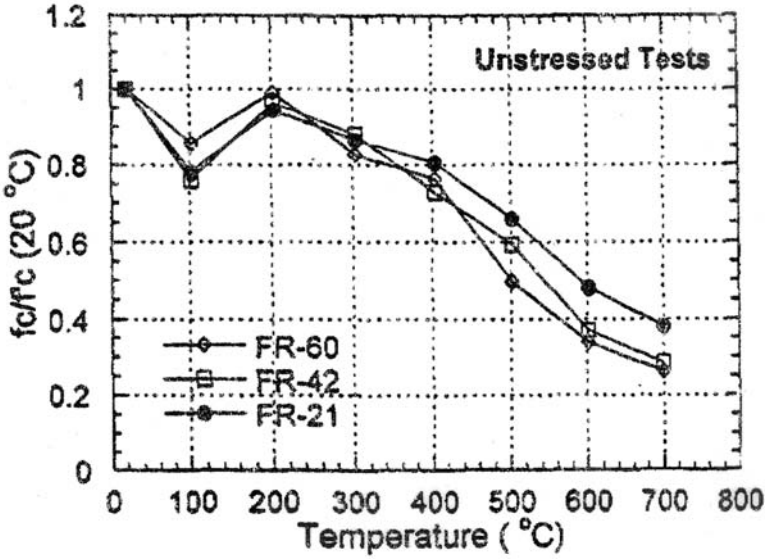

Figure 29 Elastic modulus vs temperature. *Source*: T. Furumura, T. Abe, and Y. Shinohara, "Mechanical Properties of High Strength Concrete at High Temperatures," *Proc. of 4th Weimar Workshop on High Performance Concrete: Material Properties and Design,* held at Hochschule für Architektur und Bauwesen (HAB), Weimar, Germany pp. 237–254, 4–5 October 1995.

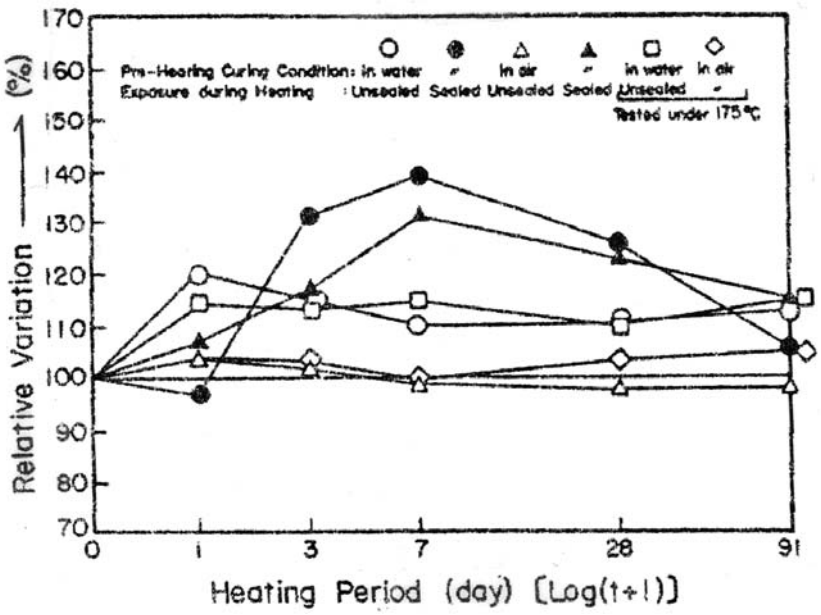

Figure 30 Effect of curing conditions prior to elevated-temperature exposure on relative compressive strength. *Source*: K. Hirano et al., "Physical Properties of Concrete Subjected to High Temperature for MONJU," Paper P2-25, Power Reactor and Nuclear Fuel Development Corporation, Tokyo, Japan.

The age at which the concrete is subjected to elevated-temperature exposure has little effect on the strength-temperature response as long as the concrete has adequate curing (e.g., 90 d). A comparison of residual unstressed compressive strength results for a nuclear power plant concrete (Temelin NPP) at ages of 28-d and 90-d for temperatures to 280°C is presented in Fig. 31.[56] Residual compressive strength results for sealed and unsealed specimens cast from a NPP siliceous aggregate concrete at curing ages of 3 months and 1 year are presented in Fig. 32.[39] These results indicate that some improvement in residual compressive stress due to more extended curing occurs, but it was not significant.

As long as the rate of heating does not produce significant thermal gradients, the rate of heating has a secondary effect on the concrete strength-temperature response, particularly at high temperatures. The effect of rate of heating on residual strength of crushed basalt concrete is presented in Fig. 33.[57] These results indicate that the rates of heating had an insignificant effect on residual strength for temperatures of 600°C and 800°C. However, the heating rate had an effect on the residual compressive strength at lower temperatures. Exposure times at temperature beyond 1 h had an effect on the residual compressive strength, but this effect diminished as the level of exposure temperature increases, with the majority of strength loss occurring in the first 2 h of temperature exposure (Fig. 34). The effect of duration of temperature exposure (exposure periods to 42 d) on the relative strength change of sealed and unsealed gravel and limestone concretes at exposure temperatures to 180°C is shown in Fig. 35.[28] For all temperatures investigated, and for sealed and unsealed conditions, the river gravel concrete generally exhibited a slight strength increase. The compressive strength of the limestone concrete was relatively constant with increasing exposure period for the unsealed condition, but exhibited a decline in compressive strength with increasing temperature level for the sealed condition. The explanation for this

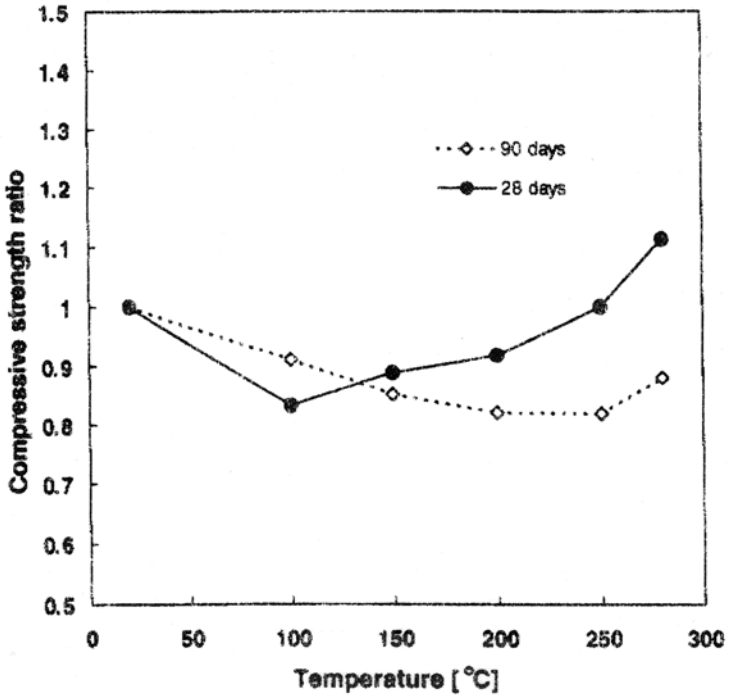

Figure 31 Effect of temperature on compressive strength ratio of concrete. *Source*: F. Vodak et al., "The Effect of Temperature on Strength—Porosity Relationship for Concrete," *Construction and Building Materials* **18**, 529–534 (2004).

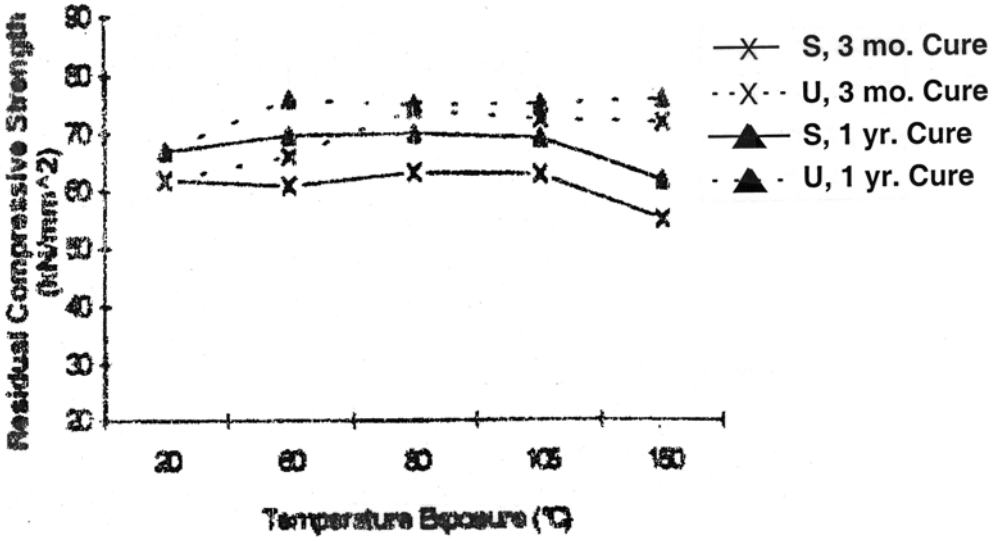

Figure 32 Effect of curing age and exposure condition on residual compressive strength (S = sealed, U = unsealed). *Source*: J. Guo and P. Waldron, "Deterioration of PCPV Concrete," *Nuclear Engineering and Design* **198**, 211–226 (2000).

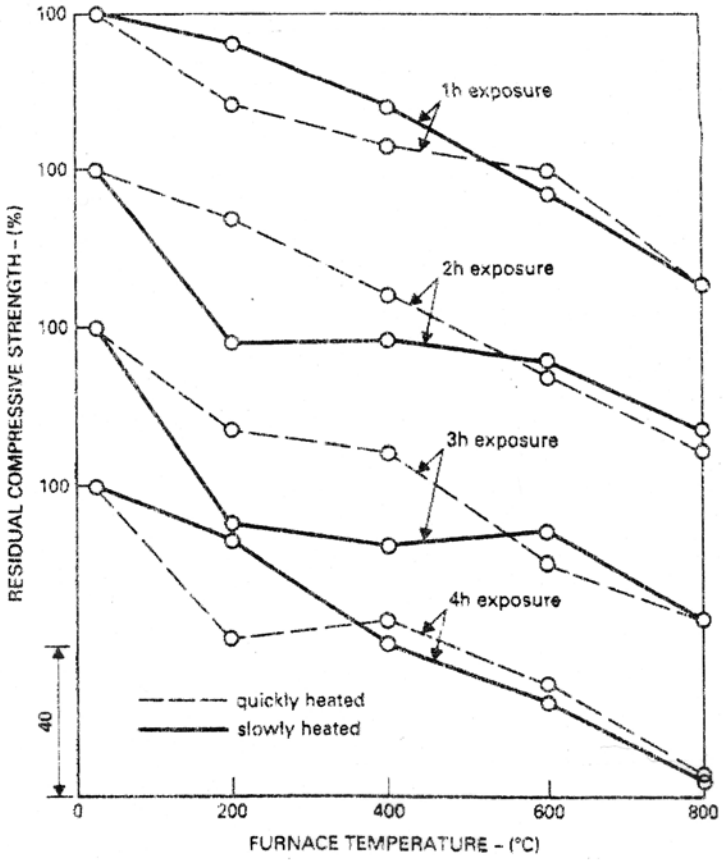

Figure 33 Effect of rate of heating on residual strength of slowly cooled concrete. *Source*: G. T. C. Mohamedbhai, "Effect of Exposure Time and Rates of Heating and Cooling on Residual Strength of Heated Concrete," *Magazine of Concrete Research* **38**(136), 151–158 (September 1986).

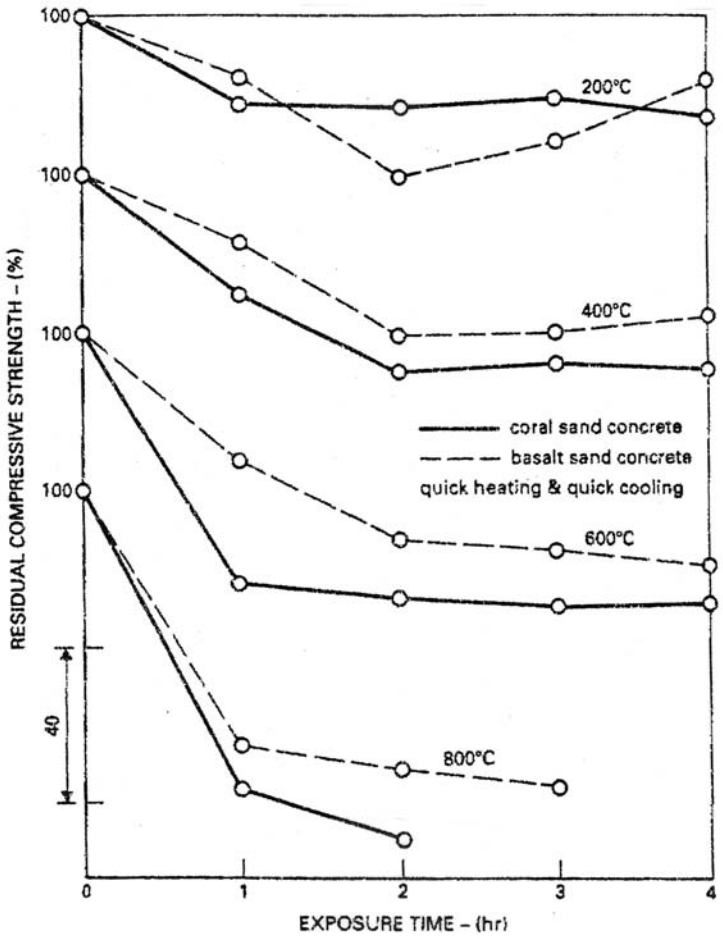

Figure 34 Effect of exposure time on residual strength of coral sand and basalt sand concretes. *Source*: G. T. C. Mohamedbhai, "Effect of Exposure Time and Rates of Heating and Cooling on Residual Strength of Heated Concrete," *Magazine of Concrete Research* **38**(136), 151–158 (September 1986).

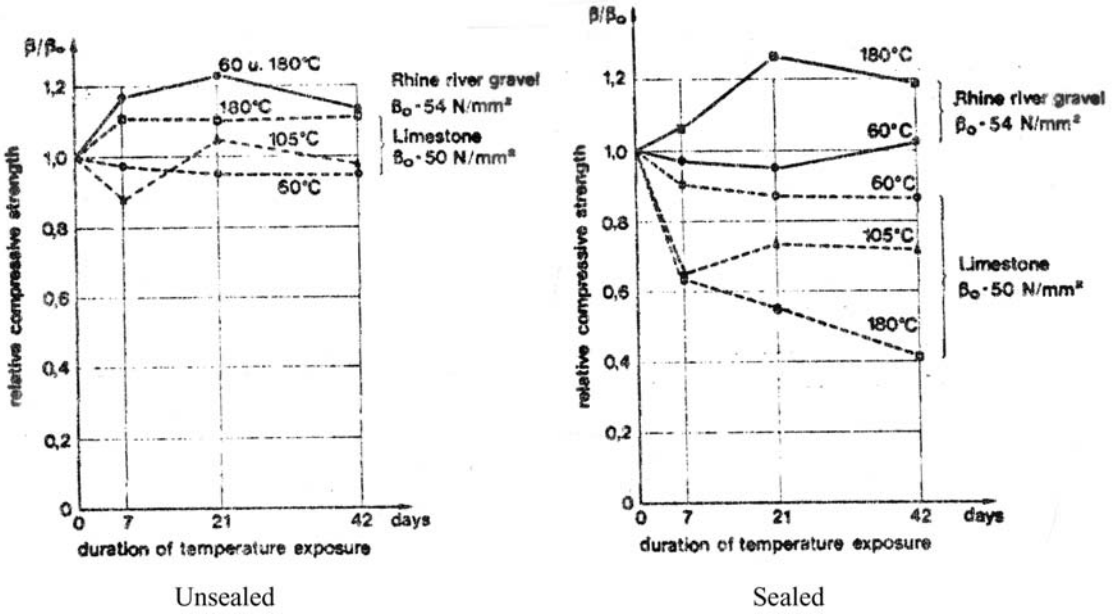

Figure 35 Relative strength development of concrete exposed to elevated temperature. *Source*: R. Kottas, J. Seeberger, and H. K. Hilsdorf, "Strength Characteristics of Concrete in the Temperature Range of 20° to 200°C," Paper HO1/4 in *5th International Conference on Structural Mechanics in Reactor Technology*, p. 8, Elsevier Science Publishers, North-Holland, The Netherlands, August 1979.

behavior was that the strength loss of the limestone concrete was caused by changes in the microstructure of the hydrated cement paste when exposed to hydrothermal conditions. In the river gravel concrete the strength loss was counteracted by a reaction between the silicates of the fine aggregate particles and the $Ca(OH)_2$ of the hydrated cement paste.

The aggregate type is one of the main factors influencing the compressive strength of concrete at elevated temperature. Figure 36 presents a comparison of stressed, unstressed residual, and unstressed compressive strength results for carbonate and siliceous aggregate concretes at temperatures to 871°C (Ref. 40). Results of this study indicate the influence of the aggregate type, show the beneficial effect of stressing the specimens (within limits) while heated, and indicate that unstressed results obtained at temperature exceed those obtained under unstressed residual conditions (i.e., hot strength results were generally greater than residual strength results). The influence of aggregate type on results is further illustrated in Fig. 37 where the compressive strength of limestone and other concretes is presented.[4,*] It was noted in this reference that for the temperature range shown in the figure, quartz and basalt aggregate are less sensitive to temperature effects than the limestone aggregate concrete.

Results in the literature indicate that the original concrete strength (NSC), type of cement, aggregate size, heating rate, and water/cement ratio have little affect on the relative strength vs temperature characteristics; exposure times at temperatures beyond 1 h had an effect on residual compressive strength, but this effect diminished as the level of exposure temperature increased, with the majority of strength loss occurring in the first 2 h. Age of concrete is important in so far as concretes with relatively

*See also Fig. 72.

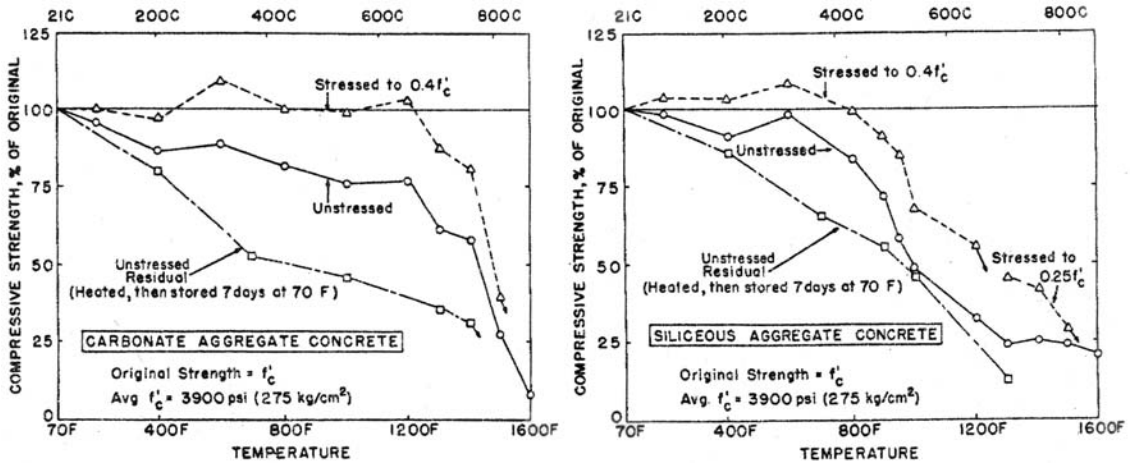

Figure 36 Effect of exposure time on residual strength of carbonate and siliceous aggregate concretes. *Source*: M. S. Abrams, "Compressive Strength of Concrete at Temperatures to 1600°F," SP-25 *Temperature and Concrete,* American Concrete Institute, pp. 33–58, 1971**.**

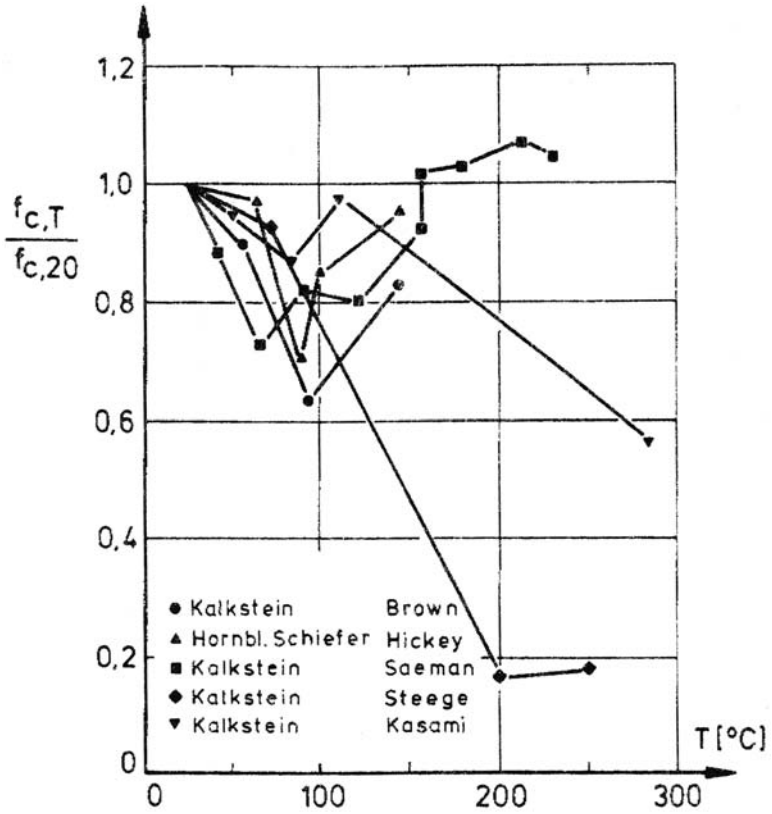

Figure 37 Compressive strength of concretes with limestone and other aggregate types. *Source*: U. Schneider, "Behaviour of Concrete at High Temperature," HEFT 337, Deutscher Ausschuss für Stahlbeton, Wilhelm Ernst & Sohn, Munich, Germany, 1982.

incomplete hydration of cement may indicate a strength increase for temperature up to 400°C due to accelerated hydration; maximum test temperature influences the strength recovery in that after exposures to above about 600°C there is no strength recovery; aggregate/cement ratio has a significant affect on strength of concrete exposed to high temperature with the reduction being proportionally smaller for lean mixtures than for rich mixtures. Type of aggregate appears to be one of the main factors influencing concrete strength at high temperature with siliceous aggregate concrete having lower strength (by percentage) at high temperature than calcareous and lightweight concrete; and stressed specimens resulted in higher compressive strength at high temperature than unstressed specimens.

Thermal Cycling

Thermal cycling, even at relatively low temperatures (65°C), can have some deleterious effects on concrete's mechanical properties (i.e., cyclic heating generally gives lower strengths than a single heating).[45] The effect of temperature cycling on a limestone aggregate concrete is presented in Fig. 38[58] and in Fig. 39[59] for a sealed limestone concrete. Results indicate that the compressive, tensile, and bond strengths, and the modulus of elasticity are reduced, and that Poisson's ratio is increased.[58,59] As shown in Fig. 39, the sealed limestone concrete exhibited a 50% loss of strength after 14 cycles at 150°C. At higher temperatures (200°C to 300°C), the first thermal cycle causes the largest percentage of damage, with the extent of damage markedly dependent on aggregate type and is associated with loss of bond between the aggregate and cement paste matrix.[58]

Tensile Strength

The tensile strength of concrete is important because it determines the ability of concrete to resist cracking. At room temperature, concrete's tensile strength generally varies from 7 to 11% its compressive strength. Direct measurement of concrete's tensile strength is seldom made because of difficulties in gripping the specimen to apply loads. An indication of concrete's tensile strength can be obtained by the splitting-tension and flexure tests. The splitting-tension test is an indirect test for tensile strength of concrete in that a horizontal concrete cylinder is loaded in compression through bearing strips placed along two axial lines that are diametrically opposite on the specimen.[60] Flexural strength of concrete is expressed in terms of modulus of rupture that is determined from beam specimens loaded in four-point bending until failure occurs. Because the modulus of rupture is calculated based on linear-elastic conditions, it is a fictitious value, but convenient for comparison purposes. For normal strength concretes tested at room temperature, the modulus of rupture is 60 to 100% higher than the direct tensile strength and 100 to 133% the splitting-tension strength.[31] Most tests to determine elevated-temperature effects on concrete tensile strength used splitting-tension tests with the residual tensile strength determined.

Unstressed residual tests of a normal-strength (38.1-MPa) and high-strength (61.1-MPa) calcareous aggregate concrete were conducted to evaluate the effect of elevated temperature on the direct-tensile and splitting-tensile strengths.[61] The experimental results, Fig. 40, show that the residual tensile strengths for both NSC and HSC decreased similarly and almost linearly with increasing temperature. Also, tensile strengths measured by the splitting-tension test were consistently higher than those obtained by the direct-tension test. Results presented in Ref. 52, in which residual tensile-strength ratio results were determined

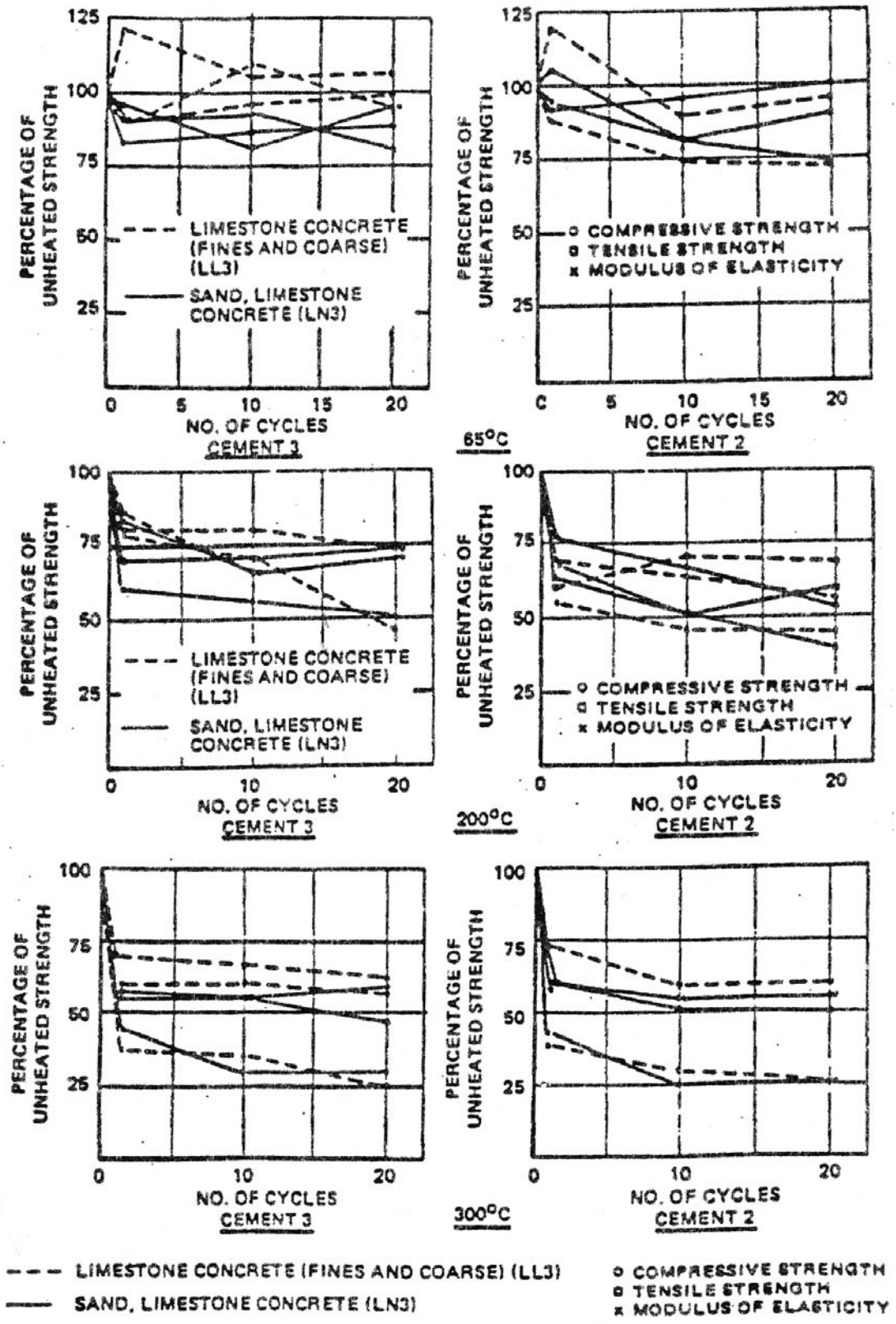

Figure 38 Effect of temperature cycles on limestone concretes. *Source*: D. Campbell-Allen and P. M. Desai, "The Influence of Aggregate on the Behavior of Concrete at Elevated Temperature," *Nucl. Eng. and Design* **6**(1), 65–77 (August 1967).

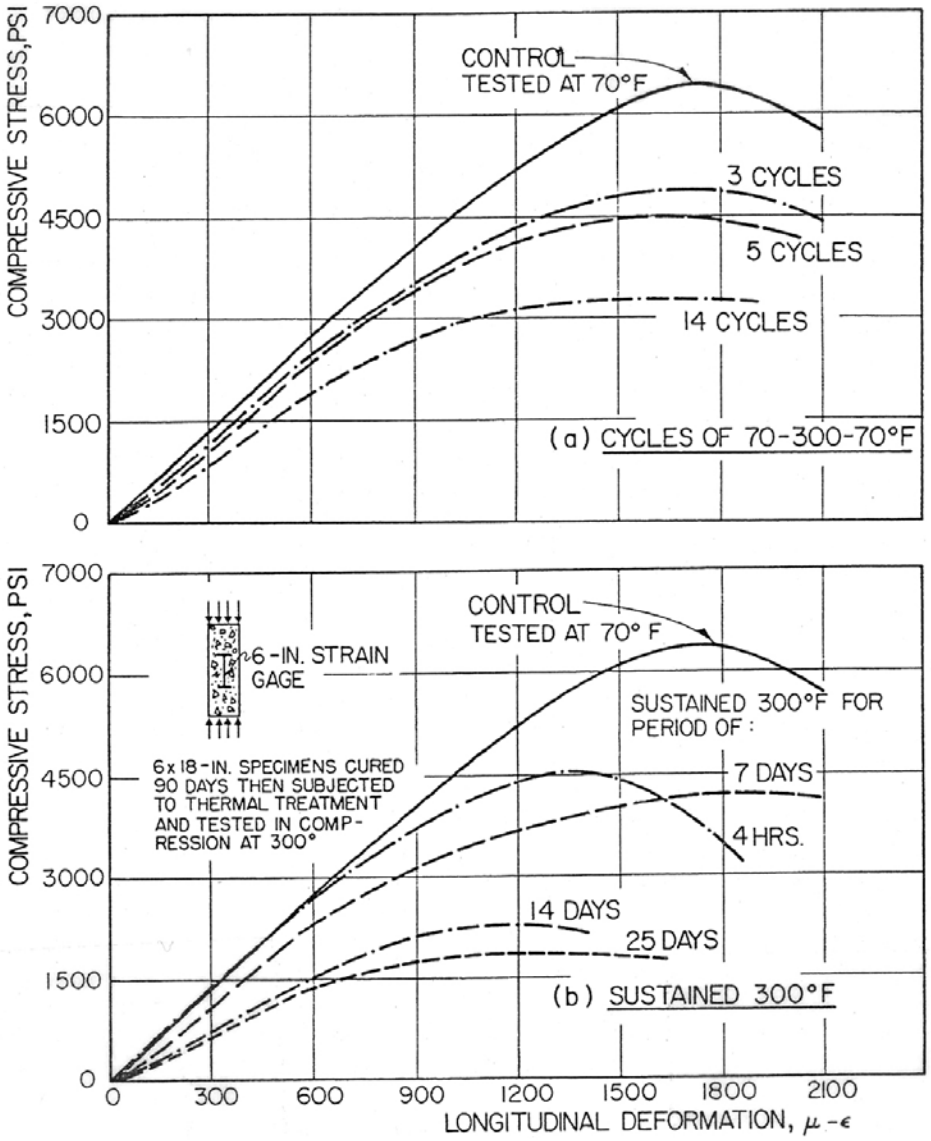

Figure 39 Influence of thermal cycling on σ-e response of sealed concrete tested at 300°F (149°C). *Source*: V. V. Bertero and M. Polivka, "Influence of Thermal Exposures on Mechanical Characteristics of Concrete," Paper SP 34-28 in Special Publication 34, Vol. I-III, American Concrete Institute, Farmington Hills, Michigan, 1972.

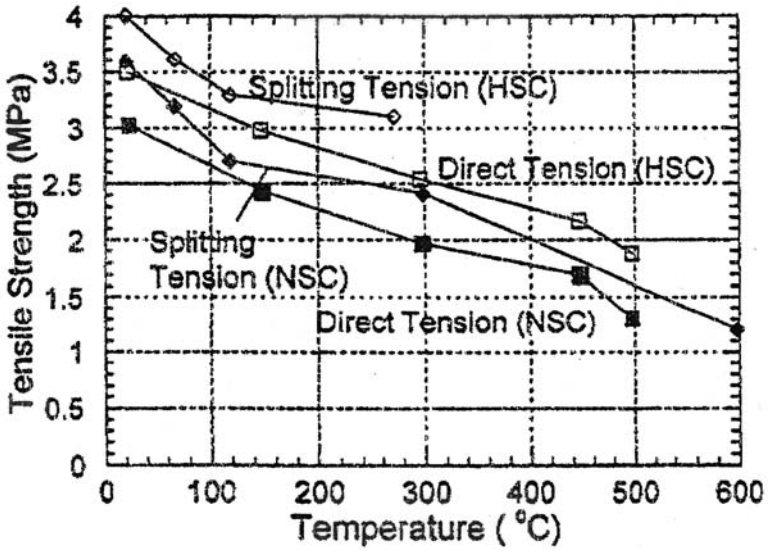

Figure 40 Residual tensile strengths of HSC and NSC. *Source*: A. N. Noumowe et al., "Thermal Stresses and Water Vapor Pressure of High Performance Concrete at High Temperature," *Proc. 4th International Symposium on Utilization of High-Strength/High-Performance Concrete, Paris, 1996*.

at temperatures of 300°C and 600°C for unsealed specimens, indicate that the residual ratios decrease with the rise of heating temperature, except for alumina cements there was little difference in results up to 600°C for several cement types investigated, and there was no significant variation in residual ratio results resulting from different water/cement ratios utilized (i.e., 0.45, 0.55, and 0.65). The influence of exposure condition on the splitting-tensile strength has been investigated.[39] Residual splitting-tensile strength results for sealed and unsealed specimens cast from a NPP siliceous aggregate concrete at curing ages of 3 months and 1 year are presented in Fig. 41.[39] Unlike the residual compressive strength results obtained in the investigation, the tensile strength of sealed concrete specimens that had experienced temperature exposure is higher than that for unsealed specimens (except at 150°C). Comparing compression and tensile results, the splitting-tensile strength appears to be more sensitive to the effect of moisture content as well as to microcracking caused by the temperature exposure. A comparison of the effect of elevated-temperature exposure on residual compressive, tensile (splitting-tension), and bend strengths (notched beams) for a siliceous gravel concrete exposed to temperatures up to 600°C is presented in Fig. 42.[62] Results in the figure indicate that the residual tensile strength, either splitting-tensile or notched beam, is affected more significantly as the temperature increases than the compressive strength.

Modulus of rupture results presented in Ref. 63 show that an increase in temperature beyond room temperature caused the modulus of rupture to decrease to minimum values between 38°C and 65°C. The modulus of rupture was reduced to 50% and 10% compared to room temperature values, for rich and lean mixtures. A further increase in temperature produced a slight increase in the modulus of rupture compared with room temperature values with rich mixes showing a large increase in modulus of rupture with increase in temperature to 121°C with the values being 20% higher than the room temperature results. Changes in flexural strength of Portland cement containing gravel or limestone aggregate heated to

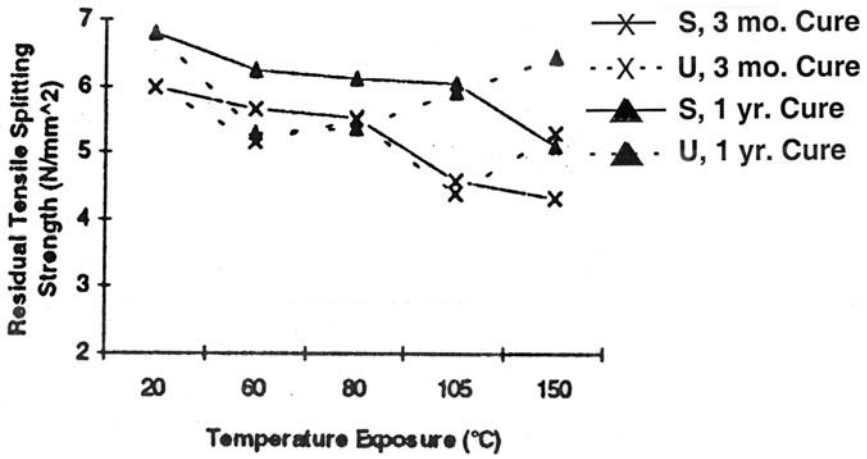

Figure 41 Effect of curing age and exposure condition on residual splitting-tensile strength (Solid line = sealed, dashed line = unsealed). *Source*: J. Guo and P. Waldron, "Deterioration of PCPV Concrete," *Nuclear Engineering and Design* **198**, 211–226 (2000).

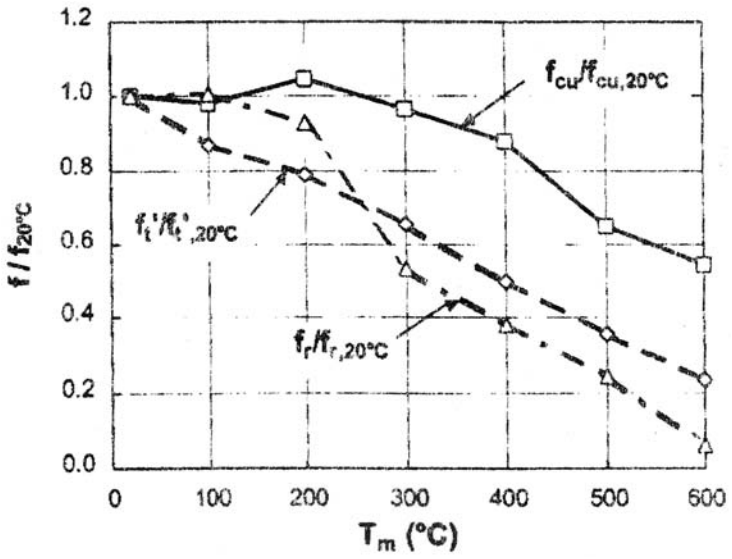

Figure 42 Comparison of the effect of elevated-temperature exposure on residual compressive, tensile (splitting-tension), and bend strengths (notched beams) of siliceous aggregate concrete. *Source*: B. Zhang et al., "Relationship Between Brittleness and Moisture Loss of Concrete Exposed to High Temperatures," *Cement and Concrete Research* **32**, 363–371 (2002).

temperatures up to 260°C were studied.[45] The results showed that the unsealed gravel and limestone concretes heat treated at 79°C exhibited a slight increase in flexural strength, whereas concrete heat treated at 121°C and 260°C exhibited a loss of flexural strength. The gravel concrete showed a lesser degree of flexural strength loss than the limestone concrete at elevated temperature. Flexural strength results have been presented for concrete in which the cement was partially replaced by fly ash (i.e., 10, 20, or 30%) and the specimens subjected to elevated-temperature exposures of 100, 200, or 250°C for 1-, 2-, or 3-h durations.[64] Figure 43 presents the variation of maximum flexural strength with temperature for the control and three mixes with different partial placements of cement with fly ash exposed to elevated temperature for 60 min. Figure 44 shows the variation of residual flexural strength with percentage fly ash for three different exposure temperatures and times. Conclusions of this study were that the fly ash consistently showed the same pattern of flexural behavior (i.e., trend) with temperature as that exhibited by concrete without fly ash for thermal exposures up to 250°C; the exposure time had an effect on the residual flexural strength of concrete, but the majority of strength loss occurred within the first hour of exposure.

Conclusions from the limited tensile test data available in the literature are that the aggregate type and mixture proportions have a significant effect on the tensile strength vs temperature relationship; the decrease in tensile strength of calcareous aggregate concrete is twice as high as that of siliceous aggregate concrete at 500°C; concretes with lower cement content have lower reduction in tensile strength than those with higher cement content; the rate of heating has minimal effect on tensile strength at high temperature; and the residual tensile strength is somewhat lower than the tensile strength measured at elevated temperature.

Shrinkage and Creep

Shrinkage of concrete is important because of its effect on movement of the structure and its tendency to induce cracking. Shrinkage occurs as a result of two effects: (1) drying or (2) autogeneous volume change. Drying shrinkage results from the loss of absorbed water and is generally the more predominant of the two effects. Autogeneous shrinkage is more prevalent in mass concrete structures where the total moisture content remains relatively constant; it results from continued cement hydration reducing the free -water content (products of hydration occupy less volume than the sum of the separate volumes of the components). Several factors affect concrete drying shrinkage: (1) cement and water contents (shrinkage

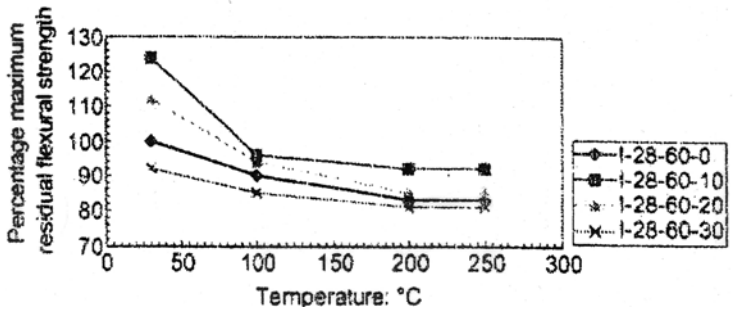

Figure 43 Variation of flexural strength with temperature. *Source*: M. P. Raju, M. Shobha, and K. Rambabu, "Flexural Strength of Fly Ash Concrete Under Elevated Temperatures," *Magazine of Concrete Research* **56**(2), 83–88 (March 2004).

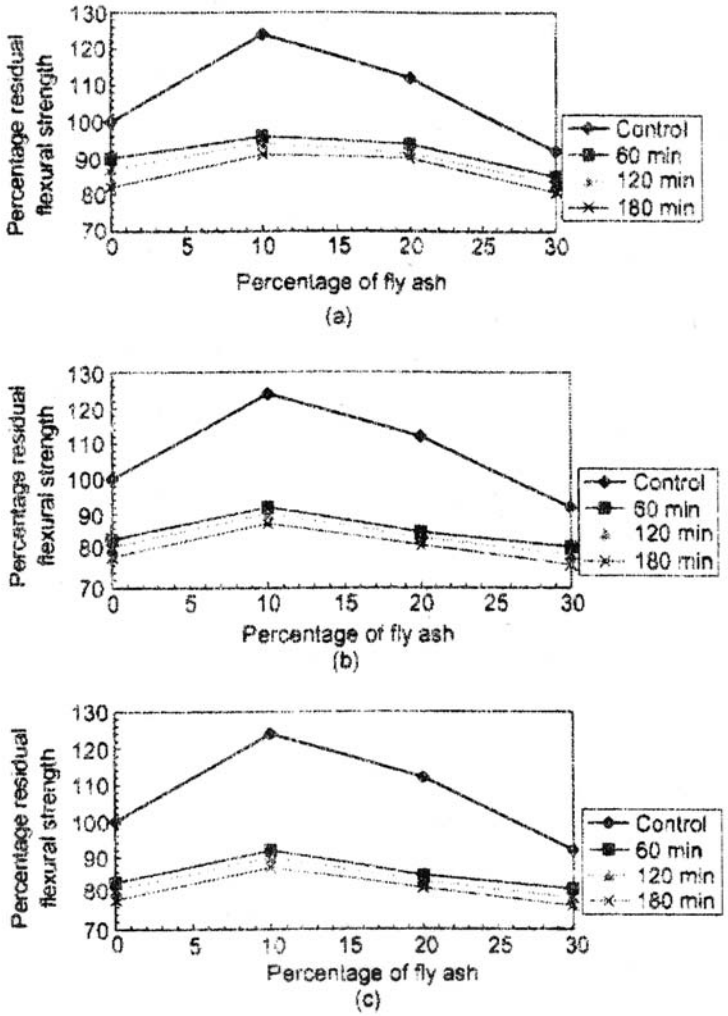

Figure 44 Variation of percentage residual flexural strength for (a) 100°C, (b) 200°C, and (c) 250°C. *Source*: M. P. Raju, M. Shobha, and K. Rambabu, "Flexural Strength of Fly Ash Concrete Under Elevated Temperatures," *Magazine of Concrete Research* **56**(2), 83–88 (March 2004).

varies directly with water-cement ratio);[65] (2) composition and fineness of cement; (3) type and gradation of aggregate (shrinkage inversely proportional to size and amount of coarse aggregate-sandstone, slate, basalt and trap rock produce concretes having greater shrinkage than quartz, limestone, dolomite, granite and feldspar aggregate concretes); (4) admixtures (those that reduce water requirement reduce shrinkage); (5) moisture and temperature conditions; and (6) amount and distribution of reinforcement. The effects of several variables influencing autogeneous shrinkage are summarized in Fig. 45.[66] In mass structures where the concrete is maintained below 100°C, shrinkage will not be a significant factor over the 30- to 40-year design life of a structure such as a PCPV.[67] The rate and magnitude of drying shrinkage generally increase with temperature.

Creep can be defined as the increase in strain in a structural member with time due to sustained stress. Because creep affects strains, deflections, and stress redistribution, it is important with respect to

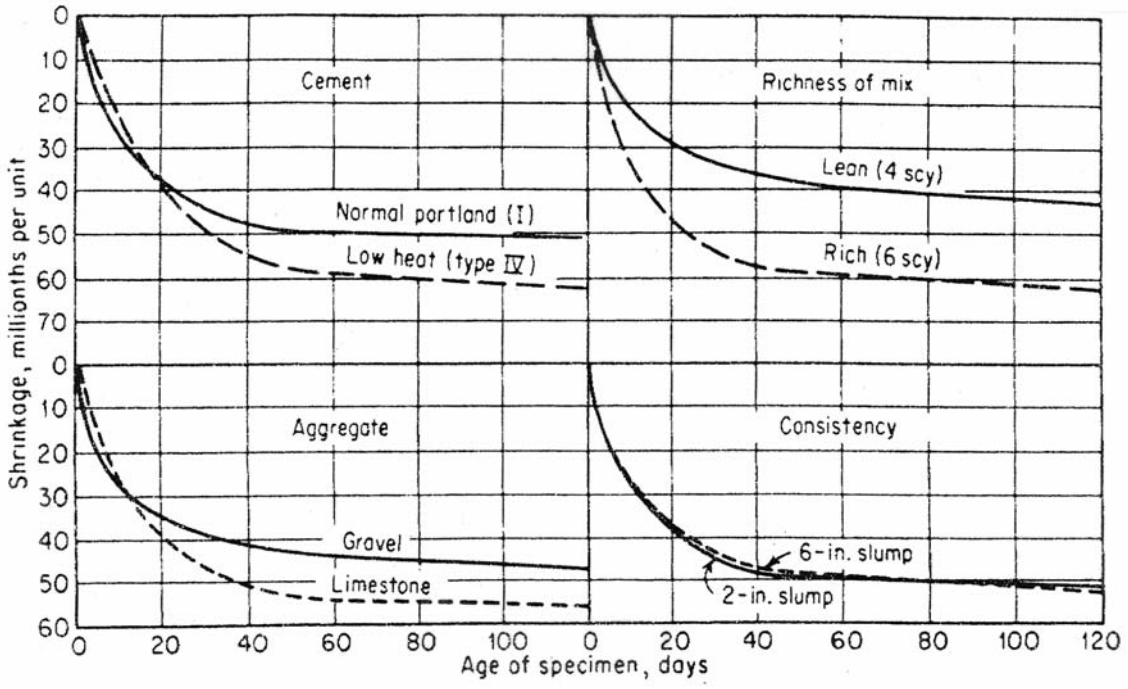

Figure 45 **Effect of several factors on autogenous shrinkage of concrete.** *Source*: G. E. Troxell, H. E. Davis, and J. W. Kelly, "Composition and Properties of Concrete," 2nd Ed., McGraw-Hill, New York, 1968.

structural analysis. Creep may also be viewed from another standpoint: if a loaded specimen is restrained from movement (constant net strain), creep will manifest itself as a progressive decrease in stress with time (stress relaxation). Although creep is generally considered only for specimens loaded in compression, creep of concrete in tension also occurs and is on the same order of magnitude as creep in compression.[68] Also, upon release of the sustained load, an initial elastic recovery of strain occurs followed by creep recovery that can continue for several days. The magnitude of creep recovery is greater for concrete specimens that were loaded later in their cure cycle, and it is inversely proportional to the period of sustained stress.

Several theories for the creep mechanism have been proposed: viscous flow of the cement-water paste, closure of internal voids, crystalline flow of aggregate, and seepage into internal voids of colloidal (adsorbed) water formed by cement hydration.[31] Some investigators[69] divide creep into two types: (1) basic creep under conditions of hygrometric equilibrium caused by molecular diffusion of the gel and absorbed water, causing a partially viscous (irrecoverable) and partially delayed elastic (partially recoverable) behavior; and (2) drying creep caused by a mechanism similar to that involved in free shrinkage due to desiccation. Basic creep has been defined as the load-induced, time-dependent deformation of a specimen which is loaded after achieving thermal, hygral, chemical, and dimensional stability at first heating to a given temperature.[70] Creep of specimens that are loaded after achieving stability at temperature higher than the temperature at loading can be termed basic creep. Drying creep is a function of the moisture loss from the concrete and is related to drying shrinkage. In sealed concrete, drying creep is absent and it is usually the practice to describe the creep during first heating simply as transitional thermal creep. Reference 3 provides a very complete description of the strains that develop for loaded and unloaded concrete during first heat-up, at constant temperature, during cooling, and residual

strains. Also included in this reference is a method for isolating individual strain components and performing an assessment of their magnitude.

Several physical and environmental parameters affect creep deformations of normal-weight concrete. Physical parameters inherent to the particular concrete mix include: (1) cement type (degree of hydration); (2) cement paste proportions and content (creep proportional to volume fraction of cement paste in mix); (3) aggregate properties and volume fraction [(a) aggregate restrains creep, (b) mineral character effects are presented in Fig. 46, and (c) creep tends to be inversely proportional to maximum aggregate size for uniformly graded mixes[31,71]]; (4) strength and stage of hydration [(a) creep decreases with degree of cement hydration of a mix, and (b) generally the amount of creep is inversely proportional to the concrete strength]; (5) moisture conditions of storing [creep is generally inversely proportional to the relative humidity of the medium surrounding the concrete (Fig. 47)[32]], and (6) size of mass (the larger the mass, the lower the creep). Mechanical parameters include: (1) state of stress: [under uniaxial compressive stress for stress/strength ratio < 0.4, creep is proportional to applied stress; (b) at high stress-strength levels (>0.85), creep can lead to failure; (c) creep under multiaxial compression is less than under uniaxial compression of the same magnitude in the given direction (Fig. 48); (d) creep occurs under hydrostatic compression[72–74]]; (2) age at loading [specific creep decreases for increased loading age]; and (3) temperature [(a) creep follows the same general pattern as creep at room temperature—being an exponential function of time under load and a relatively linear function of stress up to a stress-strength

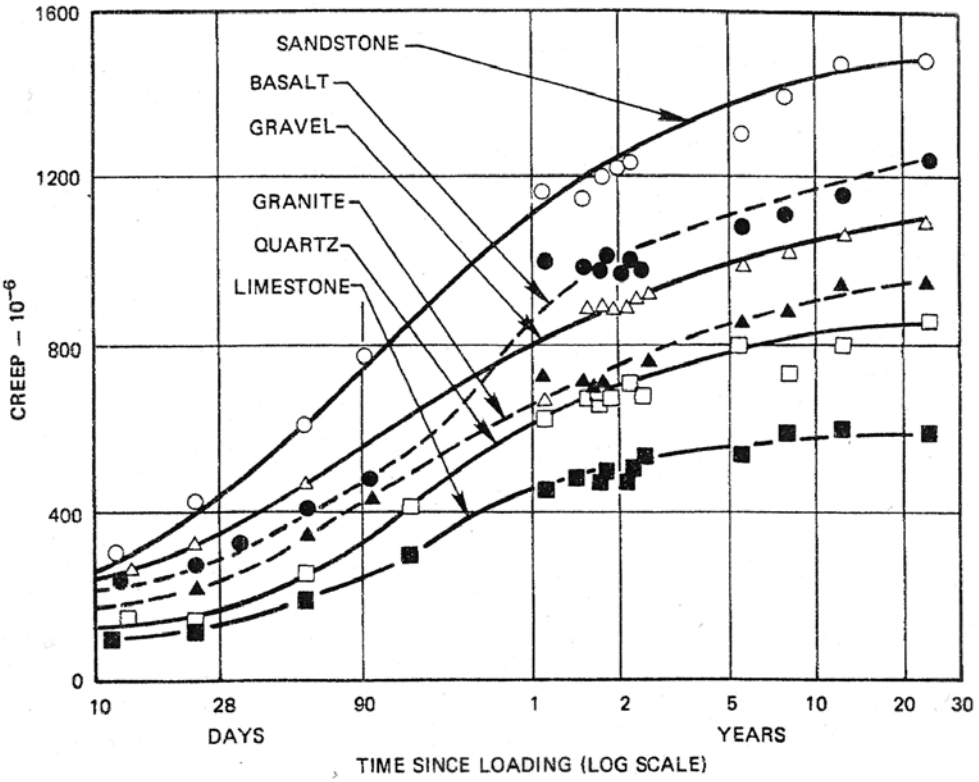

Figure 46 Creep of concrete with different aggregates (aggregate/cement ratio = 5.67, w/c = 0.59, stress = 56 kg/cm^2). *Source*: G. E. Troxell et al., *Composition and Properties of Concrete,* 2nd Ed., McGraw-Hill, New York, 1968.

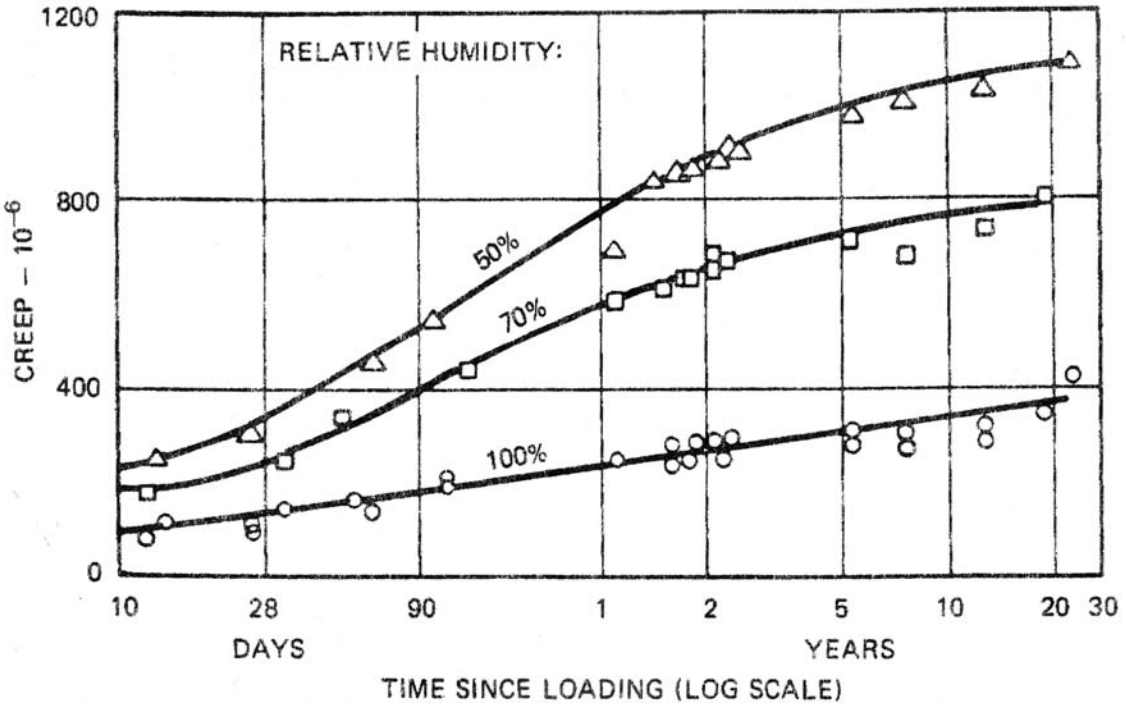

Figure 47 Creep of concrete stored at different relative humidities. *Source:* A. M. Neville, *Properties of Concrete*, Pitman, London, United Kingdom, 1970.

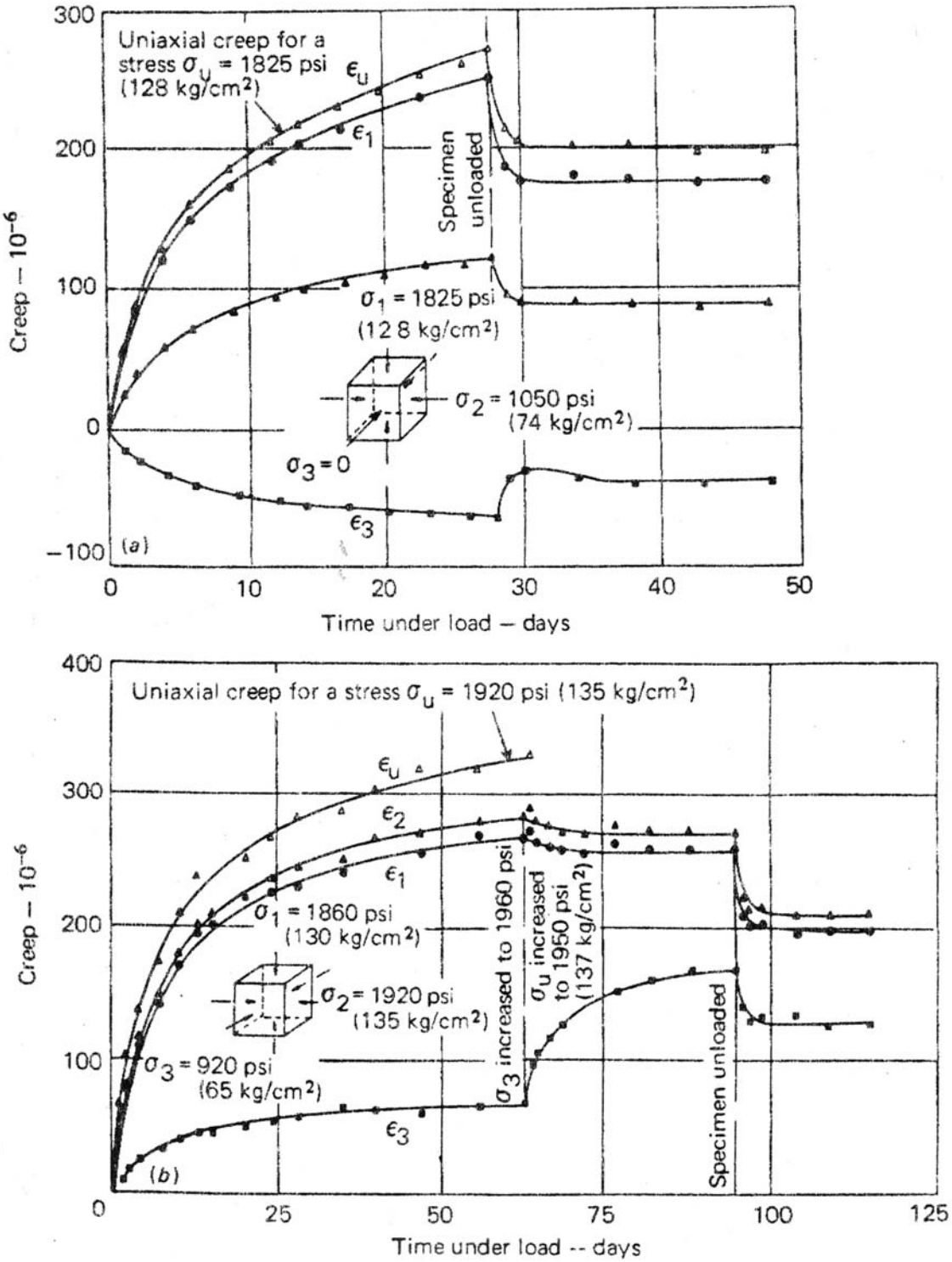

Figure 48 **Typical creep-time curves under multiaxial compression: (a) biaxial, and (b) triaxial.** *Source*: A. M. Neville, *Creep of Concrete: Plain, Reinforced and Prestressed*, North-Holland Publishing Company, Amsterdam, The Netherlands, 1970.

ratio of ~0.4; (b) sealed specimens exhibit less creep than unsealed; (c) creep definitely increases with temperature up to at least 50°C and probably increases with temperature up to 150°C (Fig. 49); and (d) the degree of creep recovery appears to be more dependent on stress level than temperature].[47,75]

As noted in Ref. 76, the effects of temperature on the creep of hardened cement paste can be broadly classified as thermal and structural. The thermal effect of temperature is that which is due to the temperature at loading, being seated in the molecular agitation caused by temperature. The structural effect will depend on the maximum exposure temperature, on the assumption that cooling down to the loading temperature does not reverse any structural changes caused by heating or cause structural changes of its own. The above assumption regarding the cooling will be true only if differential thermal strains within the specimen are minimized by a slow rate of cooling and if hydration is not allowed to take place. It was shown that (1) the thermal effect of temperature on creep can be modeled by an Arrhenius-type rate theory, (2) the structural effect of temperature on creep can be classified as that due to loss in strength and that due to stabilization process, and (3) in the range 300°C to 635°C, the above two processes are opposed to each other (i.e., strength is reduced causing an increase in creep potential, while stabilization, reflected by percentage weight loss, is increased causing a decrease in creep potential).

Like all solid materials, creep of concrete increases with temperature. Below 100°C, concrete creep at moderate stress levels originates in the cement paste, probably because of the mutual approach of adjacent laminar particles of cement gel, which is facilitated by the presence of water in gaps between the particles.[6] Temperature effect on creep, presented in Fig. 50,[33] is caused by acceleration of the diffusion of the solid components and water along gaps between the particles. At moderate temperature levels ($T < 105$°C), hydration (aging) accelerates, but at $T > 100$°C the reverse of this effect takes place (dehydration accelerates creep). Above 100°C, drying of the concrete is very rapid with an associated

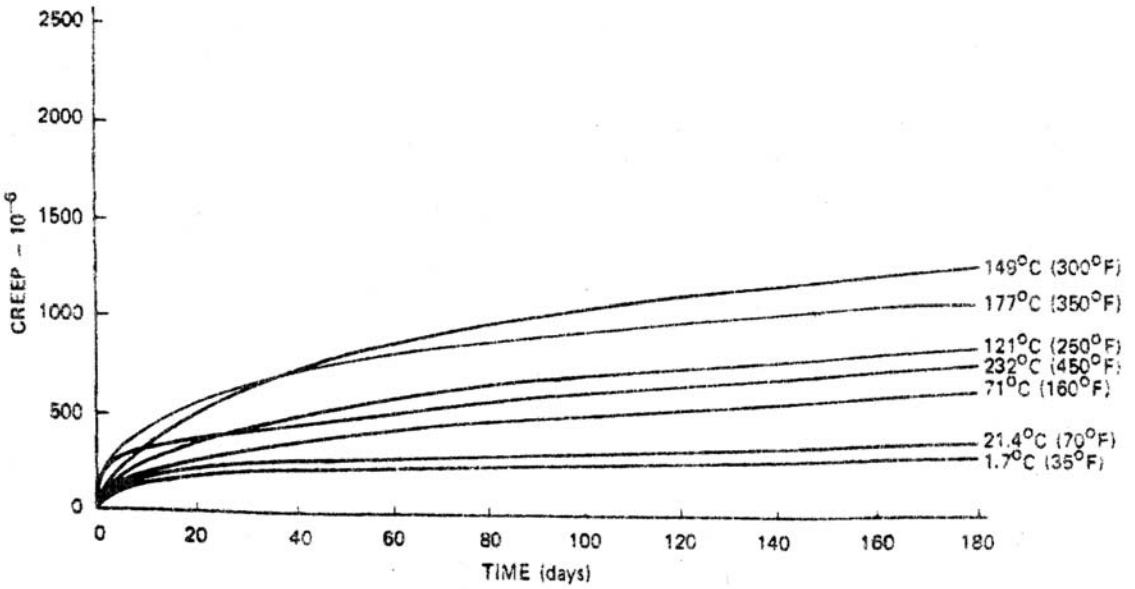

Figure 49 Creep of sealed concrete at various temperatures. *Source*: K. W. Nasser and R. P. Lohtia, "Mass Concrete Properties at High Temperatures," *J. Am. Concr. Inst.* **68**(3), 180–81 (March 1971).

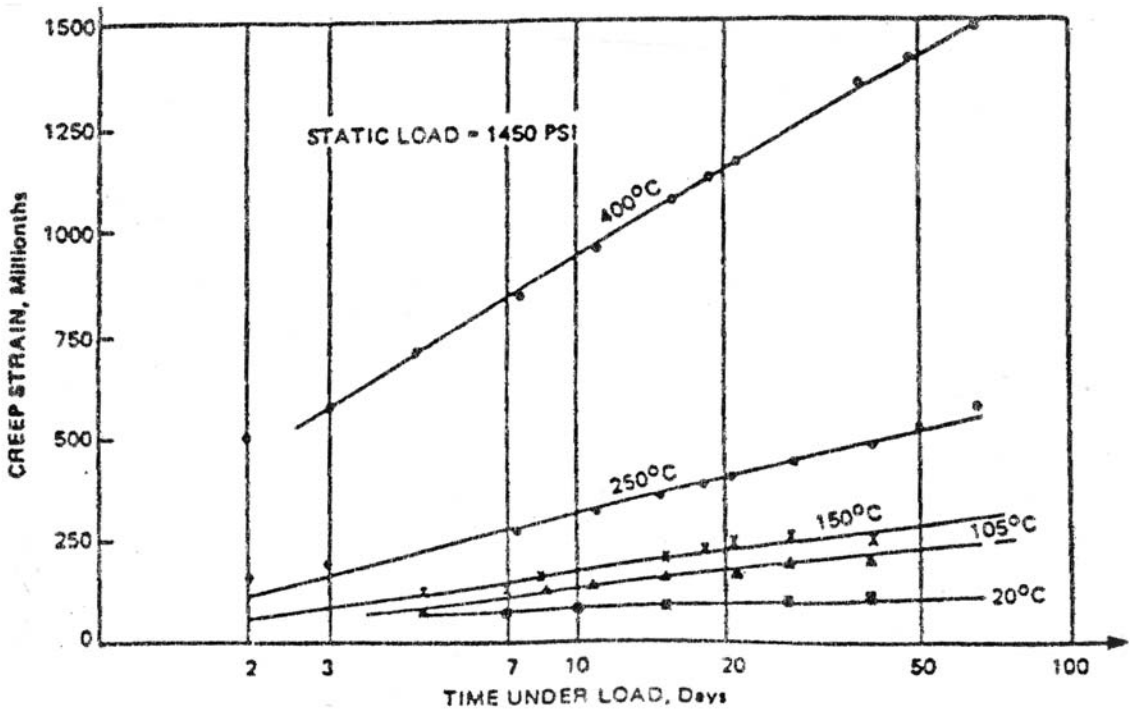

Figure 50 Creep of Portland cement/porphyry concrete at various temperatures. *Source*: A. C. Marechal, "Variations in the Modulus of Elasticity and Poisson's Ratio with Temperature," Paper SP 34-27 in Special Publication SP-34, Vol. I-III, American Concrete Institute, Farmington Hills, Michigan, 1972**.**

increase in the creep rate until a stable moisture condition is reached.[33] In addition to the moisture content and drying effects, the size and shape of the structural member are also important in that they affect the time and rate of moisture loss [i.e., large section members such as walls or a base mat in a nuclear power plant require extended periods of time (days or years) for the moisture to diffuse out of the structure]. Results presented in Ref. 77 indicate that when the magnitudes of creep strains in unsealed concrete are compared with the magnitudes of sealed ones (mass concrete), the creep of sealed concrete is greater with it being 0.7 to 5 times greater than the corresponding values for unsealed concrete above a temperature of 93°C.

Creep data under elevated-temperature conditions using sealed specimens to represent mass concrete are limited because of the difficulty in sealing the specimens to prevent moisture loss. Several steady-state creep tests have been conducted in support of development of prestressed concrete reactor vessels for high-temperature gas-cooled reactor applications. Test temperatures were generally limited to the ASME Code limit of 65°C, although some data are available at higher temperatures (see Fig. 49).

Reference 78 summarizes a 5-year investigation on creep and other properties of concrete for prestressed concrete reactor vessels (PCRVs). The creep tests were made on sealed concrete specimens to simulate the mass concrete. The test parameters included temperatures of 23, 43, and 71°C, nominal stress levels of 30, 45, and 60% of the reference compressive strength, and ages at loading of 28, 90, and 270 d. Additional tests were conducted to determine autogeneous length change and drying shrinkage of the concrete, the effect of testing temperature (23, 43, and 71°C) on compressive strength, and the influence of up to five thermal cycles (23°F to 71°F to 23°F) on compressive strength, splitting-tensile strength,

modulus of elasticity, and Poisson's ratio. All creep specimens were cast in the vertical position with sealing of the specimen against loss of moisture accomplished by means of steel end plates and a wrapping of 1.59-mm-thick butyl rubber around the specimen. All specimens were stored at 23°F prior to testing. In Fig. 51 the total strains obtained for Mix No. 1 are plotted for the 13 test conditions investigated. Making a direct comparison of strain data obtained at different levels of stress requires that values of total strain per unit of applied constant stress be computed. The effect of temperature on total strains of concrete per unit of applied stress was for the strains to increase with an increase in temperature. Concrete tested at higher stress levels achieved higher total strains and thus exhibited the highest strains per unit of applied constant stress. Age at loading had a more significant effect on strains of concretes tested at 23°C than for concretes tested at 43°C or 71°C. For the seven groups of specimens for which creep recovery at 23°C or 71°C was obtained, about 39% of the 90-d creep recovery occurred during the first day and 65% within 10 d after unloading, independent of the previous applied stress level. At 71°C creep recovery of only one group of specimens was observed. This group experienced 31% and 52% of the 90-d creep recovery at 1 and 10 d, respectively, after unloading. In general, the drying shrinkage strains leveled off between 400 and 600 microstrains at all test conditions, with the higher drying shrinkage strains occurring at the higher temperatures where humidities were lowest. Modulus of elasticity of the creep specimens was determined during loading, subsequent unloading, and when testing the creep specimens to failure on completion of the creep phase of the program. The modulus of elasticity of the concretes ranged from 40.7 to 44.8 GPa, with an average Poisson's ratio of 0.22. The splitting-tensile strength was about 9% the compressive strength at all ages of testing. The compressive strength of

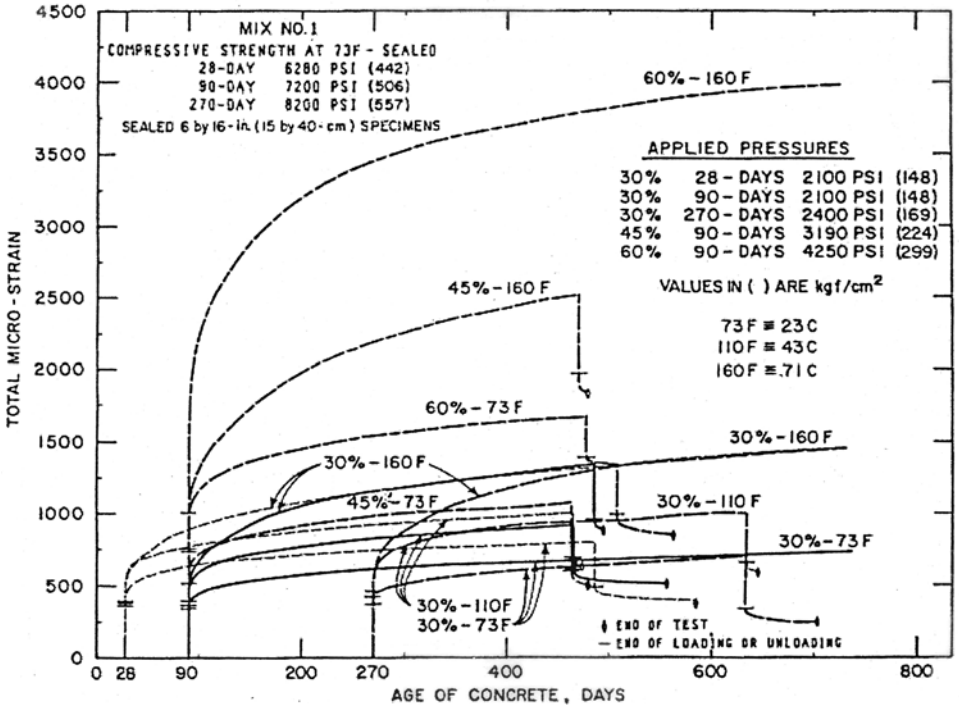

Figure 51 **Total strains for a number of test parameters.** *Source*: J. Komendant et al., "Effects of Temperature, Stress Level, and Age at Loading on Creep of Sealed Concrete," Paper SP 55-3 in *Douglas McHenry International Symposium on Concrete and Concrete Structures*, American Concrete Institute, Farmington Hills, Michigan, 1978.

specimens tested at 43°C was reduced 3 to 11% relative to specimens tested at 23°C. At 71°C, the reductions were about 11, 18, and 21% for concretes tested at 28, 90, and 270 d, respectively. Adiabatic curing resulted in a 12% increase in the 28-d compressive strength and an 8% increase in the 60-d strength in comparison to the strength of specimens cured continuously at 23°C. Thermal cycling results indicate that the compressive strength was reduced about 5% after two thermal cycles and about 2% after completion of five thermal cycles. The modulus of elasticity was reduced about 5% after the first cycle and remained stabilized at this reduced level for the subsequent four cycles. Poisson's ratio was not affected. The thermal cycles also had no significant effect on the splitting-tensile strength of the tested concretes. Long-term exposure to 71°C had a smaller impact on strength loss than short-term exposure to elevated temperature. Additional results for creep of concretes at temperatures to 65°C are available.[79]

The influence of load level and temperature on creep of NSC and high-temperature creep of NSC containing quartz aggregate is presented in Figs. 52[80] and 53,[4] respectively. Results show increased creep with increasing steady-state load and increasing temperature of exposure.

Conclusions from results presented in the literature specific to creep at elevated temperature are that the different types of concretes produced with dense aggregate materials do not have a significant effect on the steady-state creep; however, low-modulus aggregates exhibit increased creep; creep rates at higher temperatures are significantly higher than under ambient conditions; creep increases with increasing load level; sealing as it affects moisture transport is important, particularly for temperatures < 100°C; and curing of specimens at elevated temperature leads to lower creep at elevated temperature compared to specimens cured at room temperature.

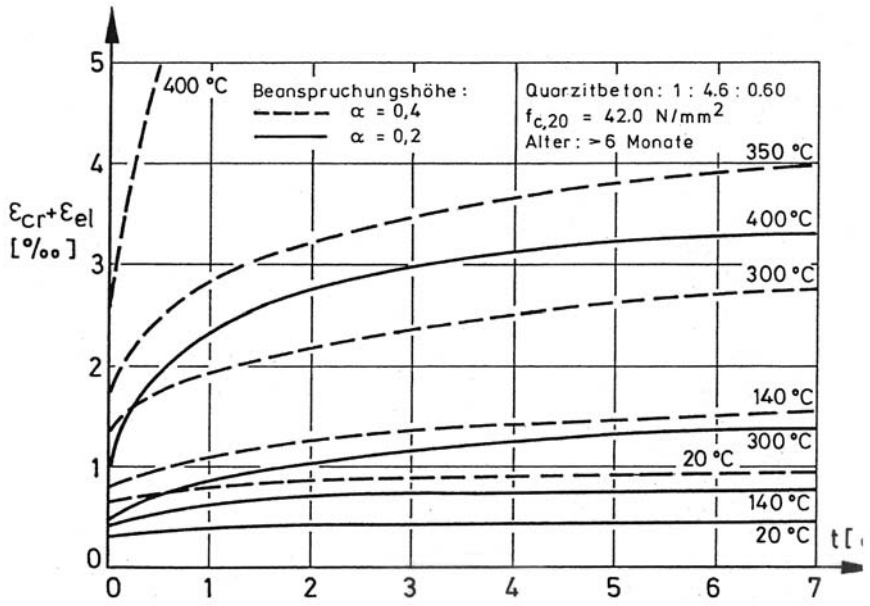

Figure 52 Influence of load level and temperature on the creep of normal concrete.
Source: H. Gross, "On High Temperature Creep of Concrete," Paper H6/5 in *Proc. 2nd International Conference on Structural Mechanics in Reactor Technology*, Elsevier Science Publishers, North-Holland, The Netherlands, 1973.

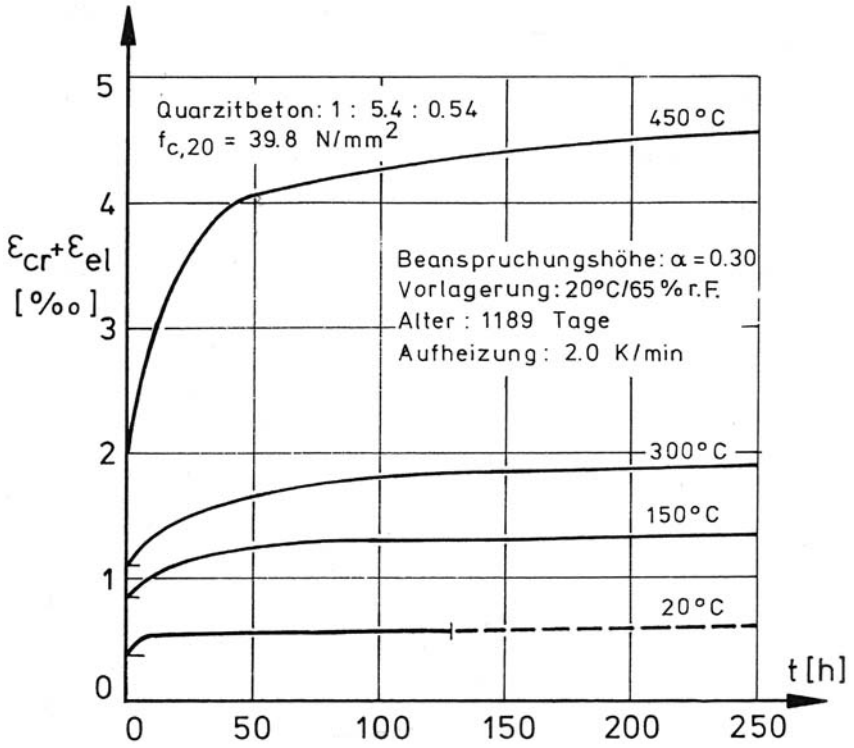

Figure 53 High-temperature creep of ordinary concrete with quartz aggregate.
Source: U. Schneider, "Behaviour of Concrete at High Temperature," HEFT 337, Deutscher Ausschuss für Stahlbeton, Wilhelm Ernst & Sohn, Munich, Germany, 1982.

Concrete–Steel Reinforcement Bond Strength

Bond arises primarily from friction and adhesion between concrete and steel and may be affected by the relative magnitude of concrete shrinkage. It is a function of (1) the concrete properties (cement type, admixtures, water-cement ratio), (2) the mechanical properties of the steel (size and spacing of lugs), and (3) rebar position within the concrete member (bond is greater for vertical bars than for horizontal bars). Permissible bond stresses are generally specified as percentages of concrete's compressive strength. Although considerable research has been conducted investigating the bond between concrete and steel at room temperature, results indicating the effect of elevated-temperature exposure are somewhat limited.

In testing specimens fabricated from river gravel concretes containing embedded plain, round steel bars,[81] it was found that the residual bond stress after subjecting the specimens to 300°C for 90 d and then cooling to room temperature was only about 50% the reference value before heating. Figure 54 indicates the importance of reinforcement type.[82] This figure shows that ribbed bars experienced a loss of bond strength only above 400°C, but the smooth bars lost strength after only a small temperature increase. A comparison of the effects of elevated temperature on ribbed and plain round bars for different concrete strengths is presented in Fig. 55.[83] The effect of bar diameter on bond strength after elevated temperature for ribbed and plain round bars is presented in Fig. 56.[84] Bond-stress-slip results as a function of temperature are presented in Fig. 57 for cold deformed steel and prestressing steel reinforcement.[85] Figure 58 presents a comparison of bond strengths of cold-deformed steel, heavily rusted plain round bars, plain round bars, and shaped prestressing strand.[85] The effect of elevated-temperature exposure time

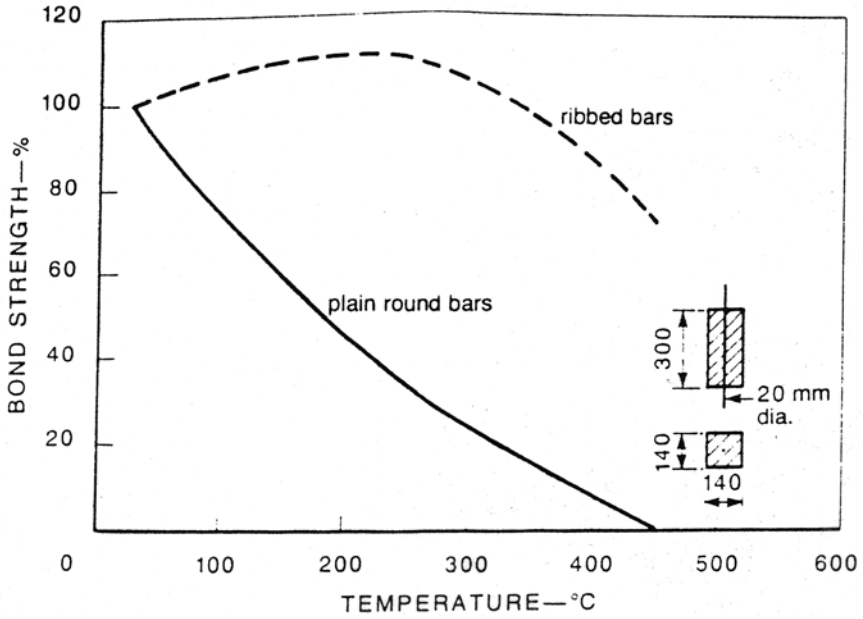

Figure 54 Bond strength of ribbed and plain round bars. *Source*: A. F. Milovanov and G. D. Salmanov, "The Influence of High Temperature Upon the Properties of Reinforcing Steels and Upon Bond Strength Between Reinforcement and Concrete," *Issledovanija po zharoupornym betonu I zhelezobetonu,* pp. 203–223, 1954.

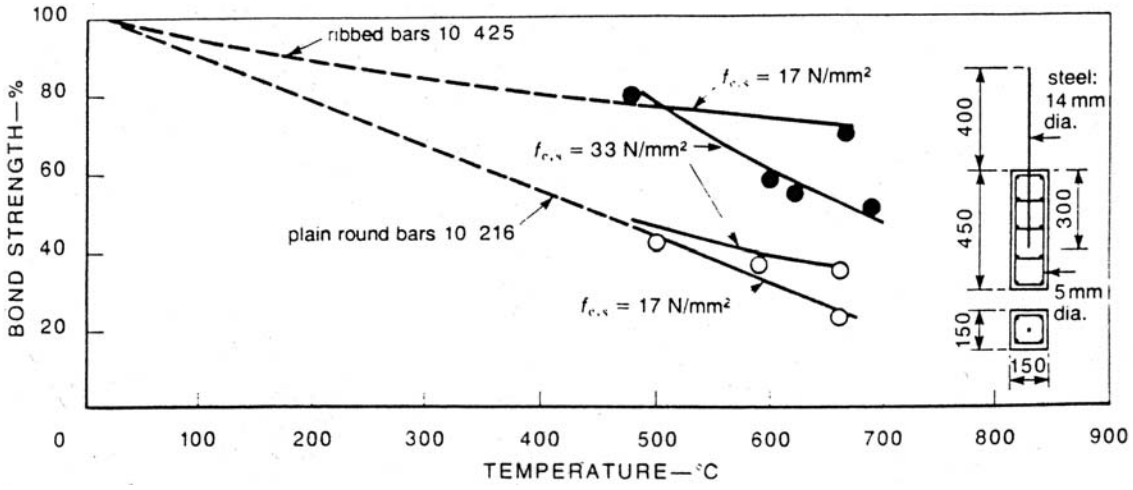

Figure 55 Bond strength of ribbed and plain round bars for different concrete compressive strengths. *Source*: H. V. Reichel, "How Fire Affects Steel-to-Concrete Bond," *Building Research and Practice* **6**(3), 176–186 (May/June 1978).

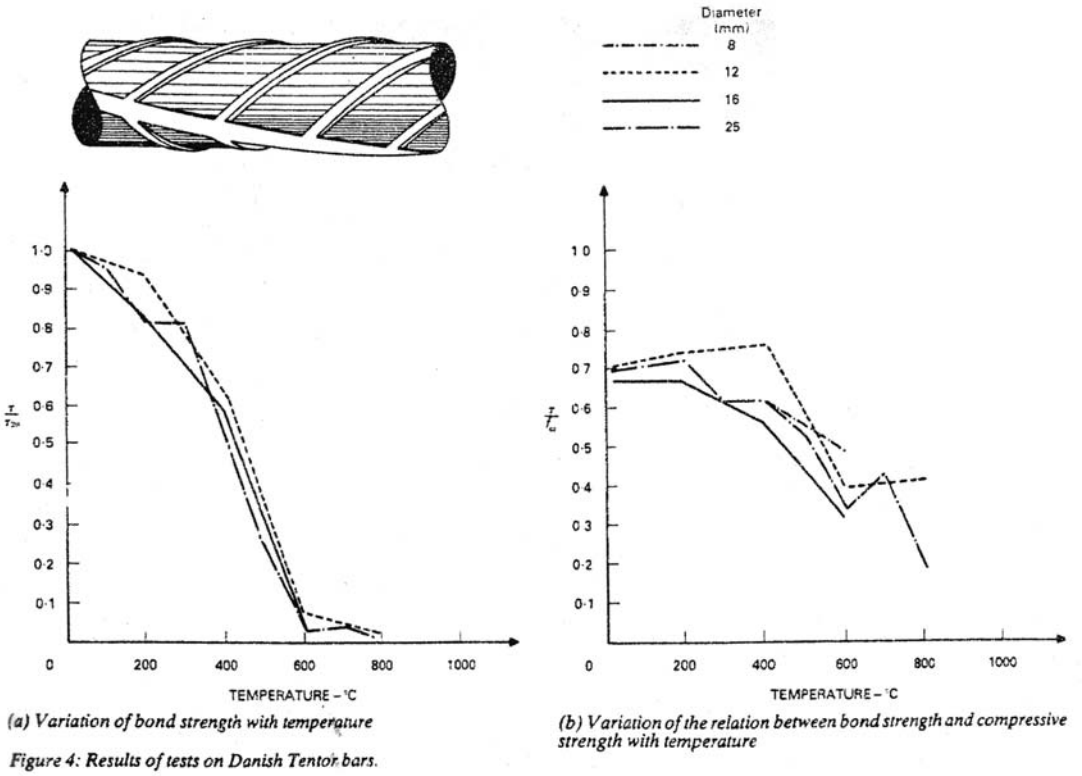

(a) Variation of bond strength with temperature

(b) Variation of the relation between bond strength and compressive strength with temperature

Figure 4: Results of tests on Danish Tentor bars.

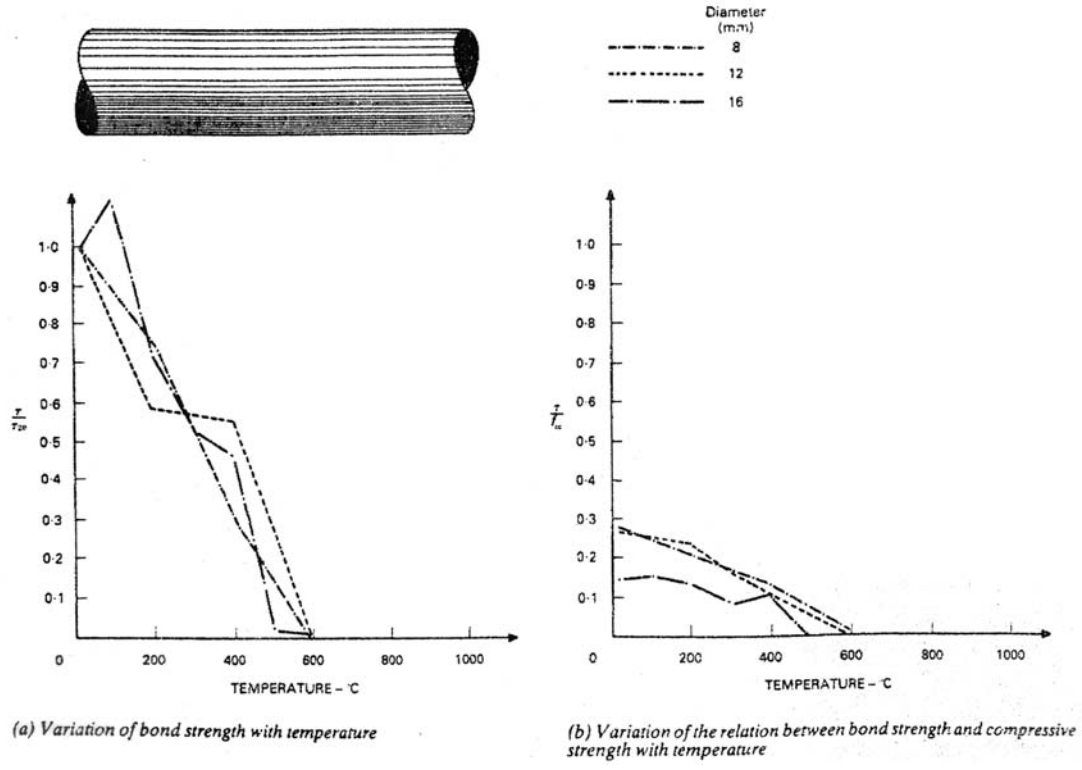

(a) Variation of bond strength with temperature

(b) Variation of the relation between bond strength and compressive strength with temperature

Figure 56 Effect of bar diameter on bond strength after elevated-temperature exposure for ribbed and plain round bars. *Source*: K. Hertz, "The Anchorage Capacity of Reinforcing Bars at Normal and High Temperatures," *Magazine of Concrete Research* **34**(121), 213–220 (December 1982).

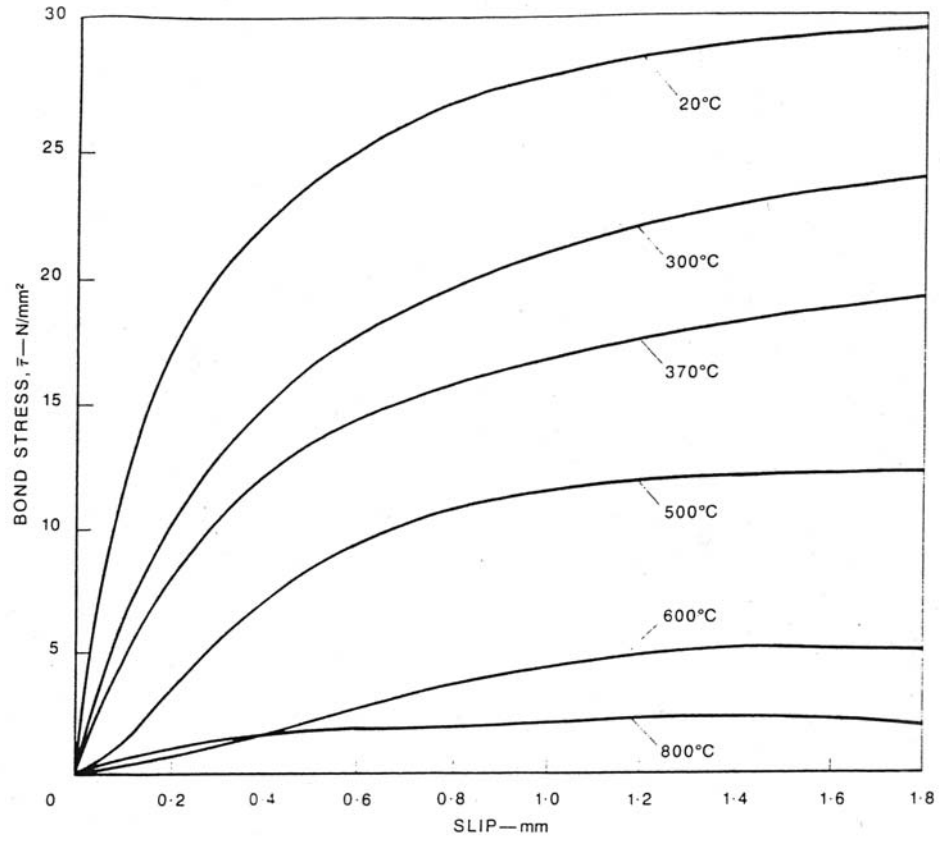

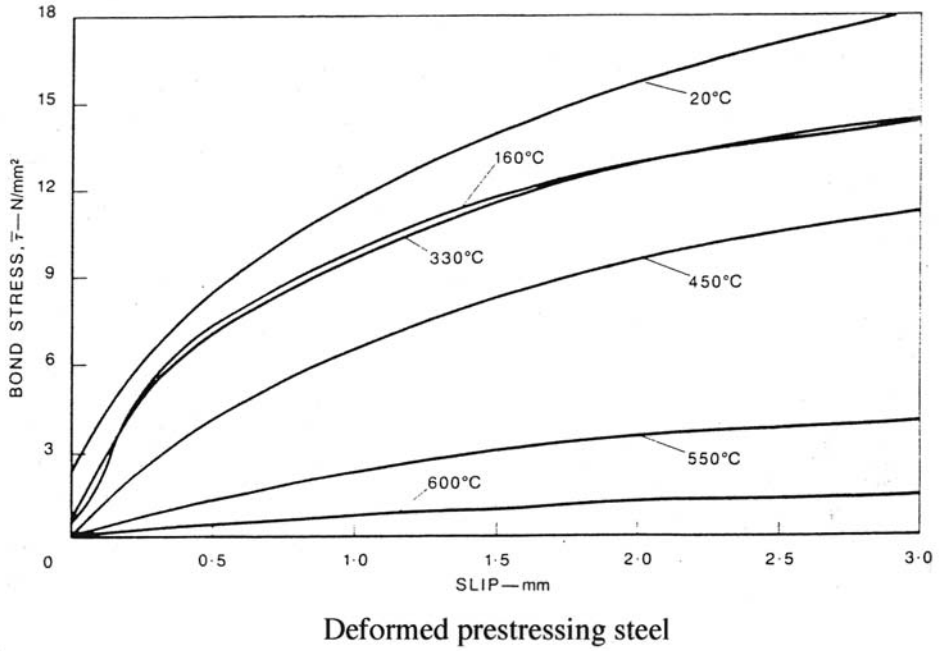

Figure 57 Bond-slip relationship at elevated temperature for cold deformed steel and deformed prestressing steel. *Source*: U. Diederichs and U. Schneider, "Bond Strength at High Temperature," *Magazine of Concrete Research* **33**(115), 75–83 (June 1981).

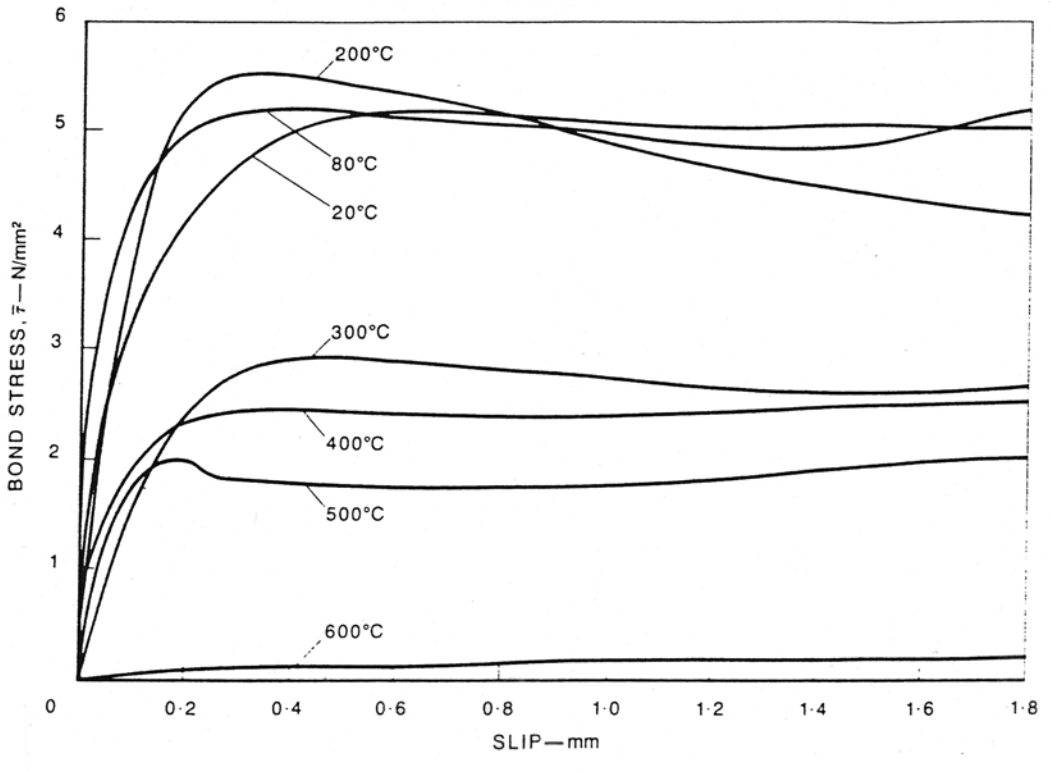

Rusted plain round mild-steel bars.

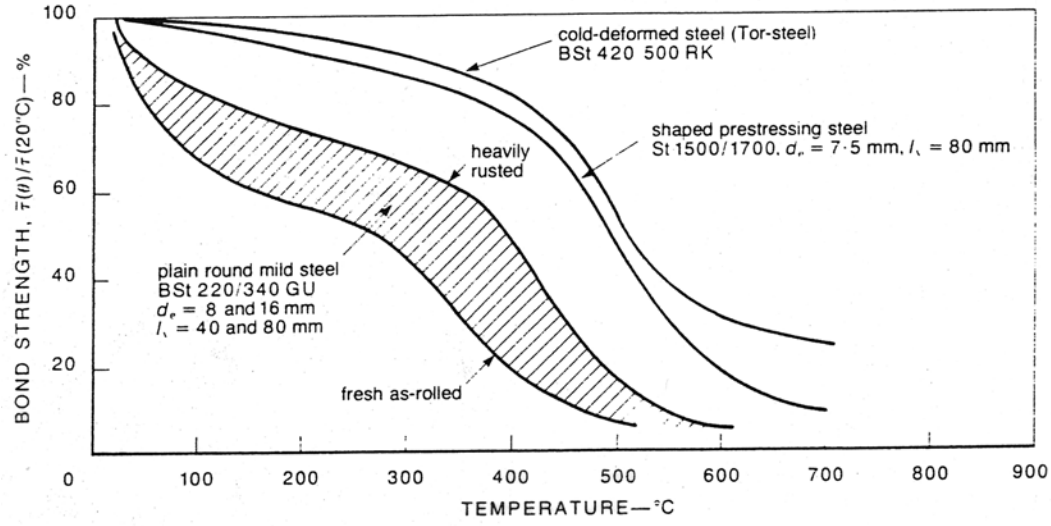

Relative bond strength of various reinforcing bars

Figure 58 Relative bond strength as a function of temperature. *Source*: U. Diederichs and U. Schneider, "Bond Strength at High Temperature," *Magazine of Concrete Research* **33**(115), 75–83 (June 1981).

(0.5 to 3 h) on the residual bond strength of No. 3 bars embedded in a concrete cube is presented in Fig. 59.[86] A substantial decrease in bond strength was observed at temperatures greater than 200°C, and the bond strength decreased with increasing exposure time. The influence of type aggregate on the bond strength is presented in Fig. 60.[87] The effect of curing conditions (e.g., in water unsealed, sealed, in air

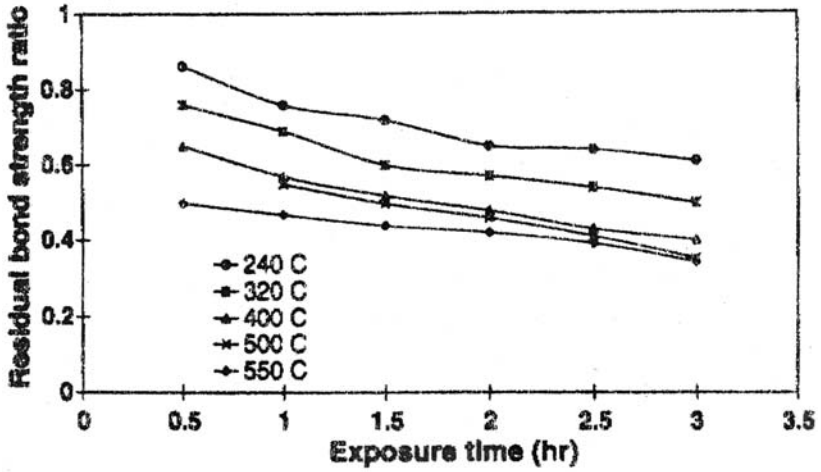

Figure 59 The effect of elevated-temperature exposure time on the residual bond strength of No. 3 bars embedded in a concrete cube. *Source*: C-H. Chiang and C-L. Tsai, "Time-Temperature Analysis of Bond Strength of a Rebar After Fire Exposure," *Cement and Concrete Research* **33**, 1651–1654 (2003).

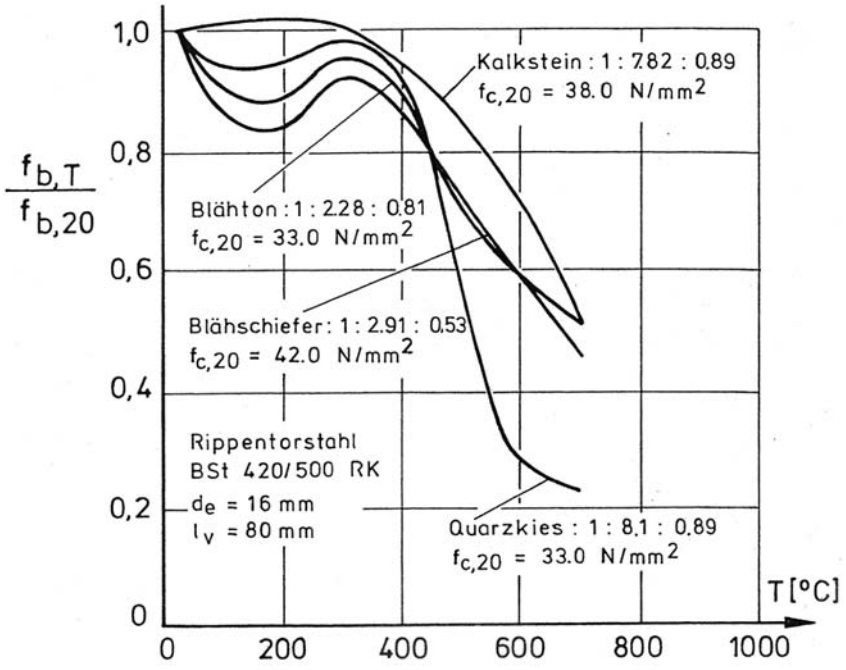

Figure 60 Bond between concrete and deformed bars exposed to high temperature. *Source*: H. Sager et al., "High Temperature Behavior of Reinforcing and Prestressing Steels," *Sonderforschungs-Bereich* **148**, Part II, pp. 51–53, Technical Universitat Braunschweig, Germany, 1980.

unsealed) prior to elevated-temperature exposure on the relative variation in bond strength at start of pull-out for a hard sandstone aggregate concrete after various heating periods at 175°C is presented in Fig. 61.[36] The bond strength for specimens unsealed during heating exhibited up to about a 30% decline for heating exposures of 3 d or less, but specimens that were sealed exhibited practically no reduction as a result of temperature exposure. Prolonged elevated-temperature exposure for sealed specimens exhibited a positive effect on the bond strength, and for the unsealed specimens a recovery in bond strength to the point that at 91-d exposure it was reduced by 10 to 15% relative to control results. Other results[85,88] indicate that the loss in bond strength between concrete and steel reinforcement at temperatures < 65°C is small (≤15%).

Conclusions from results presented in the literature specific to concrete-reinforcing steel bond at elevated temperature are that ribbed bars exhibit improved performance relative to plain round bars, surface roughness increases the performance for plain round bars, the bond strength decreases as the exposure temperature increases, at high temperatures (≥200°C) the time at temperature affects the bond strength, the diameter of ribbed steel reinforcement (8 to 25 mm) does not have a significant effect on bond strength, residual bond strengths of specimens sealed during temperature exposure perform better than unsealed specimens (≤175°C), curing conditions are important at moderate elevated-temperature exposures (≤400°C), a clear influence of the water/cement ratio and concrete strength on bond strength at elevated-temperature exposure has not been observed, the type of aggregate has a significant effect on the high-temperature bond strength, and at temperatures < 65°C the bond strength is relatively unaffected.

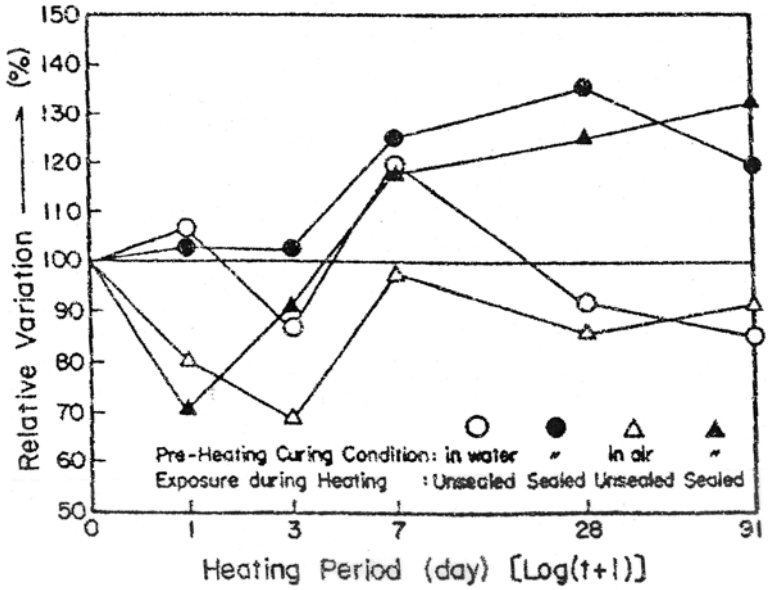

Figure 61 Relative variation in bond strength at start of pull-out for a hard sandstone aggregate concrete after various heating periods at 175°C.
Source: K. Hirano et al., "Physical Properties of Concrete Subjected to High Temperature for MONJU," Paper P2-25, Power Reactor and Nuclear Fuel Development Corporation, Tokyo, Japan.

Long-Term Exposure (Aging)

During the nominal 40-year design life of nuclear power plants, certain concrete components may be subjected to moderately elevated temperatures that could affect the concrete's mechanical properties. In conducting safety evaluations for these components, the significance of concrete component aging needs

be taken into account. Unfortunately, only a limited number of data have been identified related to the effects of long-term elevated-temperature exposure on concrete properties. Surprisingly, although Portland cement concretes have been in existence for more than 160 years, relatively little documented information is available on the aging of concrete structures that are not being acted upon by environmental stressors.[89] When concrete is fabricated with close attention to the factors related to the production of good concrete (e.g., material selection, production control, desirable properties, and costs), the concrete will have infinite durability unless subjected to extreme external influences (e.g., overload, elevated temperature, industrial liquids and gases).[31]

An investigation has been conducted to determine the changes in mechanical properties of a limestone aggregate concrete after exposure to temperatures of 75°C and 300°C for periods up to 8 months and 600°C for 1 month.[90] For thermal exposure to 75°C, compressive and splitting-tensile strengths after 8 month's exposure were 98 and 94%, respectively, of their reference values. However, on exposure to 600°C for just 1 month, compressive and splitting-tensile strengths were only 23 and 38%, respectively, of their reference values. In companion mixes where either fly ash or blast furnace slag was used, improvement in retention of mechanical properties occurred after exposure to sustained high temperatures as a result of partial replacement of the cement.

The effect of long-term exposure (up to 13 years) at moderate elevated temperature (65°C) on the mechanical properties of a limestone aggregate concrete was investigated.[91] These tests were somewhat unusual because the specimens were first subjected to a simulated temperature-vs-time cement hydration cycle. Also, because the concrete mix was being evaluated for an application that experienced exposure to sulfate-bearing groundwater at elevated temperatures (~65°C), both ordinary and sulfate-resistant Portland cements were investigated. Specimens, after being subjected to the simulated cement hydration cycle, were stored either in water at 19°C (control specimens) or in a sodium sulfate solution of 2000 ppm at 65°C. Frequently during the test program, the sodium sulfate solution was changed, which required cooling to room temperature; the specimens were therefore also subjected to thermal cycling. Results of the study indicated that there was no evidence of long-term degradation in compressive strength for any of the concrete mixes and heat treatments utilized, and that for a given compressive strength the dynamic modulus of elasticity was lower for the concrete that had been heated. Cooling down and reheating the limestone and flint aggregate mixes for a total of 87 cycles did not appear to cause a degradation in strength.

A 5-year testing program was conducted to determine the effects of long-term exposure to elevated temperature on the mechanical properties of concrete used in constructing the radioactive underground storage tanks at Hanford Engineering Development Laboratory (HEDL).[92] Tests were conducted using specimens fabricated from the same mix proportions and materials specified for the concrete used to fabricate the tanks (20.7- and 31.0-MPa design compressive strengths). Concrete strength, modulus of elasticity, and Poisson's ratio values were determined from specimens subjected to either 121, 177, or 232°C for periods of up to 33 months. The effect of thermal cycling was also investigated. Results showed that the compressive strengths in general tended to decrease with increasing temperature and also with length of exposure; however, with the exception of the cylinders exposed to 232°C, all compressive strength results obtained after a 900-d exposure exceeded the design values noted previously. Splitting-tensile strength results also decreased somewhat with increasing temperature and length of exposure. Modulus of elasticity was affected most significantly by the elevated-temperature exposure; after 920 d of heating at 232°C, it had a value of only 30% the value obtained from an unheated control specimen. Poisson's ratio, although exhibiting somewhat erratic values, was relatively unaffected by either the magnitude or the length of elevated-temperature exposure. Thermal cycling (~18 cycles) to 177°C produced moderate reductions in compressive strength (5 to 20%), significant reductions in modulus

(30 to 50%), and slight reductions in Poisson's ratio (0 to 20%). Time-dependent (creep) and physical property data were also obtained from specimens cast from the concrete mixes.

Associated with the laboratory investigation described in the previous paragraph was a study to confirm the laboratory results by testing samples removed from the underground storage tanks and process buildings at HEDL.[93] Cores 76-mm in diameter were obtained over the length of the haunch wall, and footing of a single-shell tank that was built in 1953; contained waste for about 8 years; reached temperatures in the range of 127°C to 138°C; and experienced a radiation field of 0.10 to 0.13°C/kg/h (400 to 500 R/h). Although considerable scatter was obtained from the data because of different concrete pours and different environmental exposure, after about 29 years of exposure only one data point fell below the 20.7-MPa design compressive strength. Figure 62 presents compressive strength results from cores obtained from structures at HEDL and compares them to values based on the laboratory results.

A study has been carried out to examine the effect of temperature on sealed and unsealed air-entrained concrete containing fly ash, conventional water reducer, and superplasticizer.[94] The properties of compressive strength and modulus of elasticity were studied at seven different temperatures ranging from –11°C to 232°C and at seven different exposure periods from 1 to 180 d. Local crushed aggregates of 19-mm maximum size consisting primarily of dolomite and hornblend were used in the concrete

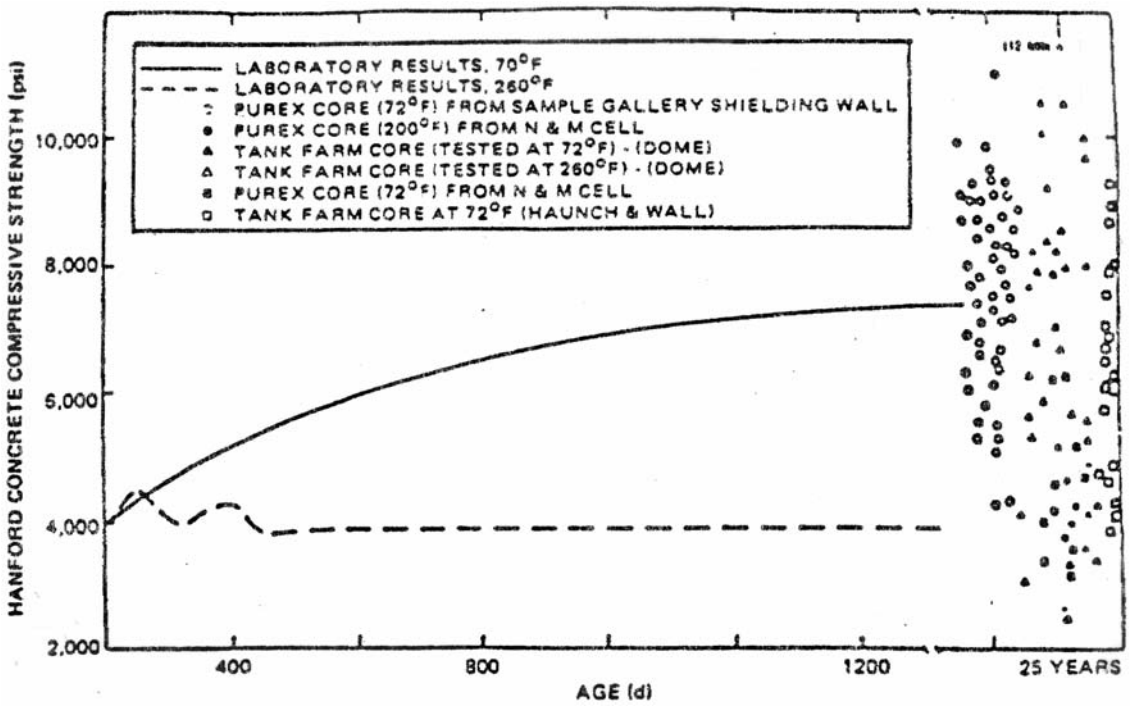

Figure 62 Comparison of laboratory and actual sample long-term compressive strength data.
Source: M. P. Gillen et al., "Strength and Elastic Properties of Concrete Exposed to Long-Term Moderate Temperatures with High Radiation Fields," RHO-RE-SA-55 P, Rockwell Hanford Operations, Richland, Washington, 1984.

mixtures. Figure 63 presents the relationship of strength ratio (ratio of compressive strength at temperature to that obtained from unheated control specimens) and exposure time for the temperatures investigated that was obtained from sealed specimens. The corresponding relationship of the elasticity ratio (ratio of modulus of elasticity at temperature to that obtained from unheated control specimens) and exposure time obtained from sealed specimens is presented in Fig. 64. The results indicate that up to a temperature of 121°C there was no degradation in compressive strength for exposures up to 180 d. With increasing temperature, the strength decreased with the extent of strength reduction generally proportional to the exposure temperature and time at temperature (e.g., at 232°C and 180-d exposure the strength was about 50% its reference value). The modulus of elasticity started to decline monotonically at temperatures ≥ 71°C with the decline in modulus proportional to the exposure temperature and time at temperature (e.g., at 232°C and 180-d exposure the modulus was about 25% its reference value). Strength and elasticity ratios for unsealed specimens are presented in Fig. 65 and indicate improved performance relative to the sealed specimens. An explanation of the greater effect of elevated-temperature exposure on sealed (mass concrete) specimens was that in a closed system saturated steam pressure develops at high temperatures, which causes deterioration in structural properties of the cement gel.

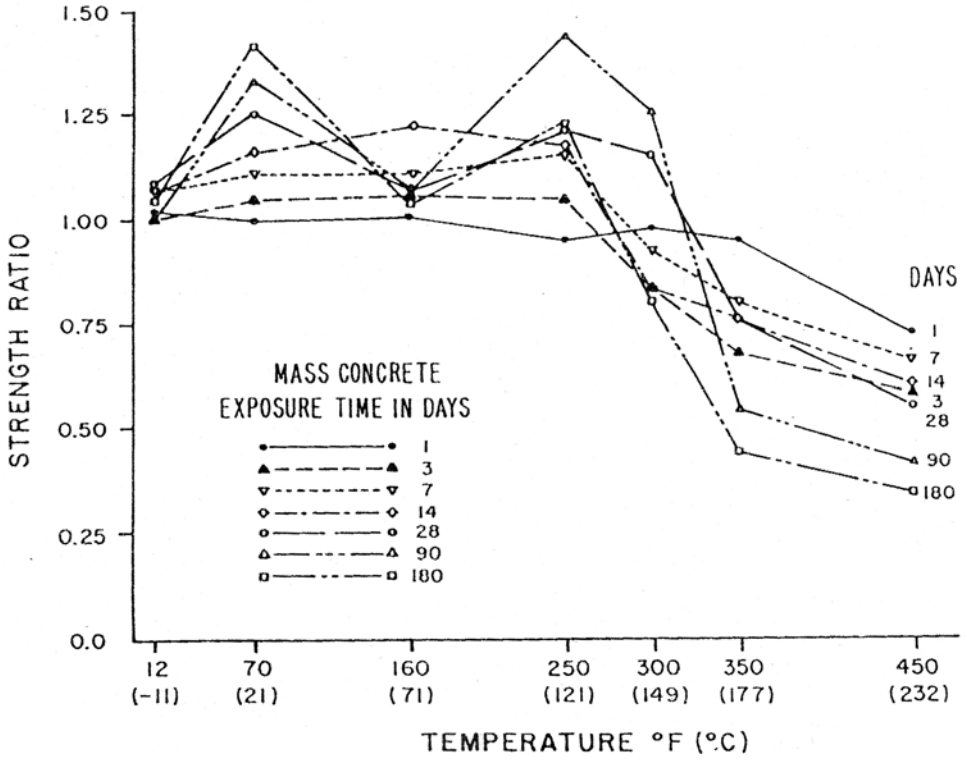

Figure 63 Relationship of strength ratio and temperature of mass concrete (sealed).
Source: K. W. Nasser and M. Chakraborty, "Temperature Effects on Strength and Elasticity of Concrete Containing Admixtures," *Proceedings of Symposium Temperature Effects on Concrete*, ASTM Special Technical Publication 858, American Society for Testing and Materials, West Conshohocken, Pennsylvania, 1985.

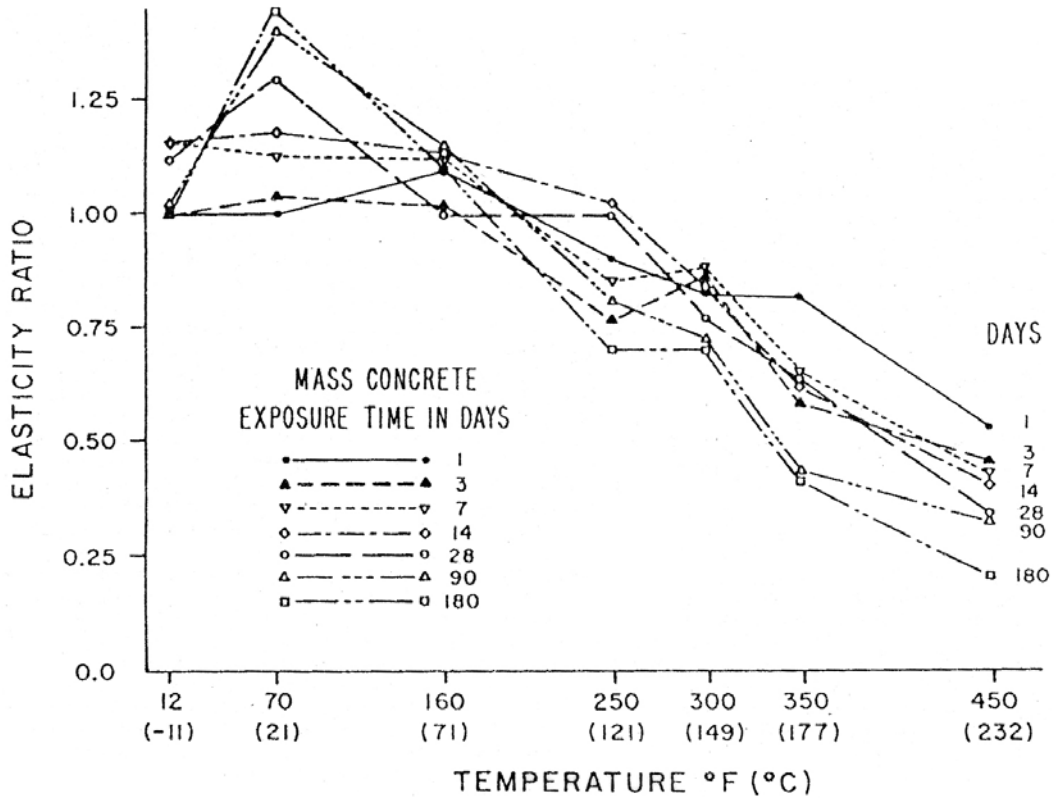

Figure 64 **Relationship of elasticity ratio and temperature of mass concrete (sealed).** *Source*: K. W. Nasser and M. Chakraborty, "Temperature Effects on Strength and Elasticity of Concrete Containing Admixtures," *Proceedings of Symposium Temperature Effects on Concrete*, ASTM Special Technical Publication 858, American Society for Testing and Materials, West Conshohocken, Pennsylvania, 1985.

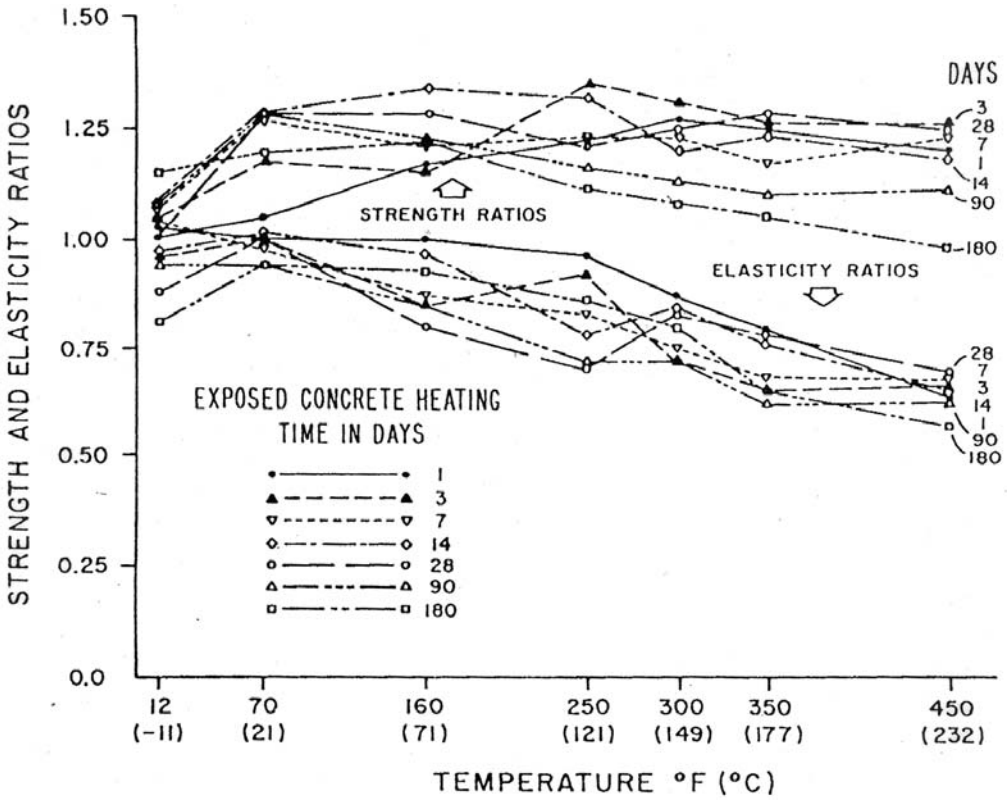

Figure 65 **Relationship of strength and elasticity and temperature of unsealed concrete.** *Source*: K. W. Nasser and M. Chakraborty, "Temperature Effects on Strength and Elasticity of Concrete Containing Admixtures," *Proceedings of Symposium Temperature Effects on Concrete*, ASTM Special Technical Publication 858, American Society for Testing and Materials, West Conshohocken, Pennsylvania, 1985.

A laboratory study has been conducted to evaluate the relative performance of limestone and dolostone aggregate ordinary Portland cement concretes under sustained exposure to high temperature.[95] After 28-d moist cure followed by 26 weeks of room temperature curing, the test specimens were exposed for up to 4 months to temperatures ranging from 76°C to 450°C, and 1 month for a 600°C exposure. Figure 66 presents residual compressive strength versus conditioning temperature (up to 450°C) after 4 months exposure for the limestone concrete.* The loss of compressive strength of specimens exposed to elevated temperature was proportional to the exposure temperature. At temperatures of 150°C and higher, an increase in length of exposure from 48 h to 4 months resulted in further decreases in strength. In all cases, any major loss in strength was found to occur within the first month of exposure. In general the leaner concretes (water/cement ratio = 0.6) were slightly less affected than the richer concretes in terms of relative strength loss after exposure.

The effect of elevated-temperature exposures either at 65°C, 90°C, or 110°C for periods up to 3.5 years was investigated in Japan in support of nuclear power plant facilities.[96] Either basalt or sandstone coarse aggregates were utilized in the concrete mixtures. Cementitious materials studied included Class B fly

*The dolostone aggregate results are not discussed because pyrite was contained in some of the aggregate particles, and it underwent slow oxidation that produced a disintegrating expansion of the aggregate and cracking of the concrete.

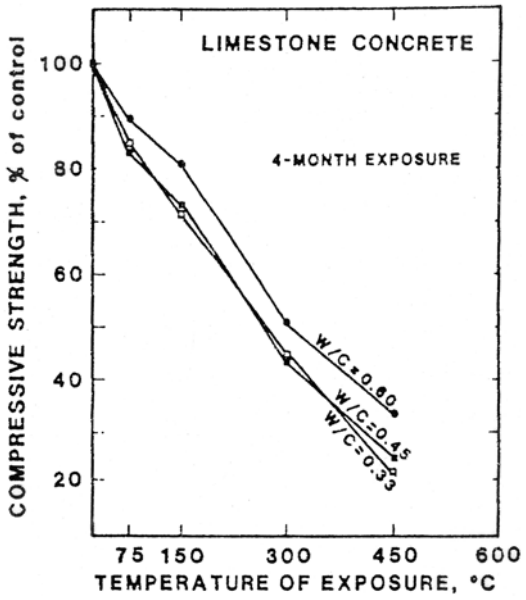

Figure 66 Compressive strength of limestone concrete after 4-month exposure to various temperatures (up to 450°C). *Source*: G. G. Carrette and V. M. Malhotra, "Performance of Dolostone and Limestone Concretes at Sustained High Temperatures," *Proceedings of Symposium Temperature Effects on Concrete,* ASTM Special Technical Publication 858, pp. 38–67, American Society for Testing and Materials, West Conshohocken, Pennsylvania, 1985.

ash, moderate heat cement plus fly ash, and normal Portland cement. Heating conditions adopted were (1) long-term heating tests [allowable temperature except for local areas (long-term) (65°C), allowable local temperature (long-term) (90°C), temperature at which water is considered to evaporate rapidly (110°C)], (2) short-term heating tests [allowable temperature (short-term) (175°C)], and (3) thermal cycling tests for up to 120 cycles [cycled heating temperatures (20°C to 110°C to 20°C) to simulate temperature variations during operation periods]. Three cylindrical specimens were prepared for each test condition and put under either sealed conditions, where evaporation of water was prevented, or unsealed conditions, where evaporation was allowed. From the results of heating tests, the following conclusions were obtained:

1. Under long-term heating at 65°C, 90°C, and 110°C, compressive strength after heating was greater than before heating, under both sealed and unsealed conditions. This was especially true under sealed conditions at 110°C in which the compressive strength increased for 1.5 years reaching approximately 200% that of unheated control specimens. These results are considered to be caused by the effect of autoclave curing. Under unsealed conditions, it is considered that microcracking in concrete, which was caused by moisture migration and evaporation under high temperatures, caused a degradation of compressive strength. However, the acceleration of hydration at high temperatures in any nonhydrated sections of the concrete increased the compressive strength more than degradation caused by microcracking. The results after 3.5 years were relatively unchanged from that measured after 1 year. Therefore, it was found that the compressive strength ceased to fluctuate at an early stage.

2. Under sealed conditions during heating, the increase in the elastic modulus due to heating had a tendency to increase slightly, though not as much as the compressive strength. The elastic modulus under sealed conditions remained relatively unchanged under heating, even after 3.5 years. Under unsealed conditions during heating, the modulus at temperature relative to that obtained from unheated control specimens was reduced about 50%. The reduction of the elastic modulus under unsealed conditions can be explained by the closing of microcracks at an early stage of stress. Thus, the elastic modulus of concrete heated to high temperatures, with moisture migration and evaporation present, was markedly reduced. In addition, it was found that the elastic modulus became stabilized at an early stage, not changing much from 91 d through 3.5 years, even under heating.
3. During the thermal-cycle heating test, compressive strength after heating was greater than before heating under both sealed and unsealed conditions. However, the ratio of increase was smaller than under constant heating, suggesting the influence of thermal-cycle heating. For the same number of thermal cycles, the compressive strength was consistently higher for the sealed specimens relative to that obtained from unsealed specimens. Under unsealed conditions, specimens exhibited little influence of number of cycles on compressive strength for thermal cycles numbers greater than five (i.e., little change in compressive strength value for cycles greater than five). Under unsealed conditions the modulus of elasticity exhibited a similar trend to that obtained for constant heating in that it was reduced by about 50%. A major part of the reduction occurred in the early stages of the thermal-cycle heating. Under sealed conditions during thermal cycling, the elastic modulus showed a tendency similar to that of the compressive strength, but the modulus of elasticity did not increase as much as the compressive strength of the sealed specimens.
4. The greater the weight reduction became, the greater the decrease in the elastic modulus tended to be, which indicated that moisture migration and evaporation during heating affected the reduction of elastic modulus. Therefore, to estimate the properties of massive concrete structures subjected to high temperatures accurately, it is necessary to study moisture migration in mass concrete members that are subjected to high temperatures over long periods of time.

Figure 67 presents the residual compressive strength and modulus of elasticity results, and Fig. 68 the effect of thermal cycling for the sealed and unsealed concretes.

A series of studies was conducted to evaluate the drying effect of elevated-temperature exposure on the properties of concrete.[81] Specimens made from four concrete mixes of ordinary Portland cement and river-gravel aggregate were tested to investigate the compressive, tensile, and bond strengths, moduli of elasticity, and weight loss after 90-d exposure to temperatures of 20, 35, 50, 65, 80, 110, 200, and 300°C. Moisture in specimens was allowed to evaporate freely. Residual strength tests of unheated and heated concretes were conducted at room temperature on both dried and wet specimens presoaked in water for 2 d. Exposure to sustained elevated temperature higher than 35°C showed remarkable deteriorating effects on the physical properties of concrete when moisture in concrete was allowed to evaporate. Greater reductions of strengths and weights after exposure were associated with mixes having higher mix water contents. Strengths did not decline linearly as the temperature rose and were minimal at around 50°C. Dry compressive strengths of heated concretes indicated approximately 10% loss when heated at 50°C with practically no change when heated at higher temperatures up to 110°C, 20% loss at 200°C, and 30% loss at 300°C. Wet compressive strengths of heated concretes indicated larger losses than dry strengths, and more than 20% loss when heated at only 35°C. Reductions in tensile and bond strengths and modulus of elasticity of heated concretes were greater than obtained in compressive strengths. Tensile strength tests indicated approximately 30% loss upon exposure to temperatures of 50°C to 65°C, and less strength loss at higher temperatures. Bond strengths showed approximately 15% loss when heated at only 35°C, and smaller loss for higher temperatures of 50°C to 80°C, 25% loss at 110°C and more than 50% loss at 300°C. Moduli of elasticity of heated concretes indicated a tendency to decline linearly with rising

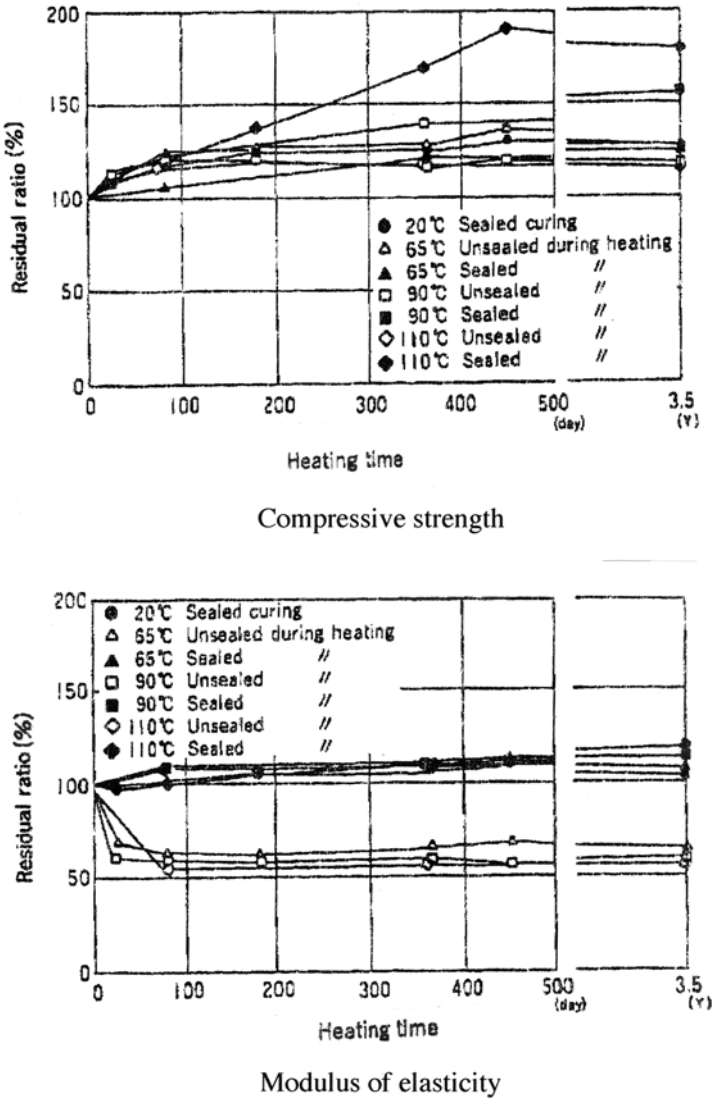

Figure 67 Long-term (3.5-year) heating effect on compressive strength and modulus. *Source*: T. Suzuki et al., "Study on the Degradation of Concrete Characteristics in the High Temperature Environment," *Concrete Under Severe Conditions: Environment and Loading*, Vol. 2, pp. 1119–1128, E & FN Spon Publishers, 1995.

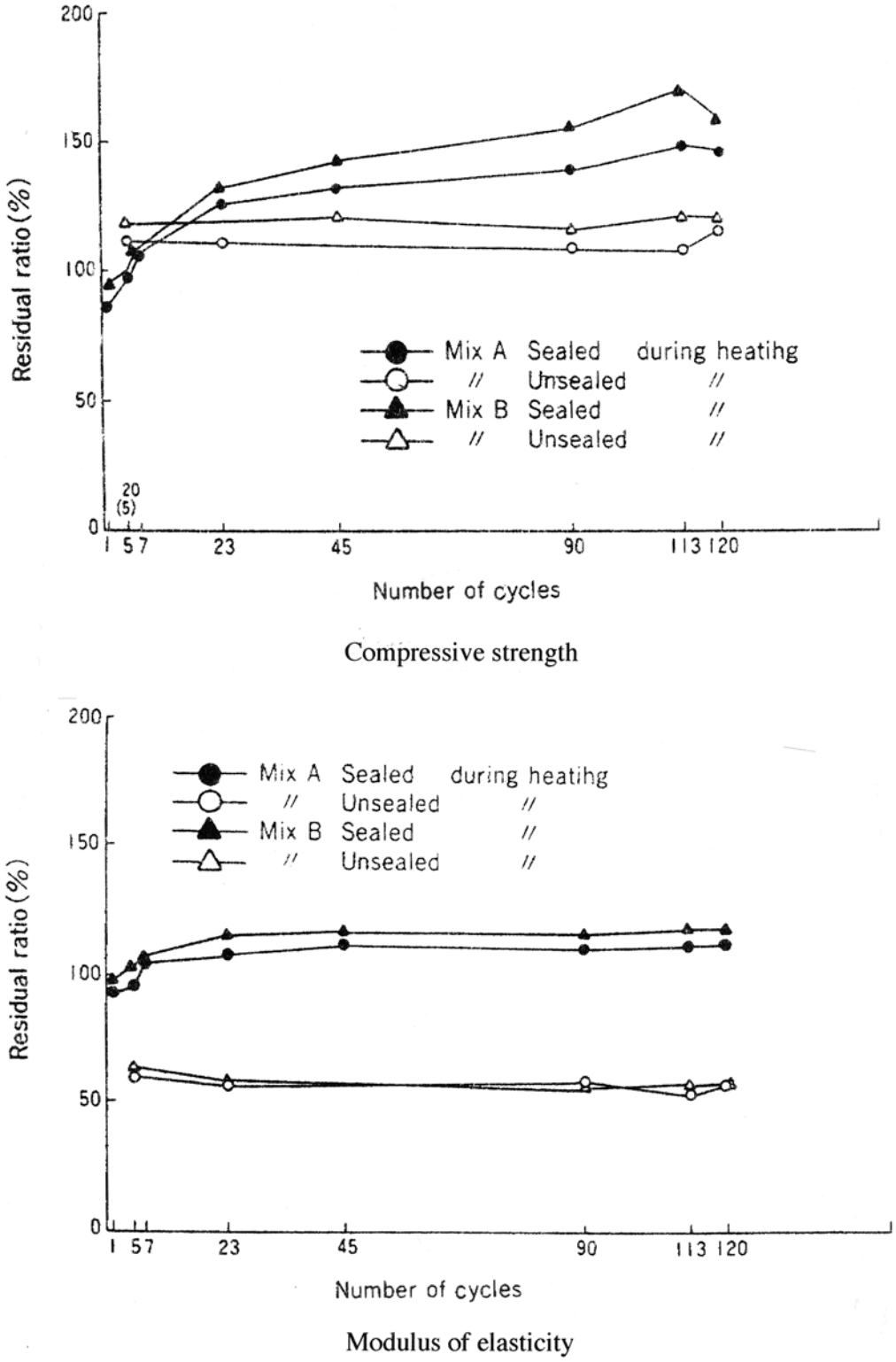

Figure 68 Effect of thermal cycling on compressive strength and modulus. *Source*: T. Suzuki et al., "Study on the Degradation of Concrete Characteristics in the High Temperature Environment," *Concrete Under Severe Conditions: Environment and Loading*, Vol. 2, pp. 1119–1128, E & FN Spon Publishers, 1995.

temperature, experiencing a 15% loss at 50°C, 25% loss at 110°C, and 50% loss at 300°C. The unusual deterioration at around 50°C in compressive, tensile, flexural and shear strengths was also indicated in subsequent investigations regardless of the kind of aggregates. However, the influence of aggregate on the properties of heated concrete was significant. Sandstone and basalt aggregate concretes indicated smaller reductions, while limestone, andesite, and serpentine aggregate concretes showed greater reductions in strengths after exposure. Changes in chemical composition in the cement paste were not noticeable under 100°C. However, the porosity was found to be affected by the exposure temperature. The unusual deterioration in strengths at around 50°C can be due to either the expansion of cement paste or to the change in porosity caused by evaporation of free water. Figure 69 presents the effect of exposure

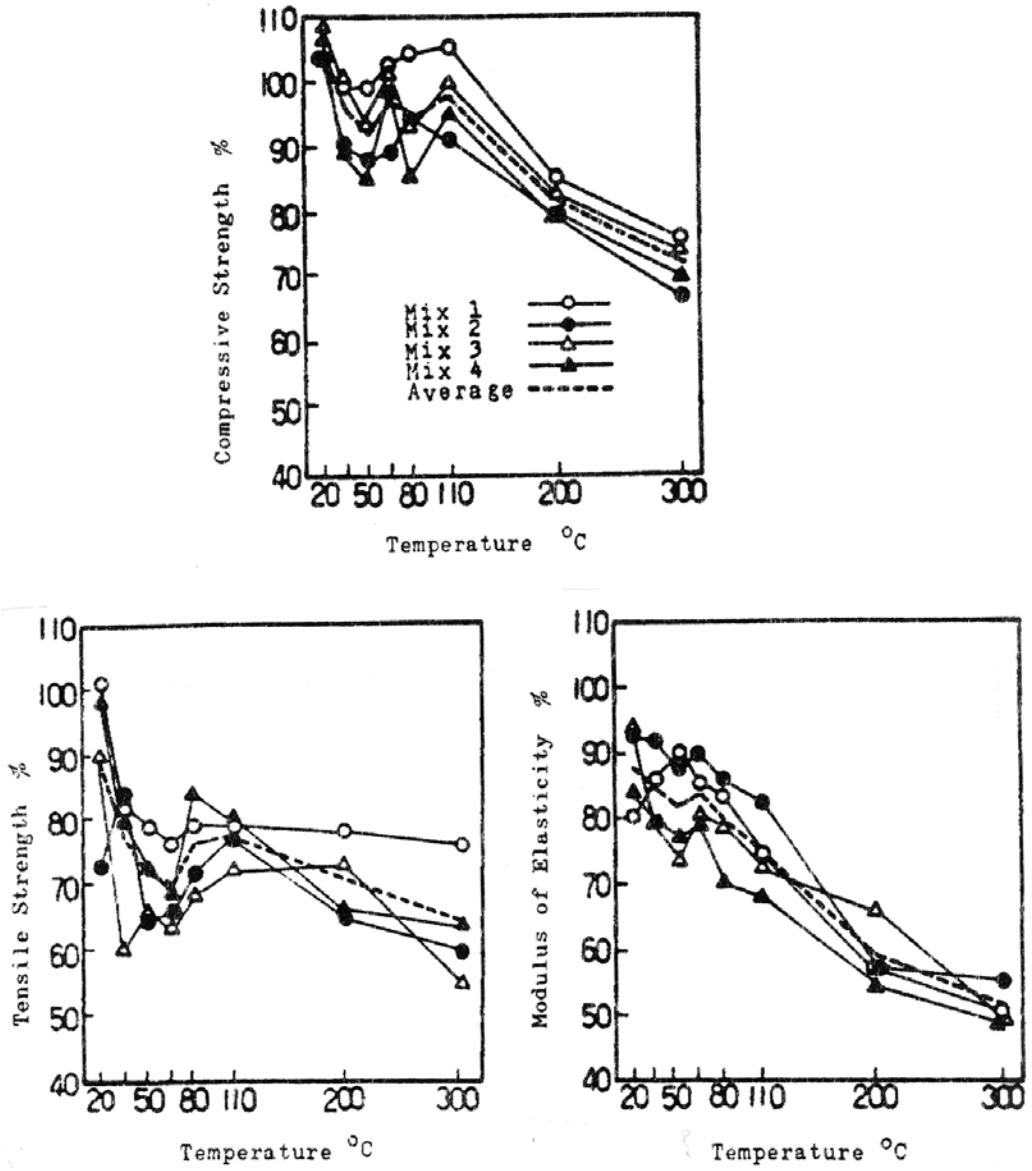

Figure 69 Effect of exposure temperature on residual compressive strength, tensile strength, and modulus of elasticity results after 90-d exposure. *Source*: H. Kasami, T. Okuno, and S. Yamane, "Properties of Concrete Exposed to Sustained Elevated Temperature," Paper Hl/5 in *Proc. 3rd International Conference on Structural Mechanics in Reactor Technology*, Elsevier Science Publishers, North-Holland, The Netherlands, 1975.

temperature on residual compressive strength, tensile strength, and modulus of elasticity results after 90-d exposure for each of the concrete mixtures investigated. Figures 70 and 71 present bond strength and weight loss results, respectively, for the different concrete mixtures. Residual compressive strength and moduli of elasticity results showing the effect of aggregate material type are presented in Fig. 72. The effect of aggregate type and temperature exposure level on shear strength* is presented in Fig. 73.

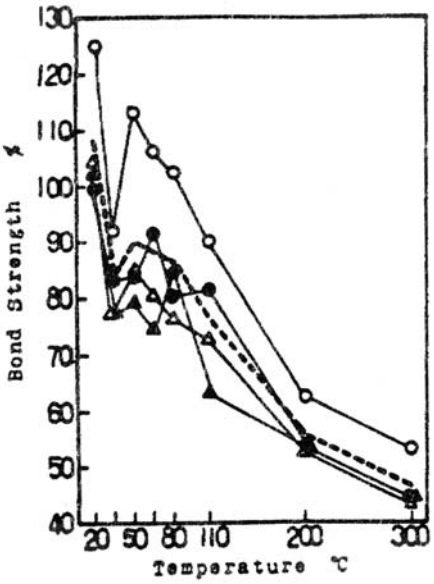

Figure 70 Bond strengths of heated concretes. *Source*: H. Kasami, T. Okuno, and S. Yamane, "Properties of Concrete Exposed to Sustained Elevated Temperature," Paper Hl/5 in *Proc. 3rd International Conference on Structural Mechanics in Reactor Technology*, Elsevier Science Publishers, North-Holland, The Netherlands, 1975.

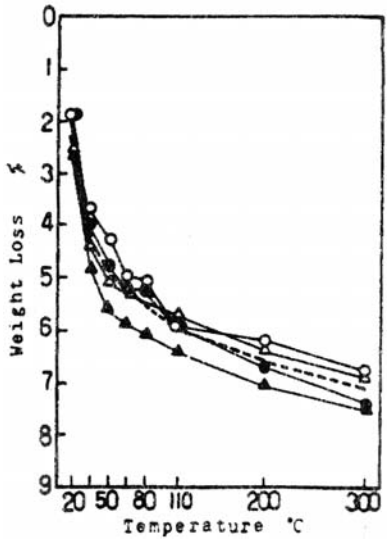

Figure 71 Weight loss of heated concrete. *Source*: H. Kasami, T. Okuno, and S. Yamane, "Properties of concrete Exposed to Sustained Elevated Temperature," Paper Hl/5 in *Proc. 3rd International Conference on Structural Mechanics in Reactor Technology*, Elsevier Science Publishers, North-Holland, The Netherlands, 1975.

*Shear is the action of two equal and opposite parallel forces applied in planes a short distance apart. Shear stresses cannot exist without accompanying tensile and compressive stresses (pure shear is applied only through torsion).

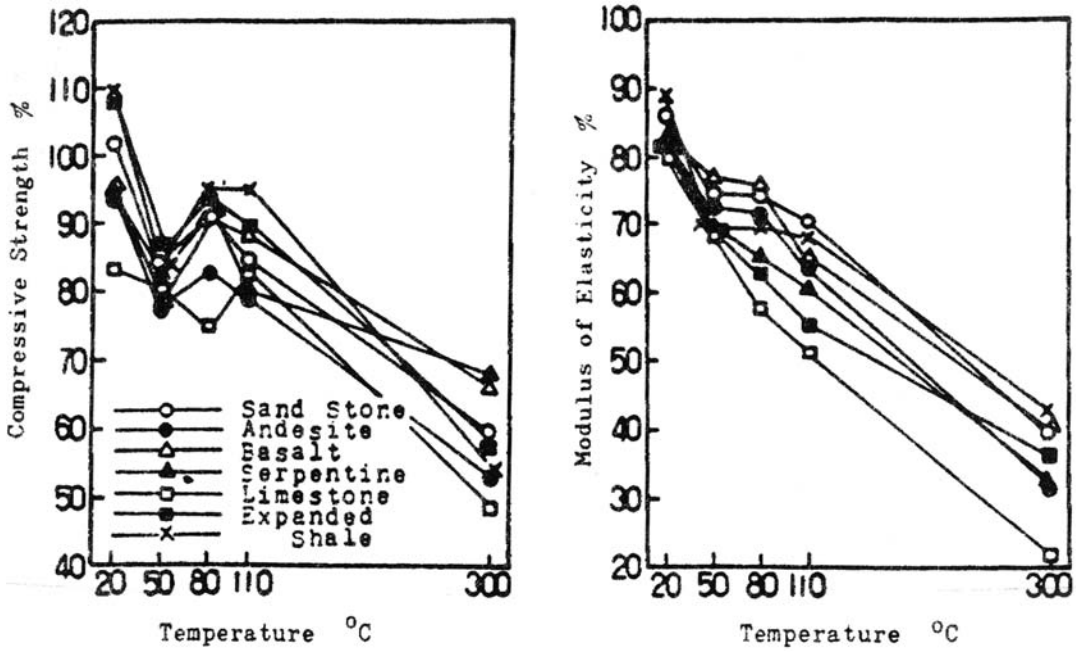

Figure 72 Compressive strength and modulus of elasticity of heated concretes. *Source*: H. Kasami, T. Okuno, and S. Yamane, "Properties of concrete Exposed to Sustained Elevated Temperature," Paper H1/5 in *Proc. 3rd International Conference on Structural Mechanics in Reactor Technology*, Elsevier Science Publishers, North-Holland, The Netherlands, 1975.

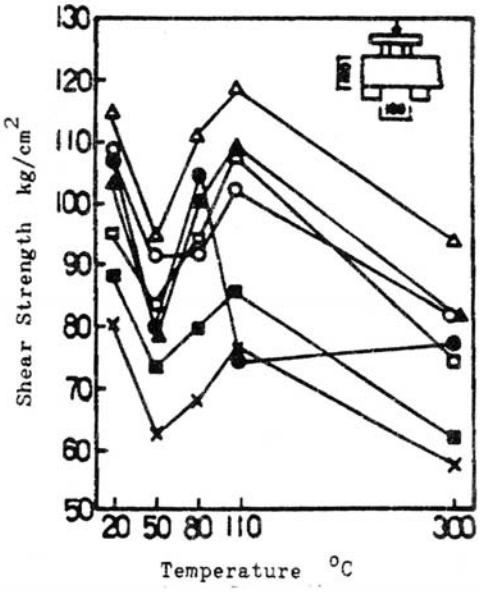

Figure 73 Shear strength of heated concrete. *Source*: H. Kasami, T. Okuno, and S. Yamane, "Properties of concrete Exposed to Sustained Elevated Temperature," Paper H1/5 in *Proc. 3rd International Conference on Structural Mechanics in Reactor Technology*, Elsevier Science Publishers, North-Holland, The Netherlands, 1975.

Radiation Shielding Effectiveness

Portland cement concrete possesses many of the physical qualities of an ideal radiation shield. It is a polyphase material consisting of particles of aggregate contained in a matrix of Portland cement paste. Gamma rays are absorbed by the high-density aggregate materials, and neutrons are attenuated by hydrogen atoms in the cement paste. A concrete shield is exposed to two sources of heat: heat transferred from hot parts of the reactor system and heat produced internally by the attenuation of neutrons and gamma rays.[97] Energy captured from slowed down fast neutrons and gamma rays entering the shield from the reactor core is deposited within the shield material and liberated as heat. The total amount of heat generated can be considerable. Different types of concrete perform differently under radiation exposure, although if heated to relatively high temperatures they all will lose waters of crystallization and become somewhat weaker and less effective in neutron attenuation.[98]

The effectiveness of concrete as a shield may be reduced under service conditions (elevated temperature) as drying reduces the hydrogen content or cracking occurs. Results of elevated-temperature exposure on shielding of heavyweight aggregate (iron limonite and magnetite limonite) concretes are presented in Fig. 74.[99] Significant changes in attenuation effectiveness were found as the concrete was heated to 100°C and 200°C, with little additional change effected on heating to 300°C. Despite the loss of neutron and gamma attenuation efficiency with increasing temperature, it was concluded that the concrete would serve as a satisfactory shield material. If increasing efficiency were required at higher temperatures, it could be accounted for in the design. The effect of different durations (1, 2, and 3 h) of high temperature (250, 500, 750, and 950°C) on the physical, mechanical, and radiation properties of heavyweight concrete has been studied.[100] Results showed that ilmenite concrete had the highest density and modulus of

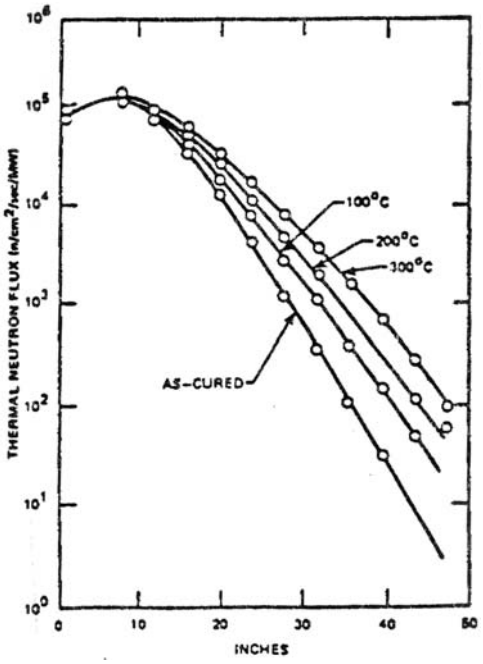

Figure 74 Thermal neutron distribution in ordinary concrete as a function of temperature. *Source*: E. G. Peterson, "Shielding Properties of Ordinary Concretes as a Function of Temperature," HW-65572, Hanford Atomic Products Operation, Richland, Washington, August 2, 1960.

elasticity and lowest percent absorption, and it also had higher values of compressive, tensile, bending, and bond strength than that obtained from either the barite or gravel concretes. Ilmenite also showed the highest attenuation of transmitted gamma rays and was most resistant to elevated temperature. As the magnitude of thermal exposure increased, the attenuation coefficient decreased.

Shielding effectiveness of concrete is also reduced if through-cracks develop. Reference 101 investigated the effect of gamma rays through a concrete shield containing straight and crooked cracks. In the immediate vicinity of the concrete surface, leakage of gamma rays through a slit contributed significantly to γ-dose rate, but diminished rapidly with distance from the surface as a result of shield thickness and scattering effects. Reference 102 investigated the shielding effectiveness of cracked concrete and developed formulas to define the resulting effects. Guidelines developed to compensate for cracking note that it might be economically advantageous to allow a concrete shield to crack and then shield the resulting radiation by other means.

Multiaxial Conditions

In large structures such as prestressed concrete pressure vessels, the concrete is stressed either biaxially or triaxially. Only limited investigations, however, have been conducted to study the multiaxial behavior of concrete at elevated temperature.

Biaxial tests of a quartzite concrete and mortar using plate-shaped specimens (200 × 200 × 50 mm) were conducted.[103] After a 2-h hold time at temperatures of either 20, 150, 300, 450, or 600°C, the specimens were loaded to failure at constant displacement rate. Specimen heating was applied at the free surfaces. A comparison of uniaxial and biaxial results for tests at 300°C and 600°C is shown in Fig. 75. Results have

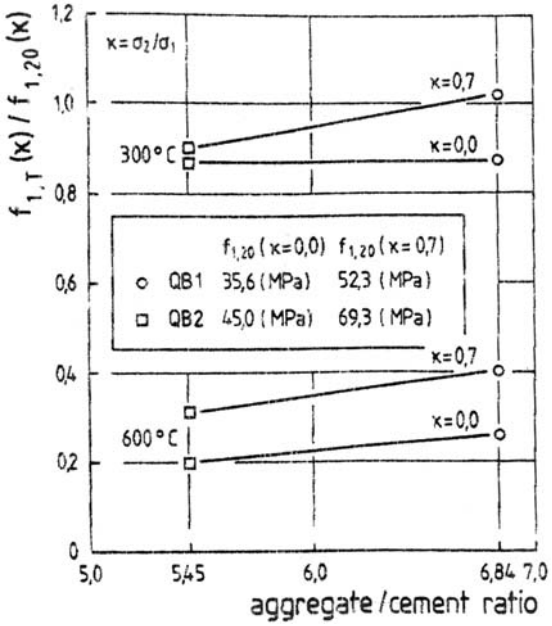

Figure 75 Comparison of uniaxial and biaxial results for tests at 300°C and 600°C. *Source*: K.-Ch. Thienel and F. S. Postasy, "Strength of Concrete Subjected to High Temperature and Biaxial Stress; Experiments and Modeling: Materials and Structures," **28**, 575–581 (1995).

been normalized with respect to corresponding strength values at room temperature and same stress ratio. The tests exhibited a smaller decrease in compressive strength for concrete with higher aggregate contents at both temperatures. Under biaxial loading, an increase in strength even appears at 300°C for the leaner mix. The strength of mortar was reduced less than that of concrete at temperatures above 300°C. The influence of stress ratio on the compressive strength for various temperatures is shown in Fig. 76. The stress ratio of the compressive strength was varied between 0 and 1, where the stress ratio represents the ratio of the applied stresses in the two principal directions. The solid and dashed lines in the figure represent the mean biaxial behavior (predicted) at each temperature noted. The failure envelopes are similar for each temperature with increasing temperature producing a larger loss of biaxial strength. The difference between uniaxial and biaxial strength increased as the temperature increased. The temperature-dependent decrease in strength was affected by the composition of the concrete in the entire range of biaxial compressive stress. The maximum aggregate size had a significant influence on behavior, while the aggregate content and water/cement ratio were less influential.

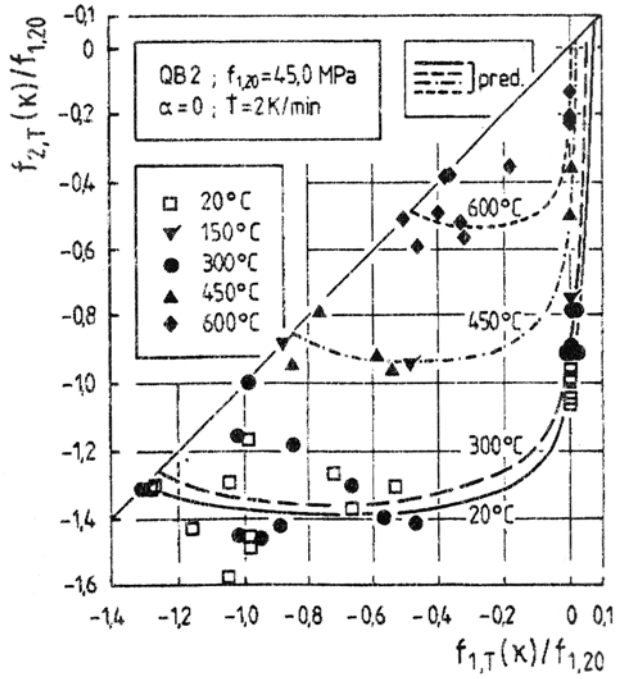

Figure 76 **Biaxial compressive strength at different temperatures.**
Source: K.-Ch. Thienel and F. S. Postasy, "Strength of Concrete Subjected to High Temperature and Biaxial Stress; Experiments and Modelling: Materials and Structures," **28**, 575–581 (1995).

Reference 104 notes that when the principal stress ratio remains constant, the biaxial strength of the concrete decreased with an increase in temperature. Loss of strength was observed at 150°C under biaxial conditions but was much lower than that obtained under uniaxial loading. Under the same elevated temperature, the biaxial strength of concrete varied with different values of principal stress ratio. When the principal stress ratio equaled 0.5, the biaxial strength of concrete at high temperature reached a maximum.

The time-dependent deformation of concrete was investigated by subjecting 15.2-cm-diameter by 40.6-cm cylindrical specimens to various stress conditions and elevated temperatures (Fig. 77). Variables included temperature (23.9°C and 65.6°C), age at loading (90, 183, and 365 d), a variety of axial and

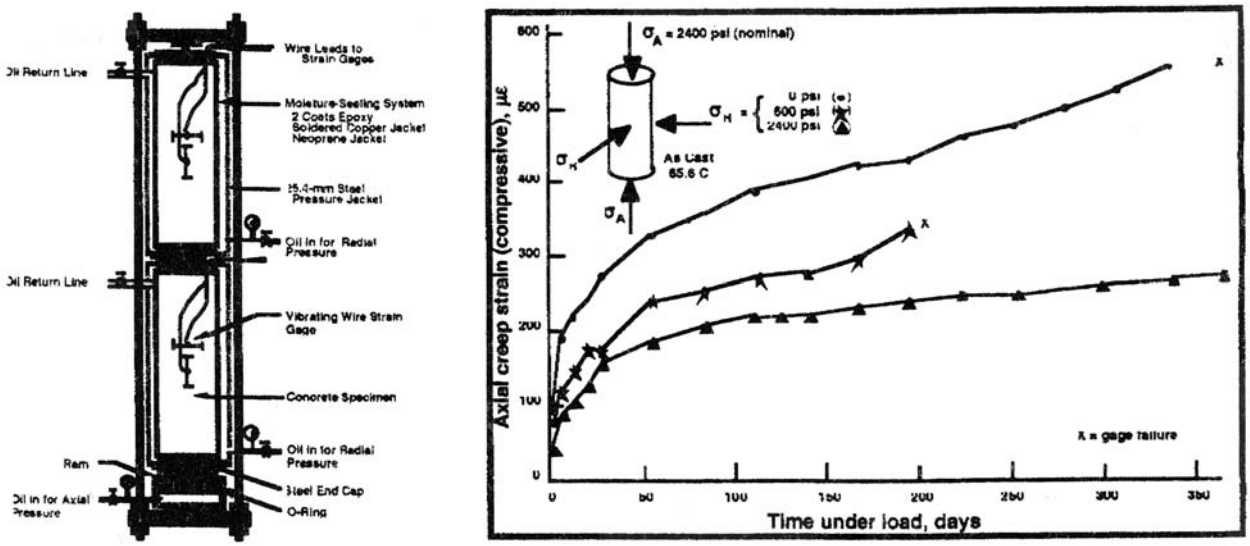

Figure 77 Investigation of the time-dependent deformation of concrete. *Source*: J. E. McDonald, "Creep of Concrete Under Various Temperature, Moisture, And Loading Conditions," SP 55, *Douglas McHenry International Symposium on Concrete and Concrete Structures,* American Concrete Institute, Farmington Hills, Michigan, 1978.

radial load combinations from 0 to 24.8 MPa, and two curing histories (air-dried and as-cast). Strains were measured using vibrating wire gages. In the investigation it was found that compressive and tensile total creep strains were generally larger for (1) a test temperature of 65.6°C than for 23.9°C, (2) an air-dried concrete than an as-cast concrete (except for low tensile creep), (3) increased time after loading, and (4) uniaxial than biaxial states of stress, and that the axial creep strains decreased with increasing confining stress.[79,105]

Thermal Spalling and Fire Resistance

The effects of very rapid and localized heating of a concrete wall or floor element is of interest in nuclear power plants in the unlikely event of a fire or where response of a structure to low probability hypothetical core disruptive accidents is considered [(e.g., molten core debris and liquid sodium coolant melt through the reactor vessel and guard vessel into the reactor area of a liquid-metal fast breeder reactor (LMFBR)]. Research on transient behavior of concrete elements under fire conditions has been conducted for many years,[106–108] with most of the tests to determine the fire resistance of specific concrete elements.

Concrete spalling tests—Spalling of concrete exposed to fire is understood to be the explosive detachment of large or small pieces of concrete from the concrete surface subjected to heating. Spalling can be divided into four categories:[108] (1) explosive dislodging of a few large pieces of concrete from the surface that can result in failure of the member affected, (2) local dislodging of relatively minor portions of the surface or the edges, (3) gradual reduction of the cross section, or (4) explosive dislodging of small pieces of concrete from the surface, which primarily occurs at high material temperatures and can expose the steel reinforcement. Factors influencing spalling include the moisture content, whether heat is applied at one or two faces, rate of temperature increase, aggregate material, the member thickness, state of stress, and presence of reinforcement. Because of the relatively high permeability of NSC, spalling is generally not a safety risk except during initial curing when concrete is in the process of drying or in some tunnel

applications. Spalling, however, is of primary importance to high-performance concrete, which exhibits reduced permeability.*

Reference 108 presents results of an extensive study conducted to evaluate spalling of concrete exposed to fire. Twenty-five tests were conducted on beam- and plate-like elements primarily to investigate the influence of the concrete moisture content. Other parameters included type aggregate (gravel and lightweight coarse aggregates), compressive stress, concrete compressive strength, thickness of element, steel reinforcement content, and one- or two-sided heating. Results of the study indicated that a high moisture content [>7% (v/v)] can give rise to severe spalling only, if in addition, one or more other unfavorable working conditions are present at the same time (i.e., two-sided heating, small thickness, compressive stress, and reinforcement). Also, it was noted that inspections of buildings after real fires revealed that the spalling that occurred was never as severe as may be expected from fire tests. This was possibly due to the heating rate being lower than that which corresponds with the standard fire-test conditions and that the concrete moisture content in these buildings was relatively low because they had been in service for several years.

Fire resistance of concrete elements—The fire endurance of materials and assemblies is established based on national and international standards.[109-111] In ASTM E 119,[109] a standard time-temperature relation is specified for use in evaluating the fire resistance of structural elements for buildings. Also provided is the furnace time-temperature for a short-duration high-intensity (SDHI) fire, which is used by many fire protection engineers where conditions are postulated that a fire will burn intensely, but die down quickly as available fuel is exhausted.[112,113] Typical unexposed surface temperatures recorded during standard fire tests for concrete slab and beam elements have been published.[114] For concrete assemblies such as these, the temperature rise depends mainly on the thickness and unit weight of the concrete, but it is also influenced by aggregate type, concrete moisture condition, air content, maximum aggregate size, and aggregate moisture condition at time of mixing.

A summary of practical information intended for use by architects, engineers. and building officials who must design concrete structures for particular fire resistances or evaluate structures as designed is given in Ref. 21. Additional information on determination of fire endurance for slabs, two-course roofs and floors, columns, and walls is available.[114] Computer program are available (e.g., FIRETEST) that estimate the temperature distribution through normal weight and lightweight concrete slabs and on the unexposed surface during either an ASTM E119 or SDHI fire test.[112] Also information is available relative to modeling the thermal behavior of concrete.[61,115–117]

Due to the unique conditions under which many of the fire tests reported in the literature were conducted (e.g., thermal gradients, use of insulating material, and structural element type), the results probably have limited application to safety evaluations of reinforced concrete structures in current and new generation nuclear power plants. However, some general conclusions that can be derived from structural fire endurance tests are pertinent: (1) fire endurance increases with increasing moisture content of the concrete; (2) fire endurance of a concrete slab increases with an increase in air content, particularly for air contents >10%, but below 7% air content the effect is not significant; (3) fire endurance of concrete slabs increases as the amount of mortar (cement, water, and sand) in the concrete increases (concretes with smaller maximum size aggregates have longer fire durations than those with larger sizes); (4) factors such as water-cement ratio, cement content, and slump have almost no influence on fire endurance within the normal ranges for structural concretes; (5) structural fire endurance of a complete concrete wall section is seldom a governing factor because it is generally much longer than the fire endurance evaluated based on the temperature rise of the unexposed surface; (6) fire endurance of slabs increases with an increase of

*High-strength (or high-performance) concretes will be discussed later.

slab thickness; and (7) in general, fire endurance increases with a decrease in unit weight (lightweight aggregate concretes have superior fire endurance relative to normal-weight concretes).[114,21]

2.2.2 Physical Properties

The physical, or thermal, properties of concrete are important both in the planning of mass concrete construction (thermal changes) and the dissipation of heat buildup during operation. The thermal expansion coefficient and modulus of elasticity data are prerequisite to computing the thermoelastic stresses that result from nonuniform heating.

As water is added to cement, an exothermic chemical reaction takes place. If the heat is generated at a faster rate than it can be dissipated, a temperature rise occurs. Factors affecting the amount and rate of heat generated during this reaction are the cement type, temperature at placement, water-cement ratio, and cement content. In mass concrete structures where there can be significant heat buildup, cracking can occur upon cooling because the exterior of the structure will cool faster than the interior. However, by using low (Type IV) or moderate (Type II) heat of hydration cements and following the procedures recommended in Ref. 118, this problem can be minimized.

Temperature variations produce expansions or contractions of concrete structures. If movement of a structure is restrained, significant internal stresses can develop, thus leading to cracking, distortions, or even destruction. In general, the density, conductivity, and diffusivity of concrete will increase with an increase in temperature. The coefficient of thermal expansion α is used as a measure of the volume change of a material subjected to a temperature differential. Dissipation of heat is important to nuclear power plant structures such as a PCPV because it affects the development of thermal gradients and the resulting thermal stresses. The basic quantities involved are (1) the coefficient of thermal conductivity k, (2) the thermal diffusivity a, and (3) the specific heat c. These quantities are related by the term $a = k/cp$, where p is the material density.

Density

The density of concrete depends on the density of its aggregate materials and its moisture content in the temperature range from 20°C to 150°C. Figure 78 presents the effect of aggregate type on the density of concretes in the temperature range from room temperature to 1400°C (Ref. 5). Storage (curing or preconditioning) conditions at lower temperature are also important because moist specimens will lose water and thus experience a greater decrease in density upon heating than specimens that have experienced drying. At temperatures from 150°C to 600°C (limestone decarbonation) the density of limestone concrete is relatively constant. Upon decarbonation weight loss occurs[119] as the concrete porosity increases until at higher temperatures when sintering take place the density may increase slightly.[5] Siliceous aggregates exhibit a somewhat steeper decrease in density with heating in the range from room temperature to 700°C. The sharper decline in density at higher temperatures is due to the large thermal expansion of the quartz. Basalt exhibits the smallest decline in density because of its lower thermal expansion.[5] Figure 79 presents bulk density as a function of temperature for a 38-MPa basalt aggregate concrete utilized for Korean nuclear power plants.[120]

Coefficient of thermal expansion

The coefficient of thermal expansion represents the volume change of a material due to temperature changes and is expressed as a change in length per degree of temperature change. The coefficient is important as a measure of the structural movement and thermal stresses resulting from a temperature

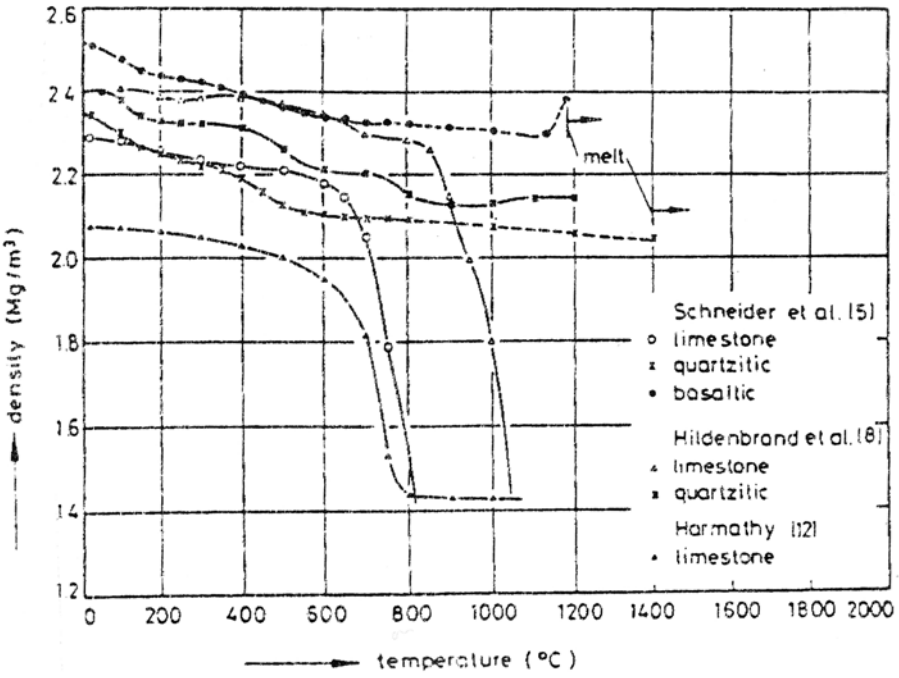

Figure 78 Density of different concretes. *Source*: U. Schneider, C. Diererichs, and C. Ehm, "Effect of Temperature on Steel and Concrete for PCRV's," *Nuclear Engineering and Design* **67**, 245–258 (1981).

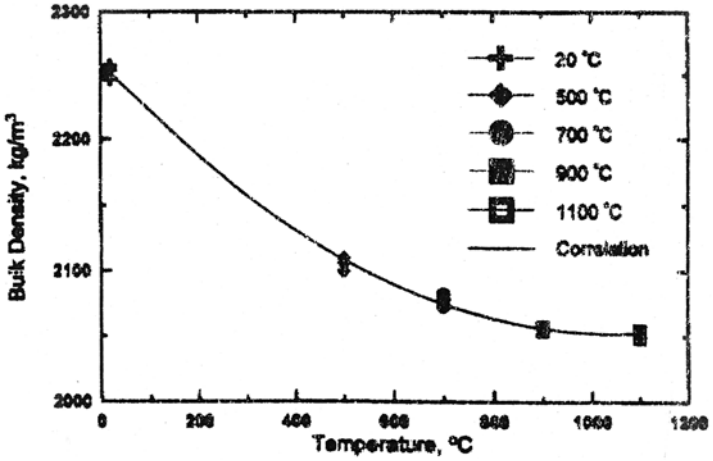

Figure 79 Density of a nuclear power plant concrete. *Source*: K.-Y. Shin et al., "Thermo-Physical Properties and Transient Heat Transfer of Concrete at Elevated Temperatures," *Nuclear Engineering and Design* **212**, 233–241 (2002).

change. Concrete's thermal expansion is a complicated phenomenon because of the interaction of its two main components—cement paste and aggregate—which each have their own coefficients of thermal expansion. Because the aggregate generally constitutes a major proportion of the mix, it primarily influences the resultant coefficient of thermal expansion. Figure 80[121] presents thermal coefficient of expansion values for neat cements, mortars, and concretes. As illustrated, values of the coefficient for concrete range from ~2.2×10^{-6} to 3.9×10^{-6} mm/mm/°C with 3.1×10^{-6} mm/mm/°C being a typical value. The coefficient is influenced by the moisture condition (applies to paste component) and has minimum values for the two extremes: dry and saturated.[119] The coefficient of linear expansion also apparently increases with increasing temperature (Fig. 81);[119] however, the effects of specimen moisture condition at test initiation (i.e., the number of thermal cycles that have been applied to the specimen) also has to be taken into consideration in determining the net specimen length change with temperature.[122]

Thermal expansion coefficients for limestone and siliceous aggregate concretes are presented in Figs. 82 and 83, respectively.[4] Results indicate an almost monotonic increase in thermal expansion coefficient for the limestone concrete until decarbonation ($CaCO_3 \rightarrow CaO + CO_2$) leads to a decrease in the coefficient. The thermal expansion of the siliceous concrete is greater than that for the limestone concrete. Basalt, due to its fine crystalline structure, exhibits a lower expansion than the siliceous concrete. Figure 84 presents the influence of temperature (20°C to 200°C) on thermal expansion coefficient of a siliceous aggregate concrete from the French Penly Nuclear Power Plant.[123]

Results presented in the literature indicate that the main factor influencing the coefficient of thermal expansion is the aggregate type; at high temperatures (600°C to 800°C) most concretes no longer exhibit an expansion and in some cases contract; moisture content, water/cement ratio, and cement type influence results at relatively low temperatures with moist concretes exhibiting higher thermal expansion values than dry concretes; and thermal expansion coefficient is inversely proportional to aggregate content.

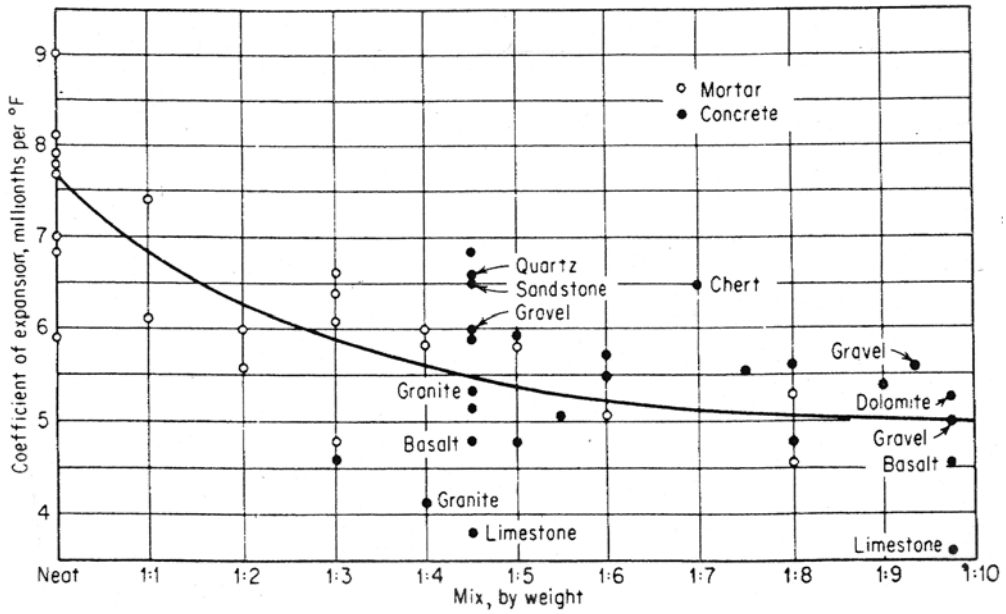

Figure 80 Coefficients of thermal expansion of neat cements, mortars, and concretes. *Source*: *Concrete Manual,* 7th Ed., U.S. Bureau of Reclamation, Denver, Colorado, 1963.

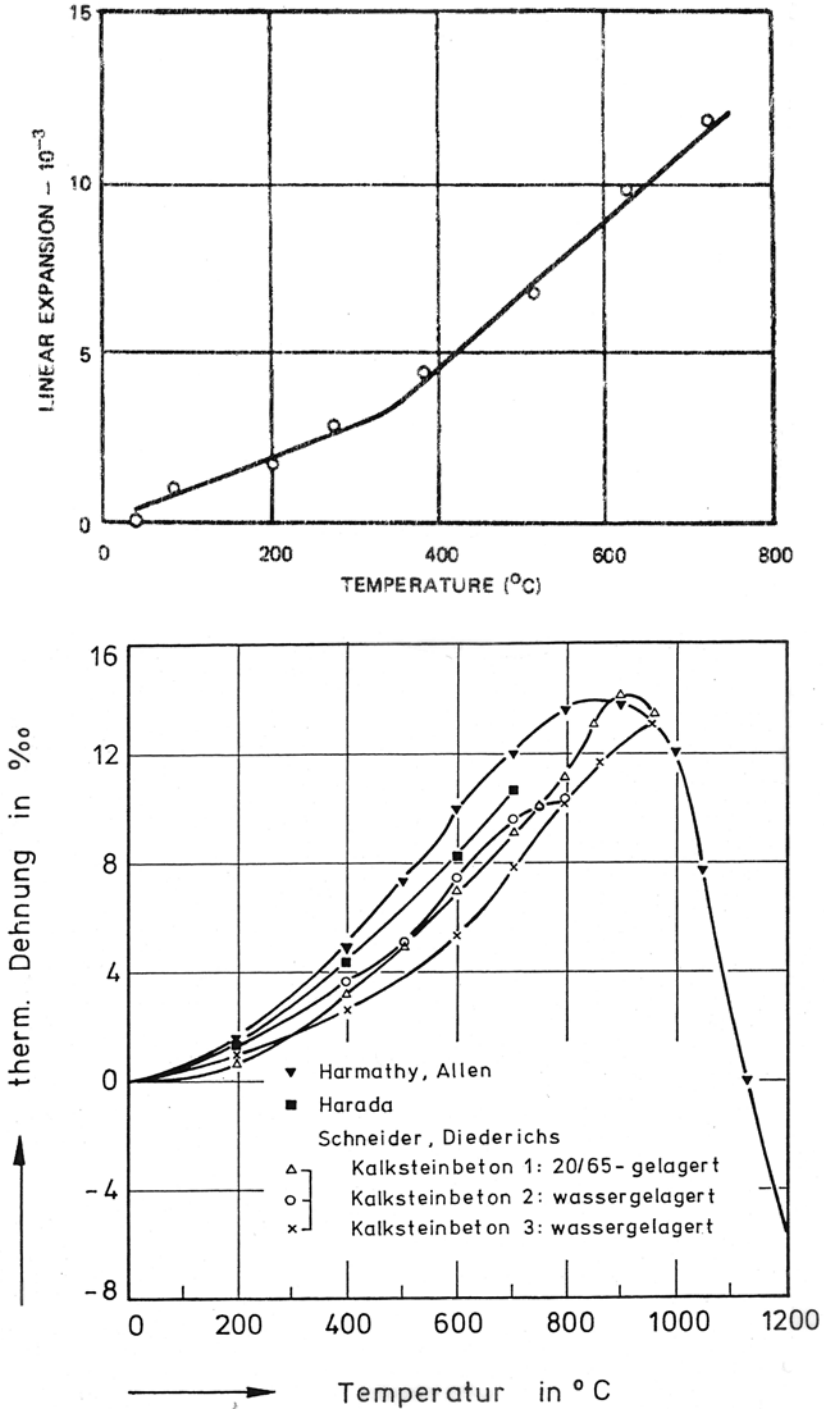

Figure 81 Linear expansion of concrete on heating. *Source*: R. Philleo, "Some Physical Properties of Concrete at High Temperature," *Research Department Bulletin 97*, Portland Cement Association, Skokie, Illinois, October 1958.

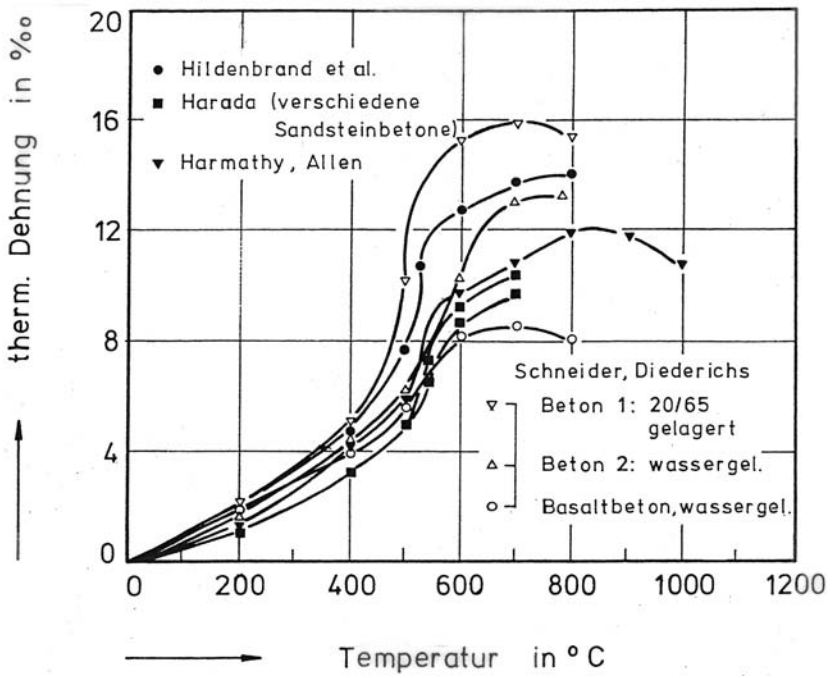

Figure 82 Thermal expansion of limestone aggregate concretes. *Source*: U. Schneider, "Behaviour of Concrete at High Temperature," HEFT 337, Deutscher Ausschuss für Stahlbeton, Wilhelm Ernst & Sohn, Munich, Germany, 1982.

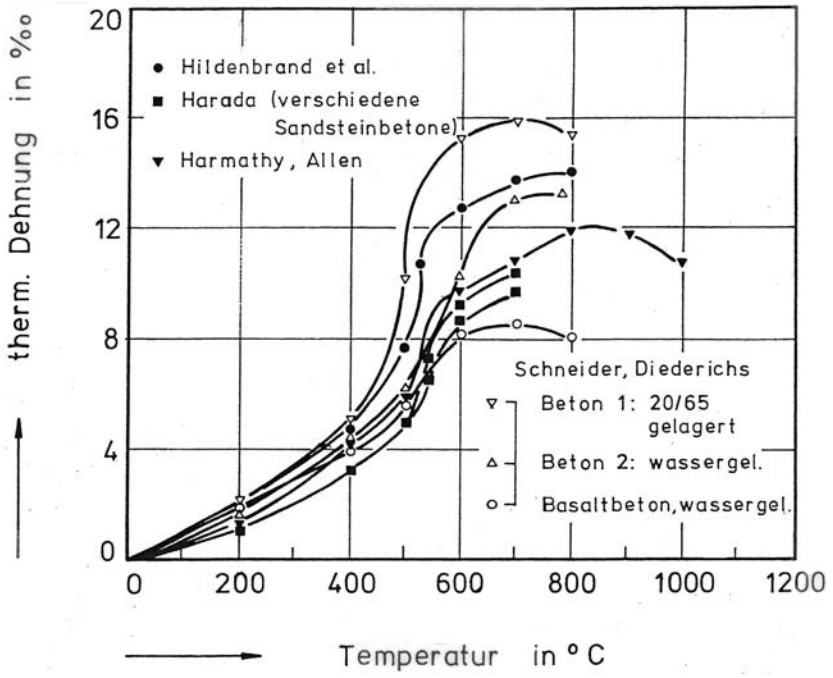

Figure 83 Thermal expansion of siliceous aggregate concretes. *Source*: U. Schneider, "Behaviour of Concrete at High Temperature," HEFT 337, Deutscher Ausschuss für Stahlbeton, Wilhelm Ernst & Sohn, Munich, Germany, 1982.

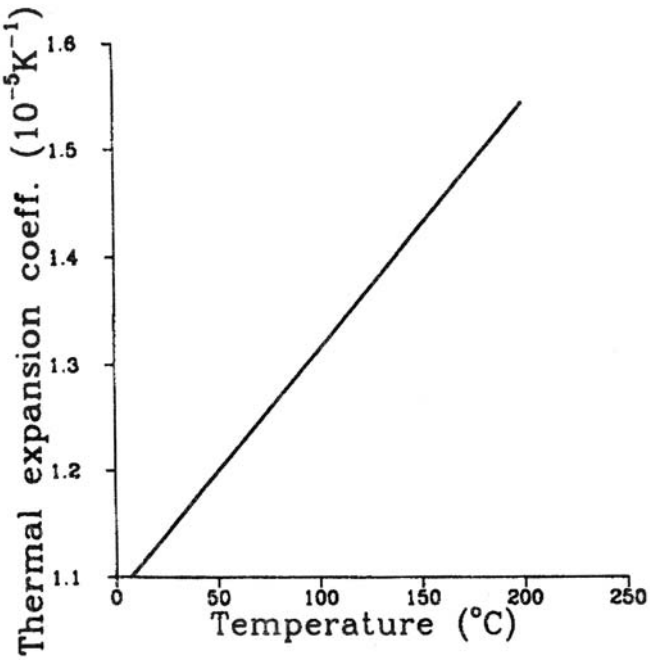

Figure 84 Temperature dependence of linear thermal expansion coefficient of nuclear power plant concrete. *Source*: F. Vodak et al., "The Effect of Temperature on Strength—Porosity Relationship for Concrete," *Construction and Building Materials* **18**, 529–534 (2004).

Thermal conductivity

Thermal conductivity is a measure of the ability of the material to conduct heat and is measured in British thermal units per hour per square foot of area of body when the temperature difference is 1°F per foot of body thickness. For PCPVs, concrete with a high thermal conductivity is generally desirable but not always used to allow a rapid dissipation of heat flux, so thermal gradients through the thickness will be minimal.

Important factors influencing the thermal conductivity of concrete are the hardened cement paste, the pore volume and distribution, and the water content. At low temperatures and with moist concrete very high values for thermal conductivity exist.[5] At higher temperatures the thermal conductivity increases slightly (see next paragraph), but decreases as it approaches 100°C. Up to 300°C to 400°C, the thermal conductivity decreases further, and as the temperature increases beyond 300°C increasing cracking develops.

Table 2 lists typical values of thermal conductivity for several concretes fabricated using a wide variety of aggregates.[124] Because the conductivity of water is approximately half that of cement paste, the lower the mix-water content, the higher the conductivity of the hardened concrete.[125] As shown in Fig. 85, thermal conductivities of concrete made with highly crystalline aggregate decrease with temperature up to 100°C, while those of concrete made with amorphous aggregate are essentially constant.[8] Figure 86 presents thermal conductivities for normal concretes having different aggregate types.[5] Figures 87 and 88 presents thermal conductivities of concrete as a function of density and moisture content and the variation of thermal conductivity as a function of temperature for several mortars and concretes, respectively.[120]

Table 2 Typical Values of Thermal Conductivity

Type aggregate	Concrete density [lb/ft^3 (kg/m^3)]	Conductivity [Btu/ft^{2}h°F/ft (MW/cm°C)]
Barite	227 (3640)	0.80 (13.9)
Igneous	159 (2550)	0.83 (14.4)
Dolomite	160 (2560)	2.13 (37)
Limestone or gravel	150 (2400)	0.75–1.00 (13–17)
Lightweight No. 1	30 (481)[a]	0.08 (1.4)
Lightweight No. 2	110 (1760)[a]	0.35 (6.1)
Pumice		0.02 (0.3)
Foam	20 (320)	0.04 (0.7)
Cinder		0.43 (7.4)
Expanded clay		0.23–0.36 (4–6.2)
Perlite or vermiculite		0.04–0.07 (0.7–1.2)

[a]Oven dried.

Source: L. L. Mitchell, "Thermal Properties," ASTM Special Technical Publication 169, pp. 129–135, American Society for Testing and Materials, West Conshohocken, Pennsylvania, October 1962.

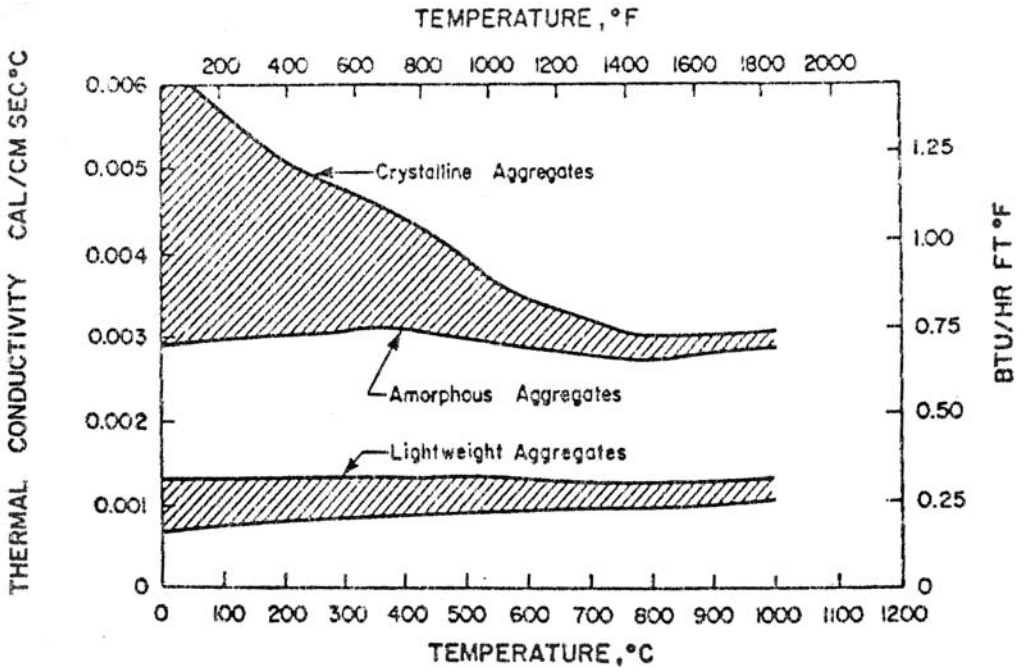

Figure 85 Thermal conductivity of Portland cement concretes. *Source*: T. Z. Harmathy and L.W. Allen, "Thermal Properties of Selected Masonry Unit Concretes," *J. American Concrete Institute* **70**, 132–142 (1973).

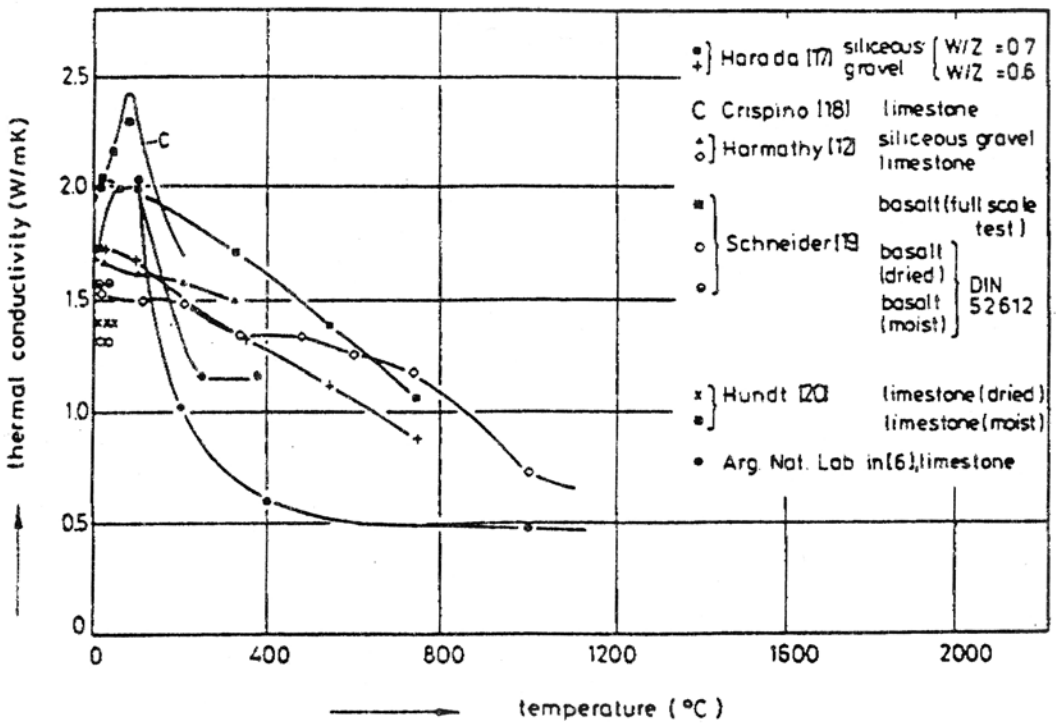

Figure 86 **Thermal conductivity of ordinary concretes with different aggregates.** *Source*: U. Schneider, C. Diererichs, and C. Ehm, "Effect of Temperature on Steel and Concrete for PCRV's," *Nuclear Engineering and Design* **67**, 245–258 (1981).

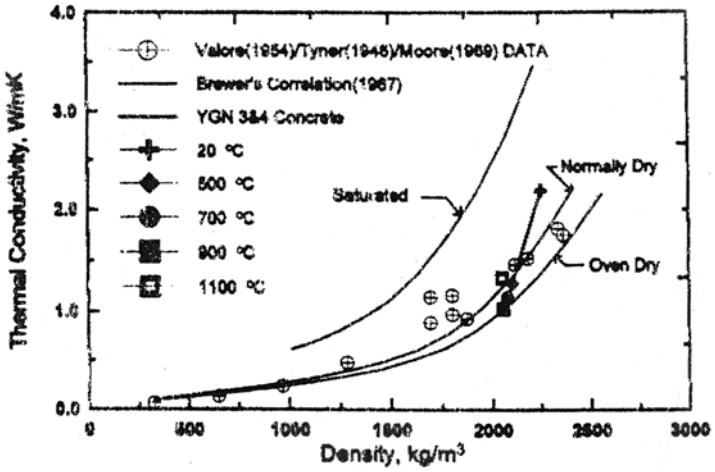

Figure 87 **Thermal conductivity as a function of density and moisture content.** *Source*: K.-Y. Shin et al., "Thermo-Physical Properties and Transient Heat Transfer of Concrete at Elevated Temperatures," *Nuclear Engineering and Design* **212**, 233–241 (2002).

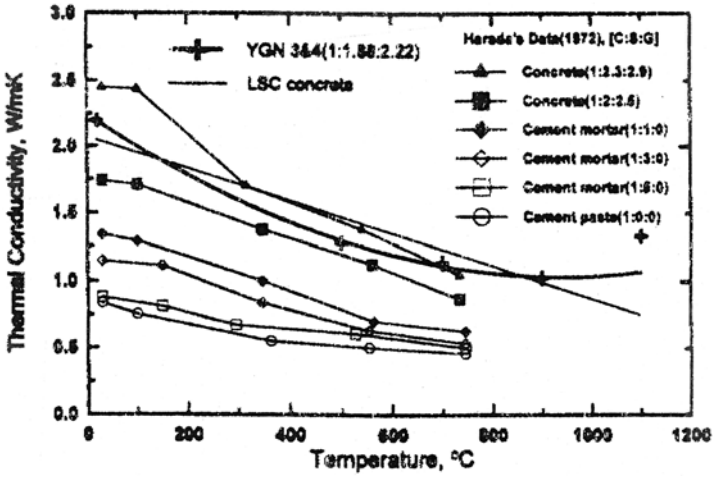

Figure 88 Thermal conductivity as a function of temperature. *Source*: K.-Y. Shin et al., "Thermo-Physical Properties and Transient Heat Transfer of Concrete at Elevated Temperatures," *Nuclear Engineering and Design* **212**, 233–241 (2002).

Figure 89 presents the influence of temperature on thermal conductivity of a siliceous aggregate concrete from the French Penly Nuclear Power Plant.[123] Results presented in the figure are based on 40 measurements at each of the test temperatures (30, 60, 90, 150, and 200°C) and are comparable to those obtained by other researchers for siliceous aggregates in this temperature range.[125,126]

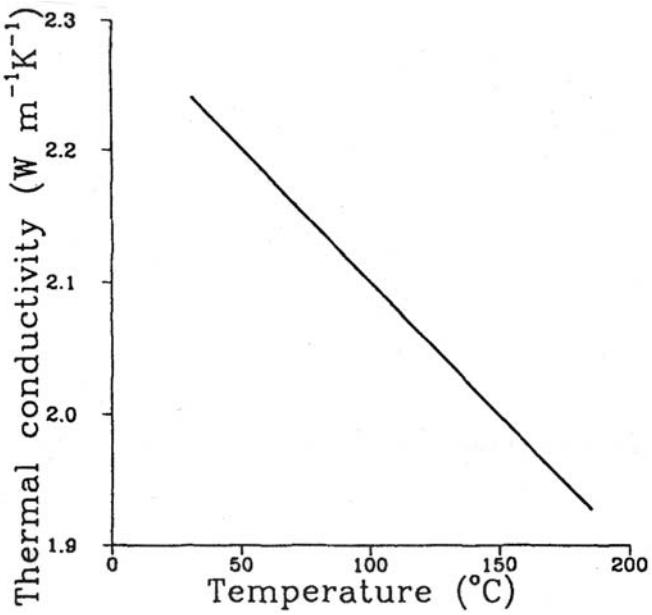

Figure 89 Temperature dependence of thermal conductivity of a nuclear power plant concrete. *Source*: F. Vodak et al., "Thermophysical Properties of Concrete for Nuclear Safety-Related Structures," *Cement and Concrete Research* **27**(3), 415–426 (1997).

Results presented in the literature indicate that the major factors influencing concrete thermal conductivity are moisture content, type of aggregate material, hardened cement paste, and pore volume and distribution. The conductivity varies linearly with moisture content. As the conductivity of the aggregate material increases, the concrete thermal conductivity increases. Concretes with lower cement paste content can be expected to have a lower conductivity than lean concrete mixtures.

Thermal diffusivity

Thermal diffusivity is a measure of the rate at which heat will diffuse through a material in all directions due to a temperature change and is thus an index of the facility with which the material will transfer heat due to a temperature change. Thermal diffusivity is important to nuclear power plant structures such as PCPVs for the same reasons cited for thermal conductivity. Thermal diffusivity of concrete is determined by the thermal properties of its constituents. Aggregates with increasing values of thermal diffusivity include basalt, rhyolite, granite, limestone, dolerite, and quartzite.[127] Factors that affect thermal conductivity generally have the same influence on thermal diffusivity. Thermal diffusivity of limestone and siliceous aggregate concretes is presented in Figs. 90 and 91, respectively.[4] Figure 92 presents the influence of temperature on thermal diffusivity of a siliceous aggregate concrete from the French Penly Nuclear Power Plant[123] and is noted to be similar to other results presented in the literature for siliceous aggregate concretes in the temperature range investigated (30°C to 200°C).[128] Figure 93 presents the thermal diffusivity of several mortars and concretes as a function of temperature.[120]

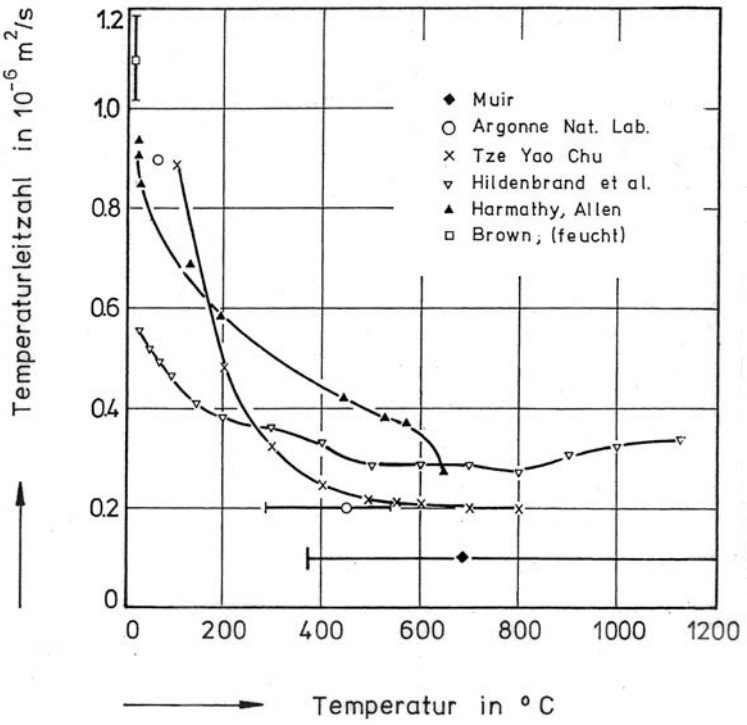

Figure 90 Thermal diffusivity of limestone concrete. *Source*: U. Schneider, "Behavior of Concrete at High Temperature," HEFT 337, Deutscher Ausschuss fur Stahlbeton, Wilhelm Ernst & Sohn, Berlin, Germany, 1982.

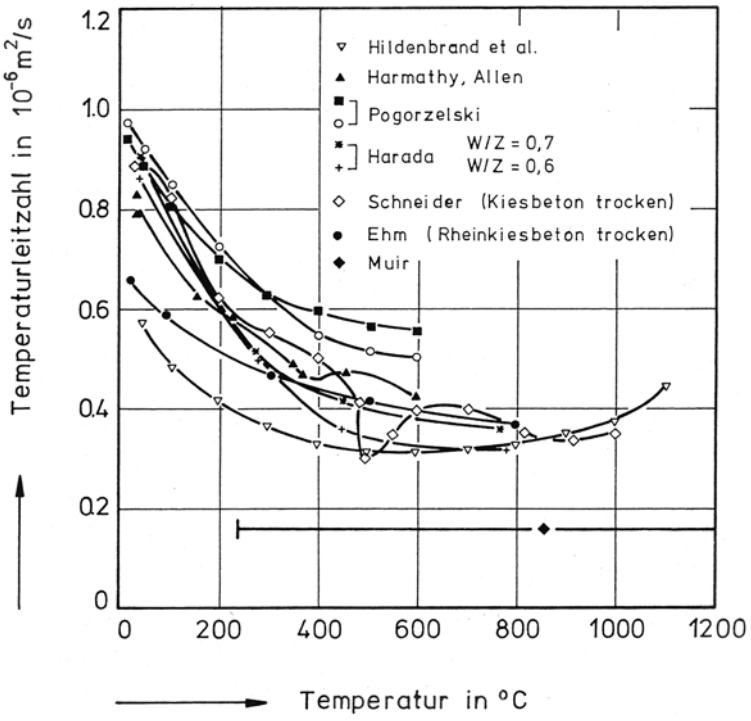

Figure 91 Thermal diffusivity of siliceous aggregate concrete. *Source*: U. Schneider, "Behaviour of Concrete at High Temperature," HEFT 337, Deutscher Ausschuss für Stahlbeton, Wilhelm Ernst & Sohn, Munich, Germany, 1982.

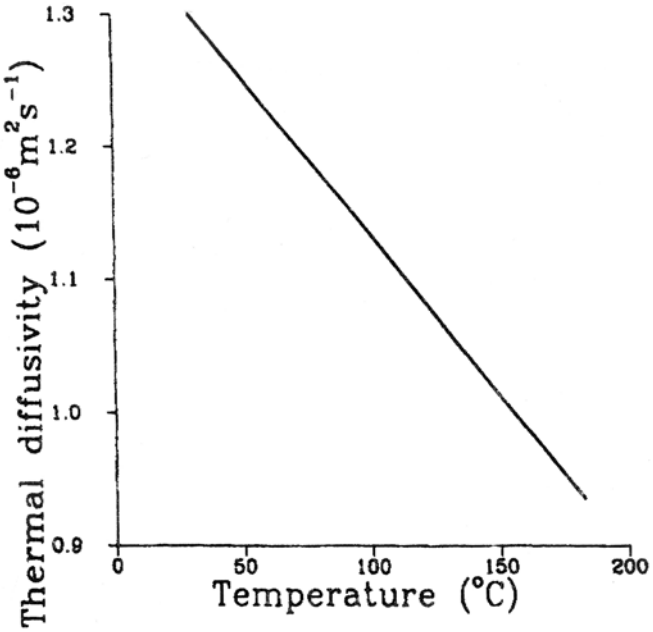

Figure 92 Temperature dependence of thermal diffusivity of a nuclear power plant concrete. *Source*: F. Vodak et al., "The Effect of Temperature on Strength—Porosity Relationship for Concrete," *Construction and Building Materials* **18**, 529–534 (2004).

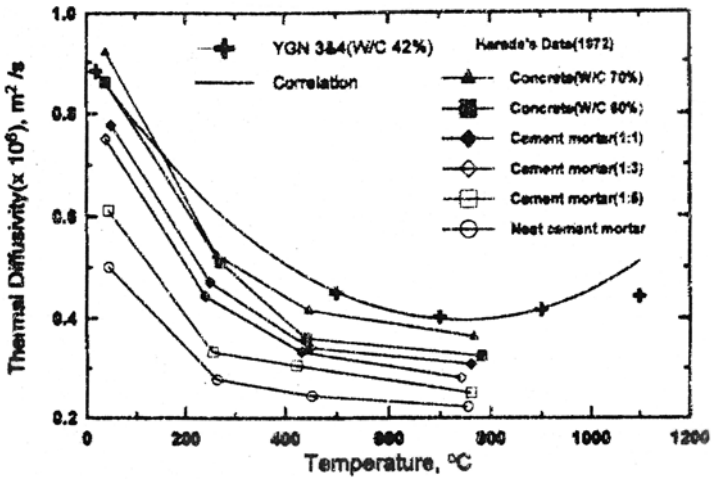

Figure 93 Thermal diffusivity variation of concrete as a function of temperature. *Source*: K.-Y. Shin et al., "Thermo-Physical Properties and Transient Heat Transfer of Concrete at Elevated Temperatures," *Nuclear Engineering and Design* **212**, 233–241 (2002).

Specific Heat

Specific heat is the amount of heat required to change the temperature of 1 lb (0.45 kg) of material 1°F (0.56°C) and thus represents the heat capacity of the material. As the moisture content in the concrete increases, the specific heat capacity increases at lower temperatures. Concrete's heat capacity rises with temperature up to about 500°C and then levels out or declines up to 1000°C as shown in Fig. 94.[8]

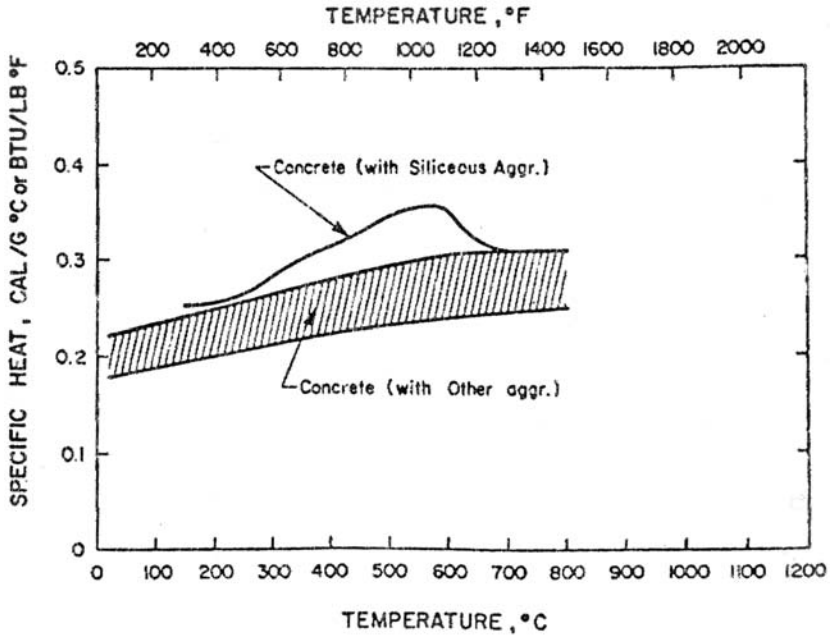

Figure 94 Thermal conductivity of Portland cement concrete. *Source*: T. Z. Harmathy and L. W. Allen, "Thermal Properties of Selected Masonry Unit Concretes," *J. American Concrete Institute* **70**, 132–142 (1973).

Figures 95 and 96 present heat capacities of limestone and siliceous aggregate concretes, respectively.[4] Additional information is provided in Figure 97, which presents the influence of temperature on the specific heat of a siliceous aggregate concrete from the French Penly Nuclear Power Plant.[123]

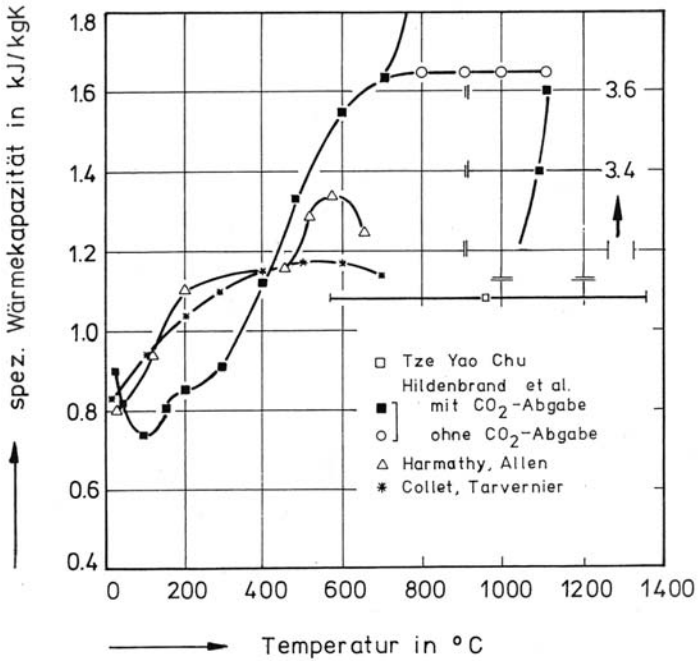

Figure 95 Specific heat capacity of limestone aggregate concrete.
Source: U. Schneider, "Behaviour of Concrete at High Temperature," HEFT 337, Deutscher Ausschuss für Stahlbeton, Wilhelm Ernst & Sohn, Munich, Germany, 1982.

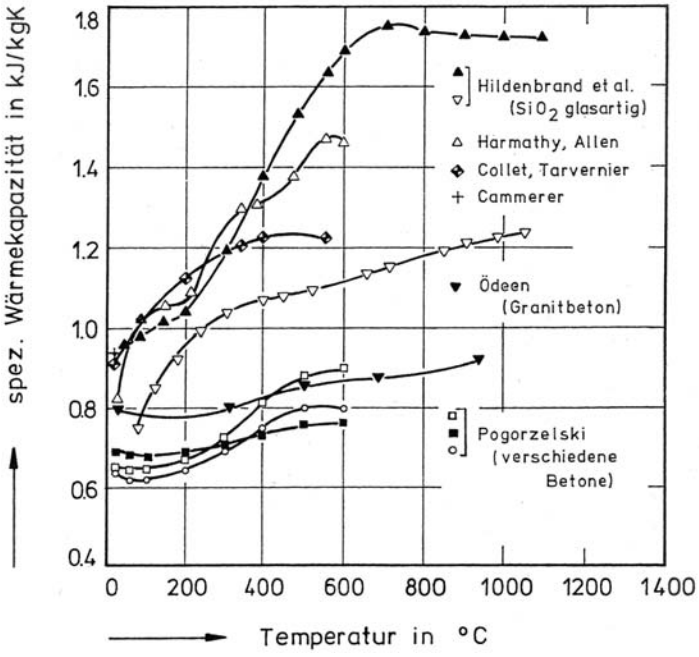

Figure 96 Specific heat capacity of siliceous aggregate concrete.
Source: U. Schneider, "Behaviour of Concrete at High Temperature," HEFT 337, Deutscher Ausschuss für Stahlbeton, Wilhelm Ernst & Sohn, Munich, Germany, 1982.

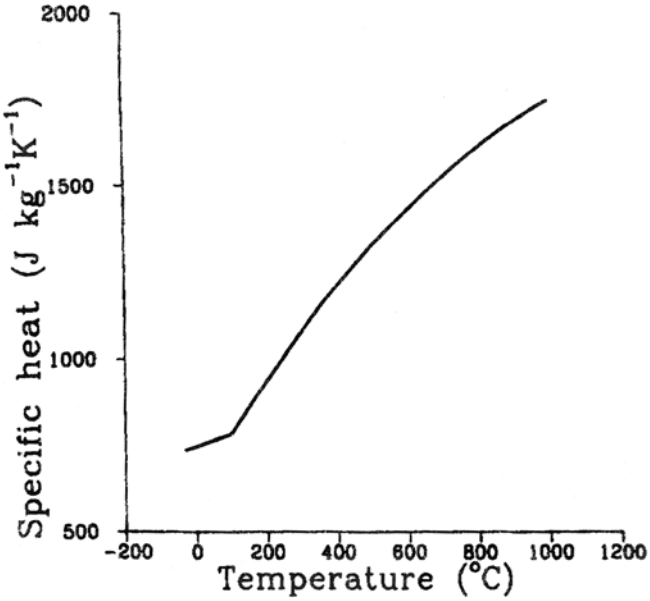

Figure 97 Temperature dependence of specific heat of a nuclear power plant concrete. *Source*: F. Vodak et al., "The Effect of Temperature on Strength—Porosity Relationship for Concrete," *Construction and Building Materials* **18**, 529–534 (2004).

3 EFFECTS OF ELEVATED TEMPERATURE ON HIGH-STRENGTH CONCRETE MATERIALS

Early research on the effects of elevated temperature on concrete material properties and performance in large measure was in support of the development of prestressed concrete pressure vessels for nuclear power plant designs. Starting in the 1980s concretes with increasing compressive strengths started to become commercially available and primarily utilized in the construction of high-rise buildings. Use of HSC* offered economic advantages because concrete column size could be reduced, thus permitting more usable space. It also had application in the construction of prestressed girders for bridge construction and other specialized applications in which high performance (e.g., low permeability) is required. Today concretes having compressive strengths up to 140 MPa and above can be produced, with strengths of 172 MPa and above attainable through use of special fabrication procedures.[129]

HSC is produced primarily through use of a relatively low water/cementitious ratio and incorporates silica fume. Because this leads to a reduced permeability relative to normal weight concretes, there has been a concern that the HSC may be more susceptible to explosive spalling under fire conditions due to the buildup of pore pressure in the cement paste. Because one of the primary applications of HSC has been to general civil engineering building structures, most recent research on elevated-temperature effects on concrete materials has shifted to an evaluation of the HSC materials under fire conditions. Because some of the newer generation reactor designs may incorporate HSC, or high-performance concretes, a limited discussion is provided below.

A comprehensive review of the experimental and analytical studies on the performance of concrete when exposed to short-term, rapid heating, such as occurs in fires, has been prepared.[130] Although the report does present some information on normal-strength concretes (NSC), the emphasis of the report is on concretes having initial high compressive strengths. Basic conclusions provided in this report follow:

- The material properties of HSC vary differently with temperature than those of NSC. The differences are more pronounced in the temperature range from 25°C to about 400°C, where higher strength concretes have higher rates of strength loss than lower strength concretes. These differences become less significant at temperatures above 400°C. Compressive strengths of HSC at 800°C decrease to about 30% of the original room temperature strengths.
- For unstressed and stressed tests of HSC, the variations of compressive strength with temperature are characterized by three stages: (1) an initial stage of strength loss (25°C to approximately 100°C), (2) a stage of stabilized strength and recovery (100°C to approximately 400°C), and (3) a stage above 400°C characterized by a monotonic decrease in strength with increase in temperature. HSC has a higher rate of compressive strength loss in the temperature range between 100°C and 400°C compared to NSC.
- For unstressed residual strength tests of HSC, the compressive strength vs temperature relationships are characterized by two stages: (1) an initial stage of minor strength gain or loss (25°C to 200°C), and (2) a stage above 200°C in which the strength decreases with increasing temperature.
- The strength recovery stage of higher strength concretes occurs at higher temperatures than lower strength concretes. Compressive strengths of HSC obtained from the stressed tests are higher than those obtained from the unstressed and unstressed residual strength tests in the temperature range of 25°C to 400°C. The application of preload reduces strength loss in this range of temperature. Varying

*High-strength concrete is defined as concrete having a compressive strength in excess of 41.4 MPa for normal-weight concretes and 27.6 MPa for lightweight concretes.[129]

the preload levels from 25 to 55% of the original compressive strength, however, does not cause significant difference in compressive strengths of HSC at elevated temperatures.

- HSC mixtures with silica fume have higher strength loss with increasing temperatures than HSC mixtures without silica fume.
- The difference between the compressive strength vs temperature relationships of normal weight and lightweight aggregate concrete appears to be insignificant based on the limited amount of existing test data.
- The tensile strength vs temperature relationships decrease similarly and almost linearly with temperature for HSC and NSC. HSC retains approximately 50% of its original tensile strength at 500°C, and NSC retains an average of 45% of its original tensile strength at this same temperature.
- Explosive spalling failure occurs more in HSC than in NSC specimens. The reported temperature range when explosive spalling occurs is from 300°C to 650°C. Factors that influence spalling include original compressive strength, moisture content of concrete, concrete density, heating rate, and specimen dimensions and shape.
- Concrete with dense pastes due to the addition of silica fume are more susceptible to explosive spalling. Likewise, HSC made with lightweight aggregate appears to be more prone to explosive spalling than HSC made of normal weight aggregate concretes. HSC specimens heated at higher heating rates and larger specimens are more prone to spalling than specimens heated at lower rates and of smaller size.
- The failure of HSC is more brittle than NSC at temperatures up to 300°C. With further increase in temperature, specimens exhibit a more gradual failure mode.
- A temperature of 300°C marks the beginning of a higher rate of decrease in modulus of elasticity for all concretes. Lightweight aggregate concretes retain higher proportions of the original modulus of elasticity at high temperature than normal weight aggregate concretes. The difference is more pronounced for unstressed residual strength tests than for unstressed tests.

4 CONCRETE MATERIALS FOR ELEVATED-TEMPERATURE SERVICE

4.1 Elevated-Temperature Cements

NSCs using Type II Portland cement have somewhat limited use for high-temperature applications for the reasons cited previously. Refractory concretes, using Portland cement as the binder, perform poorly when thermally cycled in the presence of moisture, especially when cycled to temperatures above ~430°C. (Adding a fine siliceous material to react with the calcium hydroxide formed during hydration is helpful in alleviating this problem.) Portland cement binders are rarely used for applications above 650°C; hydrothermal, calcium aluminate, or tricalcium aluminate cements are required for such applications.

Hydrothermal (non-Portland) cements have been developed for lining oil wells,[131] but they are also potentially suitable for other applications in which heat may be deleterious to normal concrete materials. The materials are basically polymer silicates whose cure initiates at an activation temperature dependent on material formulation. After curing, the cements are capable of withstanding service temperatures of up to 538°C (up to 1093°C in certain formulations) without alteration of physical or mechanical properties. Additionally, the material system can be formulated to obtain (1) compressive strengths of 68.9 to 137.9 MPa, (2) excellent adhesion to metals except for a1uminum, (3) good resistance to aggressive environments, (4) low permeability, and (5) material system costs comparable with those of special Portland cements. However, the available data generally are limited to those supplied by the manufacturer.

Aluminous or high-alumina cement is a hydraulic cement used to make concrete in much the same manner as normal Portland cement. Calcium aluminate cement is made by grinding a compound formed by fusion or sintering of (1) high-iron bauxite and limestone (low purity), (2) low-iron bauxite with limestone (intermediate purity), or (3) aluminum hydroxide and hydrated lime (high purity). Although composition varies, chemical analyses of representative cements shows the principal oxides to be as follows: CaO, 35 to 44%; $A1_20_3$, 33 to 44%; SiO_2, 3 to 11%; and Fe_20_3, 4 to 12%. The principal products of hydration at room temperature are calcium-aluminate hydrates and some colloidal a1umina.[132,133] The high-alumina cements (1) exhibit rapid strength gains (up to 96.5 MPa in 24 h and 124.1 MPa in 28 d for a water-cement ratio of 0.5), (2) are resistant to aggressive environments, (3) may be used as refractory materials at temperatures up to 1800°C when special white calcium-aluminate cement is used with fused-alumina aggregate, and (4) exhibit creep similar to that of normal concretes loaded to the same stress/strength ratio.[32] However, the high-alumina cements (1) cost several times more than normal Portland cements, (2) must be protected against water loss during curing, (3) lose strength on exposure to hot moist environments unless a rich mix has been used, (4) are generally not compatible with many additives, (5) develop heat on curing ~2.5 times that of normal Portland cement (which may develop cracking and strength reductions in thick sections), (6) may lose workability rapidly after mixing, and (7) can contribute to accelerated steel corrosion. High-purity calcium-aluminate cements are used if high strengths are desired because they have superior resistance to CO attack, provide good workability without requiring water-reducing agents, and provide a high degree of refractoriness. Plasticizer additions generally reduce the strength of calcium-aluminate concrete mixes. The use of ca1cium aluminate cements for structural and load-bearing purposes is cautioned because of the complex chemical phenomenon known as conversion, which depends on time, temperature, and the presence of water. Conversion can cause a significant decrease in strength and an increase in permeability. The effects of

conversion can be controlled in nonrefractory applications by employing mix designs and installation practices that enable the use of sufficiently low water-cement ratios.

4.2 High-Temperature Aggregates

Many common coarse aggregates are unsuitable for high-temperature service because they contain quartz, which exhibits a large volume change at ~575°C. Accordingly, crushed stone and gravel-based aggregates suitable for use are limited to diabase traprock, olivine, pyrophylite, emery, and the expanded aluminosilicates (shales, clays, and slates). The latter can be used up to temperatures in the range of 1000 to 1150°C. In principle, all refractory grains may be used as aggregates, but in practice, most aggregates for refractory concretes contain mainly alumina and silica in various forms. The most widely used aggregates are probably calcined flint or kaolin containing 42 to 45% Al_20_3 (Ref. 134). Refractory aggregates such as crushed firebrick (30 to 45% Al_20_3) are stable to temperatures of 1300°C. For temperatures up to 1600°C, aggregates such as fused alumina or carborundum can be used; for temperatures up to 1800°C, special white calcium-aluminate cement and a fused-alumina aggregate are required. Sand, gravel, and traprock aggregates are generally used in calcium-aluminate cement mixes for temperatures below 260°C. Table 3 presents examples of typical aggregates for dense refractory concretes.[134]

4.3 High-Temperature (Refractory) Concrete Mixes

Refractory concrete is defined as a granular refractory material that, when mixed with water, will harden at room temperature to support its own weight sufficiently.[134] Generally a calcium-aluminate cement is used as the binder; however, sodium silicates and certain phosphates have also been used. Refractory concretes are classified according to strength and service limit criteria.[135]

The effect of water content on physical properties is critical. The amount of water necessary for a given material will depend on a number of factors: material proportions, ambient temperature, water temperature, type and speed of mixer, and size and shape of member to be cast. Excess water can seriously degrade the strength of dense refractory concrete, Fig. 98.[136] Mixing and curing temperature can affect the type of hydrates formed in set concrete. A castable develops its full hydraulic bond because of chemical reactions between calcium-aluminate cement and water. To get maximum benefits from these chemical reactions, it is preferable to form the stable C_3AH_6 during the initial curing period. The relative amount of C_3AH_6 formed vs metastable CAH_{10} and C_2AH_8 can be directly related to the temperature at which the chemical reactions take place.[137] Hydration of calcium-aluminate cements is an exothermic reaction. The specific heat of these cements is the same as Portland cement, 0.20 cal/g. Conversion of high-alumina cement hydrates, which occurs if the cement is allowed to develop excessive heat, does not present the same problem in refractory concretes that it does in high-alumina cement concretes used for structural purposes. Three principal techniques may be used for installing refractory concretes: troweling, casting, and shotcreting.

4.4 Properties of High-Temperature Concrete

Properties of refractory concretes are both time and temperature dependent. Initial heating of a high-temperature concrete causes physical and chemical changes (largely associated with eliminating combined water) and slight volume changes (usually shrinkage). Volume change produces two independent effects: (1) reversible thermal expansion* and (2) permanent change occurring during setting

*Generally values are ~5×10^{-6} cm/cm/°C, but can be as high as 9×10^{-6} cm/cm/°C.

Table 3 Aggregates (%) Used in Dense Refractory Concretes

Typical chemical composition	Calcined fireclay	Calcined Alabama bauxite		Calcined S. A. bauxite	High purity alumina sintered or fused	Chrome ore (Phillipine)
SiO_2	45–55	34.9	25.9	7.0	0.06	5.5
Al_2O_3	40–50	60.6	70.1	87.5	99.5	31.0
Fe_2O_3	0.5–1.5	1.3	1.1	2.00	0.06	15.5
TiO_2	1.0–2.0	2.5	2.9	3.25	Trace	
CaO	0.1–0.2	0.07	0.05	Trace	Trace	0.5
MgO	0.05–0.1	0.12	0.03	Trace	Trace	16.0
Cr_2O_3						31.5
Alkalies	0.5–1.5	0.11	0.13	Trace	0.07	
Pyrometric cone equivalent	30–34	37–38	38–39	38+	Not determined	Not determined
Bulk specific gravity	2.4–2.6	2.7–2.8	2.85–3.0	3.1	3.4–3.6[a] 3.7–3.9[b]	3.9
Open-porosity	3–10	3–7	4–10	12–20	5.0[a] 0–3[b]	

[a] Sintered.

[b] Fused.

Source: W.T. Bakker, "Properties of Refractory Concretes," Paper SP 57-2 in Refractory Concrete, American Concrete Institute, Farmington Hills, Michigan, 1978.

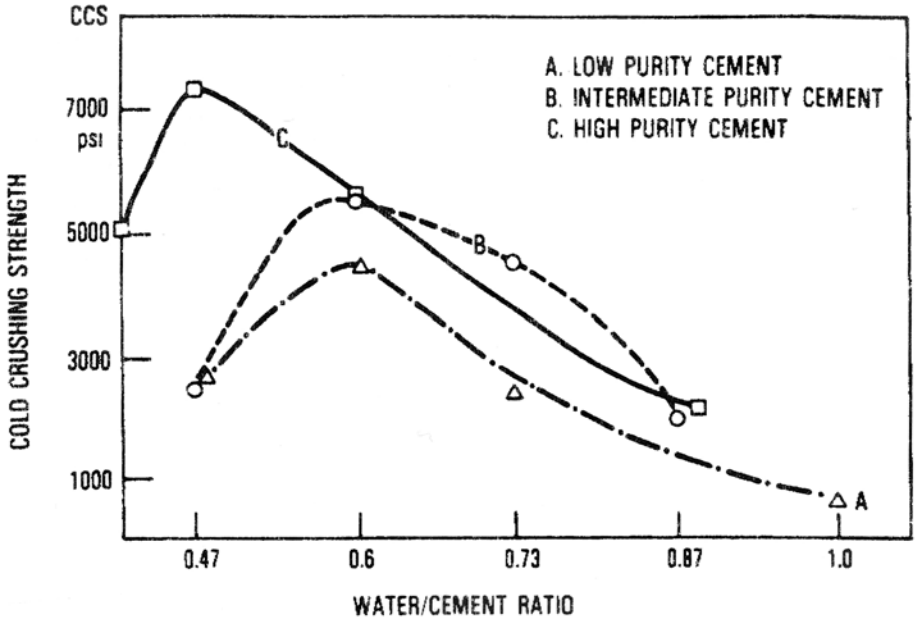

Figure 98 Effect of water/cement ratio on dried strength of dense refractory concrete. *Source*: A. V. Briebach, "A Review of Refractory Hydraulic Cement," *J. Brit. Cera, Soc.* **71**(7), 153–58.

and dehydration of the concrete and again when the glassy bond is formed at high temperatures.[138] Most normal weight high-temperature concretes will have <0.5% permanent linear shrinkage after firing at 1090°C (Ref. 137). Figure 99 presents length change as a function of temperature of a typical high-temperature concrete.[137]

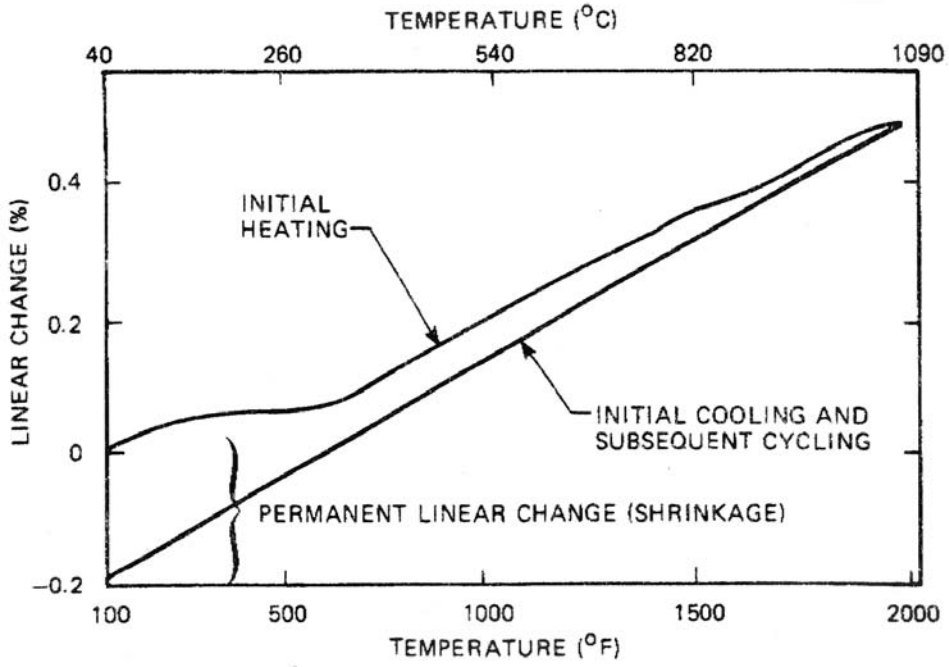

Figure 99 Length change as a function of temperature of a typical high-temperature concrete. *Source*: F. E. Linck, *Turnaround Maintenance*, Houston, Texas, October 6, 1980.

Strength properties are generally measured through compression and modulus-of-rupture tests. Generally, measurements are conducted at room temperature, probably because of difficulties in determining strains at elevated temperatures. Most high-temperature concretes have a marked decrease (25 to 50%) in strength when heated from 105°C to 540°C. Further heating from 540°C to 1090°C usually has only a slight effect on strength. At about 1090°C, initial liquid formation occurs, and the hot strength decreases considerably. Specimens heated above 1090°C and tested after cooling show a marked increase in cold strength because the liquids formed during heating vitrify on cooling to produce high cold strengths. Room-temperature compressive strengths of dense refractory concretes generally range between 13.8 and 55.2 MPa (Ref. 134). The effect of elevated temperature on modulus of elasticity is relatively minor when compared with normal Portland concrete systems. Figure 100 presents typical modulus-of-elasticity curves as a function of temperature for refractory concretes containing low- and high-purity cements.[138] Although data are limited, the modulus of elasticity tends to vary with strength, and values range from 6.9 to 55 GPa. Generally, the modulus of rupture of dense refractory concretes varies from about 4.8 to 10.3 MPa after drying at 104°C (Ref. 134). Figure 101 presents typical hot and cold modu1us-of-rupture results as a function of temperature for 40 to 50% Al_20_3 castables using a high-purity and intermediate-purity cement binder.[139] Figure 102 presents the effect of temperature on the stress-strain behavior of alumina-silicate bricks (85% alumina) tested in three-point bending.[140]

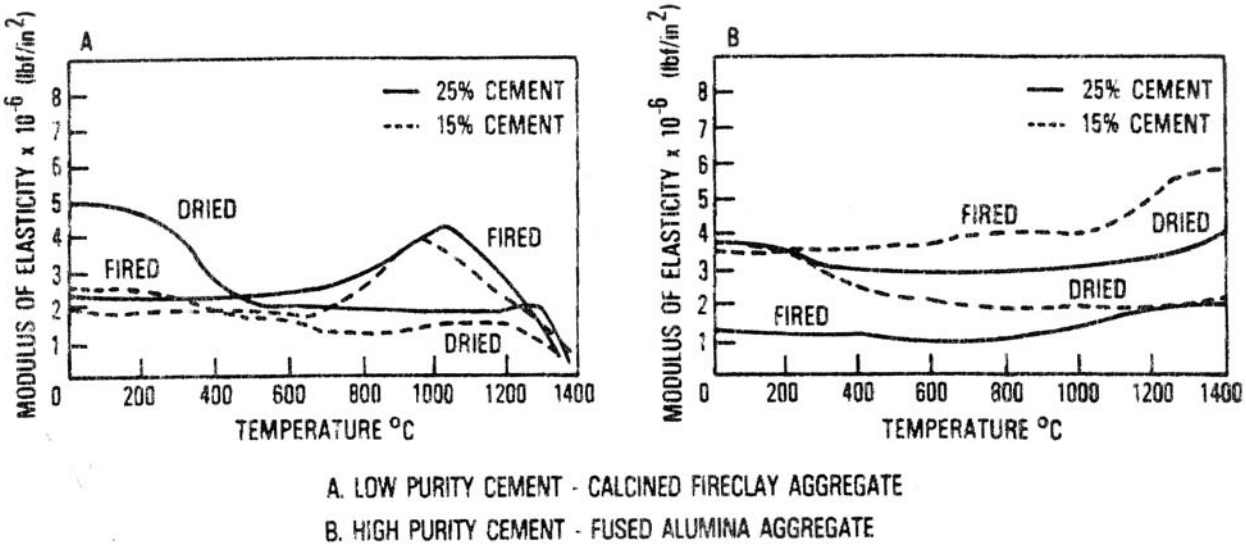

Figure 100 **Typical modulus of elasticity curves for refractory concretes containing low- and high-purity cements.** *Source*: J. M. McCullough and G. R. Rigby, "Mechanical Properties of Refractory Castables," *J. Brit. Cera. Soc*. **71**(7), 233.

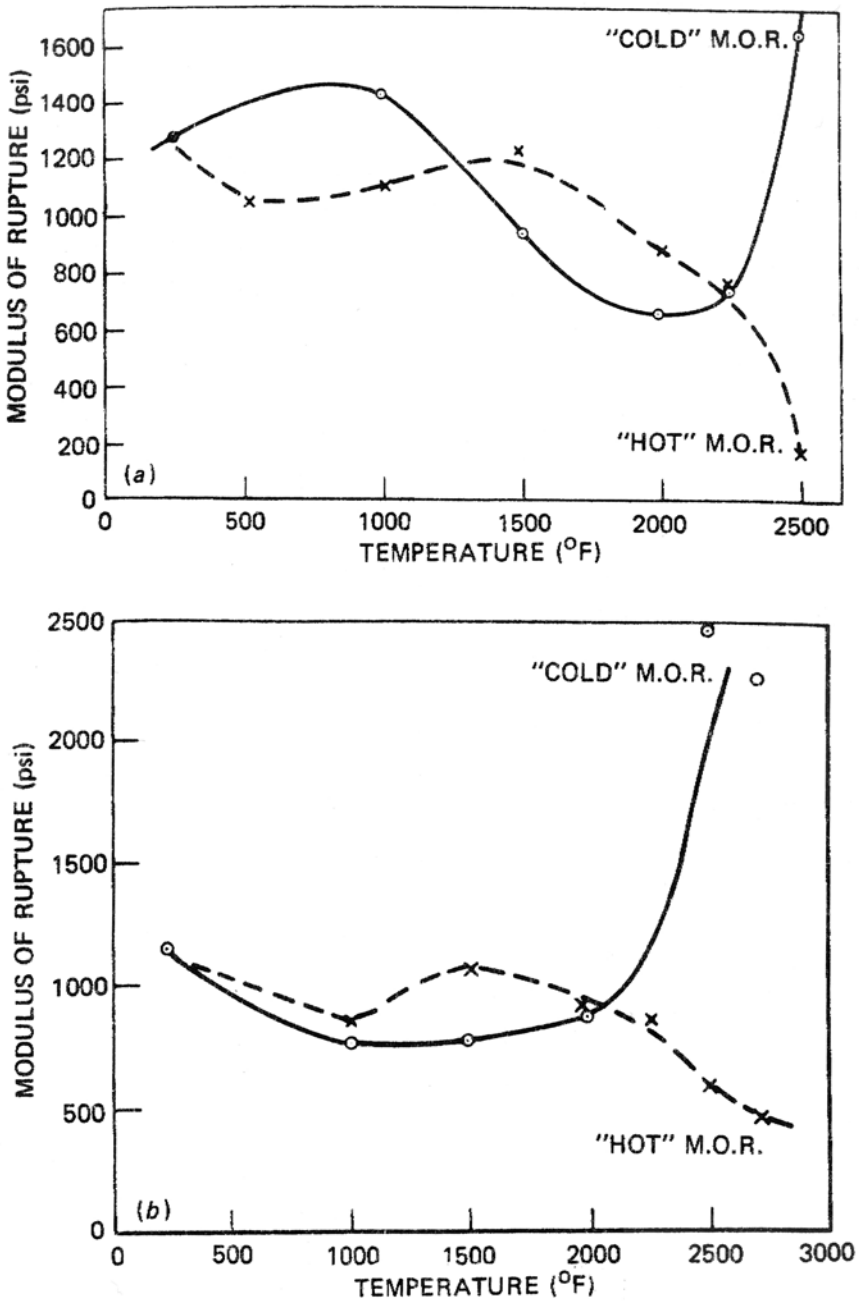

Figure 101 **Typical hot and cold modulus of rupture results for a 40–50% $A1_2O_3$ castable using (a) intermediate-purity cement and (b) high-purity cement.** *Source*: W. T. Bakker et al., "Blast Furnace Gunning in the USA," *Proceedings International Feuerafest Colloquium, Aachen, Germany, October 27–29, 1971*.

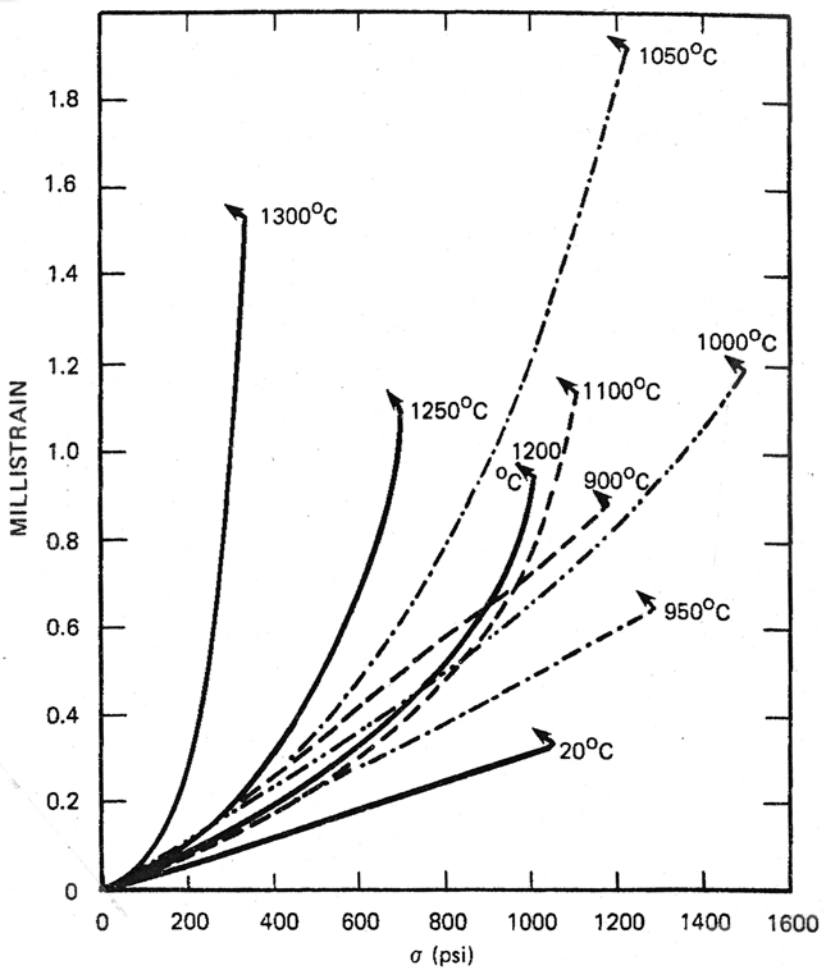

Figure 102 **Effect of temperature on stress-strain behavior of alumina-silicate bricks.** *Source*: G. C. Padgett et al., "Stress/Strain Behavior of Refractory Materials at High Temperatures," Research Paper 608, The British Ceramic Association.

For normal-weight concretes, thermal conductivity tends to increase with density and temperature (some high-alumina concretes may show a decrease with temperature) as shown in Fig. 103.[141] On first heat-up of refractories, generally a drop in thermal conductivity occurs as a result of binder dehydration; however, in actual applications as liner materials, the concrete at the cold face never gets dehydrated, so the thermal conductivity curve before dehydration is used for design. The presence of high thermal conductivity gases will significantly increase the overall thermal conductivity of the refractory 1iner.[142] Typical k factors range from about 72 W-cm m^{-2} $°C^{-1}$ for 1920 kg/m^3 material to about 144 W-cm m^{-2} $°C^{-1}$ for 2560 kg/m^3 material.[137] The specific heat of refractory concrete depends on its chemical composition and increases with temperature. Typical values range from 837 J kg^{-1} $°C^{-1}$ at 40°C to 1210 J kg^{-1} $°C^{-1}$ at 1370°C (Ref. 137). Total creep of refractory concretes does not vary much with temperature. The materials generally deform plastically at relatively low loads [~0.2 MPa] at temperatures greater than 1090°C and at high loads [3.4 to 13.8 MPa for temperatures as low as 316 to 538°C].[143] Creep evidently proceeds by the cement deforming until contacts between aggregate particles are estab1ished.[143]

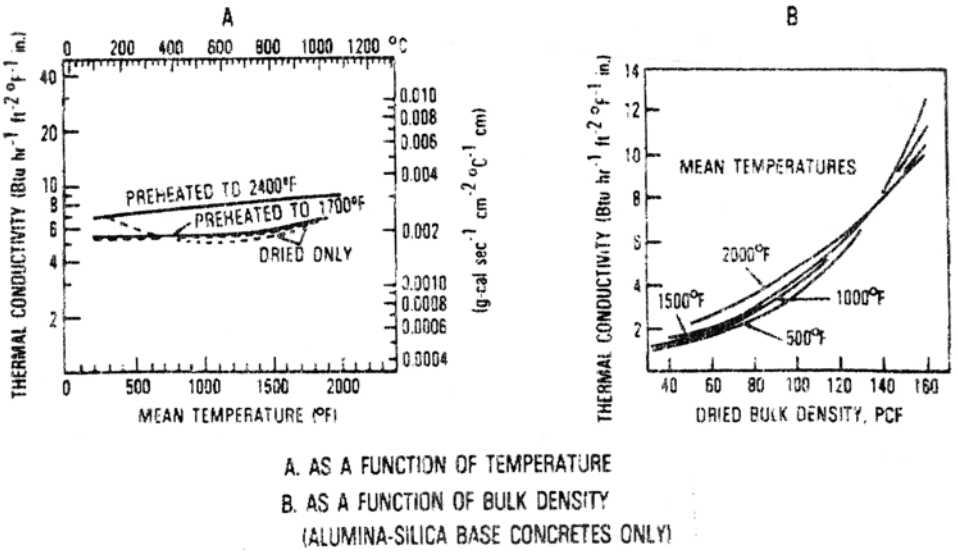

Figure 103 **Thermal conductivities of refractory concrete as a function of temperature and dried bulk density.** *Source*: E. Ruh and A. Renky, "Thermal Conductivity of Castable Refractories," *J. Am. Cera. Soc.* **46**(2), 1963.

The apparent porosity of most normal-weight high-temperature concretes is ~30 to 35% but may be as low as 20% for unfired samples because of closed pores and combined water. Permeability of concretes fired to 820°C and measured at room temperature is very low—typically 15 millidarcys, but can be as high as 1000 millidarcys. When fired to between 820°C and 1090°C, the room-temperature permeability may increase by a factor of 2 to 3 (Ref. 137).

4.5 Refractory-Insulating Concretes

Refractory-insulating concretes generally utilize calcium-aluminate cements as binders. When designed for heat retention purposes, the insulating concretes should not be subjected to impact, heavy loads, abrasion, erosion, or other physical abuse. Normally both the strength and the resistance to destructive forces decline as the bulk density decreases. However, a number of special refractory castables are available (high strength or extra strength) that have better-than-average load-bearing capabilities and can withstand abrasion or erosion much better than standard types. The lightweight refractory concretes are classified by bulk density (880 to 1680 kg/m^3) and service temperature (927°C to 1760°C).[135]

Lightweight aggregate refractory-insulating concretes require the same care in selection, aggregate gradation, and mix design as any other concrete mix. Differences in gradation and fines material content between specific aggregate types can produce variations in cement/aggregate volume, water requirements, and workability or plasticity characteristics. These variations can subsequently affect the porosity, strength, unit weight, and linear length change of the concrete. Fillers that generally consist of common refractory grains such as calcined kaolin, calcined bauxite, or kyanite (reduces high-temperature shrinkage) may be used to achieve proper grain sizing and desirable physical properties. Small amounts of finely ground plastic clay are sometimes added to a given mix to increase the workability or plasticity during placement; however, shrinkage of the concrete may increase proportionally with the clay additions, and setting time and strength may also be adversely affected. Also, short, randomly oriented fibers (stainless steel, fiberglass, tungsten, niobium, molybdenum) can be added to refractory concretes to provide improved properties relative to tensile strength, impact resistance, thermal shock resistance, and

thermal stress resistance.[144,145] Table 4[134] presents some typical lightweight aggregate materials used in refractory-insulating concretes, and Table 5[137] presents maximum service temperatures of selected aggregates mixed with calcium-aluminate cements under optimum conditions.

Properties of refractory concretes are time and temperature dependent. Porosities are higher than regular refractory concretes (on the order of up to 50%) because of the highly porous nature of the filler materials. Heat capacity is proportional to density; thus, it is low for these materials. Hot modulus-of-rupture values obtained for an expanded-clay insulating refractory concrete range from 0.6 MPa at 1482°C to 2.4 MPa at 110°C (Ref. 134). Cold compressive strengths vary between 1.4 and 3.4 MPa for materials having densities up to 800 kg/m^3 and between 6.9 and 17.2 MPa for materials having a density of 1200 to 1600 kg/m^3 (Ref. 134).

Table 4 Some Typical Lightweight Aggregate Materials Used in Refractory Concrete

Generic name	Perlite	Expanded shale (haydite)	Expanded fireclay	Alumina bubbles
Typical chemical composition, %				
Al_2O_3	19.5	24.0	27.1	99.0
SiO_2	70.0	63.0	64.3	0.8
Fe_2O_3	0.8	5.5	2.1	0.15
TiO_2	0.1	1.5	2.0	Trace
Alkaline earths	0.3	4.0	0.8	Trace
Alkalies	8.2	2.0	3.3	0.5
Bulk density, lb/ft^3 (kg/m^3)	9–11 (144–176)	55–60 (881–961)	28–32 (449–513)	34–38 (545–609)
Pyrometric cone equivalent	8–11	Not determined	27	>38
°F (°C)	2300–2450 (1260–1343)		2980 (1638)	>3400 (>1871)

Source: W. T. Bakker, "Properties of Refractory Concretes," Paper SP 57-2 in *Refractory Concrete,* American Concrete Institute, Farmington Hills, Michigan, 1978.

Table 5 Maximum Service Temperatures of Selected Aggregates Mixed with Calcium Aluminate Cements Under Optimum Conditions

Aggregate	Remarks	Maximum temperature [°F (°C)]
Alumina, bubble	Refractory, insulating	3300 (1820)
Alumina, fused	Refractory, abrasion resistant	3400 (1870)
Alumina, tabular	Refractory, abrasion resistant	3400 (1870)
Bauxite, calcined		3000 (1650)
Chrome-magnesite		3000 (1650)
Chromite	Slag resistant, high thermal conductivity, heavy	3000 (1650)
Corundum		3270 (1800)
Diatomaceous earth, calcined	Insulating	1830 (1000)
Dolomitic limestone (gravel)	Abrasion and corrosion resistant	930 (500)
Emery		2010 (1100)
Fireclay, expanded	Insulating, abrasion and corrosion resistant	2980 (1640)
Fireclay brick, crushed	Abrasion and corrosion resistant	2910 (1600)
Fireclay brick, crushed insulating	Insulating (maximum temperature depends on Al_2O_3 content)	2730 (1500)
Flint fireclay, calcined		3000 (1650)
Fly ash, expanded	Insulating (depends on composition)	2190 (1200)
Kaolin, calcined	Abrasion and corrosion resistant	3000 (1650)
Kyanite, calcined		3000 (1650)
Limestone (gravel)	Abrasion and corrosion resistant	1290 (700)
Mullite		3000 (1650)
Olivine		2500 (1370)
Perlite	Insulating	2450 (1340)
Pumice, expanded	Insulating	2000 (1090)

Table 5 (continued)

Aggregate	Remarks	Maximum temperature [°F (°C)]
Pyrophyllite[a]		2370 (1300)
Sand	Abrasion and corrosion resistant (silica content less than 90% not recommended)	570 (300)
Shale, expanded	Insulating, abrasion and corrosion resistant	2190 (1200)
Silicon carbide	High thermal conductivity	3090 (1700)
Sillimanite		2910 (1600)
Slag, blast furnace (air cooled)	Abrasion resistant	1000 (540)
Slag, blast furnace (granulated)	Insulating, abrasion and corrosion resistant	2190 (1200)
Slate, expanded	Insulating, abrasion and corrosion resistant	2190 (1200)
Trap rock, diabase	Abrasion and corrosion resistant (basic igneous rock—minimal quartz)	1830 (1000)
Vermiculite	Insulating	2010 (1100)

[a]The properties of pyrophyllite vary considerably, depending on the source and type. Note that both calcined and uncalcined pyrophyllite can be used; however, uncalcined pyrophyllite may undergo significant volume change on heating.

Source: F. E. Linck, "Turnaround Maintenance," Houston, Texas, October 6, 1980.

5 ELEVATED TEMPERATUE DESIGN CONSIDERATIONS

5.1 Significance and Current Practice

As noted previously, thermal gradients are important to concrete structures because they affect the concrete's compressive strength and stiffness. The compressive strength influences the load-carrying capacity, and the stiffness (modulus of elasticity) affects the structural deformations and loads that develop at restraints. Table 6 presents current ASME Code limits for various locations in a prestressed concrete reactor vessel (PCRV) for the appropriate conditions (normal operation and abnormal environment).[1] As noted in this table, the temperature in the concrete should not exceed 65°C at the liner-concrete interface and in the bulk concrete. Between cooling tubes (near the liner), 93°C is given as the maximum allowable. The French specification for PCRVs[146] limits temperatures in active parts of the concrete to 90°C; the British specification[147] states that if the normal operating temperature of any section of the vessel structure is such that the failure strength of the concrete at that temperature is significantly less than at ambient temperature, this will be taken into account. The British specification further notes that most concrete mixes subjected to temperatures above 100°C will suffer a reduction in compressive strength, and concrete with certain aggregates, particularly limestone, may suffer significant losses below that temperature. Figure 104 presents the BS8110 design curves for strength reduction with temperature of unsealed (a) dense concrete and (b) a lightweight aggregate concrete. Permissible temperatures for the concrete in PCRVs for gas-cooled reactors has generally been limited to the range of 45 to 80°C (Ref. 148).

5.2 Design Criteria

General Design Criteria 1. "Quality Standards and Records;" 2, "Design Bases for Protection Against Natural Phenomena;" and 4, "Environmental and Missile Design Bases," of Appendix A, "General Design Criteria for Nuclear Plants," to *10 CFR 50*, "Licensing of Production and Utilization Facilities," require, in part, that structures, systems, and components important to safety be designed, fabricated, erected, and tested to quality standards commensurate with the safety functions to be performed and that they be designed to withstand the effects of postulated accidents and environmental conditions associated with normal operating conditions.

Initially, existing building codes such as American Concrete Institute (ACI) Standard 318-71, "Building Code Requirements for Reinforced Concrete (ANSI A89.1-1972)" were used in the nuclear industry as the basis for the design of concrete structural members. However, because the existing building codes did not cover the entire spectrum of design requirements and because they were not always considered adequate, the U.S. Nuclear Regulatory Commission (USNRC) developed its own criteria for the design of Category I structures.* In particular, definitions of load combinations for both operating and accident conditions were provided, as well as a list of tornado-borne missiles and a description of the characteristics of tornados for different regions of the United States.

Using ACI 318-71 as a basis, with modifications to accommodate the unique performance requirements of nuclear plants, ACI Committee 349 developed and published in October 1976 ACI 349-76, "Code Requirements for Nuclear Safety Related Structures." The procedures and requirements described in this

*Category I structures are those essential to the function of the safety class systems and components, or that house, support, or protect safety class systems or components, and whose failure could lead to loss of function of the safety class system and components housed, supported, or protected.

Table 6 Condition Categories and Temperature Limits for Concrete and Prestressing Systems for PCRVs

Load category	Area	Temperature limits [°F (°C)]
Construction	Bulk concrete	130 (54)
Normal	Liner	
	Effective at liner-concrete interface	150 (66)
	Between cooling tubes	200 (93)
	Bulk concrete	150 (66)
	Bulk concrete with nuclear heating	160 (71)
	Local hot spots	250 (121)
	Distribution asymmetry	50 (10)
	At prestresing tendons	150 (66)[a]
	Liner interface transients (twice daily) range	100–150 (38–66)
Abnormal and severe environmental	Liner	
	Effective at liner-concrete interface	200 (93)
	Between cooling tubes	270 (132)
	Bulk concrete	200 (93)
	Local hot spots	375 (191)
	Distribution asymmetry	100 (38)
	At prestressing tendons	175 (79)
	Liner interface transients range	100–200 (38–93)
Extreme environmental	Liner	
	Effective at liner-concrete interface	300 (149)
	Between cooling tubes	400 (204)
	Bulk concrete	310 (154)
	Local hot spots	500 (260)
	Distribution asymmetry	100 (38)
	At prestressing tendons	300 (149)
	Liner interface transients range	100–200 (38–93)
Failure	Bulk concrete	
	Unpressurized condition	400 (204)
	Pressurized condition	600 (316)

[a]Higher temperatures may be permitted as long as effects on material behavior (e.g., relaxation) are accounted for in design.

Source: "Code for Concrete Reactor Vessels and Containments," Nuclear Power Plant Components, *ASME Boiler and Pressure Vessel Code*, Section III, Division 2, American Society of Mechanical Engineers, New York, New York, July 2003.

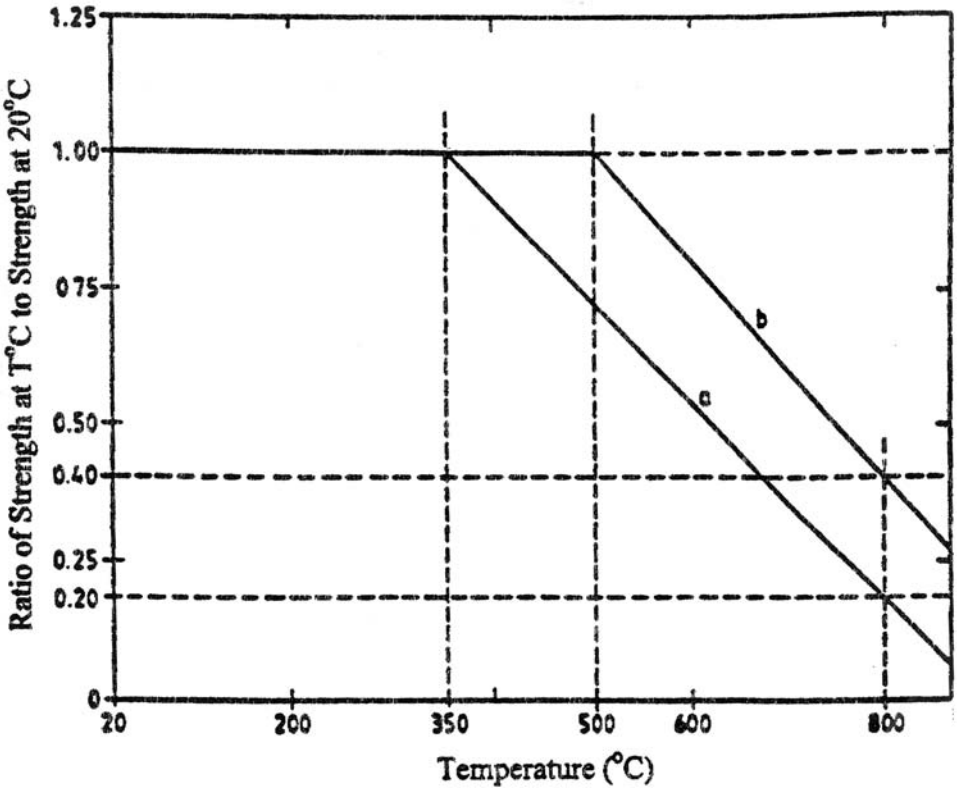

Figure 104 BS8110 design curves for strength variation with the temperature of (a) dense concrete and (b) lightweight concrete. *Source*: "Specification for Prestressed Concrete Pressure Vessels for Nuclear Reactors," BS 4975, British Standards Institution, United Kingdom, July 1973.

document are generally acceptable to the NRC staff and provide an adequate basis for complying with the general design criteria for structures other than reactor vessels and containments.* Conditions for applying the load requirements in ACI 349 are presented in U.S. Nuclear Regulatory Guide 1.142, and additional information on the design of seismic Category I structures that are required to remain functional if the Safe Shutdown Earthquake (SSE) occurs are contained in Ref. 149. Reference 150 presents a good comparison between ACI 318 and ACI 349.

Requirements for the design of concrete reactor vessels and containments are presented in ACI 359-77, ASME Section III—Division 2, "Code for Concrete Reactor Vessel and Containments."† Supplemental load combination criteria are presented in Sect. 3.8.1 of the *NRC Standard Review Plan.*[151]

National and international standards are available that provide guidance for computing concrete strength at elevated temperature: (1) Comité Europeen de Normalisation (Eurocode 2—Part 1-2, "Structural Fire Design," (2) Eurocode 4—Part 1-2, "General Rules for Structural Fire Design" and Comites Euro-International du Beton (CEB model code) Bulletin D'Information No. 208, "Fire Design of Concrete Structures," and National Building code of Finland's RakMK. Figure 105 presents a comparison of unstressed NCS results with the CEB and Eurocode Design curves.[130]

*ACI 349-76 is endorsed by U.S. Nuclear Regulatory Guide 1.142, "Safety-Related Concrete Structures for Nuclear Power Plants (Other than Reactor Vessels and Containments)."

†ACI 359-77 is endorsed by U.S. Nuclear Regulatory Guide 1.136, "Material for Concrete Containments."

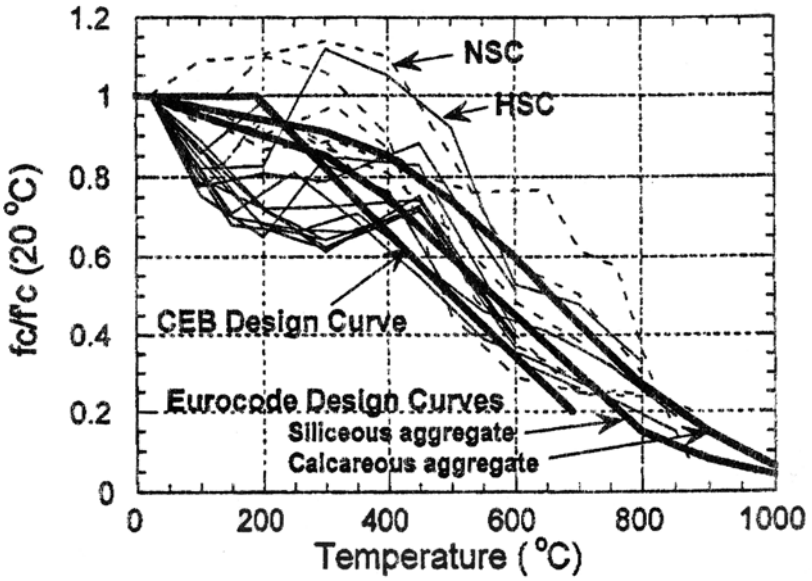

Figure 105 Comparison of unstressed NSC and HSC results with the CEB and Eurocode Design curves. *Source*: G. L. T. Phan, *Fire Performance of High-Strength Concrete: A Report of the State-of-the-Art*, NISTIR 5934, National Institute of Standards and Technology, Gaithersburg, Maryland, 1996.

5.3 Design of Reinforced Concrete Members Subjected to Elevated Temperature and Mechanical Loadings

The behavior of reinforced concrete sections at elevated temperature is of interest in the design of nuclear plant facilities for abnormal and severe environmental [bulk concrete temperature (≤93°C), local concrete hot spots (191°C)] as well as extreme environmental [bulk concrete temperature (≤149°C), local concrete hot spots (260°C)] load categories.* Also, it is important to predict the response of reinforced concrete components under hypothetical accident conditions for reactor designs in which concrete temperatures may exceed 600°C (e.g., a large sodium spill in the inerted and air-filled equipment cells of a liquid-metal fast breeder reactor).[152] The nonlinearities in material properties, the variation of properties with temperature, tensile cracking, and creep effects in the case of sustained capacity affect the buildup of thermal forces† and the deformation capacity or ductility of structural members. When severe temperatures are considered, a realistic behavior of concrete is essential in order to avoid undue and impractical design conservatisms. Examples of design procedures or considerations for elevated-temperature exposure are presented below.

American Concrete Institute (ACI) Committee 349, "Concrete Nuclear Structures," presents a design-oriented approach for considering thermal loads on reinforced concrete structures. Although the approach

*Table CB-3430-1 of Ref. 1. The low design temperatures in the Code reflect uncertainty in the concrete behavior at high temperature. Higher temperatures than those listed may be permitted in the concrete if tests are provided to evaluate the reduction in strength, and this reduction is applied to the design allowables. Also, evidence shall be provided which verifies that the increased temperatures do not cause deterioration of concrete either with or without load. Generally, to comply with the Code, structures that operate under or may see temperatures above the limiting values of the Code are provided with insulation and/or a cooling system.

†A characteristic of thermal forces in concrete members is that the forces tend to be self-relieving (i.e., high tensile forces produce cracks to lower the loads caused by temperature changes). Due to the cracks and concrete creep, the thermal stresses are nonlinear and dependent on the effect of member stiffness, which in turn varies with the magnitude of loading.

is intended to conform to the general provisions of Appendix A of ACI 349-76, it is not restricted to nuclear power plant structures. For frame structures, the thermal load is assumed to be represented by temperatures that vary linearly through the thickness of the member. A rationale is described for determining the extent of member cracking that can be assumed for purposes of obtaining the cracked structure thermal forces and moments. Stiffness coefficients and carry-over factors (carry-over loading from one section to another of a structural member) are presented in graphical form as a function of the extent of member cracking along its length and the reinforcement ratio. Fixed-end thermal moments for cracked members are expressed in terms of these factors for (1) a temperature gradient across the depth of the member and (2) end displacements due to a uniform temperature change along the axes of adjacent members. For the axisymmetric shells, the structure is considered to be uncracked for all mechanical loads and for part of the thermal loads. The thermal load is assumed to be represented by a temperature that is distributed linearly through the wall of the structure [i.e., linear temperature distribution is separated into a gradient ΔT and into a uniform temperature change $T_m - T_B$ where T_m is the mean temperature and T_B the base (stress-free) temperature]. Normalized cracked section thermal moments are presented in graphical form as a function of the reinforcement ratio and the internal axial forces and moments acting on the section. The moments have been normalized with respect to cross-sectional dimensions and the temperature gradient across the section. Examples are presented for both design of a frame and of an axisymmetric shell under mechanical and thermal loadings.

Kar[153] presents a method for analysis of two types of concrete members having uniform capacities along their lengths and subjected to a differential temperature from face to face: (1) members subjected to bending moments only, and (2) members having combined bending and axial faces. Kar's analysis is based on the hypothesis that in certain cases, the temperature load may tend to be self-limiting as a result of the formation of cracks in the member; and as the failure load condition or ultimate capacity is approached, the maximum temperature load that can occur is equal to that which is possible in the effective portion on the member-section at this load condition. (Thermal stresses are not considered as completely self-limiting, but are considered together with stresses due to other causes.) The stiffness of the member at ultimate load is used in the analysis. The effective moment of inertia is that for a cracked section with the depth of the cracked section being larger than the depth to the neutral axis. Also, the effective moment of inertia for the full member is larger than the moment of inertia of the cracked section. Recommendations made for the effective moment of inertia of concrete members reduce the necessity of iterative calculations such as required in ACI 349, "Code Requirements for Nuclear Safety Related Concrete Structures." A step-by-step approach is presented for the analysis and design of a member subjected to bending moment only and a member subjected to combined bending and axial forces.

Gurfinke1[154] used both elastic and inelastic analyses to investigate thermal effects on reinforced concrete sections subjected to axial load and bending (i.e., the incremental bending induced in the wall of an unattached containment by a given thermal differential). Results of the investigation indicated that (1) for a given section, the moment induced by a given thermal differential depends an the external axial load and bending moment to which the section is subjected; (2) upper and lower limits exist for elastically determined thermal moments in any section under a given thermal differential depending on whether the moment of inertia of the uncracked or cracked section is used; (3) at service load conditions, elastic analysis renders thermal effects that are smaller than those obtained using inelastic analysis; and (4) inelastic analysis should be used to determine thermal effects in walls of containment structures since ultimate conditions can only be determined using inelastic analysis.

Mentes et al.[155] note that thermal analysis methods can be classified into three categories, depending on the criteria used to calculate effective stiffness: (1) reduced flexural stiffness, (2) average flexural

stiffness, and (3) variable flexural stiffness. The reduced flexural method yields thermal moments that are on the unsafe side, and the combined thermal and nonthermal moments calculated may be safe or unsafe depending on the loading. Average flexural stiffness methods assume an average stiffness between the uncracked and cracked section values to account for the effects of stress level and tension stiffening and may require considerable iterative solutions. Variable flexural stiffness methods assume that members have reduced rigidities in the cracked sections and full uncracked rigidity along the rest of the member, but the methods present difficulties in including the effects of stress level and tension stiffening. These methods do, however, point out that to obtain a realistic evaluation of thermal moments in reinforced concrete members, it is necessary to consider proper stiffnesses and load interaction. The procedure for design of beams and frames is as follows: (1) assume all members uncracked, determine the mechanical load moments and amount of reinforcement required under mechanical load conditions; (2) increase the amount of reinforcement sufficiently to account for both mechanical and thermal load effects; (3) calculate the effective moment of inertia for all members; (4) calculate the equivalent fixed-end moments at all joints due to thermal loads, and add fixed-end moments due to mechanical loads; (5) using the effective moment of inertia, determine factors for distribution of fixed-end moments in the structure; (6) update the effective moment of inertia, using an equation provided, and combine moment values, then, if required, repeat this determination until satisfactory agreement between effective moment of inertia values is obtained; and (7) check that serviceability requirements are met. A flexurally restrained (but freely extendable) beam subjected to thermal load in absence of mechanical load and a portal frame subjected to combined mechanical and thermal loads are analyzed using this procedure and the results compared to those obtained using the aforementioned criteria that have been utilized to calculate effective stiffness.

Freskakis[156] examined the behavior of a reinforced concrete section (Fig. 106) by means of moment-curvature-axial force relationships that account for both the effect of temperature on the material properties and the mechanical effects induced by the tendency for thermal expansion. Of particular interest was the load carrying capacity, the thermal forces, and the deformation capacity. The effects on these properties due to variation in strength with temperature, the temperature level and its distribution across the section, the amount of reinforcing steel (0.75, 1.0, and 2.0%), and limiting values of compressive strain (0.003 and 0.004) were considered. Figures 17 and 23 presents upper and lower bound

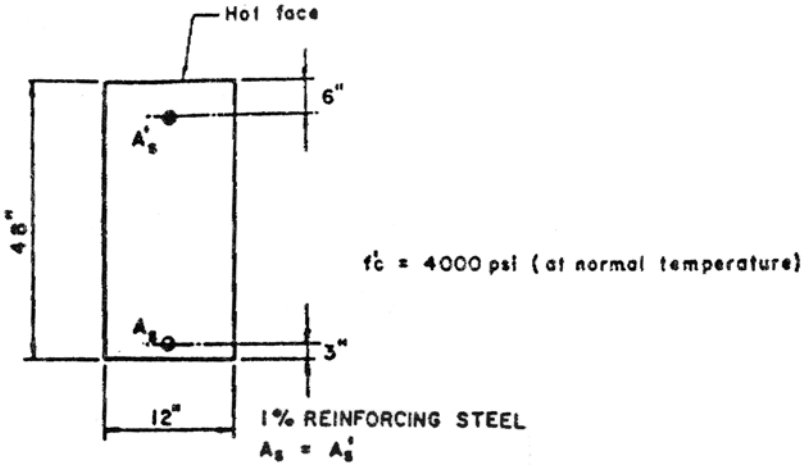

Figure 106 Reinforced concrete section examined by Freskakis. *Source*: G. N. Freskakis, "Behavior of Reinforced Concrete at Elevated Temperature," Paper 3-4, *Second ASCE Conf. on Civ. Eng. and Nuclear Power*, Vol. 1, Paper 3-5, pp. 3-5-1 to 3-5-21, Knoxville, Tennessee, September 15–17, 1980.

relationships for the concrete modulus of elasticity and residual strength, respectively, as a function of temperature. Stress-strain relationships for the concrete based on the lower and upper bound relations in these figures are presented in Figs. 107 and 108, respectively. Stress-strain relationships at various temperatures used for the Grade 60 reinforcing bars are presented in Fig 109. Thermal gradients considered in the study that had temperatures either of 149, 260, or 427°C at the face of the concrete section are presented in Fig. 110. The three thermal gradients in Fig. 110 represent short (Type I), intermediate (Type II), and long (Type III) duration thermal exposures. Results from this study for selected parameters are presented in Figs. 111 to 119. From these results, it was concluded that (1) the effect of elevated temperature is to decrease the section capacity when axial forces are present, and the net carrying capacity decreases significantly with the buildup of thermal forces; (2) in terms of bending and axial force capacity, reinforced concrete sections can be designed to sustain severe temperature gradients with levels of temperature much higher than allowed by present codes; (3) comparison of net moment capacity results based on the upper and lower bound strength and modulus of elasticity relationships indicates that either upper or lower bound relations may govern the design depending on the level and distribution of temperature across the section and the axial compression (e.g., upper bound should be considered for temperatures above 260°C and where heat of exposure is of short duration); (4) addition of reinforcing steel improves the net capacity of the sections, but the steel must be properly located in the section or a significant reduction in capacity can result; (5) where strain limits are imposed, increases in the temperature level result in significant reductions in rotational ductility; (6) for temperatures up to about 205°C, the use of a limiting concrete strain of 0.003 does not result in a significant loss in member strength, but at higher temperatures a significant reduction of strength occurs in the presence of compressive forces; and (7) the concrete tensile strength is important in the calculation of thermal forces at low elevated temperatures, but is insignificant where severe temperatures are present.

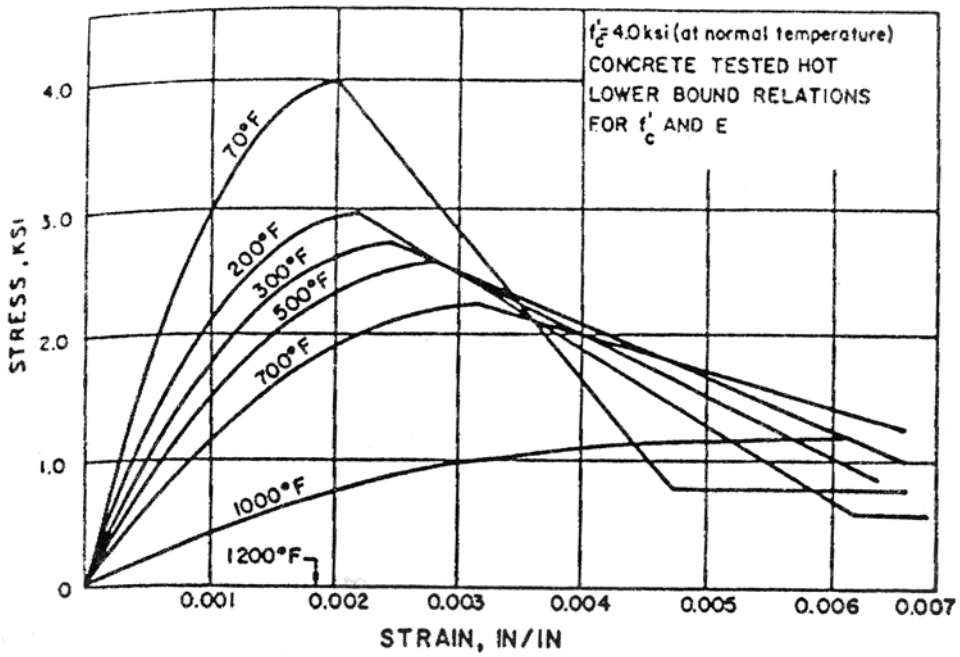

Figure 107 **Stress-strain relationships for concrete used by Freskakis (lower bound).** *Source*: G. N. Freskakis, "Behavior of Reinforced Concrete at Elevated Temperature," Paper 3-4, *Second ASCE Conf. on Civ. Eng. and Nuclear Power*, Vol. 1, Paper 3-5, pp. 3-5-1 to 3-5-21, Knoxville, Tennessee, September 15–17, 1980.

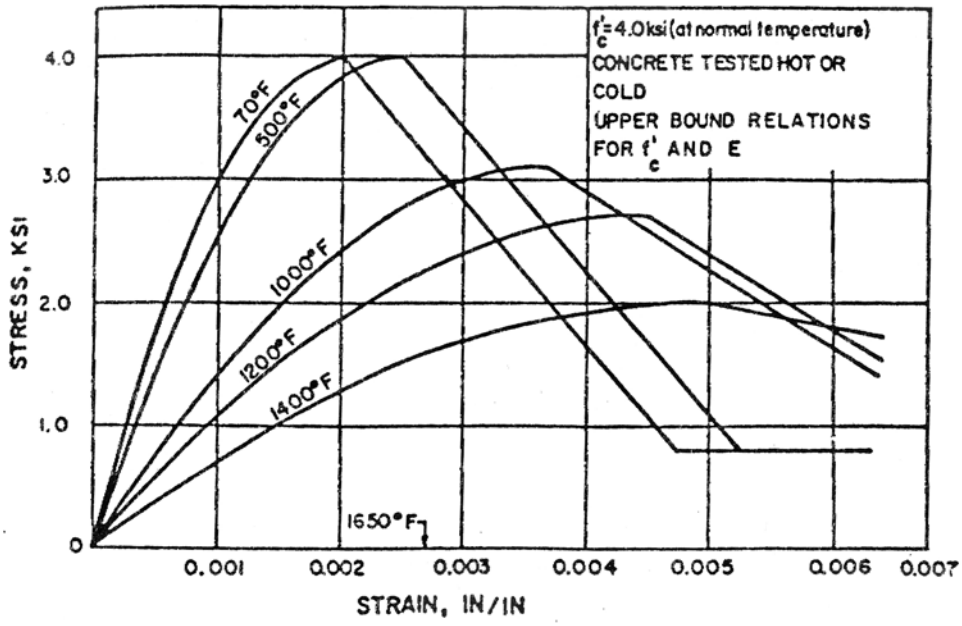

Figure 108 **Stress-strain relationships used by Freskakis (upper bound).** *Source*: G. N. Freskakis, "Behavior of Reinforced Concrete at Elevated Temperature," Paper 3-4, *Second ASCE Conf. on Civ. Eng. and Nuclear Power*, Vol. 1, Paper 3-5, pp. 3-5-1 to 3-5-21, Knoxville, Tennessee, September 15–17, 1980.

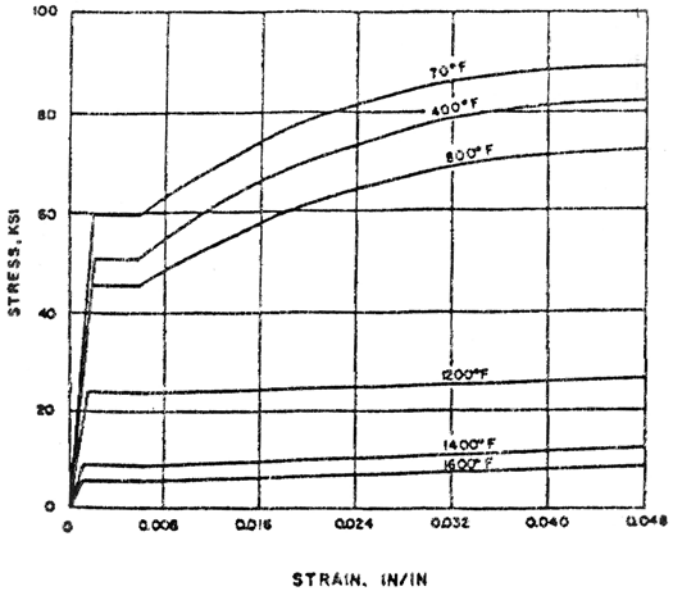

Figure 109 **Stress-strain relationships for rebars used by Freskakis.** *Source*: G. N. Freskakis. "Behavior of Reinforced Concrete at Elevated Temperature," Paper 3-4, *Second ASCE Conf. on Civ. Eng. and Nuclear Power*, Vol. 1, Paper 3-5, pp. 3-5-1 to 3-5-21, Knoxville, Tennessee, September 15–17, 1980.

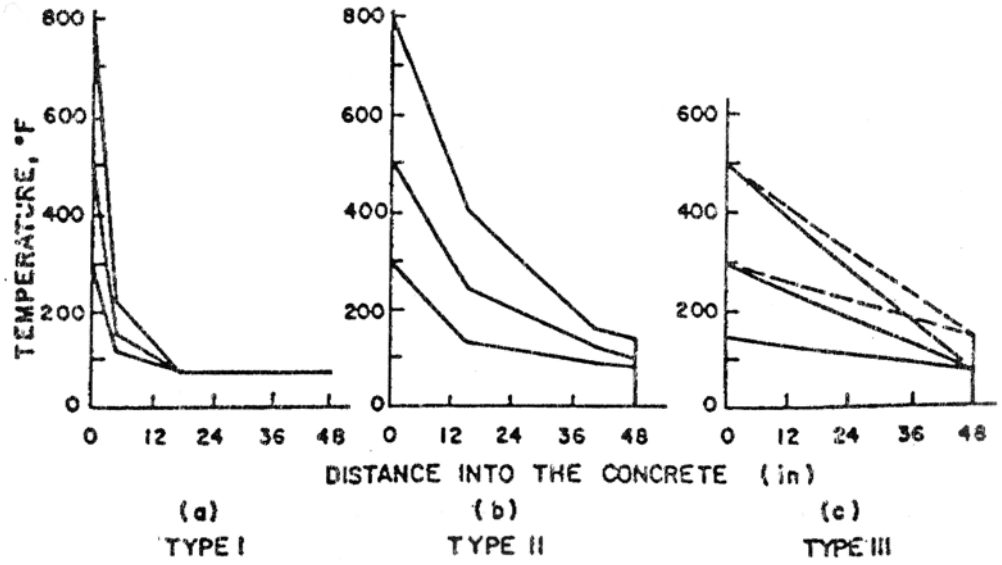

Figure 110 **Thermal gradients investigated by Freskakis.** *Source*: G. M. Freskakis, "Behavior of Reinforced Concrete at Elevated Temperature," Paper 3-4, *Second ASCE Conf. on Civ. Eng. and Nuclear Power*, Vol. 1, Paper 3-5, pp. 3-5-1 to 3-5-21, Knoxville, Tennessee, September 15–17, 1980.

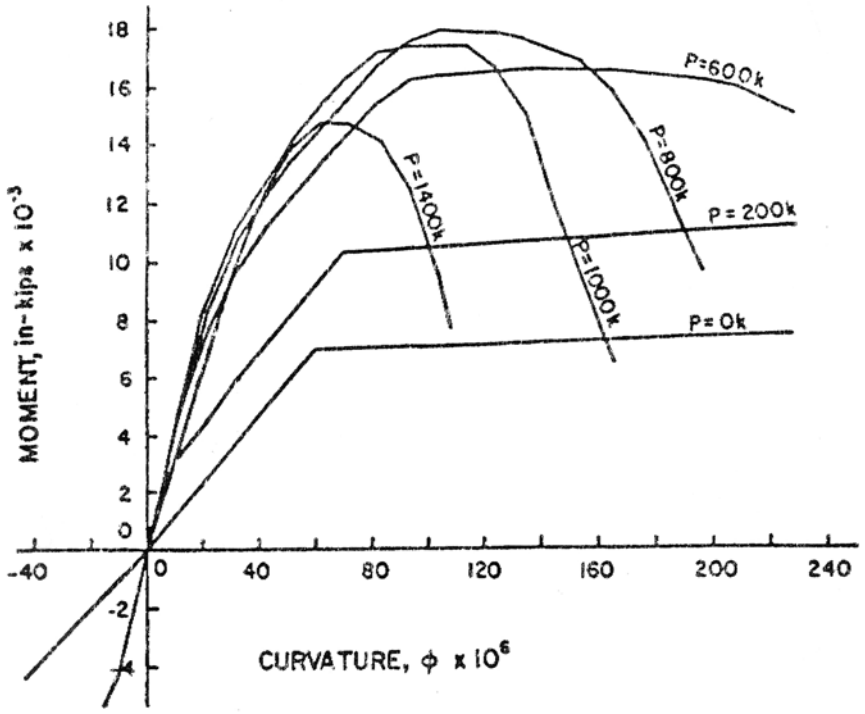

Figure 111 **M-ϕ-P relationships: normal temperature.** *Source*: G. N. Freskakis, "Behavior of Reinforced Concrete at Elevated Temperature," Paper 3-4, *Second ASCE Conf. on Civ. Eng. and Nuclear Power,* Vol. 1, Paper 3-5, pp. 3-5-1 to 3-5-21, Knoxville, Tennessee, September 15–17, 1980.

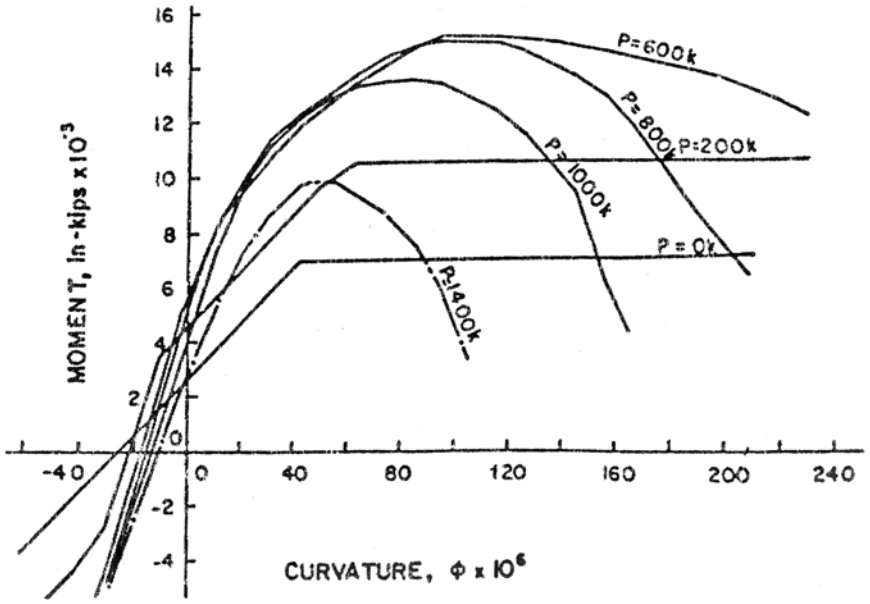

Figure 112 **M-ϕ-P relationships: T_1 = 300°F (based on lower bound relations).** *Source*: G. N. Freskakis, "Behavior of Reinforced Concrete at Elevated Temperature," Paper 3-4, *Second ASCE Conf. on Civ. Eng. and Nuclear Power*, Vol. 1, Paper 3-5, pp. 3-5-1 to 3-5-21, Knoxville, Tennessee, September.

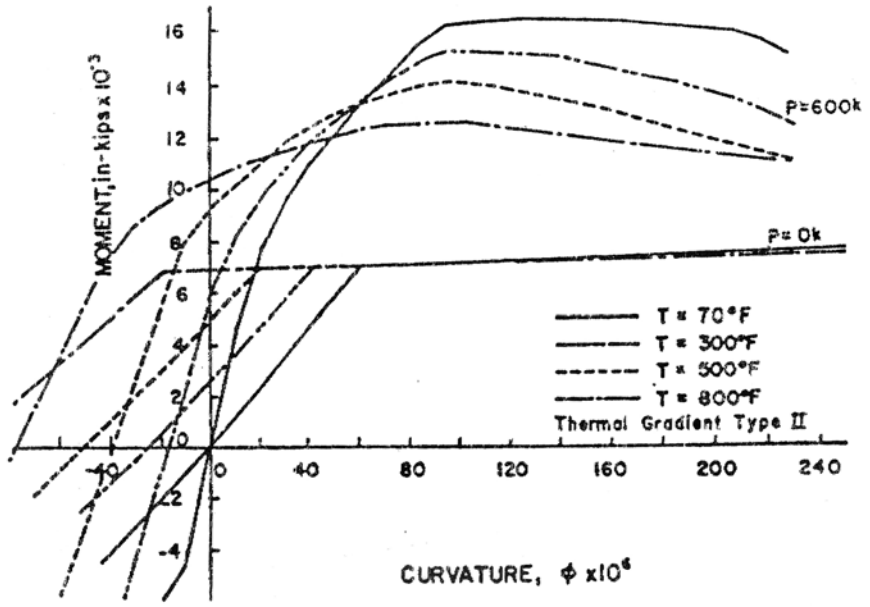

Figure 113 **Effect of temperature level on behavior (based on lower bound relations).** *Source*: G. N. Freskakis, "Behavior of Reinforced Concrete at Elevated Temperature," Paper 3-4, *Second ASCE Conf. on Civ. Eng, and Nuclear Power*, Vol. 1, Paper 3-5, pp. 3-5-1 to 3-5-21, Knoxville, Tennessee, September 15–17, 1980.

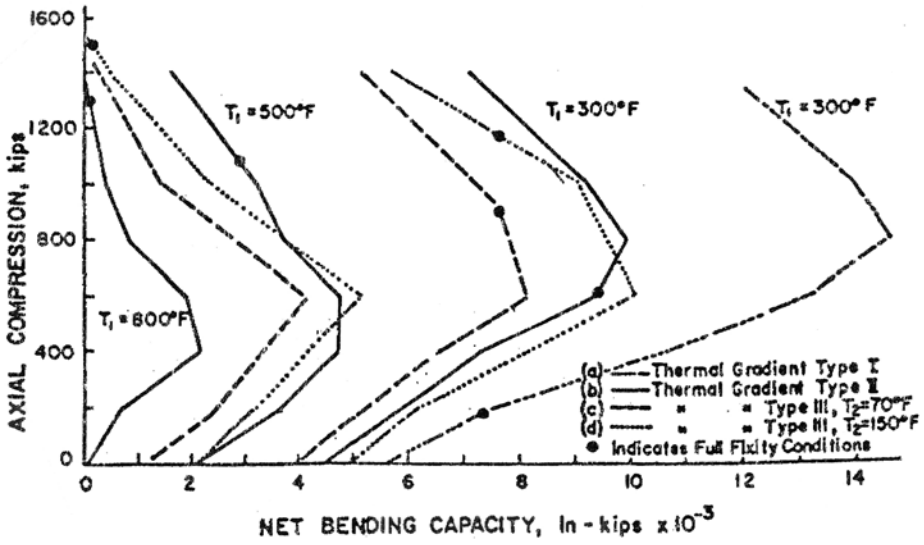

Figure 114 **Effect of temperature distribution on net bending capacity.** *Source*: G. N. Freskakis, "Behavior of Reinforced Concrete at Elevated Temperature," Paper 3-4, *Second ASCE Conf. on Civ. Eng. and Nuclear Power*, Vol. 1, Paper 3-5, pp. 3-5-1 to 3-5-21, Knoxville, Tennessee, September.

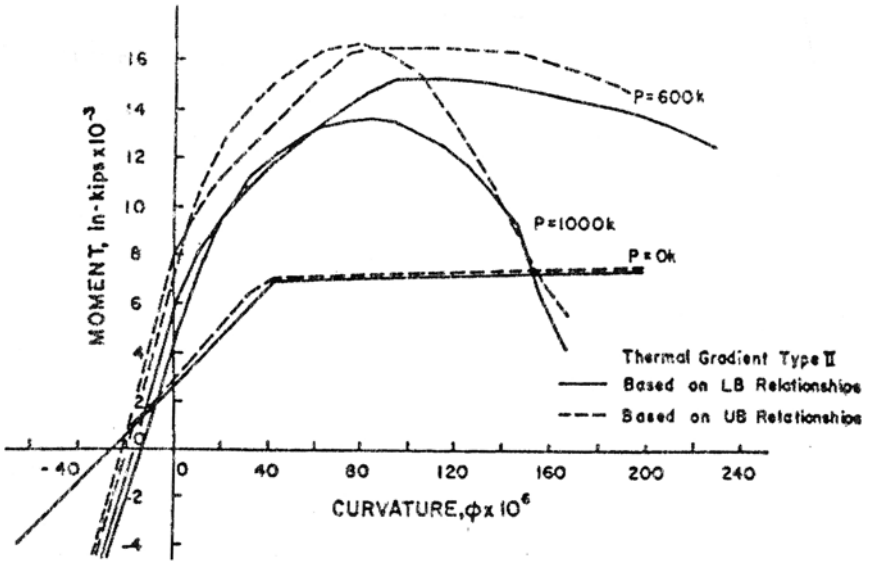

Figure 115 **N-ϕ-P diagrams based on upper and lower bound strength relations.** *Source*: G. N. Freskakis, "Behavior of Reinforced Concrete at Elevated Temperature," Paper 3-4, *Second ASCE Conf. on Civ. Eng. and Nuclear Power*, Vol. 1, Paper 3-5, pp. 3-5-1 to 3-5-21, Knoxville, Tennessee, September 15–17, 1980.

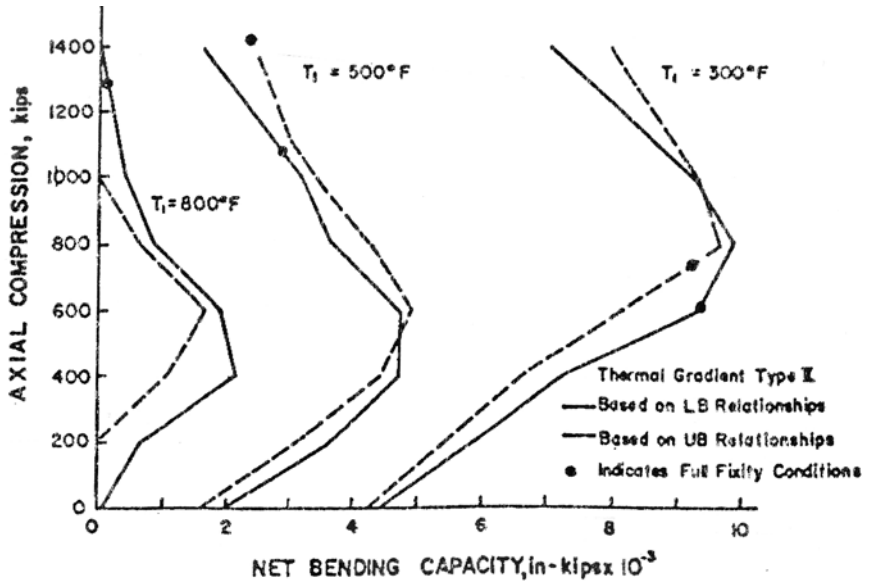

Figure 116 Net bending capacity based on upper and lower bound strength relations. *Source*: G. N. Freskakis, "Behavior of Reinforced Concrete at Elevated Temperature," Paper 3-4, *Second ASCE Conf. on Civ. Eng. and Nuclear Power*, Vol. 1, Paper 3-5, pp. 3-5-1 to 3-5-21, Knoxville, Tennessee, September 15–17, 1980.

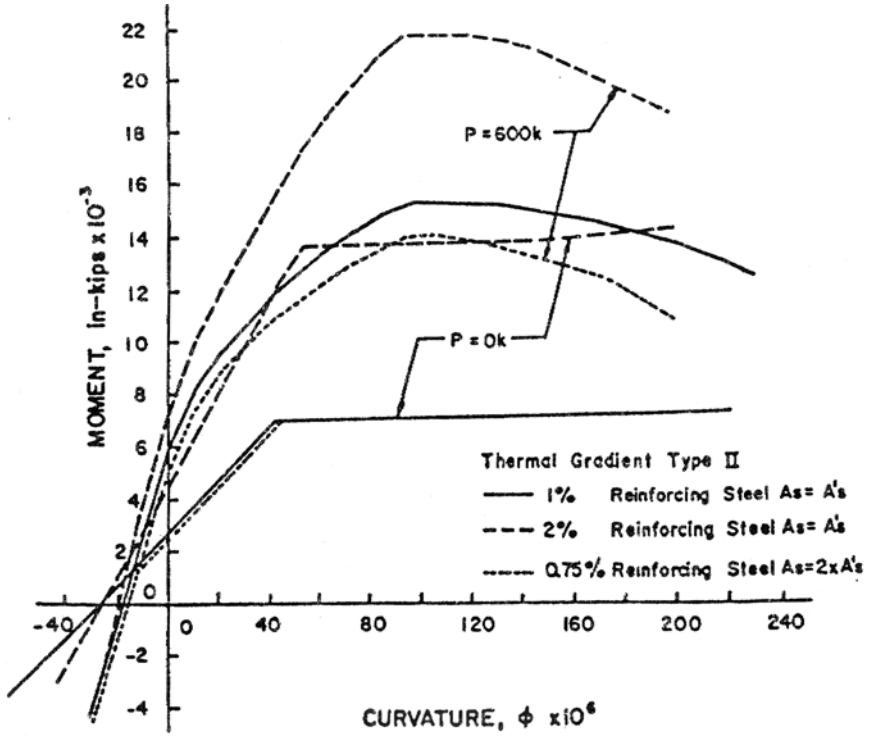

Figure 117 Effect of reinforcing steel on behavior (based on lower bound relations). *Source*: G. N. Freskakis, "Behavior of Reinforced Concrete at Elevated Temperature," Paper 3-4, *Second ASCE Conf. on Civ. Eng. and Nuclear Power*, Vol. 1, Paper 3-5, pp. 3-5-1 to 3-5-21, Knoxville, Tennessee, September 15–17, 1980.

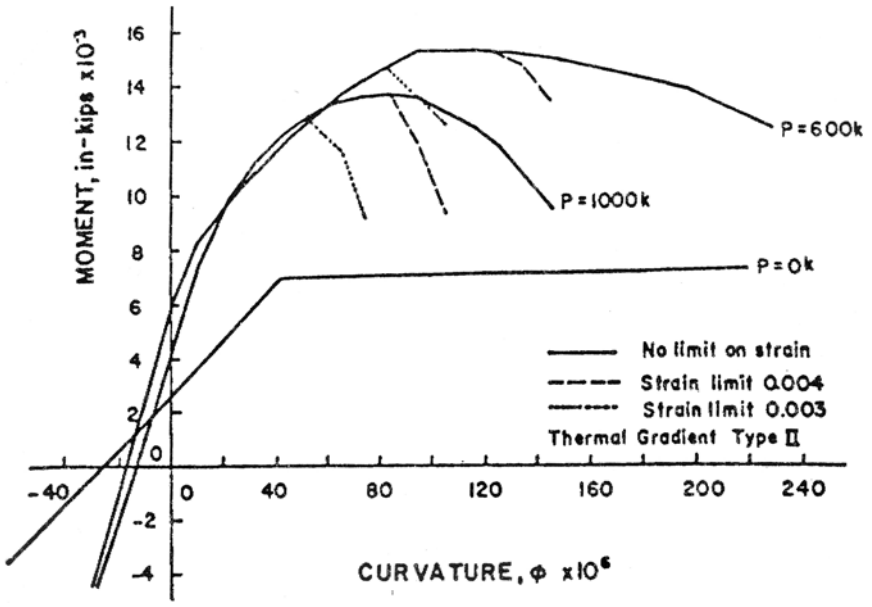

Figure 118 **Effect of strain limits on behavior: T_1 = 300°F (based on lower bound relations).** *Source*: G. N. Freskakis, "Behavior of Reinforced Concrete at Elevated Temperature," Paper 3-4, *Second ASCE Conf. on Civ. Eng, and Nuclear Power*, Vol. 1, Paper 3-5, pp. 3-5-1 to 3-5-21, Knoxville, Tennessee, September 15–17, 1980.

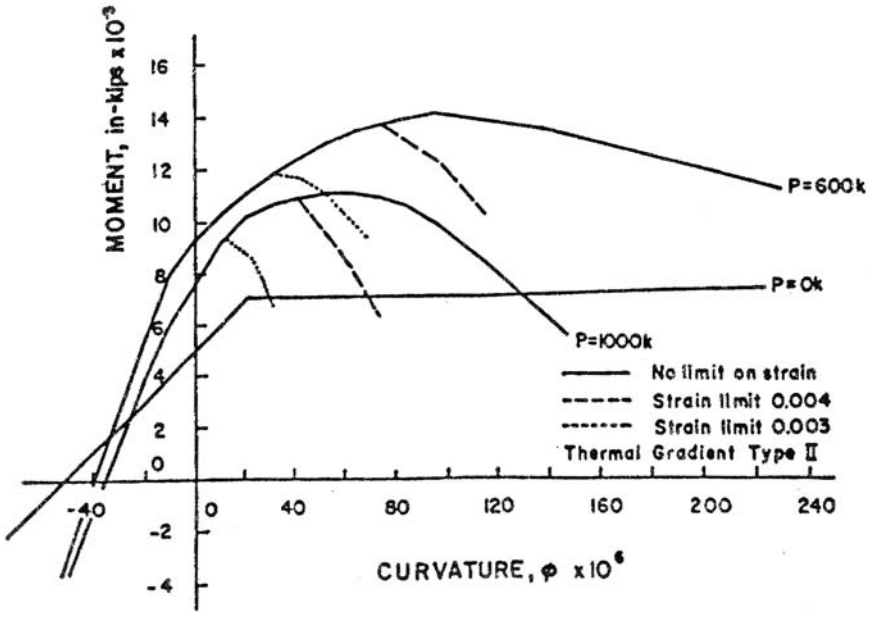

Figure 119 **Effect of strain limits on behavior: T_1 = 500°F (based on lower bound relation).** *Source*: G. N. Freskakis, "Behavior of Reinforced Concrete at Elevated Temperature," Paper 3-4, *Second ASCE Conf. on Civ. Eng. and Nuclear Power*, Vol. 1, Paper 3-5, pp. 3-5-1 to 3-5-21, Knoxville, Tennessee, September 15–17, 1980.

Information has been developed relative to prediction of the response of reinforced concrete structures to variations in temperature, humidity, and load, as well as modeling of the structures, their loading history, environmental factors, and material behavior.[157] Cracking, excessive deformation, spalling, and even partial collapse of reinforced concrete structures frequently result from variations in environmental and loading conditions not considered in design. Such distress should be minimized through incorporation of an analysis of these effects of complex environmental and loading histories into design practice. A general scheme for such a design process is illustrated by flow chart in Fig. 120, where the sequence of evaluation and analysis is indicated. Basically, it includes (1) modeling the structure, (2) modeling environmental and loading history, (3) deciding whether an environmental response analysis is required, (4) executing an environmental response analysis (when necessary), otherwise proceed directly to structural response analysis, (5) analyzing the structural response to critical loading combinations, including environmental effects when necessary, and (6) verifying that structural response compiles with performance requirements. The simplified models for selected environments and for material behavior described in the reference permit practical engineering solutions. The details of the processes using these simplified models are described below. Basic modeling aspects of the approach follow:

1. Modeling the Structure: Simplified structural analysis and determination of thermal and shrinkage distribution throughout a concrete structure, large structures are sub-structured, substructures are divided into members, members are divided into segments, and segments are divided into elements representing concrete and steel components.

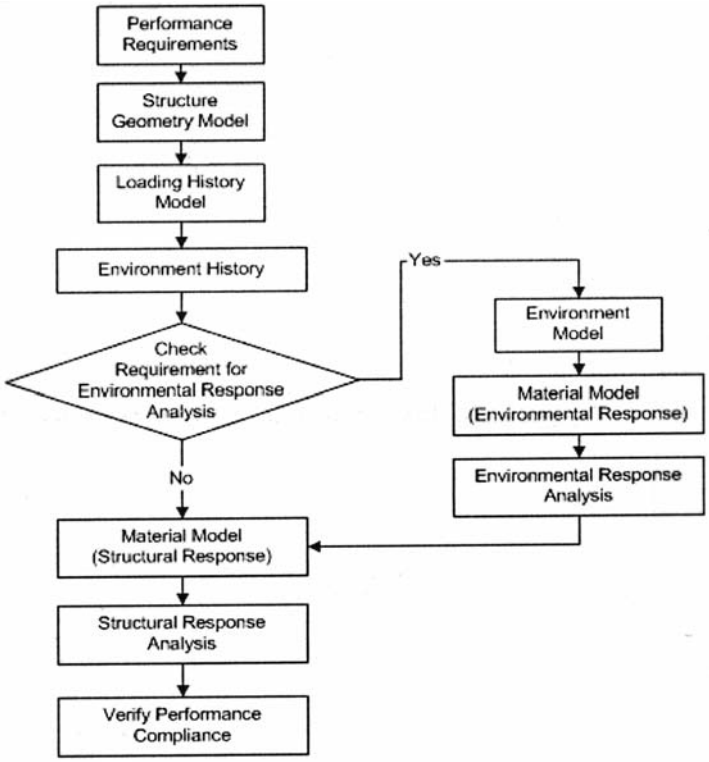

Figure 120 **Design process flow diagram.** *Source*: B. Bresler and R. H. Iding, "Effects of Normal and Extreme Environment on Reinforced Concrete Structures," Paper SP 55-11 in *Douglas McHenry Symposium on Concrete and Concrete Structures*, SP 55, American Concrete Institute, Farmington Hills, Michigan, April 1970.

2. Loading History: Important variation in loading during the life of a structure includes the following two stages: (a) Construction stage: The influence of early load history on structural response is particularly important when large loading increments develop while concrete is not fully mature. (b) Service life stage: Load increments are due to furnishing and occupancy loads in building, traffic load on bridges, etc.
3. Modeling of the Environment: Physical environmental effects can be divided into two categories: (a) normal service conditions (atmospheric environment-structural response to changes in environment depends on variations in ambient air temperature, relative humidity, wind, and sky cover); and (b) extreme conditions (fire environment modeling with important parameters in establishing models for fire environment being fire load, ventilation, compartment geometry, and surface characteristics).
4. Modeling Material Behavior: In the structure response analysis, two types of strains are calculated: (1) free strains associated with changes in the environment in the absence of any restraint or stress, which includes thermal and shrinkage strains, and (2) stress-related strains (instantaneous and time-dependent) including degradation of material such as cracking or crushing of concrete including instantaneous strains, steel and concrete response in tension and compression, effect of temperature on instantaneous strain, creep strain, and effect of temperature on creep strain.
5. Modeling Free Volume Changes: The first step in analyzing environmental response is to determine unrestrained free volume change due to moisture movement and temperature change. Issues to be considered include thermal volume change (e.g., boundary conditions and internal heat generation), and free shrinkage volume changes (i.e., boundary condition, shrinkage diffusivity, and surface layer).

Once all modeling assumptions have been made, it is possible to proceed with the structural analysis. A modification of direct stiffness method of matrix structural theory is used. The approach described above was applied to four case studies.[157] In the first two studies, analytical results were correlated with experimental results of studies on shrinkage in specimens of varying size. In the third study, the method was applied to the special problem in concrete construction related to response under permafrost condition. In the fourth study, the response of reinforced concrete frame to a hypothetical thermal excursion (compartment fire) was analyzed. In the first two case studies, the agreement between calculated and observed shrinkage was very good. In the third case study, the comparison of experimental and analytical results was less satisfactory; however, discrepancies could be attributed to inadequate understanding of concrete behavior at early ages. The behavior of the frame exposed to the elevated temperature (fire) definitely points to the need for better design of certain columns and connections in reinforced concrete frames exposed to certain types of fires. The overview of the methodology and the results point out a number of areas where more information is needed to predict structural response more reliably [i.e., experimental studies of plain concrete and reinforcing steel properties under combined variable environment (temperature, humidity) with variable stress history (short-term cycling as well as long-term sustained and variable loads)]. Additional development of the models is dependent on the development of structural features in which data for model validation is developed from structures under representative loadings and environments.

5.4 Analysis Methods

There are a number of sophisticated methods for analyzing the short-term elastic and long-term time-independent loading of complex structures.[158] These methods are sufficiently developed for three-dimensional, elastic, short-term deformations, but for determination of long-term time-dependent behavior and prediction of ultimate strength and behavior in the load range approaching failure conditions, methods such as the finite-element or finite-differences, may require refinements. Difficulties

are encountered due to limited knowledge on (1) nonhomogeneity of structural concrete; (2) nonlinear stress—strain relationship for concrete and lack of suitable constitutive relationships under combined stress conditions; (3) continuously changing topology due to crack propagation under increasing load; (4) lack of suitable failure criteria for concrete under combined stress conditions; (5) creep and shrinkage of concrete; and (6) effect of anchorage or pullout, dowell and interlock forces in cracked and uncracked sections. The performance of cement-based materials under elevated temperatures is very complicated and difficult to characterize. Current constitutive models are generally calibrated from isothermal conditions in which the transitional effects in variable temperature, humidity, chemical and mechanical loading are neglected.[159] Analyses are further complicated if the structures are subjected to loads far beyond those for which they were designed (i.e., dynamic and/or elevated-temperature loading).*

As noted in the previous section, procedures for design of reinforced concrete members for elevated-temperature exposure often involve simplifying assumptions, the validity of which becomes questionable for extreme environmental conditions. Accurate analytical modeling is possible only if the phenomenon modeled is well understood. For example, uncertainties may exist with respect to the strength and deformation of concrete due to the stochastic nature of its material properties.[160,161] Statistical approaches, however, have been developed for inclusion of these effects into structural analyses (i.e., Latin hypercube sampling technique[162–164] for prediction of effects of creep and shrinkage in concrete and Bayesian statistical approach[165] to predict the long-term creep and shrinkage of concrete. Also, computer codes such as DYNAPCON[166,167] and TEMP-STRESS[168–171] have been developed at Argonne National Laboratory to predict the response of concrete structures subjected to loads beyond those for which they were designed. The TEMP-STRESS code involves not only thermal stress considerations but also the prediction of temperature and moisture distribution within the structure. Use of TEMP-STRESS (as well as other elevated-temperature codes) is restricted, however, because of limited representative structural features data that can be used to verify and calibrate the code, particularly with respect to the various types of failure at high temperature. Also, many of these codes have been developed only for two- dimensional modeling problems of concrete. Three-dimensional computer codes capable of handling reinforced concrete structural problems at elevated temperature require further development. A listing of needs that are required to develop and/or refine computer codes for simulating concrete behavior at elevated temperature is available.[172]

*Response of structures to overload conditions requires a nonlinear constitutive model to describe material behavior, and the mode of failure exhibited by concrete introduces localized violation of the compatibility requirements of continuum mechanics.

6 REVIEW OF SELECTED ELEVATED-TEMPERATURE STRUCTURAL FEATURES TESTS

As noted previously, the properties of concrete can be significantly affected by changes in temperature. Concrete's thermal properties are more complex than for most materials because not only is the concrete a composite material whose components have different properties, but its properties depend on moisture content and porosity. While the properties of the steel reinforcement are relatively well understood, the interaction with concrete is not (i.e., at ambient temperatures the bonding between the reinforcement and concrete is considered complete when structural analyses are conducted; however, with an increase in temperature and/or load the bond deteriorates). Prediction of the performance of concrete structural elements at elevated temperatures is further complicated due to the presence of cracks that form. At high temperatures, correlation of cracking patterns predicted by analytical procedures with experimental results is difficult.[172] Due to the problems involved in the analytical treatment of concrete structural members, especially at elevated-temperature conditions, model tests (structural features) are often used to develop data under representative conditions. The results of these tests are then used in both the validation and the refinement of computer codes. However, the availability of data from elevated-temperature experiments in which concrete members have been subjected to controlled conditions is very limited. Available results are primarily concerned with testing of specific structural features in support of development of analytical procedures, or model tests related to gas-cooled or breeder reactor development. Also, a number of fire tests results are available (see Sect. 2.2.1). Results obtained from several of these studies are summarized below.

6.1 Structural Features Tests

At Shimizu Construction Co., Ltd.,[173] two series of experiments were carried out using 16 reinforced concrete beams to verify the thermal stress design method (TSDM) for reinforced concrete members. The thermal stress under consideration was the one that occurs only when the flexural deformation caused by a temperature gradient across the member cross-section is restrained, whereas the longitudinal deformation caused by the mean temperature change was not included. Nine tests were conducted with heating (T-tests) and seven tests without heating (S-tests). Pertinent parameters for each of these tests are presented in Table 7. A schematic of the test setup is shown in Fig. 121. In the T-test series, the temperature difference between the bottom and top surfaces of the beam was maintained by circulating hot water (60°C or 80°C) and cold water (15°C), respectively. When a steady-state temperature was attained, axial load (N) was applied by Jack No. 1 in Fig. 121 and a restraining bending moment (M*) by Jack No. 2. Figure 122 presents a typical pattern used for heating and application of loads. The S-tests used the same loading device at atmospheric temperature. In these tests, the relationship between bending moment and curvature was investigated up to yielding of the steel to compare results with the T-tests. Figure 123 presents the state of cracking in Test T7 of Table 7. The values adjacent to the cracks in the figure show the extent of crack propagation at the particular magnitude of bending moment noted. Conclusions from the study were that (1) where structural portions considered are not affected by the boundary conditions of the structure in the case of a comparatively short period of loading, the TSDM calculated thermal stresses correlate well with results obtained from both the T- and S-tests; and (2) under the same experimental conditions with respect to loading, thermal stress effects can be evaluated from the moment-curvature relationship obtained at normal temperature without necessarily performing the heating experiment.

Table 7 Pertinent Parameters for Reinforced Concrete Beam Tests (Shimizu Construction Co., Ltd.)

Kinds of test	Test beam number	Reinforcement (number and size)	Reinforcement ratio (%)	Material age of concrete (day)	Compressive strength of concrete (kgf/cm^2)	Tensile strength of concrete (kgf/cm^2)	Modulus of elasticity of concrete ($\times 10^5 kgf/cm^2$)
Test–T	T1	4–D16	0.50	40	258	24	2.48
	T2	4–D16	0.50	33	267	23	2.32
	T3	4–D16	0.50	32	294	29	2.50
	T4	4–D19	0.71	56	305	28	2.66
	T5	4–D19	0.71	40	300	24	2.52
	T6	4–D19	0.71	28	282	24	2.42
	T7	4–D19	0.71	27	296	24	2.60
	T8	4–D22	0.97	21	275	24	2.49
	T9	4–D22	0.97	39	296	24	2.53
Test–S	S1	4–D16	0.50	29	281	22	2.64
	S2	4–D16	0.50	26	238	21	2.39
	S3	4–D19	0.71	26	275	26	2.28
	S4	4–D19	0.71	27	282	24	2.47
	S5	4–D19	0.71	33	257	26	2.34
	S6	4–D22	0.97	22	281	23	2.40
	S7	4–D22	0.97	35	286	26	2.40

Source: K. Irino et al., "Studies on Thermal Stress Design Method for Reinforced Concrete Members of Nuclear Power Plant," Paper J4/5, Vol. J, *Trans. of 7th Ind. Conf. on St. Mech. in Reactor Technology,* pp. 209–219, Chicago, Illinois, August 22–26, 1983.

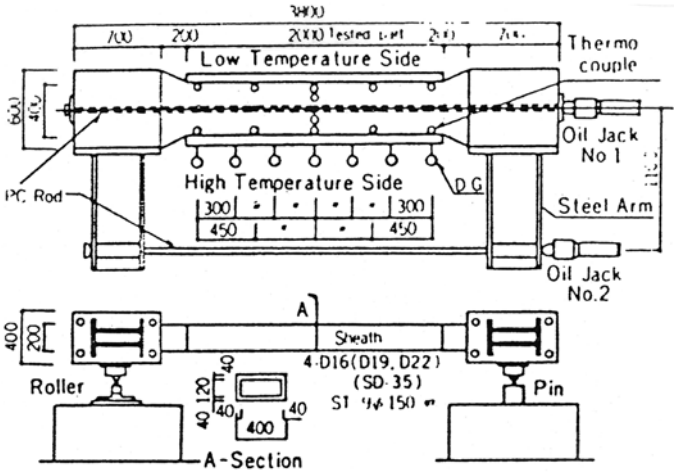

Figure 121 Test setup for investigating effect of thermal gradients on RC beam performance. *Source*: K. Irino et al., 'Studies on Thermal Stress Design Method for Reinforced Concrete Members of Nuclear Power Plant," Paper J4/5, Vol. J, *Trans. of 7th Ind. Conf. on St. Mech. in Reactor Technology*, pp. 209–219, Chicago, Illinois, August 22–26, 1983.

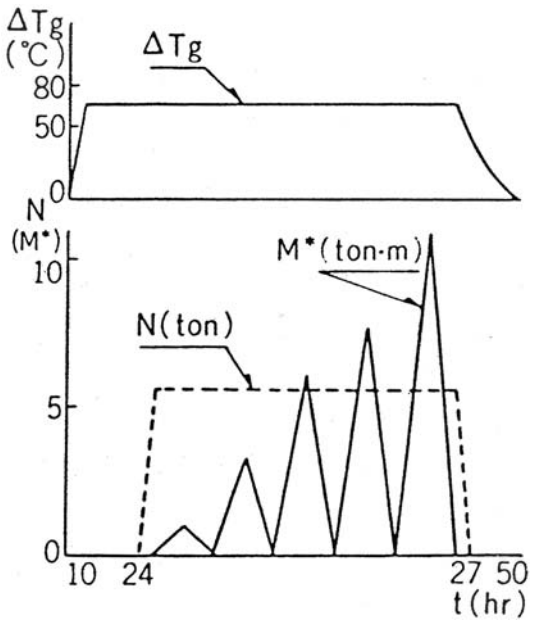

Figure 122 **Typical pattern used for heating and application of load to RC beam specimens.** *Source*: K. Irino et al., 'Studies on Thermal Stress Design Method for Reinforced Concrete Members of Nuclear Power Plant," Paper J4/5, Vol. J, *Trans. of 7th Ind. Conf. on St. Mech. in Reactor Technology*, pp. 209–219, Chicago, Illinois, August 22–26, 1983.

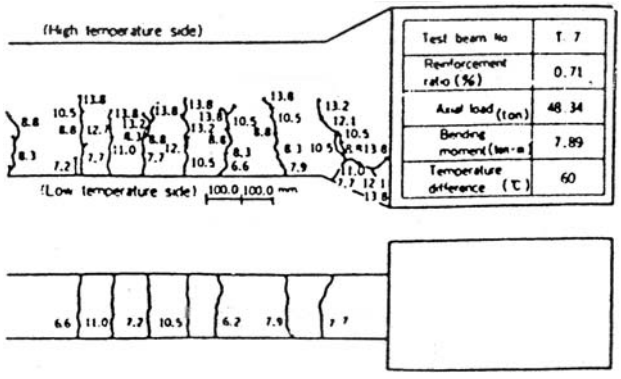

Figure 123 **Typical cracking pattern (Test T7 Table 7).** *Source*: K. Irino et al., 'Studies on Thermal Stress Design Method for Reinforced Concrete Members of Nuclear Power Plant," Paper J4/5, Vol. J, *Trans. of 7th Ind. Conf. on St. Mech. in Reactor Technology*, pp. 209–219, Chicago, Illinois, August 22–26, 1983.

An additional series of tests was conducted in the research laboratories of Shimizu Construction Co., Ltd.[174] to demonstrate the decreasing trend of bending moments and axial forces caused by cracking and creep in reinforced concrete structures. The three types of test articles (A, B, and C) used in the experiments are shown in Fig. 124. Test parameters are summarized in Table 8. A thermal gradient was applied to the column section of the models by circulating water at 80°C and 20°C in rubber bags attached to the hot and cold surfaces, respectively. The experimental setup for both applying loads and restraint is shown in Fig. 125. Models A and C had thermal deformations constrained, whereas Model B had the restraint at the model base removed so that thermal deformation could freely occur. Results of the investigation indicate that (1) where restraint is imposed, the reduction in the axial force is 3 to 5 times larger relative to that obtained for the restraining moment just after the start of testing; (2) the lower the beams rigidity (reinforcement ratio), the greater the decrease in the restraining effect against thermal deformation of a column member; and (3) both the restraining axial force and restraining moment gradually decrease with time after start of heating, eventually approaching a constant value.

Researchers at the Technical Research Institute of Ohbayashi Corporation[175] conducted heating and heating-plus-seismic loading tests at temperatures to 175°C using various concrete structural members (i.e., beams, cylindrical walls, H-section walls, and 1/10-scale models of the inner concrete (I/C) structure in a fast breeder reactor). The concrete members with relatively simple cross-sections were tested to assess the characteristics of thermal stresses and thermal cracks and the behavior of these members under combined loads. Heating and heating-plus-loading tests of the I/C structure were performed to confirm the structural performance under design loading conditions. Thirteen reinforced concrete beam specimens were tested to investigate thermal stresses and ultimate bending and shear strengths. Test variables were

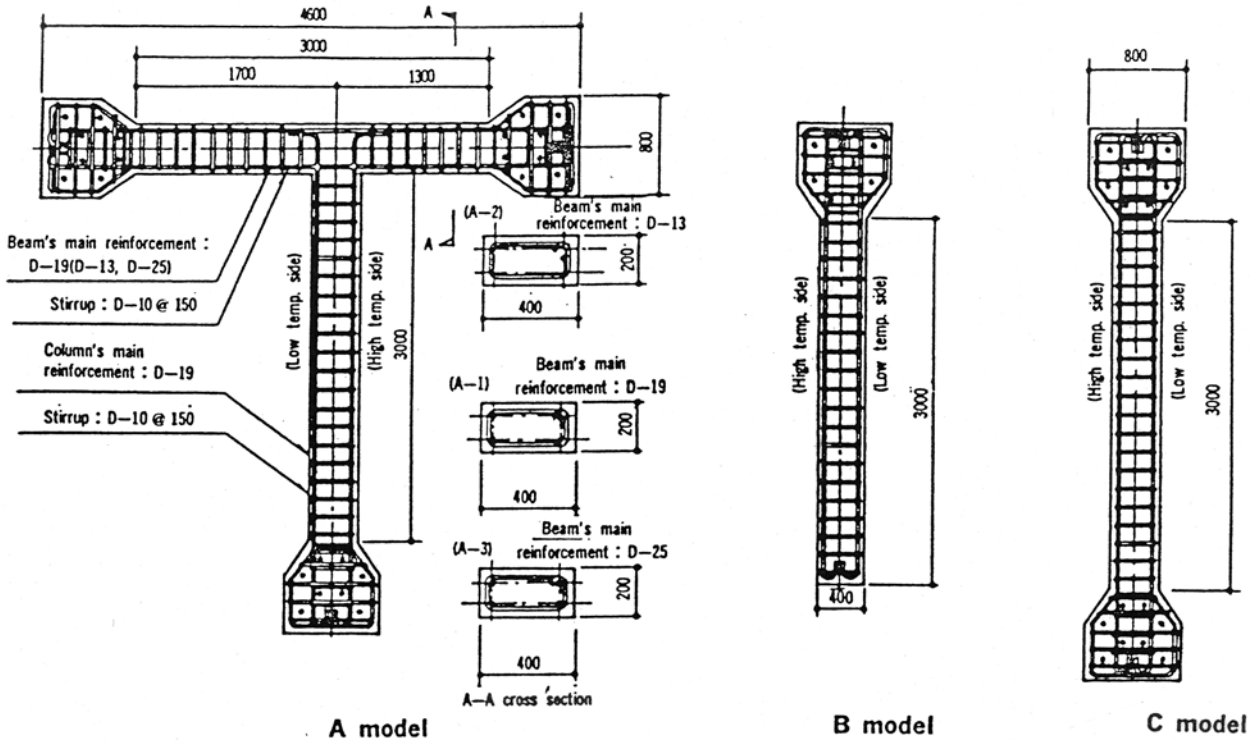

Figure 124 **Test articles used to demonstrate the decreased trend of bending moments and axial forces due to cracking and creep in RC structures.** *Source*: G. T. Ikoma and N. Tanaka, "Restraining Force and Moment of Reinforced Concrete Beam Column Under a Sustained Long-Term Temperature Crossfall," Vol. H, *Trans. of 9th Ind. Conf. on St. Mech. in Reactor Technology*, pp. 201–208, Lausanne, Switzerland, August 17–21, 1987.

Table 8 Test Parameters for RC Structural Element Tests (Shimizu Construction Co., Ltd.)

Test pieces		Reinforcement		Reinforcement ratio (one side)	Restraint	Concrete strength in the air (kgf/cm²)					
						At the start (normal temp.)		At the end (normal temp.)		At the end (80°C)	
		Number and Diameter		(%)		Compressive strength	Young's modulus	Compressive strength	Young's modulus	Compressive strength	Young's modulus
A model	A-1	B	4D19	0.7	Yes	241.2	2.33×10^5	243.5	2.27×10^5	244.3	2.24×10^5
		C	4D19	0.7							
	A-2*	B	4D13	0.4		159.5	1.86×10^5	152.0	1.72×10^5	151.4	1.27×10^5
		C	4D19	0.7							
	A-3	B	4D25	1.2		229.6	1.81×10^5	260.2	2.25×10^5	234.3	1.80×10^5
		C	4D19	0.7							
B model	B	C	4D19	0.7	No	241.2	2.33×10^5	243.5	2.27×10^5	244.3	2.24×10^5
C model	C-1*	C	4D19	0.7	Yes	159.5	1.86×10^5	152.0	1.72×10^5	151.4	1.27×10^5
	C-2	C	4D19	0.7	Yes	229.6	1.81×10^5	260.2	2.25×10^5	234.3	1.80×10^5

B: Beam, C: Column (1 kgf=9.8N)
(*): Test piece in which cracks occurred before testing

Source: T. Ikoma and N. Tanaka, "Restraining Force and Moment of Reinforced Concrete Beam Column Under a Sustained Long-Term Temperature Crossfall," Vol. H, *Trans. of 9th Ind. Conf. on St. Mech. in Reactor Technology*, pp. 201–208, Lausanne, Switzerland, August 17–21, 1987.

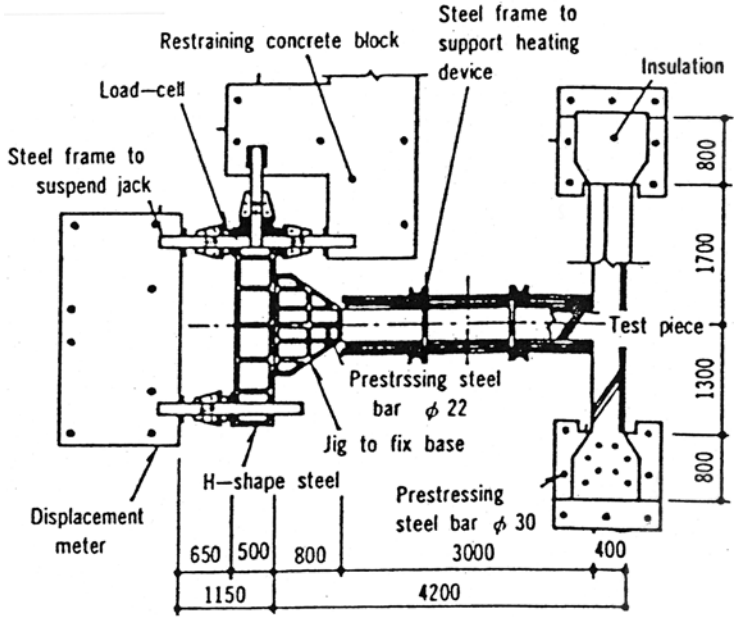

Figure 125 Setup for applying loads and restraint to test articles in Fig. 124. *Source*: T. Ikoma and N. Tanaka, "Restraining Force and Moment of Reinforced Concrete Beam Column Under a Sustained Long-Term Temperature Crossfall," Vol. H, *Trans. of 9th Ind. Conf. on St. Mech. in Reactor Technology*, pp. 201–208, Lausanne, Switzerland, August 17–21, 1987.

temperature (room, 90°C, and 175°C), loading conditions (pure flexure and combined flexure and shear), size (80 by 70 by 400 cm and 40 by 35 by 200 cm), and reinforcement ratio. Eight specimens were heated at the upper surface only, two specimens were heated at both upper and lower surfaces, and three specimens were unheated. Seven reinforced concrete cylindrical specimens (200 cm ID, 20 cm wall thickness and either 200 cm or 350 cm high) were tested to investigate thermal stresses and ultimate shear strengths. Variables in the tests were temperature condition (room, 90°C, and 175°C), loading conditions (torsional and lateral loadings), and reinforcement ratio. Five of the specimens were heated at the inner surface. H-section wall specimens (flange wall; steel plate concrete, web wall; reinforced concrete) were tested to investigate the structural behavior of a wall when adjacent walls were heated. Test variables were temperature (room and 175°C), size (660 cm long by 480 cm wide by 550 cm high, and approximately 330 cm long by 240 cm wide by 275 cm high), and web wall reinforcement ratio. Three of the specimens were heated at the outer surface of one flange wall. Two 1/10-scale I/C specimens were tested to investigate behavior of the I/C structure. One was heated and the other unheated. The loading conditions were selected to simulate design seismic loads as well as thermal loads (T_{max} = 110°C) for a sodium-leakage accident condition. Temperature dependence of concrete material properties were also evaluated for use in the nonlinear finite-element analyses of the test articles. Investigation results showed that (1) thermal deformations and stresses in specimens subjected to temperatures in excess of 100°C were markedly influenced by the temperature dependencies of the materials, especially thermal shrinkage of the concrete; (2) at early load stages for cylindrical specimens subjected to torsional or lateral loads, the thermal stresses and cracks that developed had prominent influence on behavior; however, at the ultimate stages of loading for the heated and unheated specimens, there was little difference in behavior (this was also true for the H-section wall specimens subjected to lateral loads even though a thermal strain of ~1000 με occurred in vertical reinforcement in the web wall); and (3) for the I/C structures, the behavior of the heated and unheated models was similar to that observed for the cylindrical and H-section specimens, and the ultimate strength of the I/C models was about four times greater than the design seismic load.

A second study conducted at the Technical Research Institute of Ohbayashi Corporation[176] investigated the effects on temperature distribution, moisture migration, and strain variation due to heating of a simulated section of a mass concrete wall. Cube specimens 1500 mm in dimension, such as shown in Fig. 126, were tested either with or without venting systems. Five surfaces of each specimen were sealed

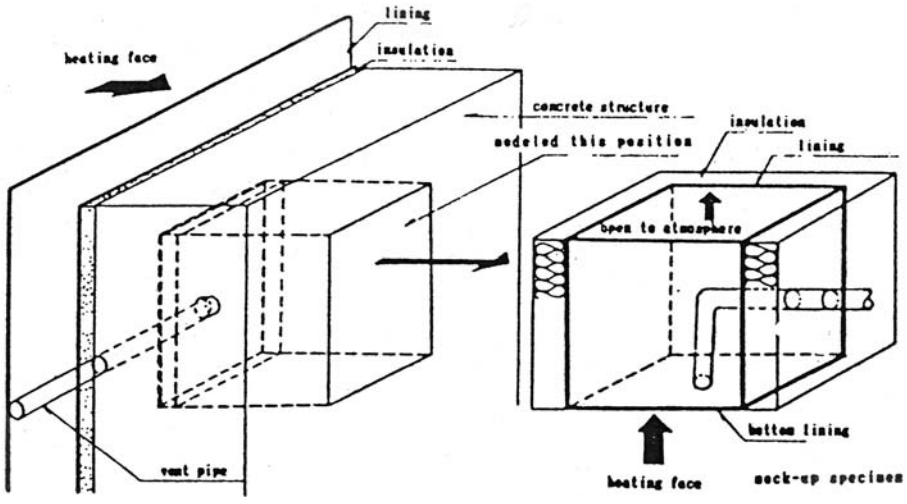

Figure 126 **Simulated section of mass concrete wall.** *Source*: T. Takeda et al., "Experimental Studies on Characteristics of Concrete Members Subjected to High Temperature," Vol. H. *Trans. of 9th Intl. Conf. on St. Mech. in Reactor Technology*, pp. 195–200, Lausanne, Switzerland, August 17–21, 1987.

and insulated with glass wool. During a test the bottom surface of the specimen was heated to 175°C over a 2- to 3-h period, and the temperature was maintained at this level for 91 d. Table 9 summarizes the testing conditions for this series of tests. Items measured during a test included temperature, moisture, concrete strain, water discharge from the venting system, and compressive strength and modulus of elasticity of concrete after heating. Figure 127 presents details and measurement positions for a typical

Table 9. Summary of Conditions for Simulated Mass Concrete Wall Section Tests

Items	Conditions	Items	Conditions
1) Types of specimen	Specimen with a venting system and without a venting system Two specimen in total	8) Exposure condition during heating	Top surface of the specimen is exposed to air
2) Shape and dimension of specimen	150 ×150 ×150 cm Cube	9) Temperature Control method	Electric capacity controller and temperature controller
3) Age when heated	Greater than 91 days	10) Measuring method	
4) Heating period	3 months	a. Moisuture content	Electrode method
5) Heating temperature	Surface temperature of the concrete of the bottom lining inside is constantly set at 175°C	b. Temperature	C-C thermo-couple for high temperature
		c. Inside strain	Embedment type strain gage
6) Heating method	Electric panel heater	d. Water discharge from vent pipe	Store the cooled vapor discharged from venting system
7) Curing conditions until heating begins	In-situ curing	e. Strength and elastic modulus	Core specimen

Source: T. Takeda et al., "Experimental Studies on Characteristics of Concrete Members Subjected to High Temperature," Vol. H. *Trans. of 9th Intl. Conf. on St. Mech. in Reactor Technology*, pp. 195–200, Lausanne, Switzerland, August 17–21, 1987.

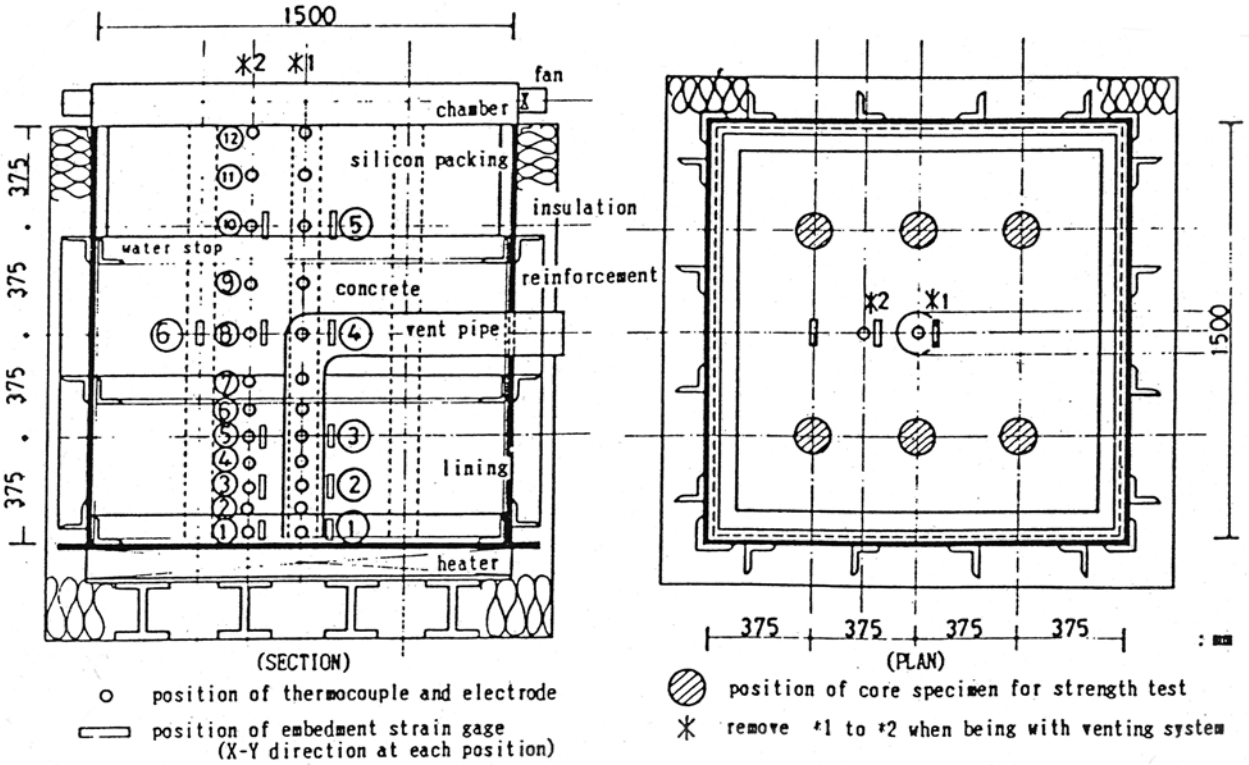

Figure 127 Details of simulated section of mass concrete wall and measurement positions. *Source*: T. Takeda et al., "Experimental Studies on Characteristics of Concrete Members Subjected to High Temperature," Vol. H, *Trans. of 9th Intl. Conf. on St. Mech. in Reactor Technology,* pp. 195–200, Lausanne, Switzerland, August 17–21, 1987.

specimen. Concrete temperature distributions at various times since the start of heating for a vented and nonvented specimen are presented in Fig. 128 and show that the temperature increase in the specimen without venting was slightly less than that for the specimen with venting, but after equilibrium was attained, the temperature distribution in the two types of specimen was almost identical. The moisture content of the specimen without a venting system decreased at a slower rate than that for the specimen with venting, Fig. 129. At 91 d after heating, the moisture distribution showed similar patterns for the two types of specimens, but the high moisture content zone was greater for the nonvented specimen. Water discharge from the venting system, shown in Fig. 130, increased relatively rapidly for the first 7 d of heating and then gradually decreased with a total of 150 L (70 L/m^2 of bottom liner) discharged over the

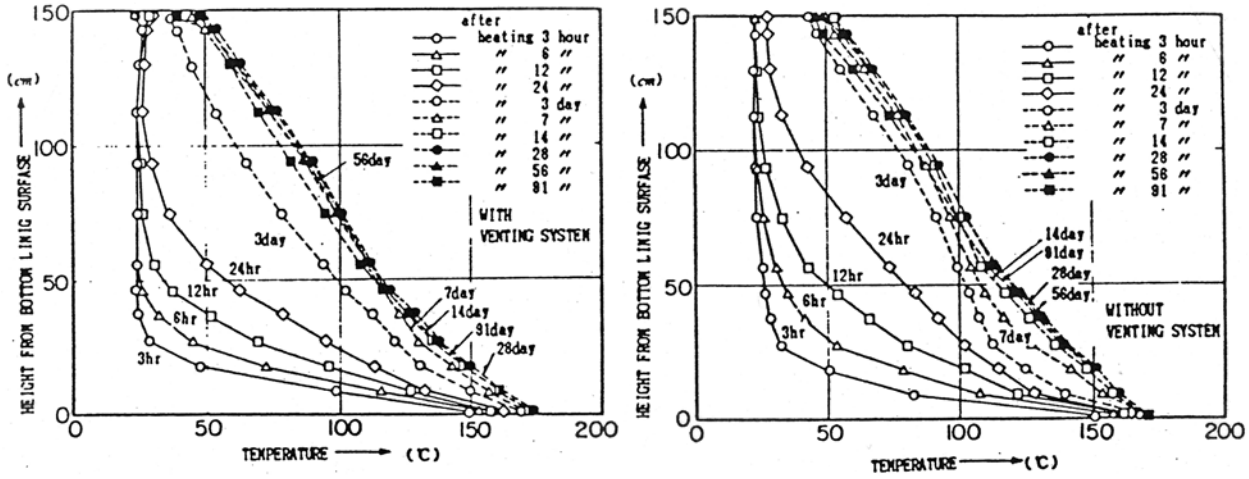

Figure 128 Temperature distribution at various times in simulated mass concrete wall with and without a venting system. *Source*: T. Takeda et al., "Experimental Studies on Characteristics of Concrete Members Subjected to High Temperature," Vol. H, *Trans. of 9th Intl. Conf. on St. Mech. in Reactor Technology*, pp. 195–200, Lausanne, Switzerland, August 17–21, 1987.

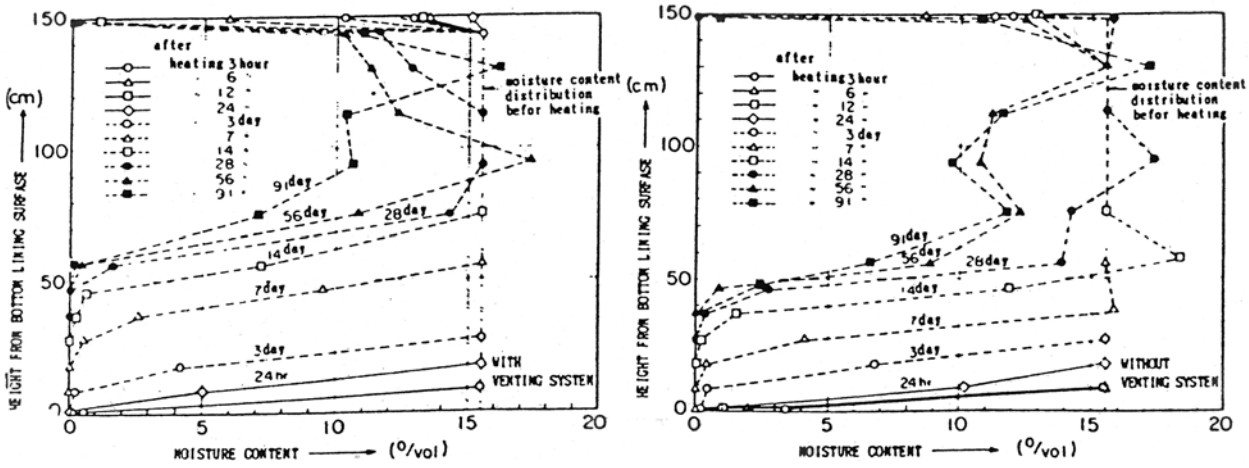

Figure 129 Moisture distribution at various times in simulated mass concrete wall section with and without a venting system. *Source*: T. Takeda et al., "Experimental Studies on Characteristics of Concrete Members Subjected to High Temperature," Vol. H, *Trans. of 9th Intl. Conf. on St. Mech. in Reactor Technology*, pp. 195–200, Lausanne, Switzerland, August 17–21, 1987.

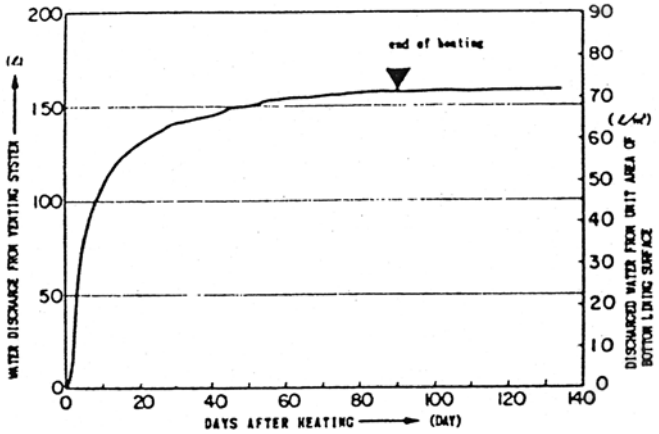

Figure 130 Water discharge from vent pipe of simulated mass concrete wall section. *Source*: T. Takeda et al., "Experimental Studies on Characteristics of Concrete Members Subjected to High Temperature" Vol. H, *Trans. of 9th Intl. Conf. on St. Mech. in Reactor Technology*, pp. 195–200, Lausanne, Switzerland, August 17–21, 1987.

91-d test duration. As the temperature increased, the concrete strains near the bottom liner (heated face) increased, and as heating continued the concrete strains at the unheated face increased with time, Fig. 131. Core samples removed from the specimens at conclusion of a test and tested at room temperature were used to determine the effect of heating on the concrete's compressive strength and modulus of elasticity. Test results for strength and modulus of elasticity are shown in Figs. 132 and 133, respectively. Reference values for strength and modulus of elasticity obtained from water-cured and sealed control specimens are

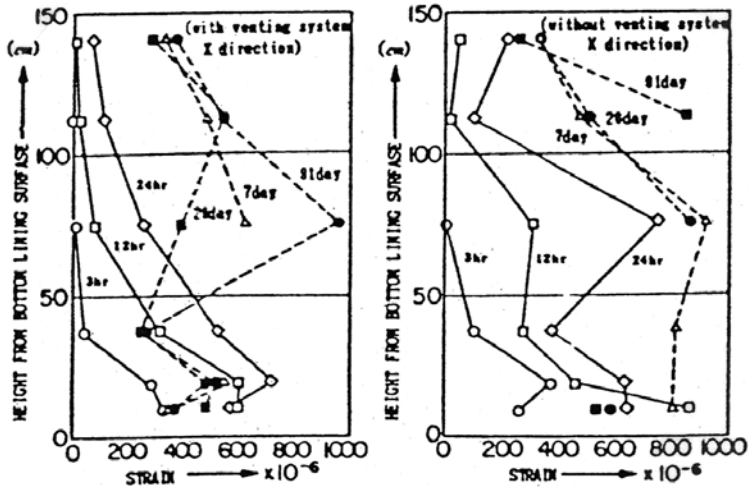

Figure 131 Change in strain distribution with time in simulated mass concrete wall section with and without venting. *Source*: T. Takeda et al., "Experimental Studies on Characteristics of Concrete Members Subjected to High Temperature," Vol. H, *Trans. of 9th Intl. Conf. on St. Mech. in Reactor Technology*, pp. 195–200, Lausanne, Switzerland, August 17–21, 1987.

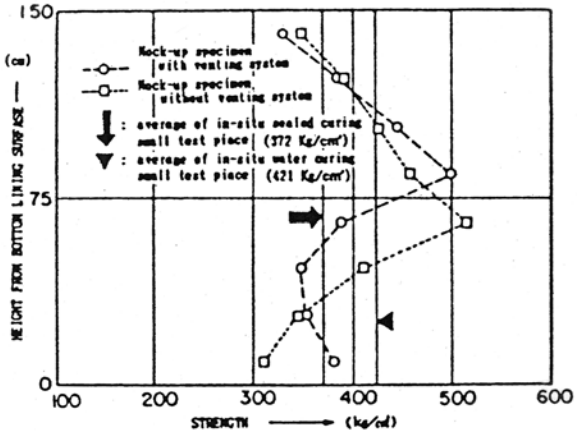

Figure 132 **Compressive strength test results at selected locations in simulated mass concrete wall section with and without venting.** *Source*: T. Takeda et al., "Experimental Studies on Characteristics of Concrete Members Subjected to High Temperature," Vol. H, *Trans. of 9th Intl. Conf. on St. Mech. in Reactor Technology*, pp. 195–200, Lausanne, Switzerland, August 17–21, 1987.

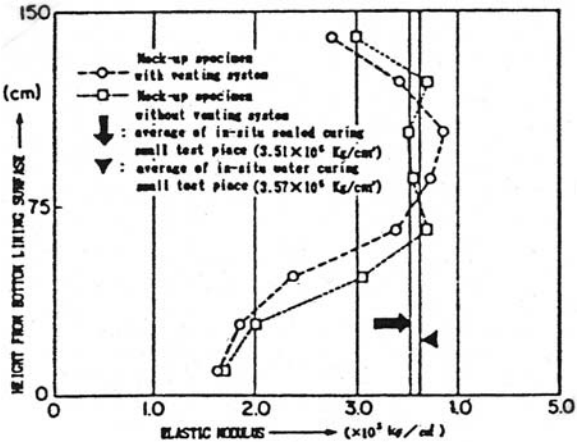

Figure 133 **Modulus of elasticity test results at selected locations in simulated mass concrete wall section with and without venting.** *Source*: T. Takeda et al., "Experimental Studies on Characteristics of Concrete Members Subjected to High Temperature," Vol. H, *Trans. of 9th Intl. Conf. on St. Mech. in Reactor Technology*, pp. 195–200, Lausanne, Switzerland, August 17–21, 1987.

also shown in the appropriate figure. The effect of the elevated temperature was most significant on the concrete modulus of elasticity, which decreased up to about 40%, relative to sealed control specimens, near the bottom face of the specimen. Compressive strength results at all locations in the test specimens exceeded the design strength (240 kg/cm^2).

At the Central Research Institute of Electric Power Industry (CRIEPI),[177] reinforced concrete structures were subjected to elevated temperatures (room to 300°C) to determine the effect on their behavior of (1) change in physical properties of materials, (2) difference in coefficients of thermal expansion between steel reinforcement and concrete, and (3) creep and drying shrinkage of concrete due to water movement. Table 10 summarizes the status of the theoretical and experimental investigations (as of September 1987). The overall objective of the investigations is to develop elevated-temperature design methods for reinforced concrete structures. Figures 134–139 present schematics of the test articles utilized in the extensive CRIEPI test program. Objectives of the various experimental studies are (1) temperature stress tests (Figs. 134 and 135)—measure temperature stress directly and comprehend the influence of creep and drying shrinkage of concrete on temperature stress in reinforced concrete members; (2) shear resistance tests (Fig. 136)—evaluate influence of internal stress, caused by coefficients of thermal expansion of concrete and rebar, on shear transfer behavior, and confirm the shear resistance capacity of reinforced concrete at elevated temperature; (3) material creep test (Figs. 137 and 138)—determine creep and drying shrinkage of concrete at various temperature conditions; (4) flexural creep test of reinforced concrete beams (Fig. 139)—evaluate the influence of creep and drying shrinkage of concrete on the long-term flexural behavior of reinforced concrete beams; (5) flexural test of reinforced concrete beam with lap splice—determine influence of internal stress on the strength and deformation capacities of a lap splice section of a reinforced concrete beam; and (6) anchorage and bond tests—evaluate the influence of the internal stress on the anchorage strength of reinforced concrete. Throughout the test program, an ordinary

Table 10 Identification/Status (September 1987) of Experimental and Analytical Investigations at CRIEPI

	Finished	Continued
Experiment	(1) Investigation of temperature dependence of physical properties of concrete and reinforcement (2) Flexural behaviour of RC beams at elevated temperatures up to 500℃ (3) Flexural behaviour of RC beams with axial compressive stress at elevated temperatures up to 200℃	(1) Creep of concrete at elevated temperature (2) Flexural creep of RC beams at elevated temperatures (3) Temperature stress test of RC beams (4) Shear resistance of RC members at elevated temperatures
Theoretical Investigation	(1) Temperature dependence of physical properties of concrete and reinforcement (2) Estimation method of flexural behaviour of RC beams at elevated temperatures (3) Estimation method of flexural behaviour of RC beams with axial compressive stress at elevated temperatures	(1) Application of Finite Element Method (2) Estimation of creep of concrete material and RC beams (3) Estimation of temperature stress

Source: "High-Temperature Concrete-Testing and Data," *8th CRIEPI/EPRI FBR Workshop,* Palo Alto, California, September 23–25, 1987.

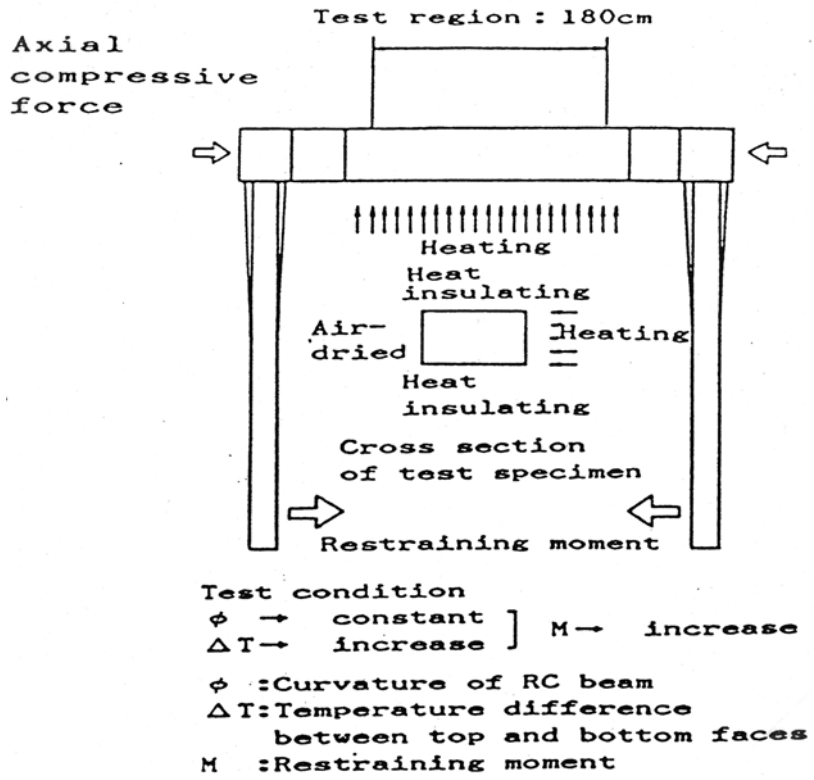

Figure 134 Temperature stress test sponsored by CRIEPI. *Source:* "High-Temperature Concrete-Testing and Data," *8th CRIEPI/EPRIFBR Workshop,* Palo Alto, California, September 23–25, 1987.

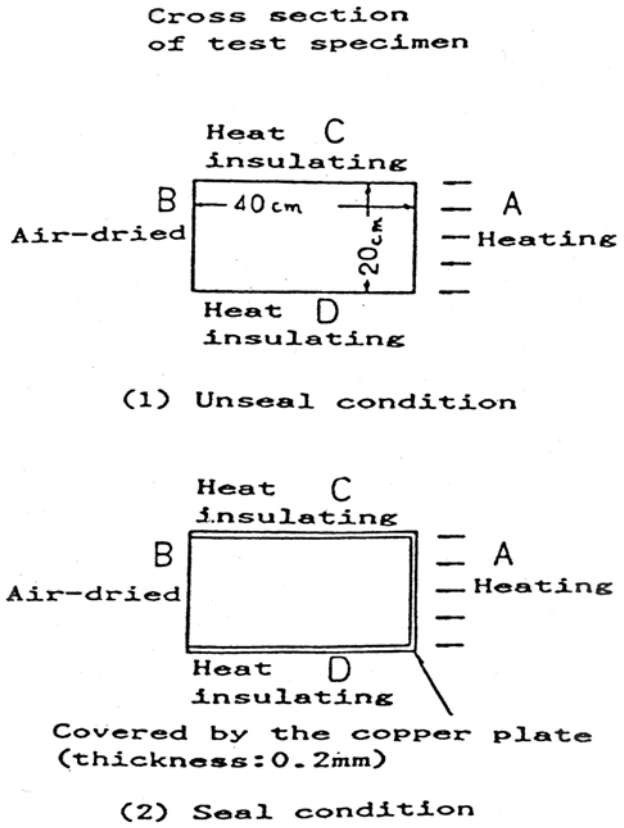

Figure 135 Sealed and unsealed conditions for reinforced concrete beams in temperature stress test series sponsored by CRIEPI.
Source: "High-Temperature Concrete-Testing and Data," *8th CRIEPI/EPRI FBR Workshop,* Palo Alto, California, September 23–25, 1987.

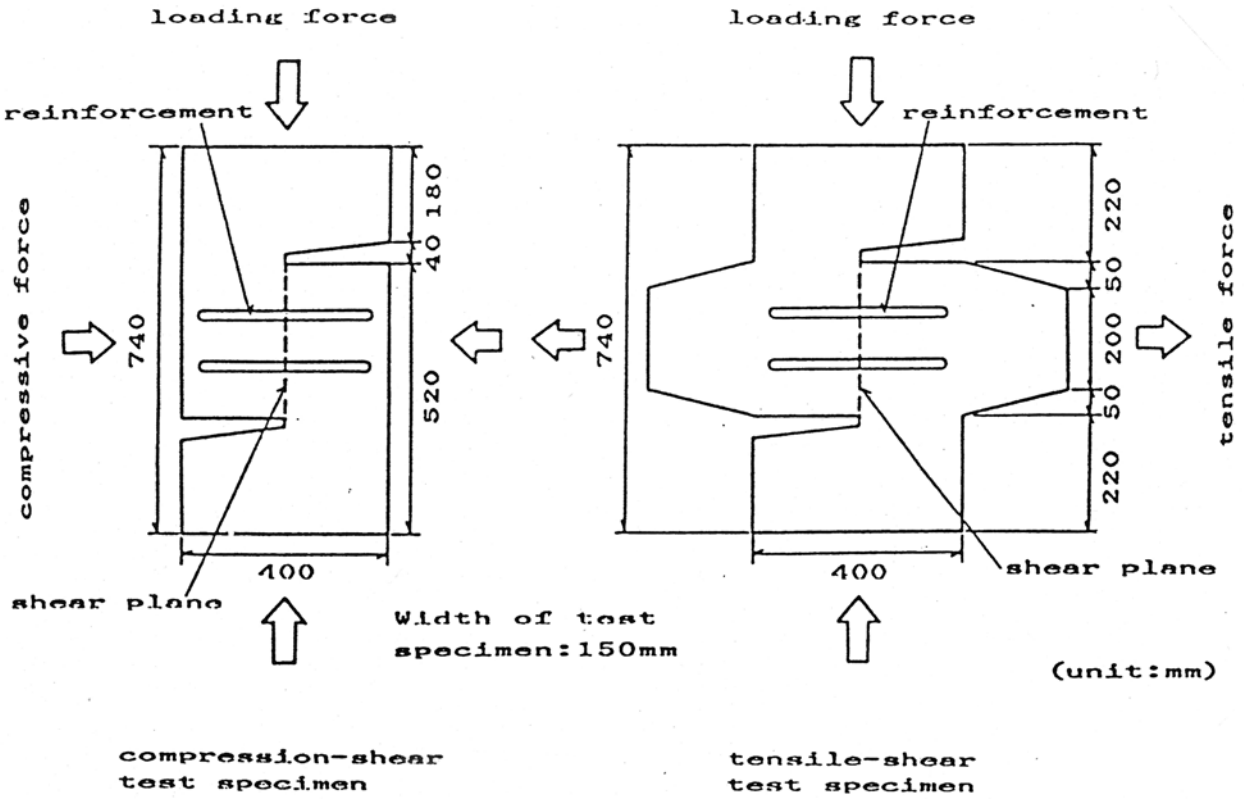

Figure 136 Shear resistance test article used in CRIEPI test program. *Source:* "High-Temperature Concrete-Testing and Data," *8th CRIEPI/EPRIFBR Workshop,* Palo Alto, California, September 23–25, 1987.

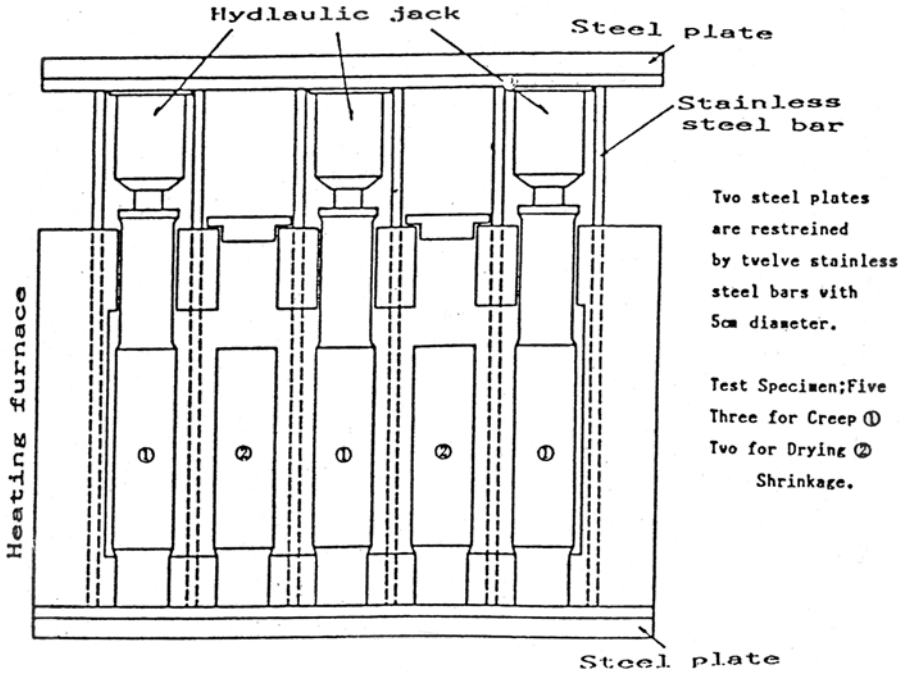

Figure 137 Creep apparatus used in CRIEPI test program. *Source:* "High-Temperature Concrete-Testing and Data," *8th CRIEPI/EPRI FBR Workshop*, Palo Alto, California, September 23–25, 1987.

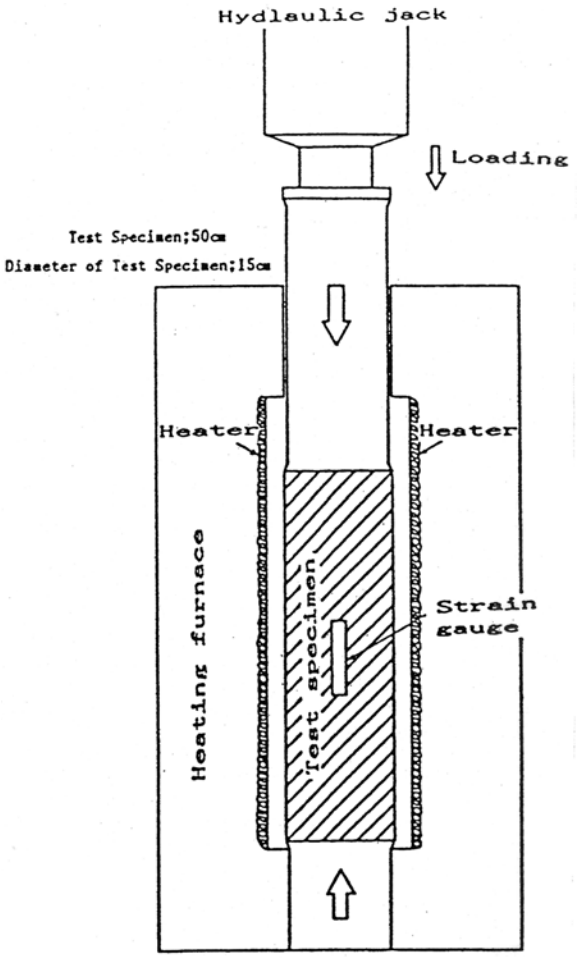

Figure 138 Close-up of creep specimen used in CRIEPI test program. *Source:* "High-Temperature Concrete-Testing and Data," *8th CRIEPI/EPRI FBR Workshop*, Palo Alto, California, September 23–25, 1987.

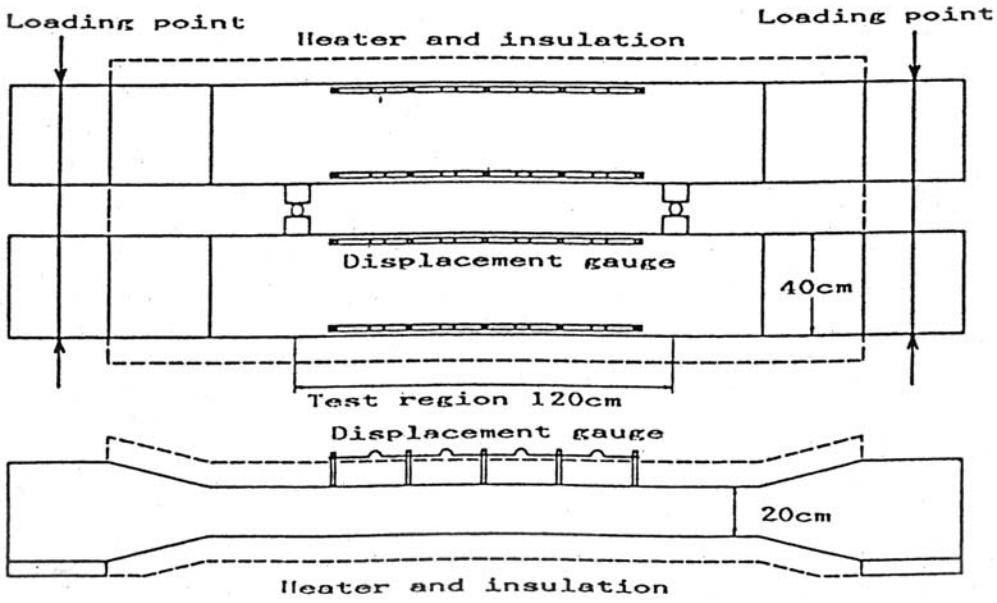

Figure 139 Test setup used for CRIEPI flexural creep tests of reinforced concrete beams at elevated temperature. *Source:* "High-Temperature Concrete-Testing and Data," *8th CRIEPI/EPRI FBR Workshop*, Palo Alto, California, September 23–25, 1987.

Portland cement concrete (greywacke and tuff coarse aggregate; chert, andesite, slate, granite and sandstone fine aggregate) having a compressive strength of 400 kgf/cm^2 was utilized.

Two reinforced concrete beam specimens, Fig. 140, representing portions of the walls or slabs of the fuel storage pool of a boiling-water reactor (BWR) building, were tested to evaluate the effect of thermal

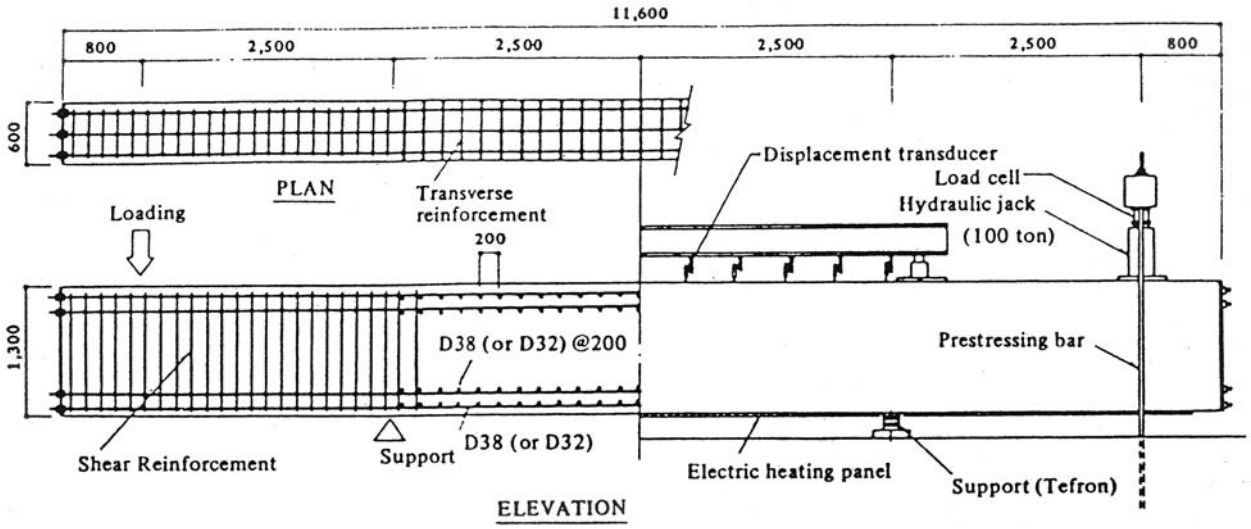

Figure 140 Reinforced concrete beam specimens tested to evaluate thermal cracking and thermal stress relaxation due to cracking. *Source:* N. Shibasaki et al., "Thermal Cracking and Thermal Stress Relaxation of Reinforced Concrete Member Tested by Full Sized Beam Specimens," Paper J4/2, Vol. J, *Trans. of 7th Intl. Conf. on St. Mech. in Reactor Technology*, p. 179–187, Chicago, Illinois, August 22–26, 1983.

cracking and thermal stress relaxation due to cracking.[178] Properties of the specimens are given in Table 11. The bottom surface of each specimen was heated over a 48-h period from room temperature (10°C) to 65°C using electric resistance panels. The temperature was then maintained at this level throughout the test duration. The upper surfaces of the beams were exposed to room air. After the temperature distributions in the beam cross-sections attained steady state, restraint moments were applied by hydraulic jacks at both ends of the specimens to return the free bending deformation to zero (i.e., thermal-stress-only condition was simulated). The restraining moments were then gradually increased until ultimate conditions were attained. Crack patterns in specimen D38 (Table 11) due to thermal stress only and thermal stress plus mechanical load are shown in Fig. 141. Cracking occurred along transverse reinforcing bars with maximum crack widths of 0.10 mm and 0.18 mm occurring in specimens D38 and D32, respectively, as a result of thermal stress only. Measured crack widths were compared with values calculated using several published crack-width formulas (i.e., CEP-FIP formula,[179]) and the calculated values were slightly larger.

Table 11 Properties of Reinforced Concrete Beam Specimens Tested to Investigate Thermal Cracking and Thermal Stress Relaxation

Specimen			D38		D32	
Reinforcement arrangement			D38 (#12) – 6 bars		D32 (#10) – 6 bars	
Reinforcement ratio (%)			0.877		0.611	
Concrete cover (mm)			90		90	
Transverse reinforcement arrangement			2 Layers – D38 @200mm		2 Layers – D32 @200mm	
Mechanical properties of materials	Rebar	Yield strength (kg/cm^2)	4000		3819	
		Modulus of elasticity ($\times 10^6$ kg/cm^2)	1.93		1.94	
	Concrete	Compressive strength (kg/cm^2)	10°C (51 days)	65°C (51 days)	10°C (67 days)	65°C (67 days)
			253.2	258.8	234.4	229.5
		Modulus of elasticity ($\times 10^5$ kg/cm^2)	2.88	2.20	2.49	2.25
		Tensile strength (kg/cm^2)	24.4	20.7	24.4	19.2
		Coefficient of thermal expansion ($\times 10^{-5}$/°C)	0.695	—	—	—
Temperature difference between top and bottom surface (°C)			45.5		48.0	

Source: N. Shibasaki et al., "Thermal Cracking and Thermal Stress Relaxation of Reinforced Concrete Member Tested by Full Sized Beam Specimens," Paper J4/2, Vol. J, *Trans. of 7th Ind. Conf. on St. Mech. in Reactor Technology*, p. 179–187, Chicago, Illinois, August 22–26, 1983.

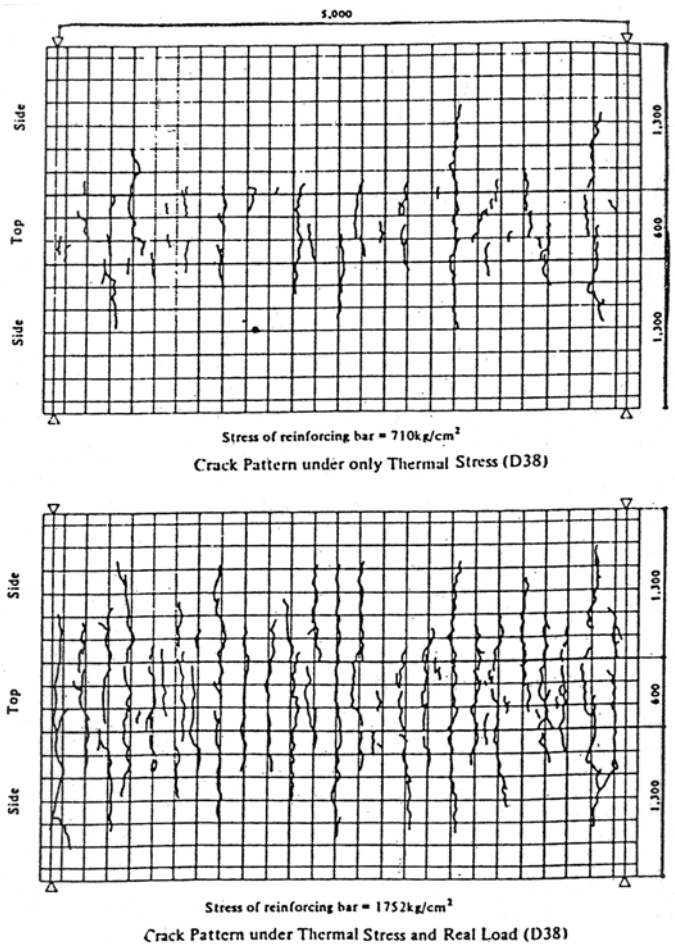

Figure 141 Crack patterns for specimen D38 (Table 11) due to thermal stress only and thermal stress with loading. *Source:* N. Shibasaki et al., "Thermal Cracking and Thermal Stress Relaxation of Reinforced Concrete Member Tested by Full Sized Beam Specimens," Paper J4/2, Vol. J, *Trans. of 7th Intl. Conf. on St. Mech. in Reactor Technology*, p. 179–187, Chicago, Illinois, August 22–26, 1983.

Nine reinforced concrete beams (Fig. 142) were tested to evaluate the thermal stress produced by restraining the deflections produced by a thermal gradient.[180] Table 12 summarizes material properties and test parameters for the study. Figure 143 presents the test apparatus. Axial force and moment acting on the specimens were produced using hydraulic jacks positioned as shown in the figure. Two primary types of specimens were tested: Type T and Type E. The loading procedure for the Type T tests included (1) specimen heated to 75°C at one face while cooled at 10°C on opposite face, specimen allowed to freely deflect; (2) after temperature distribution reached steady-state (~19 h), external axial force was applied as well as a pure moment at each end to restrain free thermal deflection; and (3) pure moment was increased until ultimate load was reached. The procedure for the Type E tests included (1) axial force and pure moment loads were applied to the specimen, (2) while maintaining the external loads, the specimen was allowed to deflect freely as it was heated to 50°C at one face and cooled to 10°C on opposite face; (3) after temperature distribution reached steady-state (~17 h), free thermal deflection was restrained by applying pure moment; (4) while holding above state, specimen was allowed to freely deflect while temperature at hot face was rapidly increased to 95°C; (5) while in an unsteady-state of nonlinear temperature distribution across the beam, pure moment was applied to restrain the free thermal deflection; and (6) pure moment was increased until ultimate load was reached. Test durations were kept short to reduce creep effects. When comparing the relationship between external thermal moment and external moment for all specimens, the following was observed: (1) thermal moments decrease with an increase in

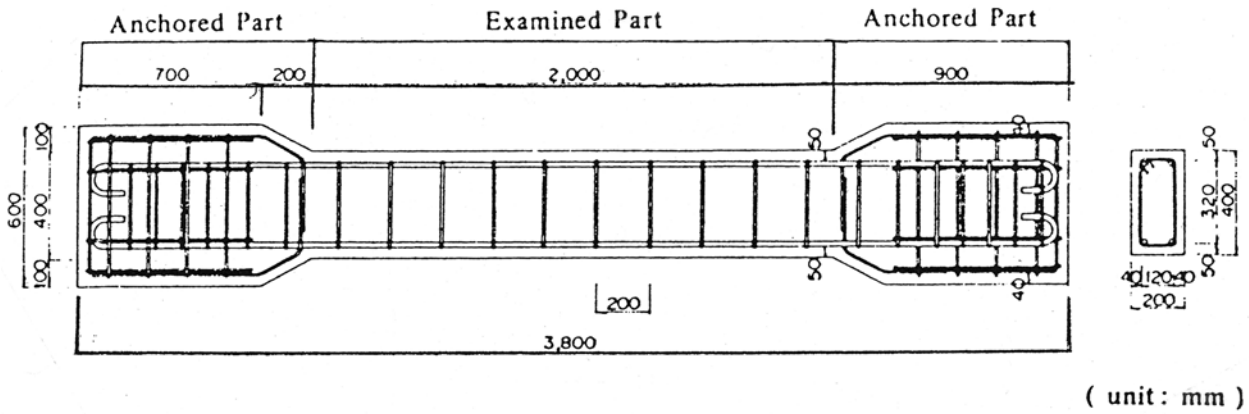

Figure 142 Test specimen utilized to evaluate thermal stress produced by restraining deflections produced by thermal gradients. *Source:* N. Shibasaki et al., "An Experimental Study on Thermal Stress of Reinforced Concrete Members Under Short-Term Loading," Paper J4/3, Vol. J, *Trans. of 7th Ind. Conf. on St. Mech. in Reactor Technology*, pp. 189–197, Chicago, Illinois, August 22–26, 1983.

Table 12 Material Properties and Test Parameters for Reinforced Concrete Thermal Gradient Experiments Conducted to Evaluate Stresses Produced by Restraining Deflections

Experimental Procedure		Type-T					Type-E			
Specimen		TC−0.71	TC−1.27	TO−0.71	TT−0.71	TT−1.27	EC−0.71	EC−1.27	ET−0.71	ET−1.27
External Axial Force (ton)		−10		0	15		−10		15	
External Moment (ton·m)		Optional					1.0		2.0	
Temperature Difference at Steady-state (°C)		60					35			
Hot Side Water Temperature at Unsteady-state (°C)							95			
Amount of Reinforcement (%)		0.71	1.27	0.71	0.71	1.27	0.71	1.27	0.71	1.27
Concrete	Compressive Strength (kg/cm^2)	301	326	313	333	269	302	299	290	289
	Tensile Strength (kg/cm^2)	30.1	28.5	27.6	26.4	29.5	26.4	25.4	28.6	26.5
	Young's Modulus ($\times 10^5 kg/cm^2$)	3.21	3.08	2.94	3.33	3.12	3.14	3.59	3.28	2.70
Re-bar	Yield Strength (kg/cm^2)	3700	3800	3700	3700	3800	3700	3800	3700	3800
	Ultimate Strength (kg/cm^2)	5230	5430	5230	5230	5430	5230	5430	5230	5430
	Young's Modulus ($\times 10^6 kg/cm^2$)	1.98	1.98	1.98	1.98	1.98	1.98	1.98	1.98	1.98

TC−0.71
- Percentage of Tensile Reinforcement
- Identification of Axial Force C: Compression, O: Non-axial Force, T: Tension
- Type of Experimental Procedure

Source: N. Shibasaki et al., "An Experimental Study on Thermal Stress of Reinforced Concrete Members Under Short-Term Loading," Paper J4/3, Vol. J, *Trans. of 7th Intl. Conf. on St. Mech. in Reactor Technology*, pp. 189–197, Chicago, Illinois, August 22–26, 1983.

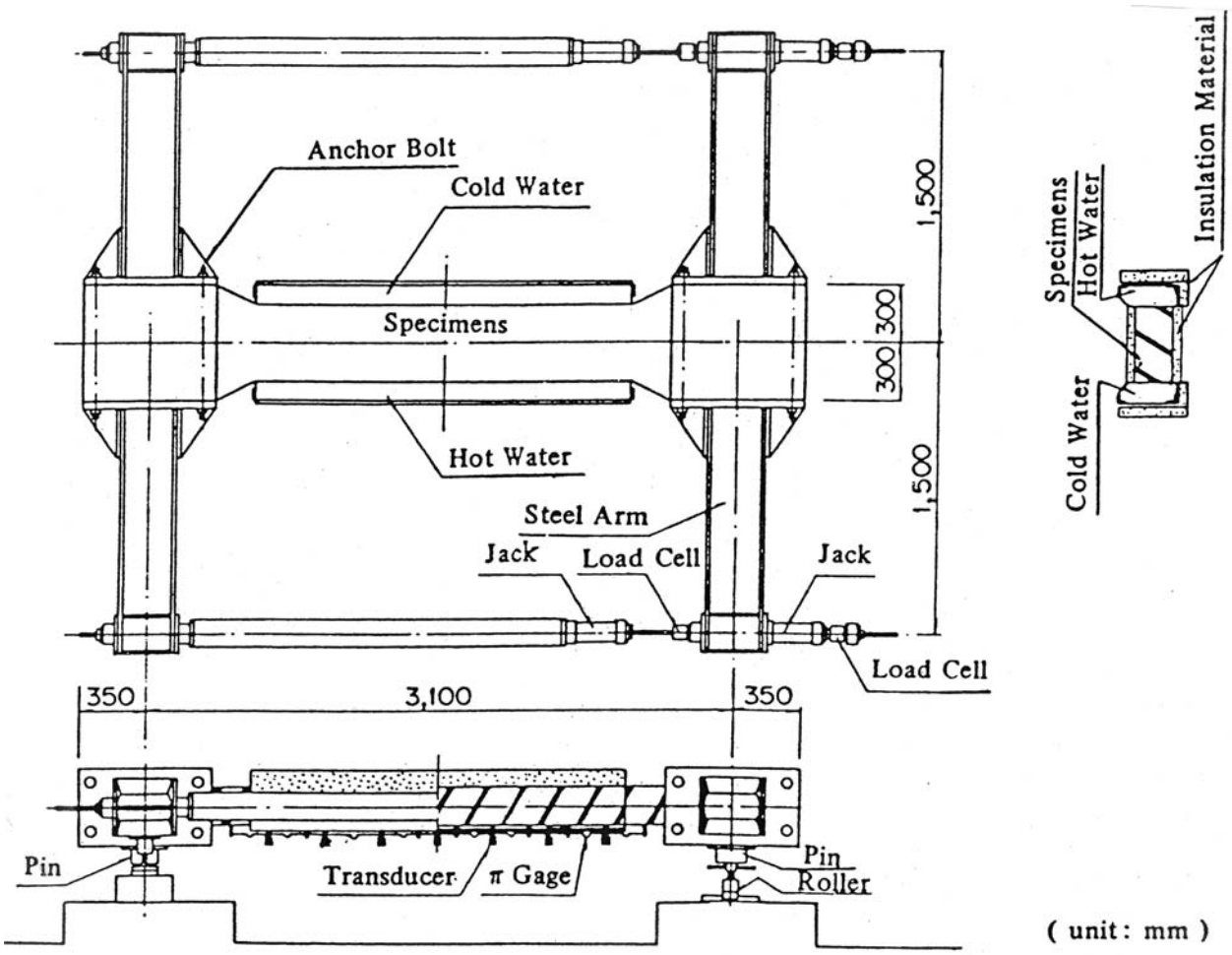

Figure 143 **Apparatus used to test specimen shown in Fig. 142.** *Source:* N. Shibasaki et al., "An Experimental Study on Thermal Stress of Reinforced Concrete Members Under Short-Term Loading," Paper J4/3, Vol. J, *Trans. of 7th Ind. Conf. on St. Mech. in Reactor Technology*, pp. 189–197, Chicago, Illinois, August 22–26, 1983.

external moments; (2) when specimens are subjected to the same axial forces, thermal moments increase as the amount of steel reinforcement increases; and (3) when the specimens have the same amount of steel reinforcement and different axial forces are applied, thermal moments decrease with increasing compressive load, nonaxial loading, and tensile loading.

Four beam specimens (Fig. 144) having identical dimensions and steel reinforcement were tested to investigate the time-dependent thermal effects either with or without application of external forces.[181] Test parameters are summarized in Table 13. All surfaces of the specimens, except those exposed to ambient conditions, were sealed with neoprene rubber sheets to prevent moisture migration. The test apparatus used to apply thermal moment and the sustained external moment is shown in Fig. 145. Thermal gradients of 40°C and 70°C at the heating surface were selected to simulate operating conditions in a nuclear power plant. A "thermal" moment was applied by mechanical jacks at both ends of a specimen to cancel out the deflection induced by the thermal gradient. The sustained external moment was applied and kept constant during the testing period by spring elements. Any changes in curvature during the ~4-month test period was adjusted by controlling the moment so that the thermal curvature was kept constant at zero (i.e., reduction in thermal moment was observed by measuring the change of the

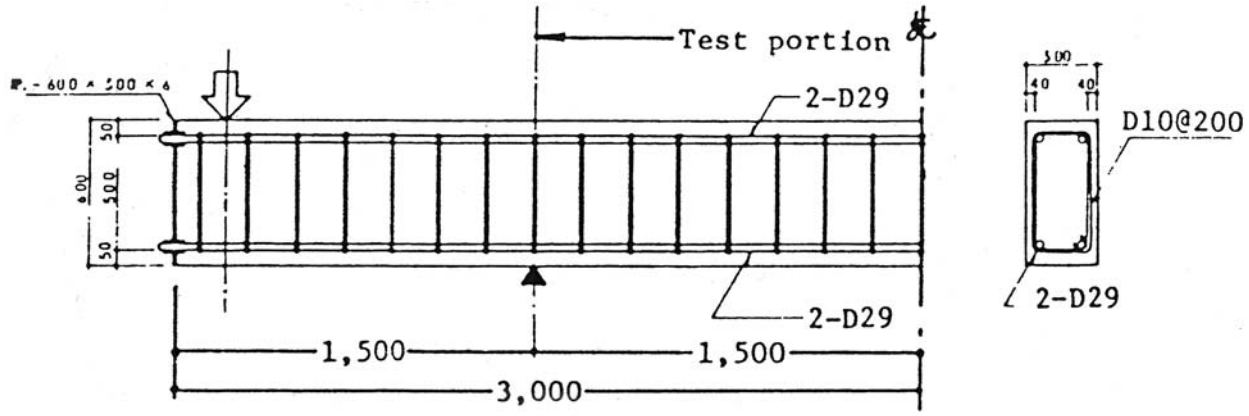

Figure 144 Test specimen utilized to investigate the time-dependent thermal effects either with or without application of external forces. *Source:* N. Shibasaki et al., "Thermal Stress Relaxation and Creep Tests of Reinforced Concrete Beams Under Long Term Thermal Effects and Loadings," Paper J4/4, *Trans. of 7th Int. Conf. on St. Mech. in Reactor Technology,* pp. 199–207, Chicago, Illinois, August 22–26, 1983.

Table 13 Parameters of Reinforced Concrete Beam Specimens Tested to Investigate Time-Dependent Thermal Effects Either With or Without External Forces

Test specimen	Test type	ΔT (deg. C)	M_F (t.m)	T_i (°C)
RH-1	Relaxation	40	0	70
RH-2	Relaxation	40	6.9	70
MH-1	Creep	40	6.9	70
MC-1	Creep	0	6.9	-

where ΔT : thermal gradient across the depth of beams
M_F : external moment
T_i : temperature at heated surface

Source: N. Shibasaki et al., "Thermal Stress Relaxation and Creep Tests of Reinforced Concrete Beams Under Long Term Thermal Effects and Loadings," Paper J4/4, *Trans. of 7th Int. Conf. on St. Mech. in Reactor Technology,* pp. 199–207, Chicago, Illinois, August 22–26, 1983.

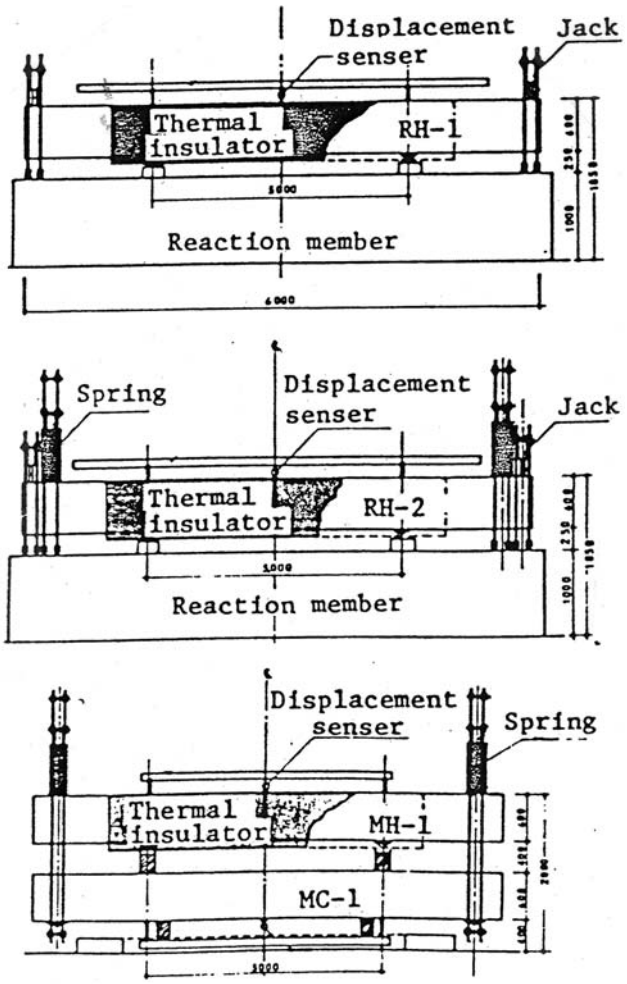

Figure 145 Apparatus used to apply thermal moment and sustained external moment test specimen shown in Fig. 144. *Source:* N. Shibasaki et al., "Thermal Stress Relaxation and Creep Tests of Reinforced Concrete Beams Under Long Term Thermal Effects and Loadings," Paper J4/4, *Trans. of 7th Int. Conf. on St. Mech. in Reactor Technology*, pp. 199–207, Chicago, Illinois, August 22–26, 1983.

moment). When subjected to a constant thermal gradient only, results showed that due to development of cracks the thermal moment decreased rapidly early in the loading stage. Crack widths estimated using a model such as proposed in Ref. 179 were considerably smaller than the test results at 4 months loading, probably due to the thermal effects such as concrete creep at elevated temperature.

A reinforced concrete box structure (Fig. 146) was subjected to thermal and mechanical loads to determine the general behavior of reinforced concrete at elevated temperatures and to develop a data base for verification and/or calibration of analytical procedures.[182] The test was conducted in two phases. The purpose of Phase I (concrete age 4–5 months) was to evaluate the response of the structure to a simulated sodium spill. Cracking patterns, temperatures, strains, displacements, and changes in stiffness of the structure were evaluated while the cell was heated to 205°C at ~6°C/h, maintained at temperature for

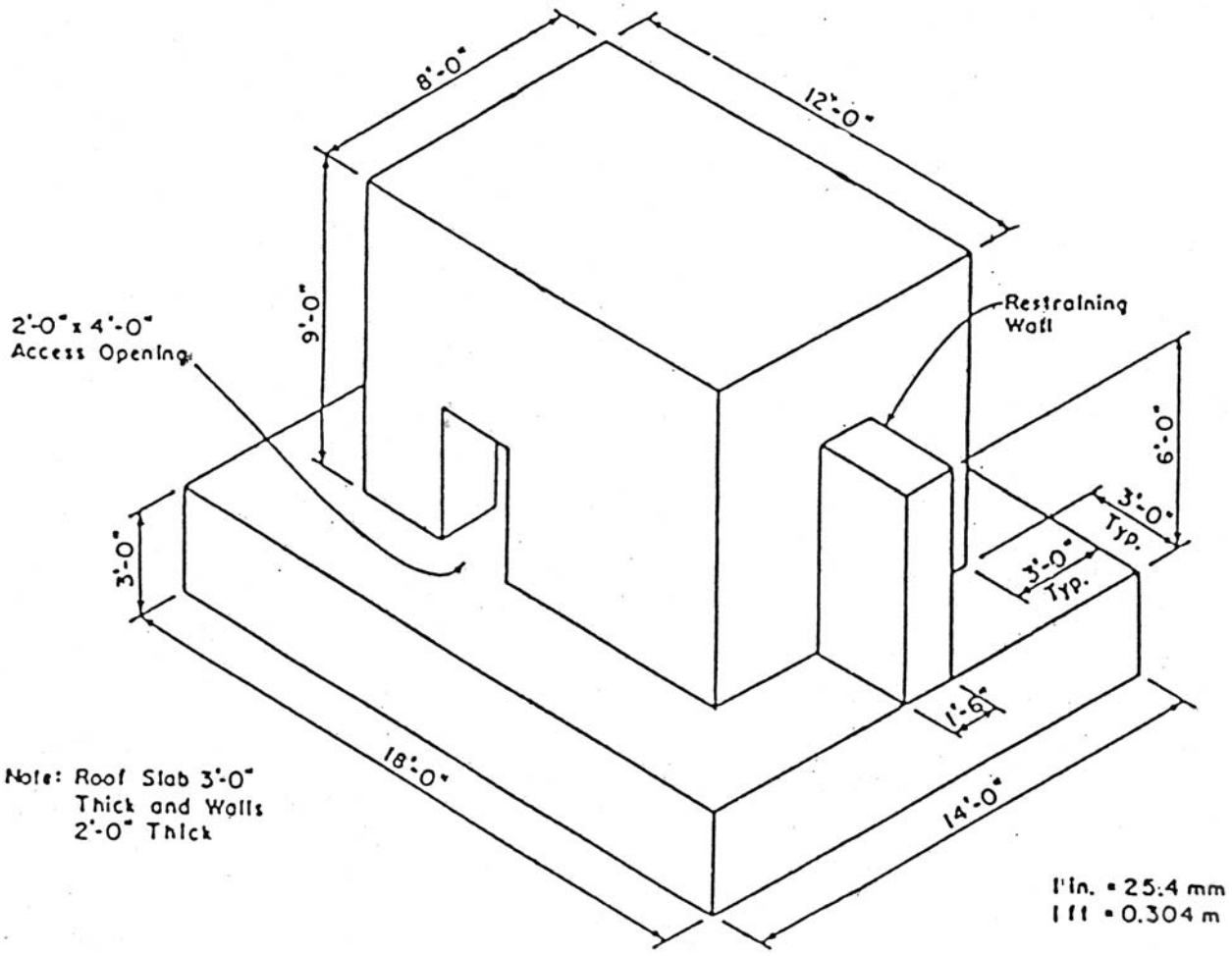

Figure 146 Reinforced concrete box structure subject to thermal and mechanical loads to determine the general behavior of reinforced concrete at elevated temperature. *Source:* G. N. Freskakis, "High Temperature Concrete Testing," *8th CRIEPI/EPRI Workshop*, Agenda Item 7.2, Palo Alto, California, September 23–25, 1987.

100 h, and cooled down. Mechanical load tests were conducted before heatup and after cooldown. Results of Phase I were that (1) stresses in the reinforcing steel increased during heatup, stabilized during the constant temperature period (stresses highest in top slab and near top of walls), and decreased during the cooldown period (stresses, however, were higher than expected); (2) bending moments were large during initial stages of heatup but dropped sharply as cracking developed (high moments occurred near top of walls and in top slab); (3) small, almost negligible, axial forces occurred; (4) cracks that occurred in exterior walls were extensive but uniform having small crack widths and closed after cooldown; (5) substantial water release and seepage through the cracks occurred; (6) stiffness was reduced 60% after heating; and (7) approximate analysis methods produced good agreement with experimental results at the center of cell except at restraints and discontinuities that were not accounted for in the analysis (further analytical verification is required to eliminate the factor required to account for two-dimensional effects and associated conservatism). The overall physical condition of the test structure at conclusion of the investigation was judged to be very good. The purpose of Phase II (concrete age 20 months) was to simulate temperature conditions of a second sodium spill in a plant in order to determine if the plant could be reused after an initial spill. Items measured and test procedures utilized were the same as for Phase I.

Although detailed results were not available for inclusion in the reference, some general comments were made relative to the Phase II test: (1) exterior cracking was the same as occurred in Phase I (delayed in opening), and the cracks closed on cooldown; (2) no additional water was released, and (3) results of the mechanical load tests indicated that the section stiffness had increased 25% since Phase I. The overall physical condition of the test structure at conclusion of Phase II was also judged to be very good.

6.2 Model Tests in Support of PCRV Development

In the *ASME Code for Concrete Reactor Vessels and Containments*[1] the use of models in support of the development of PCRVs is required where accurate analytical procedures for the ultimate strength and behavior in the range approaching failure have not been established or when models of a prototype with similar characteristics to those of the current design have not been constructed and tested. The models are required to maintain similitude, including that of materials, to the prototype design and be geometrically similar with respect to the principal dimensions of the prototype in a scale ratio consistent with test purposes as listed in Section CB-3340 of Section III, Division 2 of Ref. 1.

Model testing requirements also are noted in the French and British codes. The French Code[146] requires that each vessel design be subjected to the construction and testing of at least one representative prestressed concrete model geometrically similar to the structure with principal dimensions in a ratio at least equal to 1:6. The British Code[147] provides that the validity and accuracy of any method or computer program shall be demonstrated using known solutions, and, if necessary, they shall be checked against measurements made on models or previously completed vessels in order to verify the analysis method or computer program. Table 14[183] provides a summary listing of most of the PCRV-related model tests that have been conducted. Also included in the table are the type of test, scale, and investigating agency. Summarized below are results of several investigations that have involved the testing of models that included elevated-temperature conditions.

6.2.1 Single-Cavity PCRV Model Tests

Electricité de France.[184] Three 1:6-scale models of EDF3 (Chinon III), such as shown in Fig. 147, were tested. The first two models were identical except the first did not have a gas-tight liner. The third model was used for thermal experiments to determine the influence of relatively high temperatures, the interaction of the concrete and liner following an insulation fault, and the effects of elevated temperature on the loads of the most exposed tendons. Conclusions derived from these tests were that (1) loss of prestressing force under temperature effects was due to steel relaxation and differential expansion between the steel and concrete, (2) drying shrinkage resulted at relatively low hot-wall temperatures (80°C) and was irreversible on cooling, (3) the liner can become highly compressed locally due to the presence of a liner defect (or constraint), (4) application of a second thermal cycle did not result in increased shrinkage beyond that experienced from the first thermal cycle, and (5) tests at temperatures up to 143°C indicated an increase in the coefficient of thermal expansion.

Tests at ambient temperature (to determine the effects of prestressing and of pressure) and under unusual thermal conditions were undertaken on the 1:5-scale model of EDF4 (St. Laurent I) shown in Fig. 148. During an increase in temperature, cracks occurred in the outer walls of the model. Measurements showed that the concrete coefficient of thermal expansion was considerably greater than that assumed in the design calculations and was related to the moisture condition of the concrete.

Table 14 Summary of PCRV Model Tests

Organization	Test Item	Scale	Project	Number of Models	Test for*
1. French AEC	Head, PCRV	Not Known	G-2, G-3	2	A, B, C
	Cylindrical PCRV	1/10	G-2, G-3	3	A, B, C
	Cylindrical Vessels	I.D. 0.76 m I.H. 2.29 m	Safety Studies	25	C, D
	Cylindrical Vessel	Unavailable	G-2, G-3	2	A, B, C
2. Societe d'Etudes et d'Equipments d'Enterprises (SEEE), France	Cylindrical PCRV	1/6	EDF-3	3	A, B, C, D
	Cylindrical PCRV	1/10	EDF-3	1	T
	Cylindrical PCRV	1/5	EDF-4	2	A, B, C, T
	"Hot-Liner" Vessel	Not Known	General	1	A, B, C, T
3. Electricite de France (EDF), France	Cylindrical PCRV	1/5	Bugey I	2	A, B, C, T
	2 Layer Cylinder	1/3	General	1	
4. Central Electric Research Laboratory, England	Cylindrical PCRV	1/8	Oldbury	1	A, B, C, T
	Cylindrical PCRV	1/8	Pre-Oldbury	1	B, C

Table 14 (continued)

Organization	Test Item	Scale	Project	Number of Models	Test for*
5. Sir Robert McAlpine & Sons, England	Cylindrical PCRV	1/7	Prelim, PCRV	1	A, B, C, D
	Heads, PCRV	1/50	General	11	B, C
			Oldbury		
			AGR	2	B, C
	Cylindrical PCRV	1/8	Oldbury	1	A, B, C, T
	Heads, PCRV	1/50	Hinkley Point B	5	B, C
	Cylindrical PCRV	1/10	Hinkley Pont B	1	A, B, C
	Heads PCRV	1/40	HTR	15	B, C
	Multicavity PCRV	1/40	HTR	3	B, C
	Multicavity PCRV	1/14	HTR Oldbury B	1	A, B, C, D
	Heads, PCRV	1/40	Modified AGR	2	B, C
	Heads, PCRV	1/22	Modified AGR	1	B, C
	Heads, PCRV	1/50, 1/30	LMFBR	11	B, C
6. Taylor Woodrow Constr. Ltd. (TWC), England	Spherical PCRV	1/12, 1/40	Wylfa	2	A, B, C
	Cylindrical PCRV	Not Known	Wylfa	3	A, B, C
	Cylindrical PCRV	1/10	Hunteston B	1	A, B
	Heads, PCRV	1/24	Several	12	A, B, C
	Multicavity PCRV	1/10	Hartlepool	1	A, B, C
	Head, PCRV	1/13	Ft. St. Vrain	2	A, B, C, D
	Multicavity PCRV	1/30	GT-HTGR	2	A, B, C
	Cylindrical PCRV	1/40	Future HTGR	4	A, B, C
	Heads, PCRV	1/26, 1/8	Future HTGR	2	A, B, C
	Heads, PCRV	1/8	Future HTGR	2	A, B, C, T
	Boiler Closures	1/10	Hartlepool/Heysham	60	A, B, C
	Boiler Closures	1/3	Hartelpool/Heysham	4	A, B, C, T
	Restrained Concrete Elements	Not to Scale	General	500	A, C
	Closure Plug	1/18, 1/5	Pressure Vessel	45	A, B, C
	Head	1/30, 1/5	Pressure Vessel	77	A, B, C

Table 14 (continued)

Organization	Test Item	Scale	Project	Number of Models	Test for*
7. UKAEA/Imperial College, UK	Spherical PCRV	1/12	General	1	A, B, C, T
	Cylindrical PCRV (domical heads)	1/6	General		A, B, C
8. Kier Ltd., England	Spherical PCRV	1/12	Wylfa	1	A, B, C, T
9. Atomic Power Const., England	Cylindrical PCRV	1/10	Dungeness B	1	A, B, C
	Cylindrical PCRV	1/26	Dungeness B	1	B, C
	Heads, PCRV	1/72	Dungeness B	1	B, C
	Heads, PCRV	1/24	Dungeness B	3	B, C
	Heads, PCRV	1/26	Dungeness B	2	B, C
10. UKAEA, Foulness, England	Cylindrical PCRV	1/20	Safety Studies	10	C, D
11. Building Research Station, England	Cylindrical PCRV	1/10	Hinkley Point B	1	T
	Cylindrical PCRV	1/20	Hinkley Point B	4	T
12. General Atomic	Cylindrical PCRV	1/4	General	1	A, B, C
	Cylindrical PCRV	1/4	Ft. St. Vrain	1	A, B, C, D
	Multicavity PCRV	1/20	HTGR	1	A, B, C

Table 14 (continued)

Organization	Test Item	Scale	Project	Number of Models	Test for*
13. Oak Ridge National Lab.	Cylindrical PCRV	<1/5	General	4	A, B, C
	Wall, PCRV	1/6	General	1	A, T
	Closure, Steam Generator Cavity	1/15	GCFR	2	A, B, C
	Closure, Core Cavity	1/20	GCFR	1	A, B, C
	Head, PCRV	~1/30	General	2	C, D
14. University of Illinois	Head, PCRV	Not to scale	General	35	C, D
15. University of Sydney, Australia	Head, PCRV	1/20, 1/40	General	23	C, D
16. Siemens, Germany	Cylindrical PCRV (Prefabricated Blocks)	1/3		1	A, B, C
17. Krupp, Germany	Cylindrical PCRV	1/5	Gas-Cooled	1	A, B, C, T
	Head, PCRV	1/20	Reactor	1	A, B, C
18. ENEL/ISMES, Italy	Cylindrical PCRV	1/20	HTGR	4	A, B, C
	Head, PCRV	1/20	HTGR	6	A, B, C
	Cylindrical PCRV	1/10	BWR	2	A, B, C

Table 14 (continued)

Organization	Test Item	Scale	Project	Number of Models	Test for*
19. Ohbayashi-Gumi, Japan	Cylindrical PCRV	1/20	HTGR	1	A, B, C
	Multicavity PCRV	1/20		1	A, B, C
20. Cement and Concrete Inst. Trondheim, Norway	Cylindrical PCRV	1/3.6	Scandinavian PCRV (LWR)	4	A, B, C
21. A. B. Atomenergi, Studsvik, Sweden	Cylindrical PCRV	1/3.5	Scandinavian PCRV (LWR)	1	A, B, T
22. Shimizu Const. Ltd.,	Cylindrical PCRV	1/10	Hinkley Point B	1	A, B, C
		1/40	AGR	6	A, B, C
		1/40	General	1	T
	Multicavity PCRV	1/30	HTGR	3	A, B, C
	Head, PCRV		General	4	T
23. Nuclear Power Development Lab & Kashmi Kenetsu, K.K.	Cylindrical PCRV	1/20		3	A, B, T
24. PCPV Research & Development Group Kajima Corp.	Cylindrical PCRV		ORNL Model	3	A, B, C, T
	Multicavity PCRV	1/20	GA 1100 MW(e)	2	A, B, C

Table 14 (continued)

Organization	Test Item	Scale	Project	Number of Models	Test for*
25. Takenaka, Technical Research Laboratory	Head, PCRV	1/20	General	14	A, B, C
26. Central Research Institute of Electric Power Industry, Chiba, Japan	Cylindrical PCRV	1/10	HTGR	1	A, B, C, T
27. Danish Atomic Energy Commission, Riso	Closure, PCRV	1/11	Scandinavian PCRV	8	A, B, C
28. Austrian Research Center, Seibersdorf	Cylindrical PCRV		HTR	1	A, T
29. Swiss Institute of Technology (CEBAP), Lausanne	Multiactivity PCRV	1/20	HHT	1	A, B, C
30. KFA	PCRV Wall Segment	Full-section	HTR-500 THTR-300	3	A, D, T

*A - elastic response, B - design overpressure, C - failure, D - abnormal conditions, T - long-term creep and temperature.

Source: D. J. Naus, *A Review of Prestressed Concrete Reactor Vessel Related Structural Model Tests*, ORNL/GCR-80/10, Oak Ridge National Laboratory, Oak Ridge, Tennessee, 1980.

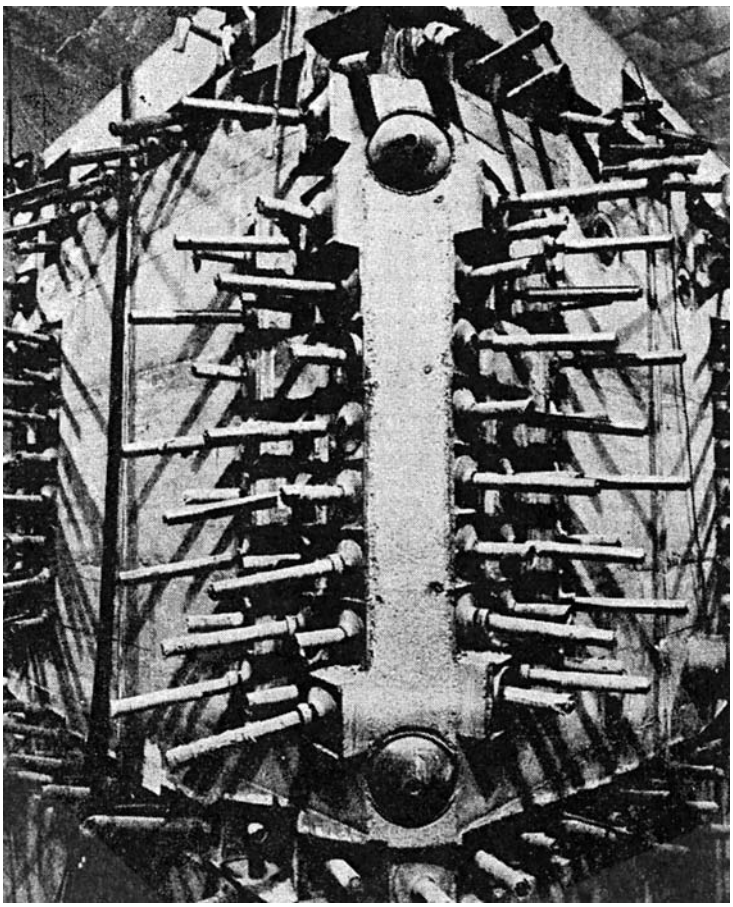

Figure 147 **EDF3 1:6-scale PCRV model.** *Source:* M. Lida and R. Ausangee, "Scale Models for Strength Testing Nuclear Pressure Vessels," Group G, Paper 44, *Prestressed Concrete Pressure Vessels*, Institution of Civil Engineers, London, pp. 497–505, 1968.

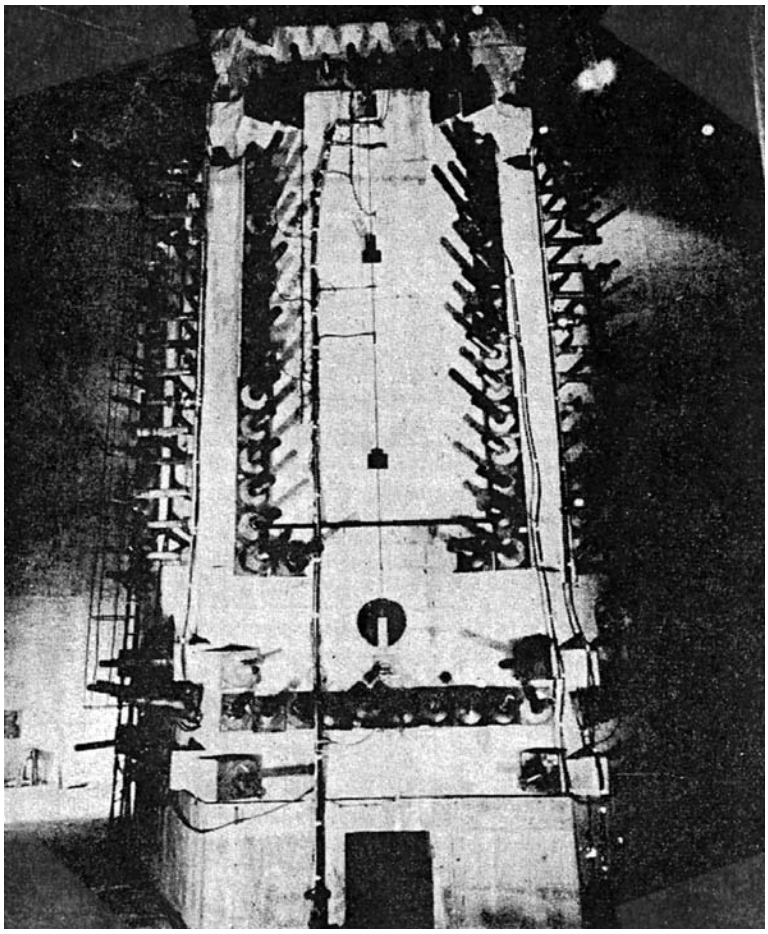

Figure 148 **EDF4 1:5-scale PCRV model.** *Source:* N. M. Lida and R. Ausangee, "Scale Models for Strength Testing Nuclear Pressure Vessels," Group G, Paper 44, *Prestressed Concrete Pressure Vessels*, Institution of Civil Engineers, London, pp. 497–505, 1968.

Sir Robert McAlpine and Sons Ltd. (United Kingdom).[185,186] The 1:8-scale model of a cylindrical PCRV shown in Fig. 149 was tested under prestress and various combinations of internal pressure and thermal loading. The test program covered 4 years and involved 5 series of tests: (1) hydraulic—up to 4.42 MPa at ambient temperature, up to 2.76 MPa at 50°C, and up to 1.79 MPa at 90°C; (2) five tests at elevated temperature under zero pressure with liner and gas ducts heated to 172°C and various fault conditions simulated by heating selected areas of the liner; (3) approximately two-thirds of top slab tendons were detensioned and 60 pressure cycles to 1.93 MPa applied at ambient and 94.5°C; (4) four 162–mm-diameter holes were placed in upper slab to simulate boiler loading holes and five tests up to 3.45 MPa were conducted at ambient temperature with half the top slab tendons tensioned; and (5) all tendons were removed from top slab and the model hydraulically pressurized at ambient temperature until failure (test was terminated at 3 times design pressure when top slab had lifted at inside edge of helical anchorage thus preventing further pressurization). It was concluded that the analysis methods were sufficiently conservative to enable them to be adopted as a design tool, the method of ultimate analysis used made a good assessment of the ultimate pressure and accurately predicted the mode of failure, cycling the load at ambient and elevated temperatures did not adversely affect elastic behavior, fault condition temperatures did not adversely affect the elastic behavior, neither the standpipe systems designed on a modular replacement basis nor the large carbon dioxide ducts caused any excessive or unexpected deflections or stresses to be set up in the concrete, and it was shown to be entirely satisfactory to stress the end slabs of a cylindrical PCPV using only a helical cable system.

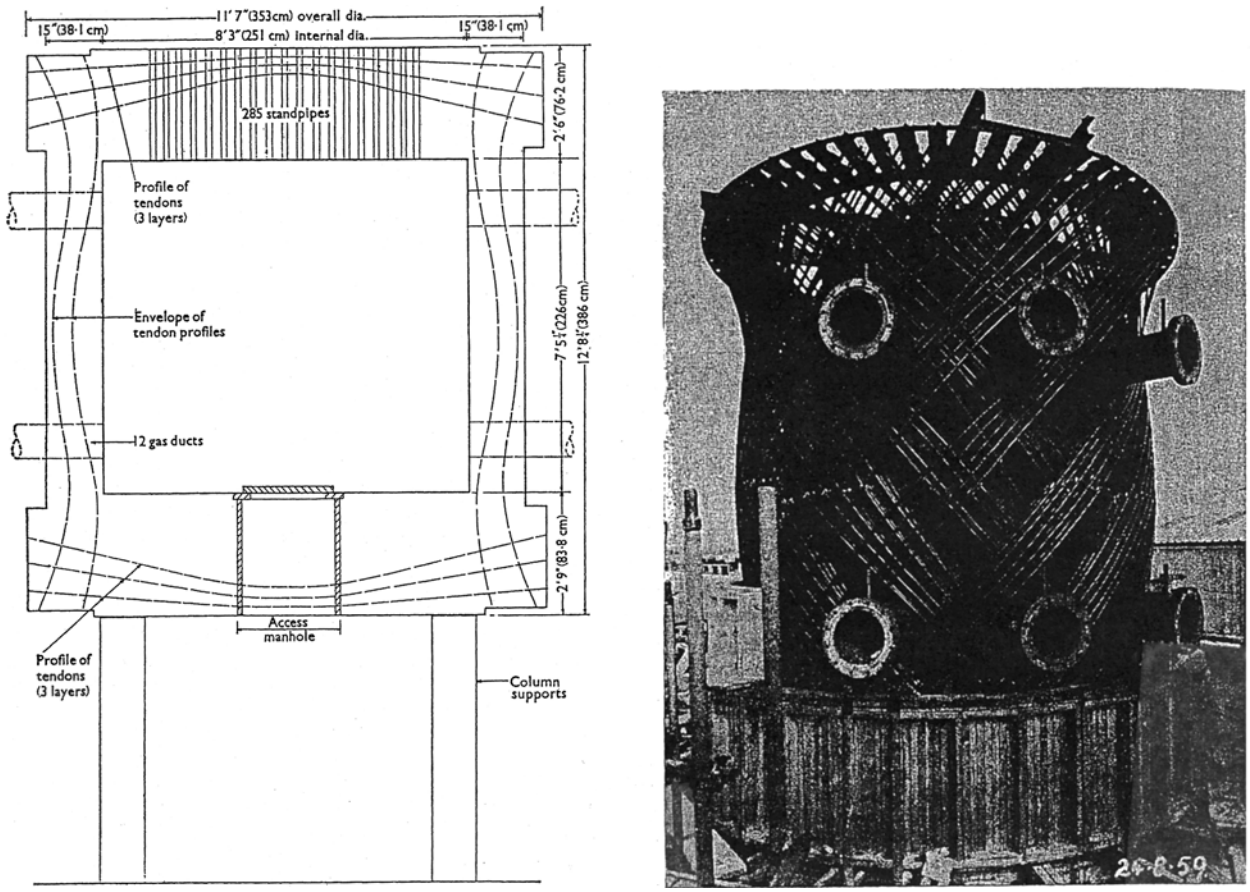

Figure 149 **1:8-scale cylindrical PCRV model.** *Source*: D. C. Price and M. S. Hinley, "Testing a l/8th Scale Cylindrical Vessel," Group G, Paper 43, *Prestressed Concrete Pressure Vessels,* Institution of Civil Engineers, London, pp. 489–496, 1968.

Kier Ltd. (United Kingdom).[187] The 1:12-scale ribbed spherical vessel shown in Fig. 150 was subjected to pressure and temperature loadings to investigate (1) elastic response to temperature and pressure loading prior to cracking. (2) cracking in a vessel that was largely unaffected by differential creep or shrinkage, and (3) the effect of aging on vessel performance. Under pressure testing, the model behavior was elastic to 1.72 MPa, and at pressures above 2.76 MPa, deflections increased rapidly with pressure. At 3.79 MPa the vessel liner failed, and the test was stopped so that the liner could be repaired. Upon repressurization, the liner again failed at 4.34 MPa. Vessel ultimate strength was then calculated to be 4.48 MPa. Temperature tests were conducted with an initial gradient of 24°C in order to avoid cracking and provide data for analysis comparisons. Long-term temperature tests were then conducted for a period of approximately 9 weeks in which the crossfall was increased in three equal stages to 36°C. During this test sequence, an internal pressure of 2.14 MPa was applied from day 40 to day 47. A temperature crossfall of 84°C was then imposed on the vessel while under a 2.14-MPa internal pressure to simulate a severe overload temperature. No extensive new cracking occurred as a result of this test, and the ability of the vessel to withstand severe temperature loading without great distress was demonstrated.

General Atomic Company (USA).[188] A 1:4-scale model of the PCRV for the Fort St. Vrain plant was fabricated and tested to meet the following objectives: (1) determine construction problems associated with use of preplaced aggregate, job-mixed concrete, liner installation, penetrations, and prestressing

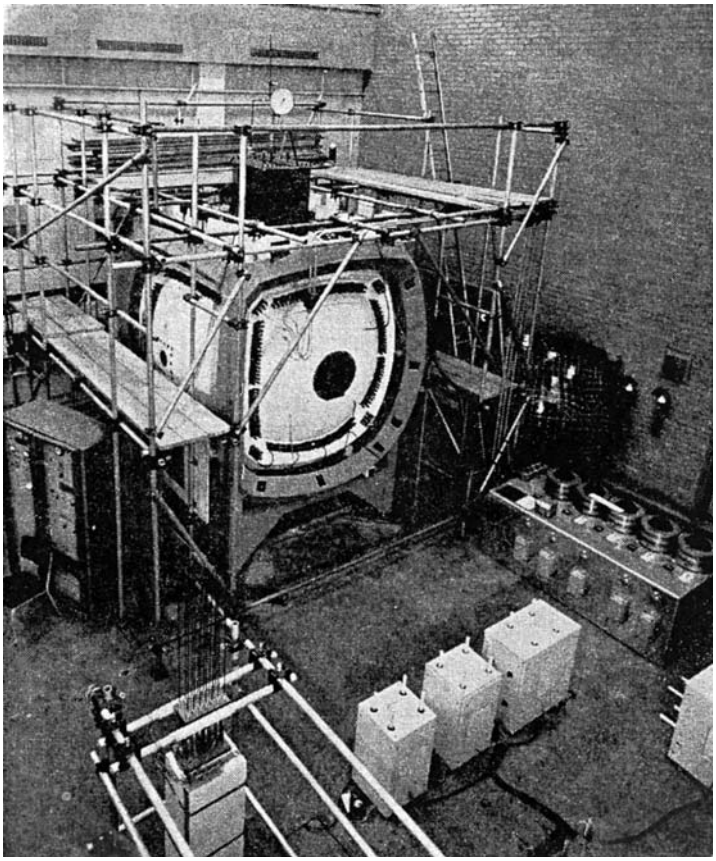

Figure 150 1:12-scale ribbed spherical pressure vessel model. *Source*: M. L. A. Moncrieff, "Comparison of Theoretical and Experimental Results for a Ribbed Spherical Vessel," Group G, Paper 42, pp. 469–479, *Prestressed Concrete Pressure Vessels*, Institution of Civil Engineers, London, 1968.

system; (2) evaluate strain and deformation response resulting from pressure, temperature, prestressing, and the combination of these forces; (3) qualitative determination of moisture loss rate; (4) observe effects of pressure cycles; (5) investigate time-temperature dependent concrete behavior; (6) evaluate gross gas leakage from a faulted liner; and (7) determine vessel response under overpressure loads. The model shown in Fig. 151 was subjected to a series of tests extending over a period greater than 2 years. Included in the test history were tests to demonstrate that the structural response of the vessel to short-term loadings up to reference pressure (4.86 MPa) was elastic, evaluate vessel performance with a constant temperature gradient of 27.8°C across the walls, and demonstrate the ability of the vessel to withstand overpressures up to 2.13 times the reference pressure without structural failure. An additional series of tests was conducted to demonstrate vessel behavior under abnormal and accident conditions (pneumatic overpressure to 1.6 times reference pressure, gas permeation tests, gas release tests, and tendon detensioning tests). Results obtained from the tests showed that the vessel response was linear up to 1.5 times reference pressure, response of vessel pressurization at temperature was not significantly different from the response at ambient when shrinkage cracks alone were present, creep rate during conditions of residual prestress and elevated temperature was lower than or equal to the measured rate of creep under prestress and ambient temperature and the creep rate in the model was less than that for reference cylinder specimens, and during overpressure tests up to 2.13 times reference pressure (2.61 times normal working pressure) no structural distress was noted although some surface cracking was

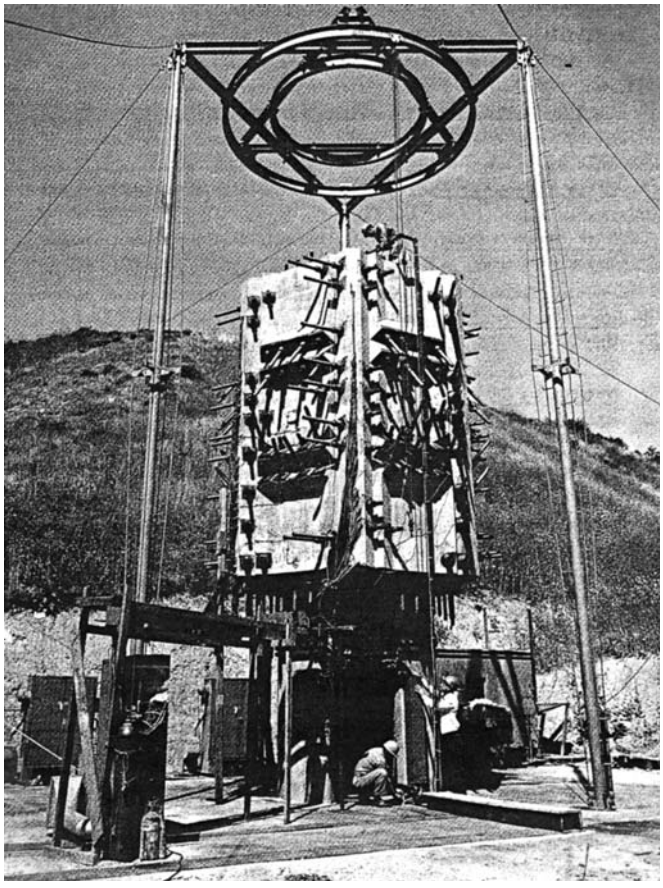

Figure 151 **1:4 scale Fort St. Vrain PCRV model.** *Source*: T. E. Northup, "Pressure and Temperature Tests and Evaluation of a Model Prestressed Concrete Pressure Vessel," GA-9673, General Atomic Co., September 15, 1969.

noted in the middle third portion of the barrel. Vessel response during the sustained prestress, transient and steady-state temperature distributions, short-time and sustained pressures, and pressure overload was calculated using a method of analysis that accounted for concrete creep, cable relaxation, cracking, and steel yielding. Results indicated that the analysis, which was based on a nonlinear superposition principle and a two-dimensional solution, agreed well with experimental results.

Austrian Research Center (Seibersdorf).[189,190] A large-scale model PCRV having a hot liner and adjustable wall temperature was constructed for use as a pressure vessel of the high temperature helium rig for the testing of high temperature reactor components. The 12-m-high by 2.6-m-diameter (1.5-m inner diameter) cylindrical vessel, as shown in Fig. 152, was designed to operate at a pressure of 10.0 MPa, a liner temperature of 300°C, and a concrete temperature of 120°C. The vessel wall section consisted of four functional parts (Fig. 153): the liner (5-mm-thick with anchor bolts), the insulating concrete, the structural concrete, and the prestressing system. Tubes that circulate nitrogen were used to control the temperature distribution in the wall. Thermal stabilization and pressure tests have been conducted on the vessel. During the first thermal cycle the vessel was carefully heated to 120°C and kept at this temperature for 100 d for thermal stabilization. During this period there initially was an increase and acceleration of viscoelastic strains and loss of prestress, but as the test period neared completion these changes had stopped and the values stabilized. Assumptions with respect to behavior and that large-scale concrete structures could operate for a prolonged period at temperatures above 100°C were verified. Prestress loss caused by creep and shrinkage of concrete was compensated for by retensioning. A pressure test to 1.15 times the operating pressure was conducted with measurements made to determine the liner and insulating concrete strains as well as the overall vessel geometric stability and tendon prestress. These measurements were noted to be in full agreement with the structural analysis that had been conducted previously. The next step was drying and stabilizing the insulating concrete at 140°C. The first test cycle with 150°C liner temperature and 80°C concrete temperature with a 50-bar internal pressure followed. Two 150°C cycles were executed followed by an increase in the liner temperature up to 200°C. In the fifth cycle, full load was applied with 300°C liner temperature, 120°C concrete temperature, and 95-bar internal pressure. Results obtained indicate that it is possible to operate a hot vessel in a stable state after a stabilization treatment is applied.

6.2.2 End Slab Model Tests

Imperial College (United Kingdom).[191] A study was conducted to investigate the behavior of unperforated and perforated circular plates with reinforced holes when subjected to radial in-plane loading and sustained uniform temperature. Two series of five specimens each, as shown in Fig. 154(a), were tested in the test rig shown in Fig. 154(b) at a test temperature of 80°C. Strains, temperatures, and loads were obtained during the tests so that creep, elastic, thermal, and shrinkage strains as well as internal stress and strain redistributions could be determined. Conclusions reached were that stresses around the perforated zones decrease as a result of differences in the rate of creep between the perforated and unperforated zone concretes, and the thermal stresses due to restrained thermal expansion on application of heat are reduced gradually as a result of thermal creep causing a redistribution of applied load stresses.

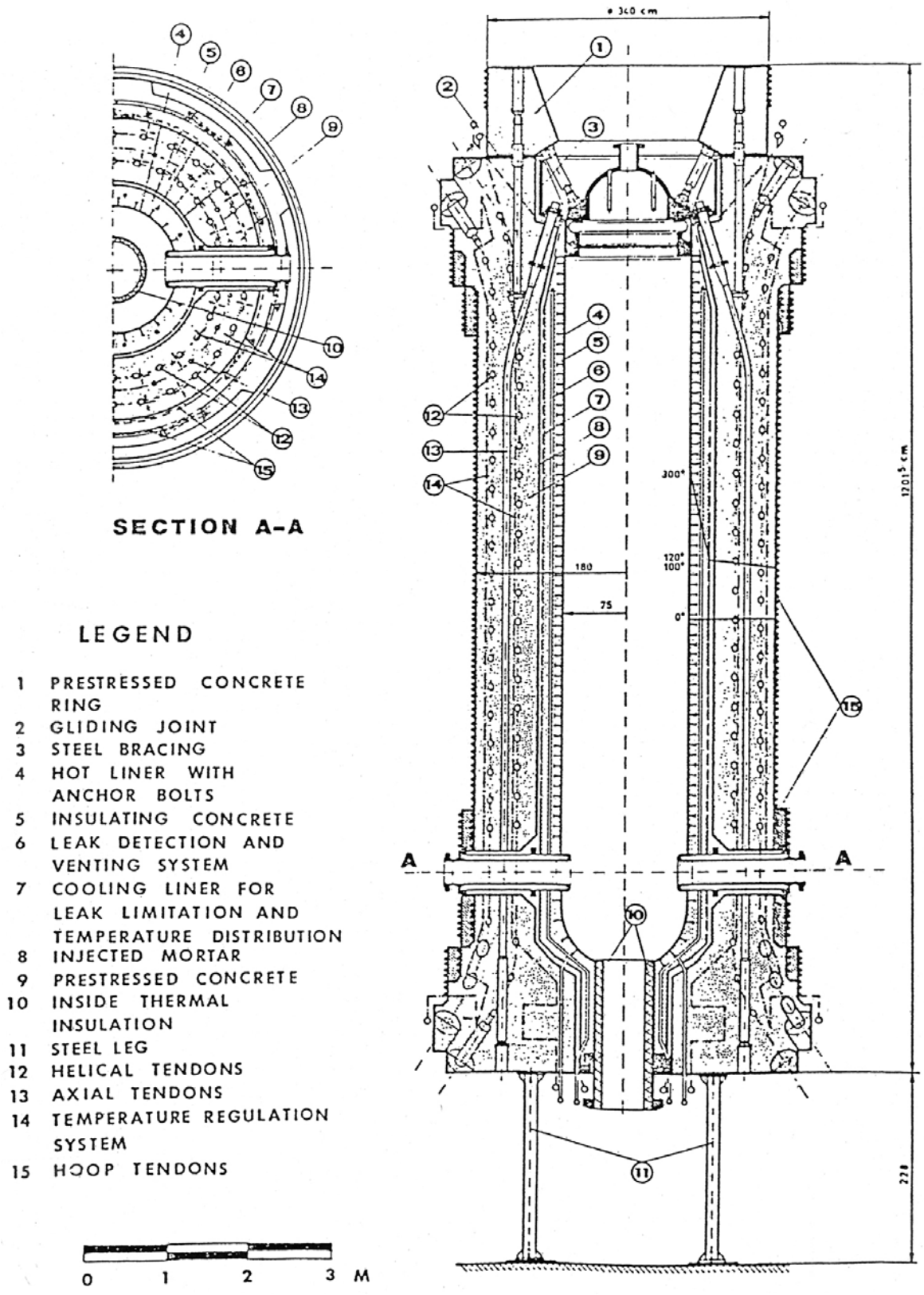

Figure 152 Austrian large PCRV model with hot liner. *Source*: J. Nemet et al., "Testing of a Prestressed Concrete Pressure Vessel with Hot Liner," Report SBB/He-3E, Reaktorbau Forschungs-und Baugesellschalft, Seibersdorf, Austria, November 1977.

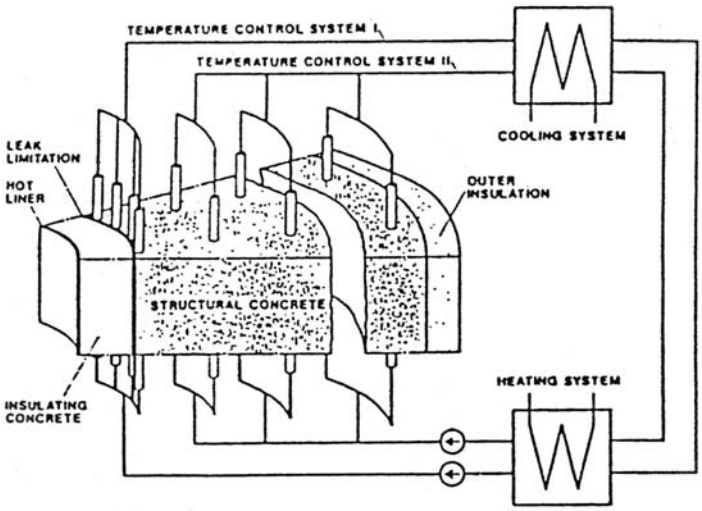

Figure 153 Section through vessel wall of Austrian PCRV model showing hot liner and adjustable wall temperature system. *Source*: J. Nemet et al., "Testing of a Prestressed Concrete Pressure Vessel with Hot Liner," Report SBB/He-3E, Reaktorbau Forschungs -und Baugesellschalft, Seibersdorf, Austria, November 1977.

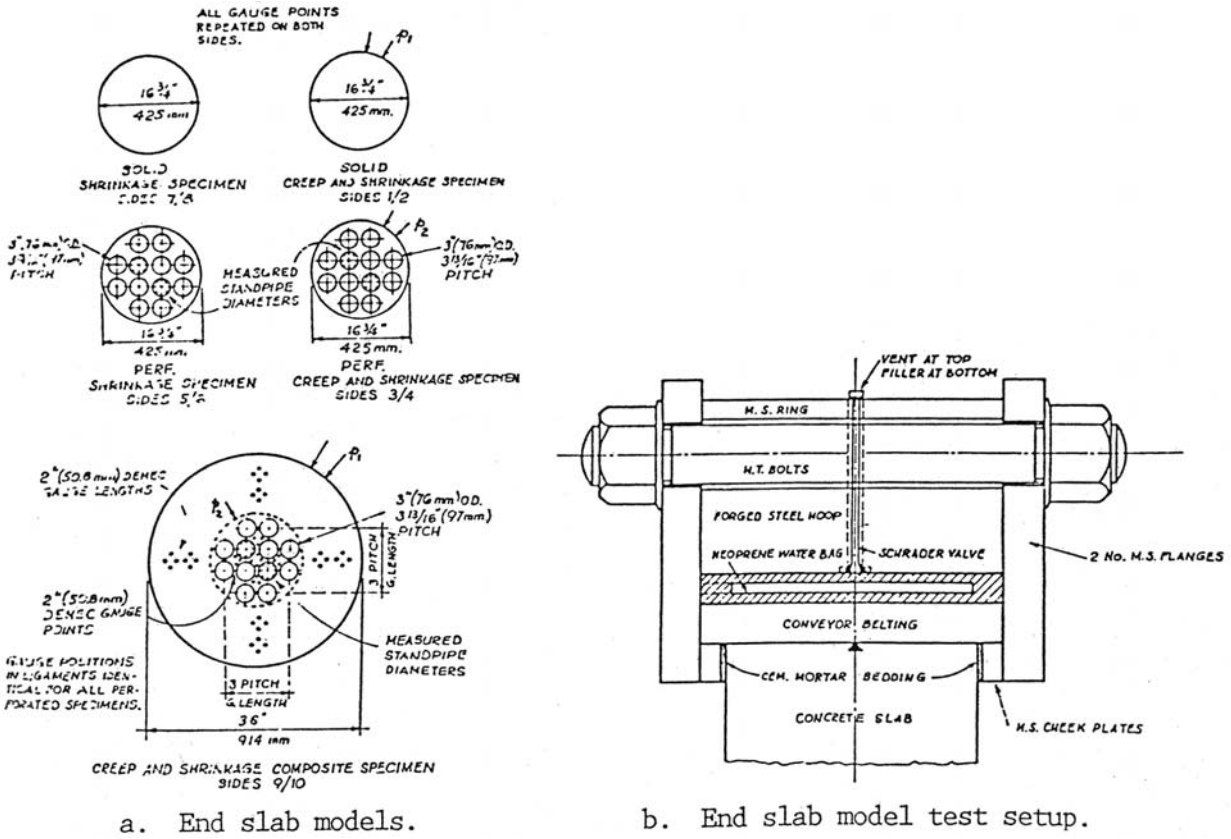

Figure 154 Unperforated and perforated plate tests. *Source*: G. D. Stefanou et al., "An Experimental Investigation Into the Behaviour of Perforated End Slabs for Concrete Pressure Vessels Under Temperature and External Load," Paper 8, *Model Techniques for Prestressed Concrete Pressure Vessels*, The British Nuclear Energy Society, London, 1968.

6.2.3 Thermal and Moisture Migration Model Tests

Building Research Station (United Kingdom).[192] An investigation was conducted to provide information on model techniques applied to temperature loading on massive concrete structures. The primary concrete shields at Hinkley Point A nuclear power station were used as the prototype. Repeated tests were made to compare, during alternations between uniform temperature and the required temperature distribution, the behaviors of models of two different geometric scales with each other and with analysis results. Four 1:20-scale and one 1:10-scale (Fig. 155) models were tested. In addition to thermal loadings, one of the

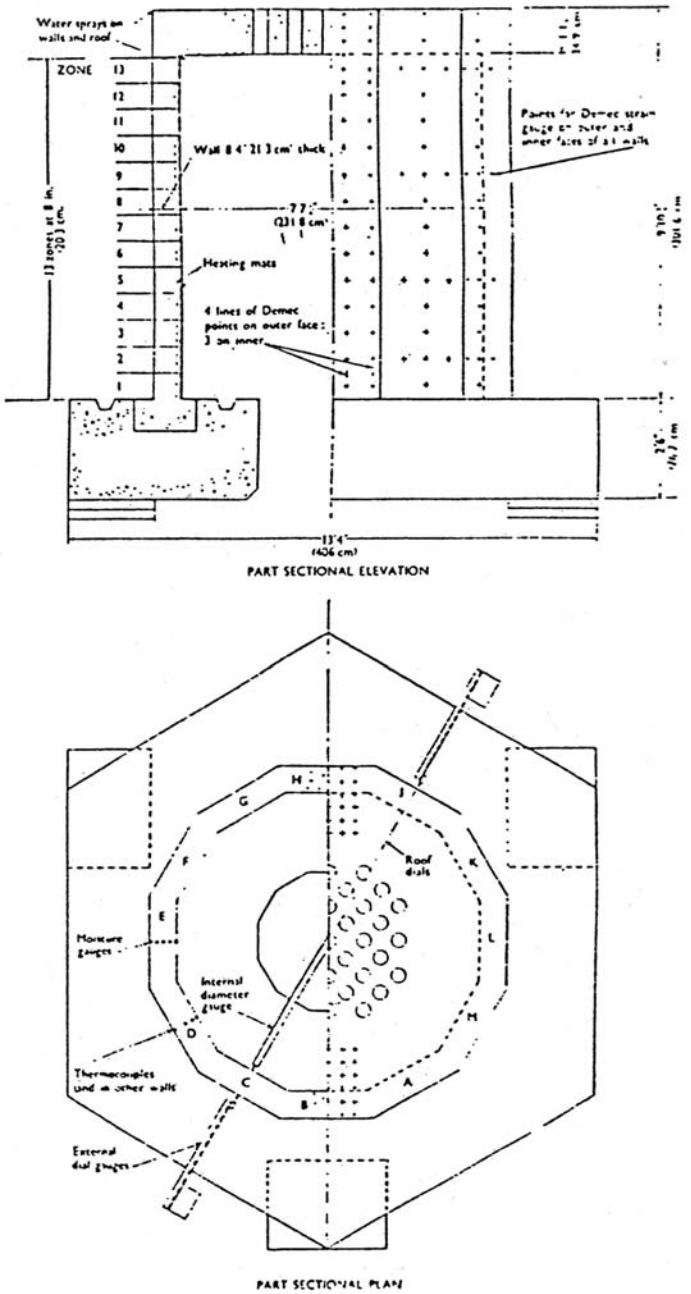

Figure 155 **1:10-scale Hinkley Pt. A primary shield model.** *Source*: C. R. Lee et al., "Behaviour of Model Concrete Structures Under Temperature Loading," Group G, Paper 46, *Prestressed Concrete Pressure Vessels*, Institution of Civil Engineers, London, pp. 517–525, 1968.

1:20-scale models was tested while under external mechanical loadings (Fig. 156). Models 1 and 2 were used to develop test techniques while the remaining three models were used for the main investigation. The majority of tests were conducted with the models subjected to superficial water sprays to maintain a saturated condition to give better stability and a better simulation of practical conditions than would have been obtained by permitting the concrete to dry. Measurements obtained during testing included temperatures, internal and external wall deflections, and vertical and horizontal strains of the inner and outer surfaces of the walls and roof. Observations from the tests were that the rate of drying was potentially much greater in the model than prototype, short-term temperature tests were insensitive to changes in the rate of heating, reasonably good agreement was noted between experiment and theory, and model techniques can be satisfactorily applied to short-term temperature loadings of massive concrete structures within normal operating conditions.

Central Electricity Research Laboratories (United Kingdom).[193,194] A 1:8-scale model of the PCRV for Oldbury was investigated (Fig. 157). The thermal testing was conducted in four phases: (1) preliminary thermal cycle of 17 d (2 d required to obtain desired inner and outer temperatures of 55°C and 29°C,

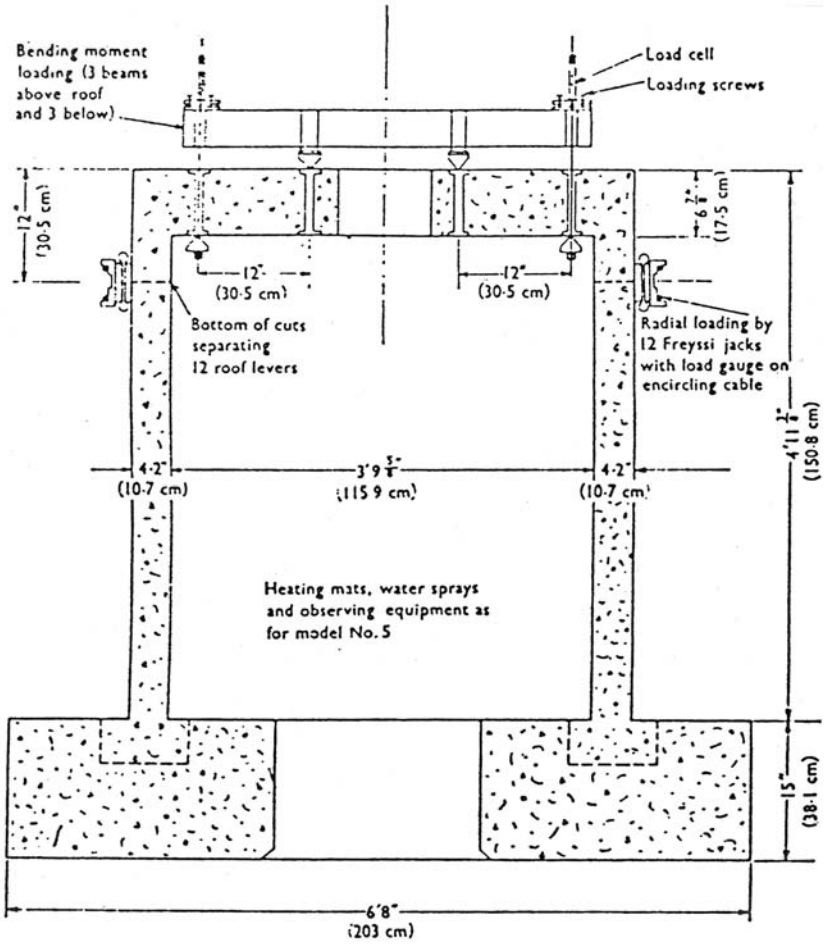

Figure 156 **1:20-scale Hinkley Pt. model mechanical load system setup.** *Source*: C. R. Lee et al., "Behaviour of Model Concrete Structures Under Temperature Loading," Group G, Paper 46, *Prestressed Concrete Pressure Vessels*, Institution of Civil Engineers, London, pp. 517–525, 1968.

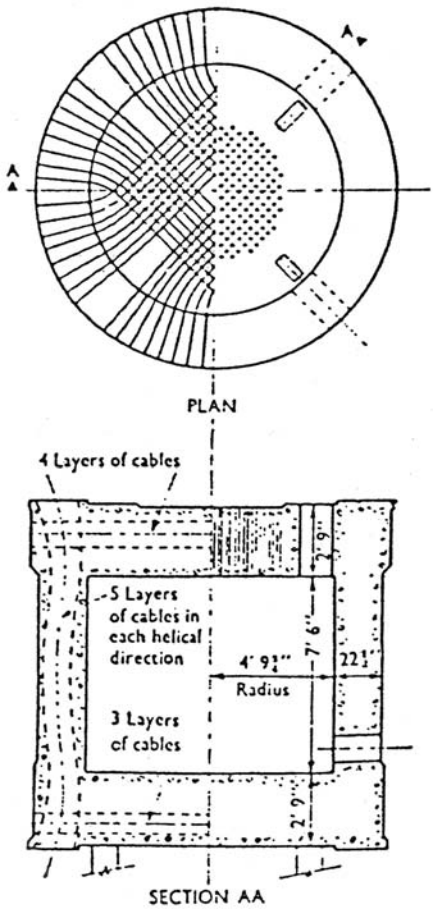

Figure 157 **1:8-scale Oldbury PCRV Model.** *Source*: I. W. Hornby, "The Behaviour of the Oldbury Model Vessel with Time Under Thermal and Pressure Loadings," Paper No. 11, *Model Techniques for Prestressed Concrete Pressure Vessels*, The British Nuclear Energy Society, London, 1968.

respectively, followed by 15 d of cooling); (2) main thermal cycle of 2 d heatup followed by 5 d of cooling; (3) superposition of pressure (2.65 MPa) onto the thermal loading (vessel pressurized, heated for 2 d, allowed to cool for 13 d, and then depressurized); and (4) same sequence as the third phase except the temperature and pressure remained 61 d followed by 16 d of cooling prior to depressurization. It was noted in the tests that several factors were to be considered in determining total strain changes: the coefficient of thermal expansion for the second and subsequent loading cycles was approximately 20% less than the initial value, so the residual thermal expansion from the first thermal cycle must be considered in subsequent loading cycles; creep strain due to a temperature increase was not understood sufficiently; creep-produced stress redistributions were neglected for long periods of loading; the variation of creep recovery with stress decrease was nonlinear; and shrinkage was neglected in the tests, but large shrinkage strains did not occur prior to the test. It was concluded that the response of the model could be predicted during the thermal and creep tests, but basic information relative to creep of concrete subjected to variable stress, temperature, and moisture content was required for estimating (modeling) long-term performance.

During commissioning tests of Oldbury, there were a small number of localized breakdowns of the liner insulation permitting the temperature to reach 180°C in the head penetration region and 90°C in the haunch region at the upper boiler instrument penetration, which could have induced cracking in the concrete. To provide input on concrete cracking, a full-scale model (3.66 m by 1.52 m thick) of the region

of the vessel local to the upper boiler instrumentation where the highest liner temperatures were recorded was fabricated and tested (Fig. 158). The test procedure included heating of the model over a 24-h period to the steady-state condition achieved in the hot spot region of the prototype, allowing the model to attain thermal equilibrium, and maintaining this condition for 3 months with the prestressing force reduced as the test progressed, permitting the model to cool to ambient, and injection of a dye between the liner and concrete to denote cracking. Core samples that were taken to determine concrete strength and to locate internal cracking revealed cracking parallel to the liner at the level of the cooling tubes. This indicated that cracking probably had occurred in the prototype vessel near penetrations at hot spots over 100°C, but the cracking was limited to the immediate vicinity of the hot spot, and the effectiveness of the liner

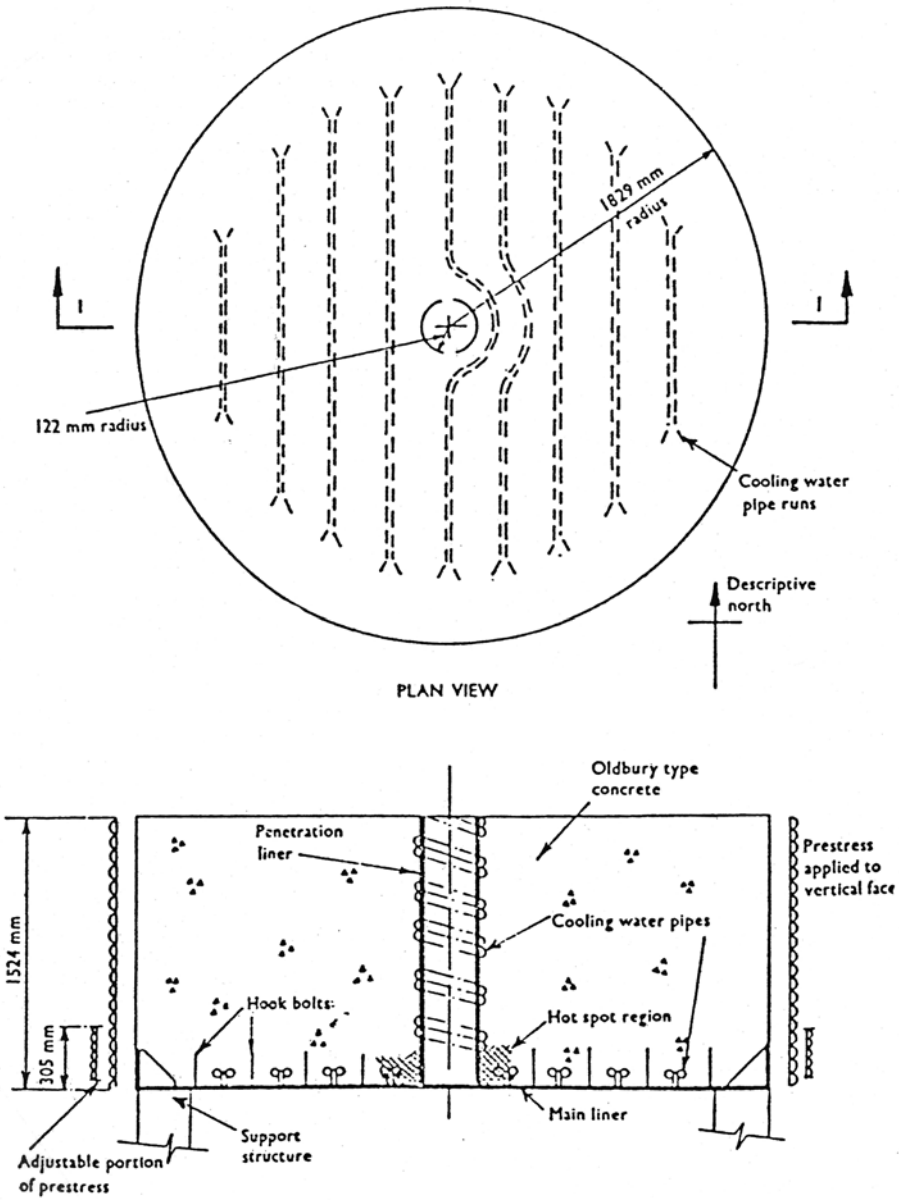

Figure 158 **Full-scale Oldbury hot-spot model.** *Source*: J. Irving et al., "A Full Scale Model Test of Hot Spots in the Prestressed Vessels of Oldbury Nuclear Power Station," Paper 7699, *Proc. Instn. Civil Engineers* **57**, June 1974.

anchorages was not jeopardized. Results also showed that there was not significant loss of strength in uncracked regions of the model where cooling tubes provided heat removal functions, and that the cracks were restricted to localized hot spots around penetrations.

Compagnie Industrialle le Travaux (Paris).[195] Two 1:5-scale models of the Bugey PCRV were constructed (Fig. 159). The first model was to determine rupture strength, and the second was for more detailed tests such as thermal tests. The model had an outside diameter of 5.5 m, a wall thickness of 1.1 m, a height of 10.7 m, and an end slab thickness of 1.4 m. Thermal tests were conducted on the second model according to the test history presented in Fig. 160(a). These tests were followed by special tests as noted in Fig. 160(b), which included a series of tests in which one, five, or all of the standpipes in the head region (Fig. 161) were heated to temperatures of 80, 100, and 120°C. During these tests buckling of the liner occurred between liner anchorages due to the large compressive strains caused by the thermal gradient. In general, the tests confirmed earlier computer analyses, and only slight modifications in the design of the anchors were required near some of the penetrations.

Centre Experimental de Researches et d'Etudes du Batiment et des Travaus Publics (CEBTP) France.[196] Following satisfactory operation of G2 and G3 in Marcoule, and with difficulties encountered in the construction of steel containments of the type EDF 1 and EDF 2, the French Atomic Energy Commission (CEA) decided to test a simplified model of the EDF 3 type and subject it to thermal cycling tests.

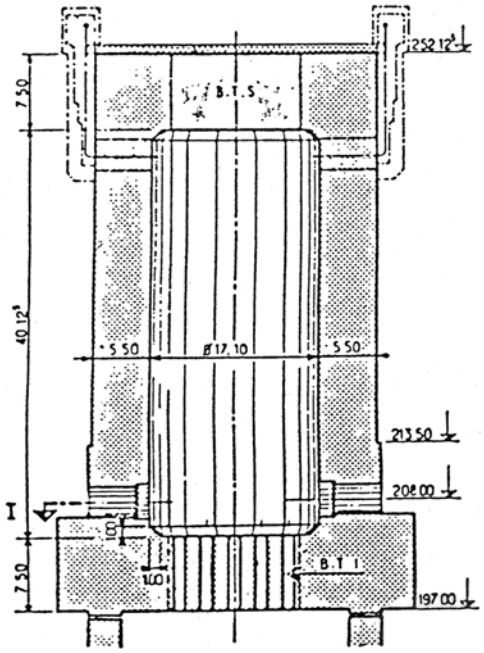

Figure 159 **1:5-scale model Bugey PCRV.** *Source*: P. Launay, "Apparatus, Instrumentation, and Concrete Models of Bugey I Prestressed Concrete Pressure Vessel," Paper SP-34-69, Session 17, *Concrete for Nuclear Reactors*, Vol. III, American Concrete Institute Special Publication SP-34, Farmington Hills, Michigan, pp. 1529–1566, 1979.

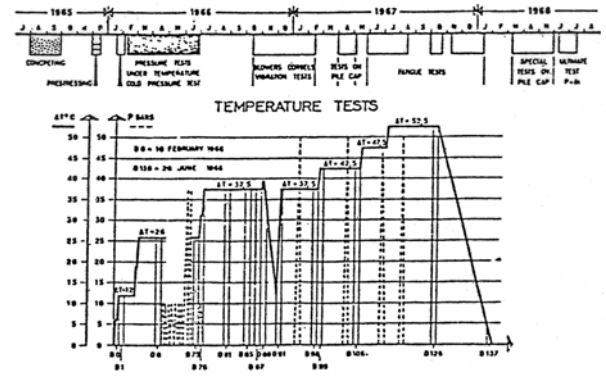

a. Temperature-time history.

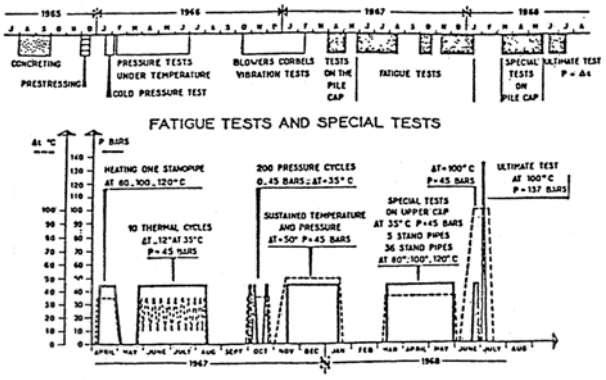

b. Special test loading history.

Figure 160 1:5-scale Bugey PCRV model test history.
Source: P. Launay, "Apparatus, Instrumentation, and Concrete Models of Bugey I Prestressed Concrete Pressure Vessel," Paper SP-34-69, Session 17, *Concrete for Nuclear Reactors*, Vol. III, American Concrete Institute Special Publication SP-34, Farmington Hills, Michigan, pp. 1529–1566, 1979.

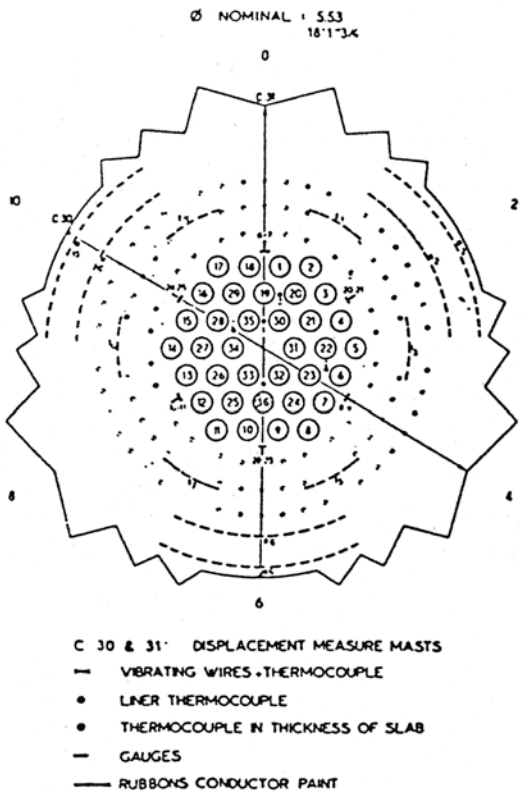

Figure 161 1:5-scale Bugey standpipe region model.
Source: P. Launay, "Apparatus, Instrumentation, and Concrete Models of Bugey I Prestressed Concrete Pressure Vessel," Paper SP-34-69, Session 17, *Concrete for Nuclear Reactors*, Vol. III, American Concrete Institute Special Publication SP-34, Farmington Hills, Michigan, pp. 1529–1566, 1979.

Figure 162 presents a cross section of the model that was prestressed vertically and horizontally. The model was a 1:10-scale version of the prototype except for the height, which was doubled so that the central region could be considered as approximating an infinitely long cylinder. The interior of the model was heated by electrical-resistance heaters, and the exterior was cooled by circulated air. Eight heating cycles were applied to the model over a period of approximately 27 months with maximum temperatures at the inside face of the model being 200°C for cycles 1–7 and 260°C for cycle 8. Temperature distributions were found to be relatively uniform along the 5-m height for a distance of approximately 0.5 m from the ends. Temperatures, strains, and overall deformations were measured during the test. Results obtained showed that calculated temperature distributions were valid for both the steady-state and transient conditions; primary cracking was vertical, forming in the center of the free section between lugs for prestressing anchorage and running the complete model length; secondary horizontal cracks also formed (it was noted that these cracks which were 8-cm long at the end of the second thermal cycle were 12–13 cm at the end of the last cycle and that their width had increased from approximately 0.33 mm to 2.25 mm); water content measurements indicated that the 7 cm of concrete next to the inside surface had dried when the temperature reached 150°C, at a temperature of 175°C the region of drying had reached

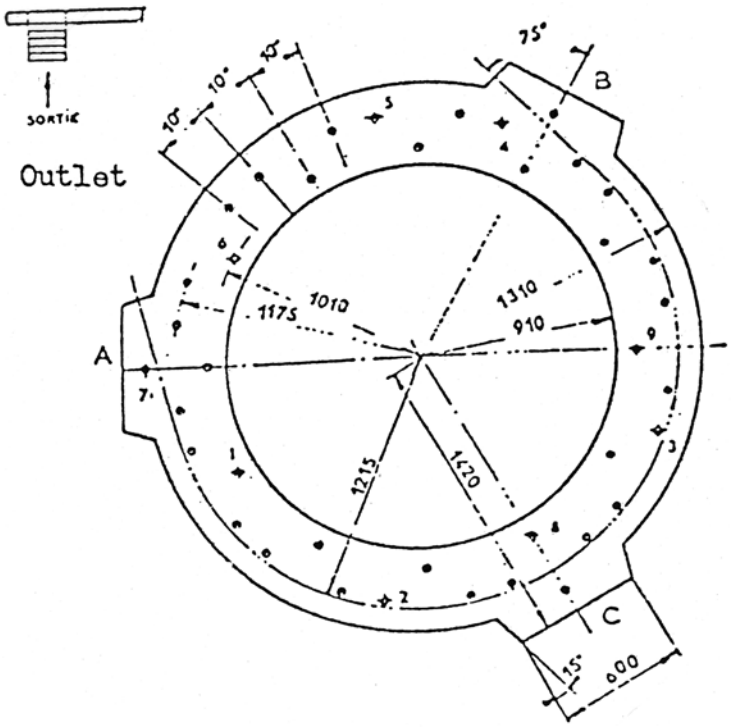

Figure 162 **Simplified 1:10-scale EDF3-type model used in thermal cycling tests.** *Source*: F. Dubois et al., "Study of a Reduced Scale Model of a Prestressed Concrete Vessel Subjected to a Large Thermal Gradient," Annales de 1'Institut Technique du Batimen't et des Travaux Publics. No. 214, October 1965.

20 cm, and at the end of the second heating cycle, drying had reached 30 cm; and prestressing losses averaged 30% and 20% at the end of all heating cycles for the horizontal and vertical tendons, respectively. Companion test specimens were also tested to determine concrete mechanical properties under the influence of temperature, and in general it was found that there was no significant compressive strength variation for specimens subjected to 150°C for periods of 7–180 d, tensile strengths decreased approximately 12% for 180 d exposure at 150°C, and the weight loss for specimens exposed to 150°C was approximately 4.6% regardless of curing period. It was concluded in the investigation that the safety factor for temperature for these vessels is high and that accidental temperature increases of the vessel can be considered without too much fear for vessel integrity.

Oak Ridge National Laboratory (USA).[197,198] A thermal cylinder experiment was designed both to provide information for evaluating the capability of analytical methods to predict the time-dependent stress-strain behavior of a 1:6-scale model of the barrel section of a single-cavity PCRV and to demonstrate the structural behavior under design and simulated thermal conditions such as could result from an accident. The model shown in Fig. 163 was a thick-walled cylinder having a height of 1.22 m, a thickness of 0.46 m, and an outer diameter of 2.06 m. It was prestressed both axially and circumferentially and subjected to a 4.83-MPa internal pressure together with a thermal crossfall imposed by heating the inner surface to 65.7°C and cooling the outer surface to 24°C. Because the model was designed to study the behavior of the barrel section of a massive concrete structure, all exposed surfaces were sealed to prevent loss of moisture, and the ends of the cylinder were insulated to prevent heat flow in the axial direction. The experiment utilized information developed from previous studies of concrete materials properties, triaxial creep, instrumentation, analyses methods, and structural models. The initial

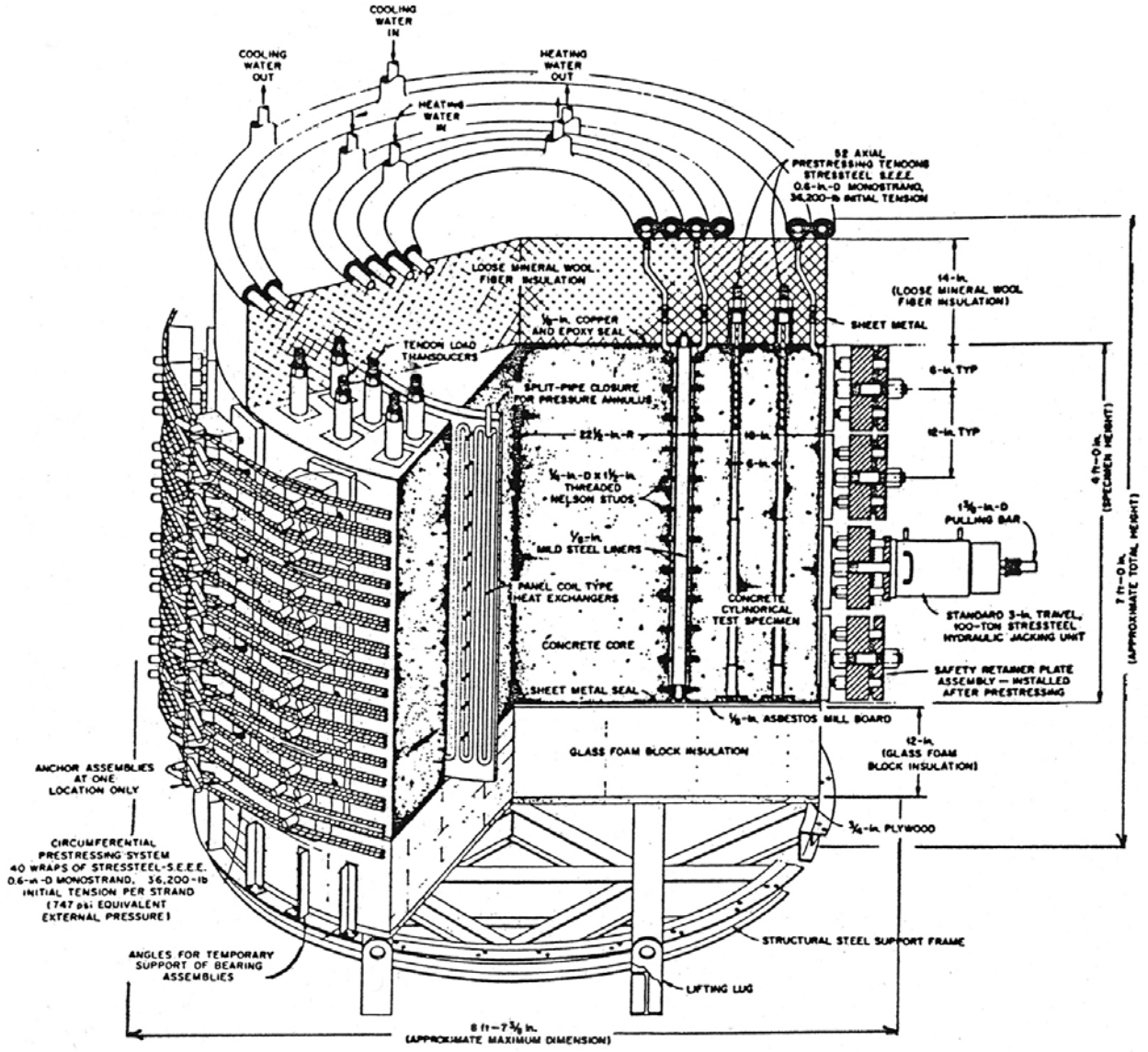

Figure 163 Isometric of ORNL thermal cylinder test structure. *Source*: J. J. P. Callahan et al., *Prestressed Concrete Reactor Vessel Thermal Cylinder Model Study*, ORNL/TM-5613, Oak Ridge National Laboratory, June 1977.

460 d of testing were divided into time periods that simulated prestressing, heatup, reactor operation, and shutdown. At the conclusion of the simulated operating period, the model was repressurized and subjected to localized heating at 232°C for 84 d to produce an off-design hot-spot condition. Comparisons of experimental data with calculated values obtained using the SAFE-CRACK finite-element computer program showed that the program was capable of predicting time-dependent behavior in a vessel subjected to normal operating conditions, but that it was unable to accurately predict the behavior during off-design hot-spot heating. Readings made using a neutron and gamma-ray backscattering moisture probe showed little, if any. moisture migration in the concrete cross-section. Destructive examination indicated that the model maintained its basic structural integrity during localized hotspot heating.

In an effort to obtain information regarding the nature of moisture movement and rate of moisture loss in a PCRV, an experimental study of moisture migration in a pie-shaped specimen representing the flow

path through a cylindrical wall of a PCRV was conducted. The model was 2.74 m in length with cross-sectional dimensions of 0.61 by 0.61 m on one end and 0.61 by 0.81 m on the other end. It was sealed against moisture loss on the small end (interior) and along lateral surfaces and exposed to the atmosphere at the other end (exterior). A series of heating lamps such as shown in Fig. 164 were used to maintain the required temperature on the simulated interior surface. Temperature distributions, shrinkage, and moisture distribution were monitored for approximately 17 months prior to application of a 44°C temperature gradient that was maintained for one year. At the end of the test, with the exception of zones nearest the ends of the specimen, moisture contents were fairly constant. Concrete strains corrected for thermal effects were small with only 1 m (that nearest open end) indicating shrinkage strain in excess of 20 millionths, implying that drying shrinkage was minimal. It was concluded that moisture migration in thick sections of concrete, such as a PCRV, is a slow process and is not likely to be a significant factor with temperature differences of 44°C or less.

Central Research Institute of Electric Power Industry (Japan).[199] An investigation was conducted to determine the effects of differential thermal creep on the behavior of a PCRV model that was subjected to a long-term temperature gradient across the wall for a duration of 4 months and to investigate the applicability of analytical methods for estimating the time-dependent behavior. The model shown in Fig. 165 was approximately 1:10-scale and was prestressed axially and circumferentially. A lead plate liner was used to seal the inner surface. During the first stage of tests the elastic behavior of the model at prestressing and during an internal design pressure test was investigated. The temperature at the inside surface of the model was then incremented in 10°C steps with the thermal crossfall maintained for 3 weeks at each increment except for the last increment which represented a $\Delta T = 40°C$ where it was maintained for 8 weeks. After thermal creep tests, the model was pressurized to failure which occurred at 3.2 times design pressure. It was concluded that the creep characteristics of the model could be predicted using a strain hardening method as well as the rate of creep if measured values of the concrete creep and thermal properties were incorporated into the analysis, and that significant stress relaxation occurs indicating the necessity of evaluating the thermal stresses in the design with due consideration given to

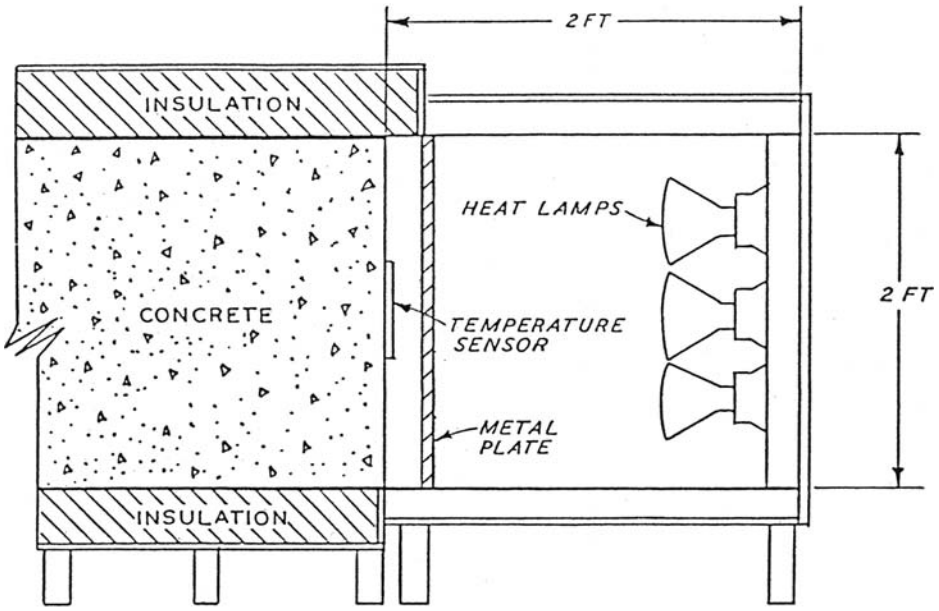

Figure 164 **Heating arrangement for moisture migration test conducted at Waterways Experiment Station.** *Source*: J. E. McDonald, *Moisture Migration in Concrete*, Technical Report C-75-1, U.S. Army Waterways Experiment Station, Vicksburg, Mississippi, May 1975.

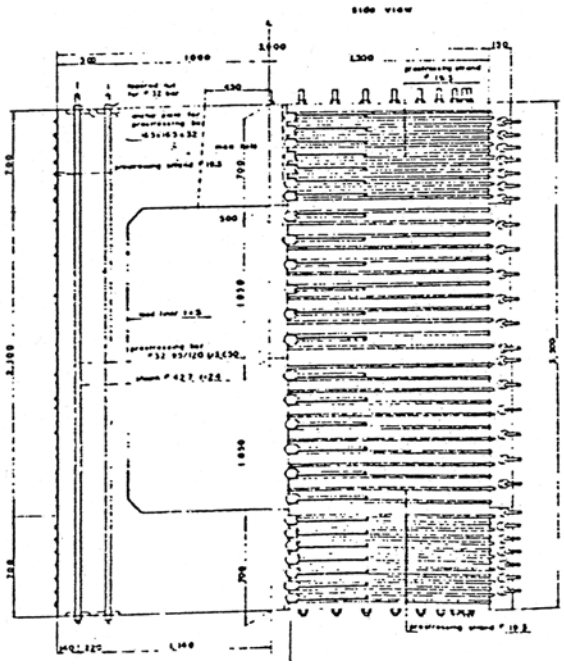

Figure 165 1:10-scale PCRV thermal creep model.
Source: H. Ohnuma et al., "Creep Behavior Under Sustained Temperature Gradient in a Model of Prestressed Concrete Reactor Vessels," Paper H 4/9, Vol. H, *Proc. of 5th Ind. Conf. on St. Mech. in Reactor Technology*, Berlin, 1979.

creep behavior of concrete at high temperature and of selecting suitable prestressing procedures to cope with the stress redistributions caused by thermal creep.

Institut für Nukleare Sicherheitsforschung der Kernforschungsanlage (Germany).[200] At KFA, the effects of a hypothetical accident that can lead to an unrestricted heatup of the reactor core in a high-temperature reactor (HTR) was investigated. For such an accident, it was assumed that all active cooling systems had failed, and during the course of the accident it takes an extended period of time before the temperature reaches a level sufficient to fail the insulation, liner, and concrete. In the experiments, sections (reinforced concrete, liner plate anchored with bolts and cooling pipes) of the PCRV 1 m by 1.5 m by 0.5 m were heated while suspended over an electric chamber furnace (Fig. 166). The facility can heat specimens up to 1500°C using a preset accident temperature-time curve. Two types of high-strength (55–60 MPa) concrete were investigated: a limestone aggregate concrete used in the THTR-300 and a basalt aggregate concrete for the HTR-500. Three tests were completed: two tests utilizing the limestone aggregate concrete without insulation and one test using the basalt aggregate concrete with 10 cm of Kaowool insulation. During a test, which may last up to 6 months, measurements were made of the temperature distribution in the concrete and insulation, pressure buildup, and water released. Calculations of water and gas release were made using a modified version of the Sandia USINT code.[201] Results of the first two tests in which the specimens were heated on the liner side to 1410°C and 1470°C showed that release of CO_2 from the calcitic concrete began at about 600°C with a maximum near 900°C; above 900°C the concrete was granular and powdered, and possessed little, if any strength; at 600°C the concrete retained 45% of its room temperature strength; above 1000°C the liner had lowered perceptibly due to creep; at a liner temperature of 1270°C, a ~3-mm-thick iron oxide layer (scale) began to peel off the liner (when a helium temperature was present, the scale did not form); at 1350–1400°C, a hole formed in the liner

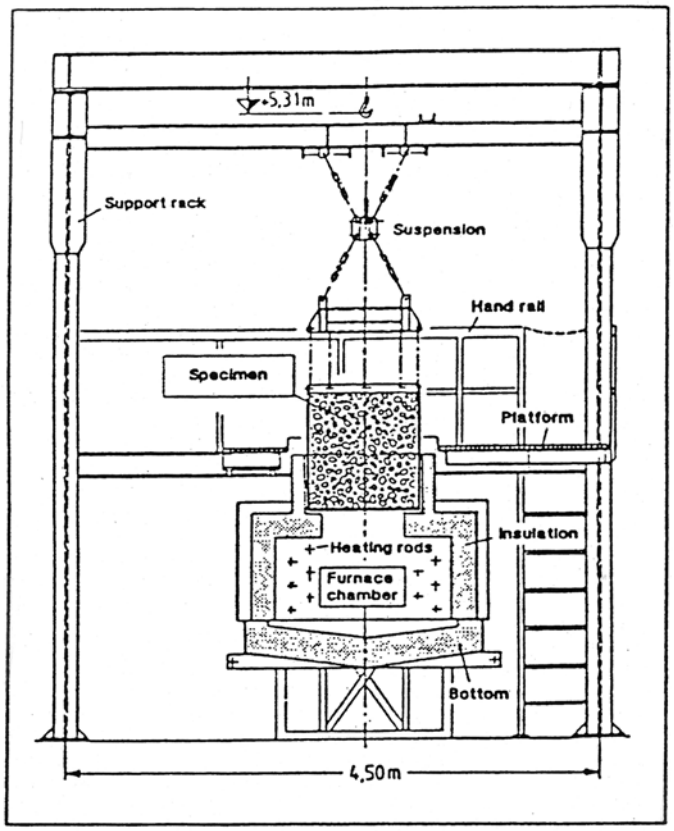

Figure 166 Experimental setup for subjecting PCRV wall sections to elevated temperature. *Source*: J. Altes et al., "Experimental Study of the Behaviour of Prestressed Concrete Pressure Vessels of High Temperature Reactors at Accident Temperatures," *Trans. of the 9th Intl. Conf. on St. Mech. in Reactor Technology*, Vol. H, Lausanne, Switzerland, August 17–21, 1987.

through which molten steel material leaked; and the side of the liner facing the concrete displayed considerable corrosion. In one test, the ability to refeed water into the cooling tubes, after a simulated failure of both trains of the liner cooling system, was investigated. Experimental results showed that for temperatures up to 450°C it was possible to refeed water into the cooling tubes to cool the concrete down to normal operating conditions (liner temperature of 50–55°C).

7 SUMMARY AND CONCLUSIONS

7.1 Summary

Under normal conditions most concrete structures are subjected to a range of temperature no more severe than that imposed by ambient environmental conditions. However, there are important cases where these structures may be exposed to much higher temperatures (e.g., jet aircraft engine blasts, building fires, chemical and metallurgical industrial applications in which the concrete is in close proximity to furnaces, and some nuclear power-related postulated accident conditions). Of primary interest in the present study is the behavior of reinforced concrete elements in designs of new generation reactor concepts in which the concrete may be exposed to long-term steady-state temperatures in excess of the present ASME Code limit of 65°C. Secondary interests include performance of concrete associated with radioactive waste storage and disposal facilities, and postulated design-basis accident conditions involving unscheduled thermal excursions. Under such applications the effect of elevated temperature on certain mechanical and physical properties may determine whether the concrete will maintain its structural integrity.

Concrete's properties are more complex than for most materials because not only is the concrete a composite material whose constituents have different properties, but its properties also depend on moisture and porosity. Exposure of concrete to elevated temperature affects its mechanical and physical properties. Elements could distort and displace, and, under certain conditions, the concrete surfaces could spall due to the buildup of steam pressure. Because thermally induced dimensional changes, loss of structural integrity, and release of moisture and gases resulting from the migration of free water could adversely affect plant operations and safety, a complete understanding of the behavior of concrete under long-term elevated-temperature exposure as well as both during and after a thermal excursion resulting from a postulated design-basis accident condition is essential for reliable design evaluations and assessments. Because the properties of concrete change with respect to time and the environment to which it is exposed, an assessment of the effects of concrete aging is also important in performing safety evaluations.

The objective of this limited study was to provide an overview of the effects of elevated temperature on the behavior of concrete materials. In meeting this objective the effects of elevated temperatures on the properties of ordinary Portland cement concrete constituent materials and concretes are summarized. The effects of elevated temperature on HSC materials are noted and the performance compared to NSCs. A review of concrete materials for elevated-temperature service is presented. Nuclear power plant and general civil engineering design codes are described. Design considerations and analytical techniques for evaluating the response of reinforced concrete structures to elevated-temperature conditions are presented. Pertinent studies in which reinforced concrete structural elements were subjected to elevated temperatures are described.

7.2 Conclusions

A substantial body of knowledge on the material properties of ordinary Portland cement concretes at elevated temperature is available. The use of these data for a quantitative interpretation of the response of reinforced concrete structural elements in nuclear power plants to long-term moderate elevated-temperature exposure (≥65°C) or design basis and hypothetical severe accident conditions needs to be carefully evaluated. In many of these elevated-temperature tests, neither representative materials nor representative environmental conditions were modeled: (1) samples were tested hot or cold, (2) moisture migration was either free or totally restricted, (3) concrete was either loaded or unloaded while heated,

(4) concrete constituents and proportions varied from mix to mix, (5) test specimen size was not consistent, (6) specimens were tested at different degrees of hydration and moisture contents, and (7) heatup rates and thermal stabilization periods varied.

Concrete in the temperature range of 20°C to 200°C can show a small strength loss. Between 22 and 120°C any strength loss that occurs is attributed to the thermal swelling of the physically bound water, which causes disjoint pressures. A regain of strength is often observed between 120°C and 300°C and is attributed to greater van der Waals forces as a result of the cement gel layers moving closer to each other during heating. Between 200°C and 250°C the residual compressive strength is nearly constant. Beyond 350°C there can be a rapid decrease in strength. The following observations can be made relative to the behavior of Portland cement concretes at elevated temperature:

1. Specimens lose more strength if moisture is not permitted to escape while heated than do those where the moisture escapes.
2. Specimens heated and then permitted to cool before testing lose more strength than those tested while hot.
3. Concrete specimens loaded during heating lose less strength than unloaded specimens.
4. The longer the duration of heating before testing, the larger the loss in strength; however, the loss in strength stabilizes after a period of isothermal exposure.
5. The decrease in modulus of elasticity caused by elevated-temperature exposure is more pronounced than the decrease in compressive strength.
6. Relative to the effect of mix proportions, low cement-aggregate mixes lose less strength as a result of heating than richer mixes, and concretes made with limestone aggregate degrade less due to heating than concrete made with siliceous aggregate.
7. The water-cement ratio has a limited effect on strength degradation of heated concrete.
8. Small test specimens generally incur greater strength losses than larger ones.
9. Specimens subjected to several cycles of heating and cooling lose more strength than those not subjected to thermal cycling.
10. The strength of concrete before testing has little effect on percentage of strength retained at elevated temperature.

In general, for structural applications involving service temperatures in the range of ambient to 300°C or 400°C, provided many temperature cycles of large magnitude are not present, Portland cement concretes are the best materials if heat-resistant aggregates (basalt, limestone, or serpentine) are used; and for limited periods of time, temperatures to 600°C could probably be tolerated by the Portland cement concretes.[3] At higher temperatures or for prolonged exposure to temperatures around 600°C, special procedures would have to be considered such as removal of the evaporable water by moderate heating.

Codes and standards for concrete technology recognize that concrete strength tends to decrease with increasing temperature. Consequently, current design procedures specify concrete temperature limits to ensure predictable concrete behavior. Analytical models for accurately predicting the response of a structure to thermal loadings for practical design considerations, where thermal environments exceed the limits contained in the code, are very complex. As a result, most existing methods utilize various types and degrees of simplification that affects the accuracy of results. Current designs for nuclear structures cover these shortcomings by appropriate conservatism in designs. When design conditions exceed established temperature limits, experimental investigations for characteristic mechanical and physical properties data and for design verification may be required to avoid undue and impractical conservatism in design.

Several research projects have been conducted to investigate the behavior of reinforced concrete structures at elevated temperature; however, the overall level of effort has not been sufficient for establishment of widely accepted elevated-temperature concrete design procedures. A review of the literature in which representative concrete structures were subjected to moderate elevated-temperature service indicates that many of these structures have performed adequately; however, some losses in strength and other properties have occurred. Results of these structural tests, together with the material properties data determined in conjunction with these tests, can serve as the basis for numerical modeling of the response of a reinforced concrete structure to a thermal excursion. Analysis methods requiring development are related to the more realistic representation of embedded reinforcing elements, modules for improved representation of time-dependent behavior, better constitutive relationships for input into computer modules, models for cracking analysis, and modeling of concrete behavior under long-term steady-state elevated temperature, or accident conditions resulting in increased thermal exposures and loadings. The end result of improved analysis methods would be the development of significantly improved rules for the analysis and design of reinforced concrete structures for temperatures that exceed those currently permitted by the Code.

If a reinforced concrete structural element in one of the new generation nuclear power plants is required to maintain its functional and performance requirements at temperatures in excess of 400°C, or at moderately elevated temperatures for extended periods of time, techniques for optimizing the design of structural elements to resist these exposures should be investigated (i.e., material selection and design). With respect to material selection, the performance of the concrete materials can be improved by (1) minimizing the moisture content through aggregate gradation, placement techniques, or use of extended-range water-reducing agents; (2) utilizing aggregates having good thermal stability and low thermal expansion characteristics such as lightweight or refractory materials; and (3) incorporating fibrous reinforcing materials such as short, randomly oriented steel fibers to provide increased ductility, dynamic strength, toughness, tensile strength, and improved resistance to spalling. Another possible approach is to design the concrete mix for higher strength so that any losses in properties resulting from long-term thermal exposure will still provide adequate design (safety) margins.

REFERENCES

1. "Code for Concrete Reactor Vessels and Containments," Nuclear Power Plant Components, *ASME Boiler and Pressure Vessel Code*, Section III, Division 2, American Society of Mechanical Engineers, New York, July 2003.

2. V. S. Ramachandran, R. F. Feldman, and J. J. Beaudoin, *Concrete Science—A Treatise on Current Research*, Hey and Son, London, 1981.

3. G. A. Khoury, "Performance of Heated Concrete—Mechanical Properties," Contract NUC/56/3604A with Nuclear Installations Inspectorate, Imperial College, London, August 1996.

4. U. Schneider, *Behaviour of Concrete at High Temperature*, HEFT 337, Deutscher Ausschuss für Stahlbeton, Wilhelm Ernst & Sohn, Munich, Germany, 1982.

5. U. Schneider, C. Diererichs, and C. Ehm, "Effect of Temperature on Steel and Concrete for PCRV's," *Nuclear Engineering and Design* **67**, 245–258 (1981).

6. Z. P. Bazant et al., *Normal and Refractory Concretes for LMFBR Applications—Vol. 1, Review of Literature on High-Temperature Behavior of Portland Cement and Refractory Concretes*, EPRI Report NP-2437, Northwestern University and Portland Cement Association, Chicago, Illinois, June 1982.

7. N. V. Waubke, "On One Physical Aspect of Strength Loss of Portland Cement Concretes at Temperatures up to 1000°C," in Brandverhalten von Bauteilen, Schriftenreisse der Deutschen Forschungsgemeinschaft, Heft 2, Technical Universität Braunschweig, Germany, November 1973.

8. T. Z. Harmathy and L. W. Allen, "Thermal Properties of Selected Masonry Unit Concretes," *J. American Concrete Institute* **70**, 132–142 (1973).

9. G. A. Khoury, B. N. Granger, and P. J. E. Sullivan, "Transient Thermal Strain of Concrete: Literature Review, Conditions Within Specimen and Behaviour of Individual Constituents," *Magazine of Concrete Research* **37**(132), 131–144 (September 1985).

10. T. Z. Harmathy, "Thermal Properties of Concrete at Elevated Temperatures," *J. of Materials* **5**, 47–74 (1970).

11. T. Z. Harmathy and J. E. Berndt, "Hydrated Portland Cement and Lightweight Concrete at Elevated Temperatures," *J. American Concrete Institute* **63**, 93–112 (1966).

12. D. H. H. Quon, *Phase Changes in Concrete Exposed to Sustained High Temperatures*, Division Report MRP/MSL 80-111(TR), Mineral Sciences Laboratories, CAANMET, Ottawa, Canada, August 1980.

13. J. F. Muir, "Response of Concrete Exposed to High Heat Flux on Surface," Research Paper SAND 77-1467, Sandia National Laboratories, Albuquerque, New Mexico, 1977.

14. T. Y. Chu, "Radiant Heat Evolution of Concrete—A Study of the Erosion of Concrete Due to Surface Heating," Research Paper SAND 77-0922, Sandia National Laboratories, Albuquerque, New Mexico, 1978.

15. G. Hildenbrand et al., "Untersuchung der Wechselvirkung von Kernschmelze und Reaktorbeton," Abschlussbericht Förderungverhaben BMFT RS 154, KWU, Erlangen, Germany, May 1978.

16. M. Takeuchi et al., "Material Properties of Concrete and Steel Bars at Elevated Temperatures," *12th International Conference on Structural Mechanics in Reactor Technology*, Paper H04/4, pp. 133–138, Elsevier Science Publishers, North-Holland, The Netherlands, 1993.

17. RILEM Committee 44-PHT, "Behaviour of Concrete at High Temperatures," U. Schneider, Ed., Kassel Universität, Kassel, Germany, 1985.

18. Comité Euro International Du Beton, "Fire Design of Concrete Structures—In Accordance With CEB/FIP Model Code 90," CEB Bulletin D'Information No. 208, Switzerland, July 1991.

19. Comité Européen de Normalisation (CEN)," prENV 1992-1-2: Eurocode 2: Design of Concrete Structures: Part 1-2: Structural Fire Design," CEN/TC 250/SC 2, 1993.

20. Comité Européen de Normalisation (CEN), "Eurocode 4: Design of Composite Steel and Concrete Structures, Part 1-2: General Rules—Structural Fire Design, CEN ENV, 1994.

21. "Guide for Determining Fire Endurance of Concrete Elements," ACI 216R-89, American Concrete Institute, Farmington Hills, Michigan, 1989.

22. L. T. Phan and N. J. Carino, "Fire Performance of High Strength Concrete: Research Needs," Applied Technology in Structural Engineering, *Proceedings ASCE/SEI Structures Congress 2000, 8–10 May 2000, Philadelphia, Pennsylvania*.

23. S. E. Pihlajavaara, "An Analysis of the Factors Exerting Effect on Strength and Other Properties of Concrete At High Temperature," Paper SP 34-19 in Special Publication SP-34, Vol. I-III, American Concrete Institute, Farmington Hills, Michigan, 1972.

24. P. J. E. Sullivan, "The Effects of Temperature on Concrete," Chapter 1 in *Developments in Concrete Technology—1*, F. D. Lydon, Ed., Applied Science Publishers, London, 1979.

25. G. N. Freskakis et al., "Strength Properties of Concrete at Elevated Temperature, *Civil Engineering Nuclear Power*, Vol. 1, ASCE National Convention, American Society of Civil Engineers, Boston, Massachusetts, April 1979.

26. E. Hognestad, "A Study of Combined Bending and Axial Load in Reinforced Concrete Members," *University of Illinois Engineering Experiment Station Bulletin* Vol. **49**(339) (November 1951).

27. R. Baldwin and M. A. North, "A Stress-Strain Relationship for Concrete at Elevated Temperature," *Magazine of Concrete Research* **25**(28) (December 1973).

28. R. Kottas, J. Seeberger, and H. K. Hilsdorf, "Strength Characteristics of Concrete in the Temperature Range of 20° to 200°C," Paper H01/4 in *5th International Conference on Structural*

Mechanics in Reactor Technology, p. 8, Elsevier Science Publishers, North-Holland, The Netherlands, August 1979.

29. Y. Anderberg and S. Thelanderson, "Stress and Deformation Characteristics of Concrete at High Temperatures, 2-Experimental Investigation and Material Behaviour Model," Bulletin 54, Lund Institute of Technology, Lund, Sweden, 1976.

30. H. Weigler and R. Fischer, "Influence of High Temperatures on Strength and Deformations of Concrete," Paper SP 34-26 in Special Publication SP-34, Vol. I-III, American Concrete Institute, Farmington Hills, Michigan, 1972.

31. G. E. Troxell et al., *Composition and Properties of Concrete*, 2nd Ed., McGraw-Hill, New York, 1968.

32. A. M. Neville, *Properties of Concrete*, Pitman, London, 1970.

33. J. C. Marechal, "Variations in the Modulus of Elasticity and Poisson's Ratio with Temperature," Paper SP 34-27 in Special Publication SP-34, Vol. I-III, American Concrete Institute, Farmington Hills, Michigan, 1972.

34. B. Wu, J. Yuan, and G. Y. Wang, "Experimental Study on the Mechanical Properties of HSC After High Temperature," *Chinese J. Civil Engineering* **33**(2), 8–15 (2000).

35. B. Wu, ZhCh Ma, and J. P. Qu, "Experimental Research on Compressive Constitutive Relationship of HPC Under Axial Loading and High Temperature," *Chinese J. of Building Structures* **20**(5), 42–49 (1999).

36. K. Hirano et al., "Physical Properties of Concrete Subjected to High Temperature for MONJU," Paper P2-25, Power Reactor and Nuclear Fuel Development Corporation, Tokyo, Japan.

37. J. Xiao and G. König, "Study of Concrete at High Temperature in China—An Overview," *Fire Safety Journal* **39**, 89–103 (2004).

38. C. Castillo and A. J. Durrani, "Effect of Transient High Temperature on High-Strength Concrete," *J. American Concrete Institute*, **87**(1) (1990).

39. J. Guo and P. Waldron, "Deterioration of PCPV Concrete," *Nuclear Engineering and Design* **198**, 211–226 (2000).

40. M. S. Abrams, "Compressive Strength of Concrete at Temperatures to 1600°F," SP-25 *Temperature and Concrete*, American Concrete Institute, pp. 33–58, 1971.

41. D. A. Campbell-Allen et al., "An Investigation of the Effect of Elevated Temperatures on Concrete for Reactor Vessels," *Nucl. Struct. Eng*. **2**, 3823–88 (1965).

42. Portland Cement Association, "Effect of Long Exposure of Concrete to High Temperatures," Concrete Information, ST 32-3-53, Skokie, Illinois.

43. D. J. Hannant, "The Effects of Heat on Concrete Strength," *Eng.* **197**(5105), 302 (February 1963).

44. T. Harada et al., "Strength, Elasticity and Thermal Properties of Concrete Subjected to Elevated Temperatures," Paper SP 34-21 in Special Publication SP-34, Vol. I-III, American Concrete Institute, Farmington Hills, Michigan (1972).

45. D. T. Lankard et al., "Effects of Moisture Content on the Structural Properties of Portland Cement Concrete Exposed to Temperatures Up to 500°F," SP-25 *Temperature and Concrete*, pp. 59–102, American Concrete Institute, Farmington Hills, Michigan, 1971.

46. H. L. Malhotra, "The Effect of Temperature on the Compressive Strength of Concrete," *Mag. Corncr. Res.* **8**(2), 382–88 (1965).

47. K. W. Nasser and R. P. Lohtia, "Mass Concrete Properties at High Temperatures," *J. Am. Concr. Inst*. **68**(3), 180–81 (March 1971).

48. S. Ohgishi et a1., "On Properties of Magnetite and Serpentine Concrete at Elevated Temperatures for Nuclear Reactor," SP 34-57 in Special Publication SP-34, Vol. I-III, American Concrete Institute, Farmington Hills, Michigan (1972).

49. F. J. Roux, "Concrete at Elevated Temperatures," Doctoral Thesis, University of Capetown, South Africa, August 1974.

50. N. G. Zoldners, "Effect of High Temperatures on Concrete Incorporating Different Aggregates," *ASTM Proc*. **60**, 1087–108 (1960).

51. *Behavior of Concrete Under Temperature Extremes*, Publication SP-39 American Concrete Institute, Farmington Hills, Michigan, 1973.

52. K. Nagao and S. Nakane, "Influences of Various Factors on Physical Properties of Concretes Heated to High Temperatures," Paper H03/1 in *11th International Conference on Structural Mechanics in Reactor Technology*, pp. 61–66, Elsevier Science Publishers, North-Holland, The Netherlands, August 1991.

53. G. A. Khoury, *Transient Thermal Creep of Nuclear Reactor Pressure Vessel Type Concretes*, Ph.D. dissertation, University of London, Vol. 1, pp. 1126; Vol. 2, pp. 418; Vol. 3, pp. 895, 1983.

54. T. Morita et al., "Residual Mechanical Properties of High Strength Concrete Members Exposed to High Temperature—Part 1. Test on Material Properties," *Summaries of Technical Papers of Annual Meeting*, Architectural Institute of Japan, Naiigata, August 1992.

55. T. Furumura, T. Abe, and Y. Shinohara, "Mechanical Properties of High Strength Concrete at High Temperatures," *Proc. of 4th Weimar Workshop on High Performance Concrete: Material Properties and Design*, held at Hochschule für Architektur und Bauwesen (HAB), Weimar, Germany, pp. 237–254, October 4–5, 1995.

56. F. Vodák et al., "The Effect of Temperature on Strength—Porosity Relationship for Concrete," *Construction and Building Materials* **18**, 529–534 (2004).

57. G. T. C. Mohamedbhai, "Effect of Exposure Time and Rates of Heating and Cooling on Residual Strength of Heated Concrete," *Magazine of Concrete Research* **38**(136), 151–158 (September 1986).

58. D. Campbell-Allen and P. M. Desai, "The Influence of Aggregate on the Behavior of Concrete at Elevated Temperature," *Nucl. Eng. and Design* **6**(1), 65–77 (August 1967).

59. V. V. Bertero and M. Polivka, "Influence of Thermal Exposure on Mechanical Characteristics of Concrete," Paper SP 34-28 in Special Publication SP-34, Vol. I-III, American Concrete Institute, Farmington Hills, Michigan (1972).

60. "Standard Test Method for Splitting Tensile Strength of Cylindrical Concrete Specimens," Part 14 of *Annual Book of ASTM Standards*, ANSI/ASTM C78-75, American Society for Testing and Materials, West Conshockon, Pennsylvania, 1975.

61. A. N. Noumowe et al., "Thermal Stresses and Water Vapor Pressure of High Performance Concrete at High Temperature," *Proc. 4th International Symposium on Utilization of High-Strength/High-Performance Concrete, Paris, 1996.*

62. B. Zhang et al., "Relationship Between Brittleness and Moisture Loss of Concrete Exposed to High Temperatures," *Cement and Concrete Research* **32**, 363–371 (2002).

63. J. C. Seaman and G. W. Washa, "Variation of Mortar and Concrete Properties with Temperature," *J. American Concrete Institute*, 385–395 (1957).

64. M. P. Raju, M. Shobha, and K. Rambabu, "Flexural Strength of Fly Ash Concrete Under Elevated Temperatures," *Magazine of Concrete Research* **56**(2), 83–88 (March 2004).

65. R. W. Carlson, "Drying Shrinkage of Concrete as Affected by Many Factors," *ASTM Proc*. **38**(II), 419–437 (1938).

66. G. E. Troxell, H. E. Davis, and J. W. Kelly, *Composition and Properties of Concrete*, 2nd Ed., McGraw-Hill, New York, 1968.

67. R. D. Browne and R. Blundell, "The Behaviour of Concrete in Prestressed Concrete Pressure Vessels," Paper H11/1 in *Proc. 1st International Conference on Structural Mechanics in Reactor Technology*, Elsevier Science Publishers, North-Holland, The Netherlands, 1971.

68. U.S. Bureau of Reclamation, *A 10-Year Study of Creep Properties of Concrete*, Concrete Laboratory Report No. Sp-38, Denver, Colorado, July 28, 1953.

69. I. Ali. And C. E. Kesler, *Creep in Concrete With and Without Exchange of Moisture with the Environment*, TAM Report 641, University of Illinois, Urbana-Champaign, 1963.

70. W. P. S. Dias, G. A. Khoury, and P. J. E. Sullivan, "Basic Creep of Unsealed Hardened Cement paste at Temperatures Between 20°C and 725°C," *Magazine of Concrete Research* **39**(139), 93–111 (1987).

71. A. M. Neville, "Discussion of the Influence of Sand Concentrations on Deformations of Mortar Bars Under Low Stress," *J. American Concrete Institute* **59**(2), 931–934 (June 1962).

72. A. M. Neville, *Creep of Concrete: Plain, Reinforced and Prestressed*, North-Holland Publishing Company, Amsterdam, The Netherlands, 1970.

73. A. M. Neville, "The Influence of Cement on Creep of Concrete and Mortar," *J. Prestressed Concrete Institute* **66**, 1008–1020, 1969.

74. K. S. Gopalarkrishan et al., "Creep Poison's Ratio on Concrete Under Multiaxial Compression," *J. American Concrete Institute* **2**, 12–18 (March 1958).

75. H. G. Geymayer, "Effect of Temperature on Creep of Concrete: A Literature Review," Paper SP 34-31 in Special Publication SP-34, Vol. I-III, American Concrete Institute, Farmington Hills, Michigan (1972).

76. W. P. S. Dias, G. A. Khoury, and P. J. E. Sullivan, "The Thermal and Structural Effects of Elevated Temperature on the Basic Creep of Hardened Cement Paste," *Magazine of Concrete Research* **23**, 418–425 (1990).

77. K. W. Nasser and H. M. Mazouk, "Creep of Concrete at Temperatures from 70 to 450°F Under Atmospheric Pressure," *J. American Concrete Institute* **78**(2), 147–150 (March–April 1981).

78. J. Komendant et al., "Effects of Temperature, Stress Level, and Age at Loading on Creep of Sealed Concrete," Paper SP 55-3 in *Douglas McHenry International Symposium on Concrete and Concrete Structures*, American Concrete Institute, Farmington Hills, Michigan, 1978.

79. J. E. McDonald, "Creep of Concrete Under Various Temperature, Moisture, and Loading Conditions," SP 55, *Douglas McHenry International Symposium on Concrete and Concrete Structures*, American Concrete Institute, Farmington Hills, Michigan, 1978.

80. H. Gross, "On High Temperature Creep of Concrete," Paper H6/5 in *Proc. 2nd International Conference on Structural Mechanics in Reactor Technology*, Elsevier Science Publishers, North-Holland, The Netherlands, 1973.

81. H. Kasami, T. Okuno, and S. Yamane, "Properties of Concrete Exposed to Sustained Elevated Temperature," Paper H1/5 in *Proc. 3rd International Conference on Structural Mechanics in Reactor Technology*, Elsevier Science Publishers, North-Holland, The Netherlands, 1975.

82. A. F. Milovanov and G. D. Salmanov, "The Influence of High Temperature Upon the Properties of Reinforcing Steels and Upon Bond Strength Between Reinforcement and Concrete," *Issledovanija po zharoupornym betonu I zhelezobetonu*, pp. 203–223, 1954.

83. H. V. Reichel, "How Fire Affect Steel-to-Concrete Bond," *Building Research and Practice* **6**(3), 176–186 (May/June 1978).

84. K. Hertz, "The Anchorage Capacity of Reinforcing Bars at Normal and High Temperatures," *Magazine of Concrete Research* **34**(121), 213–220 (December 1982).

85. U. Diederichs and U. Schneider, "Bond Strength at High Temperature," *Magazine of Concrete Research* **33**(115), 75–83 (June 1981).

86. C-H. Chiang and C-L. Tsai, "Time-Temperature Analysis of Bond Strength of a Rebar After Fire Exposure," *Cement and Concrete Research* **33**, 1651–1654 (2003).

87. H. Sager et al., "High Temperature Behavior of Reinforcing and Prestressing Steels," *Sonderforschungs-Bereich* **148**, Part II, pp. 51–53, Technical Universität Braunschweig, Germany (1980).

88. C. B. Oland and J. P. Callahan, *Bond Between Concrete and Steel Reinforcement at Temperatures to 149°C (300°F)*, ORNL/TM-6086, Union Carbide Corp., Nucl. Div., Oak Ridge National Laboratory, Oak Ridge, Tennessee, April 1978.

89. D. J. Naus, *Concrete Component Aging and Its Significance Relative to Life Extension of Nuclear Power Plants*, NUREG/CR-4652, Martin Marietta Energy Systems, Inc., Oak Ridge National Laboratory, Oak Ridge, Tennessee, September 1986.

90. G. G. Carette et al., "Sustained High Temperature Effects on Concretes Made with Normal Portland Cement, Normal Portland Cement and Slag, or Normal Portland Cement and Fly Ash," *Concrete International* **4**(7), 41–51 (July 1982).

91. A. P. Mears, "Long Term Tests on the Effects of Moderate Heating on the Compressive Strength and Dynamic Modulus of Elasticity of Concrete," Paper SP 34-20 in Special Publication SP-34, Vol. I-III, American Concrete Institute, Farmington Hills, Michigan (1972).

92. C. DeFigh-Price et al., "Effects of Long-Term Exposure to Elevated Temperature on Mechanical Properties of Concrete," ACI Symposium on Concrete and Cementitious Materials for Radioactive Waste Management," New York, November 1, 1984.

93. M. P. Gillen et al., "Strength and Elastic Properties of Concrete Exposed to Long-Term Moderate Temperatures and High Radiation Fields," RHO-RE-SA-55 P, Rockwell Hanford Operations, Richland, Washington, 1984.

94. K. W. Nasser and M. Chakraborty, "Temperature Effects on Strength and Elasticity of Concrete Containing Admixtures," *Proceedings of Symposium Temperature Effects on Concrete*, ASTM Special Technical Publication 858, American Society for Testing and Materials, West Conshockon, Pennsylvania, 1985.

95. G. G. Carrette and V. M. Malhotra, "Performance of Dolostone and Limestone Concretes at Sustained High Temperatures," *Proceedings of Symposium Temperature Effects on Concrete*, ASTM Special Technical Publication 858, pp. 38–67, American Society for Testing and Materials, West Conshockon, Pennsylvania, 1985.

96. T. Suzuki et al., "Study on the Degradation of Concrete Characteristics in the High Temperature Environment," *Concrete Under Severe Conditions: Environment and Loading*, **2**, pp. 1119–1128, E & FN Spon Publishers (1995).

97. H. Etherington, *Nuclear Engineering Handbook*, McGraw-Hill, New York, 109–111.

98. S. Glasstone and A. Sesonske, *Nuclear Reactor Engineering*, D. Van Nostrand, Princeton, New Jersey, pp. 614–615.

99. E. G. Peterson, "Shielding Properties of Ordinary Concretes as a Function of Temperature," HW-65572, Hanford Atomic Products Operation, Richland, Washington, August 2, 1960.

100. K. Sakr and E. El-Hakim, "Effect of Fire on Heavy Weight Concrete Properties," *Cement and Concrete Research* **35**, 590–596 (2005).

101. S. Miyasaka et al., "Gamma-Ray Leakage Through Slit in Concrete Shield," *Nippon Genshiryaku Gakkaishi* **11**, 2–8 (1969).

102. F. Seboek, "Shielding Effectiveness of Cracked Concrete," *Kerntechnik* **12**, 4496–501 (November 1970).

103. K.-CH. Thienel and F. S. Postasy, "Strength of Concrete Subjected to High Temperature and Biaxial Stress; Experiments and Modelling," *Materials and Structures* **28**, 575–581 (1995).

104. B. L. Hu, Y. P. Song, and G. F. Zhao, "Test on Strength and Deformation of Concrete Under Complex Stress at Elevated Temperature," *Building Science Research* **20**(1), Sichuan, pp. 47–50 (1994).

105. T. W. Kennedy, *An Evaluation and Summary of a Study of the Long-Term Multiaxial Creep Behavior of Concrete*, Research Report 3899-2, ORNL Subcontract No. 3661, University of Texas, Austin, December 1975.

106. T. Z. Harmathy, "Effect of Moisture on Fire Endurance of Building Materials," ASTM Technical Publication No. 385: *Moisture in Materials in Relation to Fire Tests*, pp. 74–95, American Society for Testing and Materials, West Conshockon, Pennsylvania, 1965.

107. H. Saito, "Explosive Spalling of Prestressed Concrete in Fire," Building Research Institute, Shinijuku, Japan, 1965.

108. W. J. Copier, "The Spalling of Normal Weight and Lightweight Concrete Exposed to Fire," Paper SP-80-7, *Fire Safety of Concrete Structures*, American Concrete Institute, Farmington Hills, Michigan, 1983.

109. "Standard Test Methods for Fire Endurance of Concrete Elements," ASTM E 119-88, American Society for Testing and Materials, West Conshockon, Pennsylvania, 1988.

110. "Fire Resistance Tests—Elements of Building Construction," ISO 834, International Organization for Standardization, 1975.

111. "Method for Fire Resistance Test for Structural Parts of Buildings," JIS A 1304, Japanese Industrial Standards, 1994.

112. J. Lefter, "Fire Safety of Concrete Slabs," *Concrete International* **9**(8), 23–28 (August 1987).

113. B. R. Ellingwood and J. R. Shaver, "Effects of Fire on Reinforced Concrete Members," *Journal of the Structural Division* **106**(ST 11), 21251–2166 (November 1980).

114. A. H. Gustaferro, "Fire Resistance," Chap. 7, pp. 212–228, in *Handbook of Concrete Engineering*, Ed. M. Fintel, Van Nostrand Reinhold Co., New York, 1974.

115. Z. P. Bazant and W. Thonuthai, "Pore Pressure in Heated Concrete Walls: Theoretical Prediction," *Magazine of Concrete Research* **31**(107), 67–76 (1979).

116. G. L. England and N. Khoylou, "Modeling of Moisture Behaviour in Normal and High Performance Concretes at High Temperatures," *Proceedings of the Fourth Weimar Workshop on High Performance Concrete: Material Properties and Design*, held at Hochschule für Architektur und Bauwesen (HAB), Weimar, Germany, pp. 53–68, October 4–5, 1995.

117. G. N. Ahmed and J. P. Hurst, "Modeling the Thermal Behavior of Concrete Slabs Subjected to the ASTM E 119 Standard Fire Condition," *Journal of Fire Protection Engineering* **7**(4), 125–132 (1995).

118. ACI COMMITTEE 207, "Mass Concrete for Dams and Other Massive Structures," *Proceedings of the Journal of American Concrete Institute* **67**(4), 273–309 (April 1970).

119. R. Philleo, "Some Physical Properties of Concrete At High Temperature," *Research Department Bulletin 97*, Portland Cement Association, Skokie, Illinois, October 1958.

120. K.-Y. Shin et al., "Thermo-Physical Properties and Transient Heat Transfer of Concrete at Elevated Temperatures," *Nuclear Engineering and Design* **212**, 233–241 (2002).

121. *Concrete Manual*, 7th Ed., U.S. Bureau of Reclamation, Denver, Colorado, 1963.

122. H. C. Hirth et al., *Final Report on Thermal Properties of Concrete at Elevated Temperature*, University of California, Berkeley, July 1980.

123. F. Vodák et al., "Thermophysical Properties of Concrete for Nuclear Safety-Related Structures," *Cement and Concrete Research* **27**(3), 415–426 (1997).

124. L. L. Mitchell, "Thermal Properties," ASTM Special Technical Publication **169**, 129–135 (October 1962).

125. T. Z. Harmathy, *Journal of Materials* **5**(47) (1970).

126. H. Abe et al., "Influence Factors of Elevated Temperatures on Thermal Properties and Inelastic Behavior of Concrete," Paper SP 34-40 in Special Publication SP-34, Vol. I-III, p. 847, American Concrete Institute, Farmington Hills, Michigan, 1972.

127. S. L. Meyers, "How Temperature and Moisture Changes May Affect the Durability of Concrete," *Rock Products*, 153–157 (August 1951).

128. R. Felicetti et al., "The Mechanical Properties of High Performance Siliceous Concrete Exposed to High Temperature; "Penly" Concrete; Uniaxial Compression," Research Project 1794/20-3-95, Milan University of Technology, Milan, Italy, March 1995.

129. "High-Strength Concrete," *Proceedings of a Workshop Held at University of Illinois at Chicago Circle, December 2–4, 1979*.

130. L. T. Phan, *Fire Performance of High-Strength Concrete: A Report of the State-of-the-Art*, NISTIR 5934, National Institute of Standards and Technology, Gaithersburg, Maryland, 1996.

131. W. A. Mallow, "Recycled Material," pp. 1097–1102 in *Proc. 3rd Materials Engineering Conference, San Diego, California, November 13–16, 1994*.

132. F. M. Lea, *The Chemistry of Cement and Concrete*, 2nd Ed., St. Martin's, New York, 1956.

133. H. F. W. Taylor, *The Chemistry of Cements*, Vol. 1, Academic, New York, 1964.

134. W. T. Bakker, "Properties of Refractory Concretes," Paper SP 57-2 in *Refractory Concrete*, American Concrete Institute, Farmington Hills, Michigan, 1978.

135. *Standard Classification of Castab1e Refractories*, Part 17 of Annual Book of ASTM Standards, ANSI/ASTM C 401-77, American Society for Testing and Materials, West Conshockon, Pennsylvania, 1980.

136. A. V. Briebach, "A Review of Refractory Hydraulic Cement," *J. Brit. Cera. Soc*. **71**(7), 153–58.

137. F. E. Linck, *Turnaround Maintenance*, Houston, Texas, October 6, 1980.

138. J. M. McCullough and G. R. Rigby, "Mechanical Properties of Refractory Castables," *J. Brit. Cera. Soc*. **71**(7), 233.

139. W. T. Bakker et a1., "Blast Furnace Gunning in the USA," *Proceedings International Feuerafest Colloquium, Aachen, Germany, October 27–29, 1971*.

140. G. C. Padgett et a1., "Stress/Strain Behavior of Refractory Materials at High Temperatures," Research Paper 608, The British Ceramic Association.

141. E. Ruh and A. Renky, "Thermal Conductivity of Castab1e Refractories," *J. Am. Cera. Soc*. **46**(2) (1963).

142. J. F. Wygant and M. S. Crowley, "Effects of High Conductivity Gases on Thermal Conductivity of Insulating Refractory Concrete," *J. Am. Cera. Soc*. **41**(5) (1958).

143. J. F. Wygant and M. S. Crowley, "Designing Monolithic Refractory Vessel Linings," *Am. Cera. Soc. Bll.* **43**(3) (1964).

144. D. R. Lankard, "Steel Fiber Reinforced Refractory Concrete," Paper SP 57-11 in *Refractory Concrete,* American Concrete Institute, Farmington Hills, Michigan, 1972.

145. Y. Ichikawa and L. A. Nelson, "Fiber Reinforced Composite Refractory Insulation System, Paper SP 57-12 in *Refractory Concrete*, American Concrete Institute, Farmington Hills, Michigan, 1972.

146. "Nuclear Reactor Vessels of Prestressed Concrete with Metal Reinforcements,' *J. Offic. Republ. Fr.*, 6119–128 (June 1970).

147. "Specification for Prestressed Concrete Pressure Vessels for Nuclear Reactors." BS4975: July 1973. British Standards Institution, London.

148. W. Fürste et al., "Prestressed Concrete Reactor Vessels for Nuclear Reactor Plants Compared to Thick-Walled and Multilayer Steel Vessels," *Second International Conference on Pressure Vessel Technology (Part 1), San Antonio, Texas, October 1973.*

149. *Standard Format and Content of Safety Analysis Reports for Nuclear Power Plants (LWR Edition)*, Regulatory Guide 1.70 (Rev. 3), Office of Standard Development, U.S. Nuclear Regulatory Commission, Washington, D.C., November 1978.

150. R. S. Orr and E. G. Hess, "ACI 318 or 349 for Radioactive Waste Facilities," Presented at *Concrete and Cementitious Materials for Radioactive Waste Management Seminar*, New York, November 1, 1984.

151. U.S. Atomic Energy Commission, "Concrete Containment," Sect. 3.8.1 in *Regulatory Standard Review Plan*, NUREG-0800, Washington, D.C., July 1981.

152. Burns and Roe, Inc., "A Comprehensive Testing Program for Concrete at Elevated Temperatures," DRS 27.13 (Rev. 6), approved by EN; RPS; 79-019, dated January 23, 1979.

153. A. K. Kar, "Thermal Effects in Concrete Members," *Trans. 4th Intl. Conf. on St. Mech. in Reactor Technology*, **J**(a), Paper J4/4, San Francisco, California, August 15–19, 1977.

154. G. Gurfinkel, "Thermal Effects in Walls of Nuclear Containments—Elastic and Inelastic Behavior," *Trans. 1st Intl. Conf. on St. Mech. in Reactor Technology*, **J**, Paper J3/7, Berlin, Germany, September 20–24, 1971.

155. G. A. Mentes et al., "Thermal Effects in Reinforced Concrete Structures," *Second ASCE Conf. on Civ. Eng. and Nuclear Power*, Vol. 1, Paper 3-5, pp. 3-5-1 to 3-5-21, Knoxville, Tennessee, September 15–17, 1980.

156. G. N. Freskakis. "Behavior of Reinforced Concrete at Elevated Temperature," Paper 3-4, *Second ASCE Conf. on Civ. Eng. and Nuclear Power*, Vol. 1, Paper 3-5, pp. 3-5-1 to 3-5-21, Knoxville, Tennessee, September 15–17, 1980.

157. B. Bresler and R. H. Iding, "Effects of Normal and Extreme Environment on Reinforced Concrete Structures," Paper SP 55-11 in *Douglas McHenry Symposium on Concrete and Concrete Structures*, SP 55, American Concrete Institute, Farmington Hills, Michigan, April 1970.

158. W. G. Dodge et al., *A Review of Analysis Methods for Prestressed Concrete Reactor Vessels*, ORNL-5173, Oak Ridge National Laboratory, Oak Ridge, Tennessee, February 1977.

159. K. J. Willam, "Constitutive Models for Engineering Materials," *Encyclopedia of Physical Science and Technology*, 3rd Ed., Vol. 3, pp. 603–633, Academic Press (2002).

160. P. A. Pfeiffer and A. H. Marchertas, "Thermal Stress-Dependent Dilatation of Concrete," *ANS/ENS 1984 International Conference, Washington, D.C., November 1984*.

161. J. R. Benjamin. "The Basics of Structural Reliability," *Nuclear Engineering and Design* **60**, 3–9 (1980).

162. M. D. McKay, "A Method of Analysis for Computer Codes," Los Alamos National Laboratory, 1980.

163. M. D. McKay, R. J. Beckman, and W. J. Conover, "A Comparison of Three Methods for Selecting Values of Input Variables in the Analysis of Output from a Computer Code," *Technometrics*, **21**(2), 239–245 (May 1979).

164. M. D. McKay, W. J. Conover, and D. C. Whiteman, *Report on the Application of Statistical Techniques to the Analysis of Computer Code*, Los Alamos Scientific Laboratory Report, LA-NUREG-6526-MS, NRC-4, 1976.

165. Z. P. Bazant and J. C. Chern, "Bayesian Statistical Prediction of Concrete Creep and Shrinkage," Report No. 83-4/665b, Center for Concrete and Geomaterials, Northwestern University, Evanston, Illinois, April 1983 [see also *ACI Journal*, pp. 319–330 (July–August 1984)].

166. A. H. Marchertas and T. B. Belytschko, "Transient Analysis of a PCRV for LMFBR Primary Containments," special issue on "Mechanics Application to Fast Breeder Reactor Safety," *Nuclear Technology* **51**(3), 433–442 (1980).

167. A. H. Marchertas, "DYNAPCON—A Computer Code for DYNamic Analysis of Prestressed CONcrete Structures," ANL-82-77, Argonne National Laboratory, Argonne, Illinois, September 1982.

168. A. H. Marchertas and R. F. Kulak, *A Coupled Heat Conduction and Thermal Stress Formulation Using Explicit Integration*, ANL/RAS 81-9, Argonne National Laboratory, Argonne, Illinois, March 1981.

169. A. H. Marchertas et al., *Structural Response Simulation under High Temperatures*, ANL/RAS 82-21, Argonne National Laboratory, Argonne, Illinois, June 1982.

170. A. H. Marchertas et al., *2-D TEMP-STRESS Code Computational Capability*, ANL/RAS-83-30, Argonne National Laboratory, Argonne, Illinois, October 1983.

171. A. H. Marchertas, "Thermo-Mechanical Analysis of Concrete in LMFBR Programs," *Nucl. Eng. and Design* **76**, 183–191 (1983).

172. A. H. Marchertas, "Experimental Needs in Simulating Concrete Behavior at High Temperatures," ANL/RAS 84-18, Argonne National Laboratory, Argonne, Illinois, August 1984.

173. K. Irino et al., "Studies on Thermal Stress Design Method for Reinforced Concrete Members of Nuclear Power Plant," Paper J4/5, Vol. J, *Trans. of 7th Ind. Conf. on St. Mech. in Reactor Technology*, pp. 209–219, Chicago, Illinois, August 22–26, 1983.

174. T. Ikoma and N. Tanaka, "Restraining Force and Moment of Reinforced Concrete Beam Column Under a Sustained Long-Term Temperature Crossfall," Vol. H, *Trans. of 9th Ind. Conf. on St. Mech. in Reactor Technology*, *Lausanne, Switzerland, August 17–21, 1987,* pp. 201–208.

175. K. Ornatsuzawa et al., "Behavior and Ultimate Strength of an Inner Concrete Structure of a Nuclear Reactor Building Subjected to Thermal and Seismic Loads," Vol. J, *Trans. of 9th Intl. Conf. on St. Mech. in Reactor Technology, Lausanne, Switzerland, August 17–21, 1987,* pp. 167–172.

176. T. Takeda et al., "Experimental Studies on Characteristics of Concrete Members Subjected to High Temperature," Vol. H, *Trans. of 9th Ind. Conf. on St. Mech. in Reactor Technology*, *Lausanne, Switzerland, August 17–21, 1987*, pp. 195–200.

177. "High-Temperature Concrete-Testing and Data," *8th CRIEPI/EPRI FBR Workshop, Palo Alto, California, September 23–25, 1987.*

178. N. Shibasaki et al., "Thermal Cracking and Thermal Stress Relaxation of Reinforced Concrete Member Tested by Full Sized Beam Specimens," Paper J4/2, Vol. J, *Trans. of 7th Ind. Conf. on St. Mech. in Reactor Technology*, *Chicago, Illinois, August 22–26, 1983*, p. 179–187.

179. *CEB-FIP Model Code for Concrete Structures*, 3rd Ed., CEB, Paris, 1978.

180. N. Shibasaki et al., "An Experimental Study on Thermal Stress of Reinforced Concrete Members Under Short-Term Loading," Paper J4/3, Vol. J, *Trans. of 7th Ind. Conf. on St. Mech. in Reactor Technology*, *Chicago, Illinois, August 22–26, 1983*, pp. 189–197.

181. N. Shibasaki et al., "Thermal Stress Relaxation and Creep Tests of Reinforced Concrete Beams Under Long Term Thermal Effects and Loadings," Paper J4/4, *Trans. of 7th Int. Conf. on St. Mech. in Reactor Technology*, *Chicago, Illinois, August 22–26, 1983*, pp. 199–207.

182. G. N. Freskakis, "High Temperature Concrete Testing," *8th CRIEPI/EPRI Workshop*, *Agenda Item 7.2, Palo Alto, California,* September 23–25, 1987.

183. D. J. Naus, *A Review of Prestressed Concrete Reactor Vessel Related Structural Model Tests*, ORNL/GCR-80/10, Oak Ridge National Laboratory, Oak Ridge, Tennessee, 1980.

184. M. Lida and R. Ausangee, "Scale Models for Strength Testing Nuclear Pressure Vessels," Group G, Paper 44, pp. 497–505, *Prestressed Concrete Pressure Vessels*, Institution of Civil Engineers, London, 1968.

185. D. McD. Eadie, "Testing of One Tenth Scale Model of the Hinkley Point B and Hunterson B Power Station Prestressed Concrete Pressure Vessel," Paper 14, *Model Techniques for Prestressed Concrete Pressure Vessels*, The British Nuclear Energy Society, London, 1968.

186. D. C. Price and M. S. Hinley, "Testing a 1/8th Scale Cylindrical Vessel," Group G, Paper 43, pp. 489–496, *Prestressed Concrete Pressure Vessels*, Institution of Civil Engineers, London, 1968.

187. M. L. A. Moncrieff, "Comparison of Theoretical and Experimental Test Results for a Ribbed Spherical Vessel," Group G, Paper 42, pp. 469–479, *Prestressed Concrete Pressure Vessels*, Institution of Civil Engineers, London, 1968.

188. T. E. Northup, *Pressure and Temperature Tests and Evaluation of a Model Prestressed Concrete Pressure Vessel*, GA-9673, General Atomic Co., September 15, 1969.

189. J. Nemet et al., "Testing of a Prestressed Concrete Pressure Vessel with Hot Liner," Report SBB/He-3E, Reaktorbau Forschungs-und Baugesellschalft, Seibersdorf, Austria, November 1977.

190. A. Witt et al., "The Prototype PCPV with Hot Liner and Elevated Wall Temperature—Experimental and Operational Experience," *Specialists' Meeting on Design, Criteria and Experience with Prestressed Reactor Pressure Vessels for Gas-Cooled Reactors*, *December 4–7, 1984*, International Atomic Energy Agency International Working Group on Gas-Cooled Reactors, IWGGCR-11, Lausanne, Switzerland. pp. 360–371.

191. G. D. Stefanou et al., "An Experimental Investigation Into the Behaviour of Perforated End Slabs for Concrete Pressure Vessels Under Temperature and External Load," Paper 8, *Model Techniques for Prestressed Concrete Pressure Vessels*, The British Nuclear Energy Society, London, 1968.

192. C. R. Lee et al., "Behaviour of Model Concrete Structures Under Temperature Loading," Group G, Paper 46, *Prestressed Concrete Pressure Vessels*, Institution of Civil Engineers, London, pp. 517–525, 1968.

193. I. W. Hornby, "The Behaviour of the Oldbury Model Vessel with Time Under Thermal and Pressure Loadings," Paper No. 11, *Model Techniques for Prestressed Concrete Pressure Vessels*, The British Nuclear Energy Society, London, 1968.

194. J. Irving et al., "A Full Scale Model Test of Hot Spots in the Prestressed Vessels of Oldbury Nuclear Power Station," Paper 7699, *Proc. Instn. Civil Engineers* **57** (June 1974).

195. P. Launay, "Apparatus, Instrumentation, and Concrete Models of Bugey I Prestressed Concrete Pressure Vessel," Paper SP 34-69, Session 17, *Concrete for Nuclear Reactors*, Vol. III, American Concrete Institute Special Publication SP-34, Farmington Hills, Michigan, pp. 1529–1566, 1979.

196. F. Dubois et al., "Study of a Reduced Scale Model of a Prestressed Concrete Vessel Subjected to a Large Thermal Gradient," Annales de 1'Institut Technique du Batimen't et des Travaux Publics, No. 214, October 1965.

197. J. P. Callahan et al., *Prestressed Concrete Reactor Vessel Thermal Cylinder Model Study*, ORNL/TM-5613, Oak Ridge National Laboratory, Oak Ridge, Tennessee, June 1977.

198. J. E. McDonald, *Moisture Migration in Concrete*, Technical Report C-75-l, U.S. Army Waterways Experiment Station, Vicksburg, Mississippi, May 1975.

199. H. Ohnuma et al., "Creep Behavior Under Sustained Temperature Gradient in a Model of Prestressed Concrete Reactor Vessels," Paper H 4/9, Vol. H, *Proc. of 5th Ind. Conf. on St. Mech. in Reactor Technology*, Berlin 1979.

200. J. Altes et al., "Experimental Study of the Behaviour of Prestressed Concrete Pressure Vessels of High Temperature Reactors at Accident Temperatures," *Trans. of the 9th Intl. Conf. on St. Mech. in Reactor Technology*, Vol. H, Lausanne, Switzerland, August 17–21, 1987.

201. J. V. Beck and R. L. Knight, *User's Manual for USINT*, NUREG/CR-1375 (SAND76-1694), Sandia National Laboratories, Albuquerque, New Mexico, 1980.

NUREG-XXXX
Dist. Category RD, R9

INTERNAL DISTRIBUTION

1. E. E. Bloom
2. J. M. Corum
3. E. Lara-Curzio
4. S. Greene
5–10. D. J. Naus
11. C. B. Oland
12. A. E. Pasto
13–14. J. J. Simpson
15. ORNL Laboratory Records-OSTI

EXTERNAL DISTRIBUTION

16. S. Ali, RES/DET/ERAB, Mail 10 D20, U.S. Nuclear Regulatory Commission, Washington, DC 20555-0001
17. C. Andrade, Ietcc, IETcc (CSIC), "Eduardo Torroja," Serrano Galvache s/n—Aptdo 19 002, E-28033, Madrid, Spain
18. H. G. Ashar, NRR/ADES/DE/EGCB, Mail 9 D3, U.S. Nuclear Regulatory Commission, Washington, DC 20555-0001
19. G. Bagchi, NRR/ADRA/DPR/PRA, Mail 12 E15, U.S. Nuclear Regulatory Commission, Washington, DC 20555-0001
20. Z. Bittnar, Czech Technical University, Fac. of Civil Eng.—Dept. of Structural Mechanics, Thakurova 7, 166 29 Prague 6, Czech Republic
21. J. Carey, Electric Power Research Institute, 3412 Hillview Avenue, Palo Alto, CA 94304
22. T-Y. Chang, RES/DET/ERAB/MSE, Mail 10 D20, U.S. Nuclear Regulatory Commission, Washington, DC 20555-0001
23. N. C. Chokshi, RES/DRAA/OERAB, Mail 9 F39, U.S. Nuclear Regulatory Commission, Washington, DC 20555-0001
24. Commander and Director, USAE Waterways Experiment Station ATTN: CEWES-IM-MI-R Alfreda S. Clark CD Dept. I #1072, 3909 Halls Ferry Road, Vicksburg, MS 39180-6199
25. R. Danisch, Framatome ANP Freyeslebenstrasse 1, 91058 Erlangen, Germany
26. B. R. Ellingwood, Professor of Civil Engineering, Georgia Institute of Technology, School of Civil & Environ. Engineering, 790 Atlantic Avenue, Atlanta, GA 30332-0355
27. M. Evans, RES/DET/ERAB, Mail 10 D20, U.S. Nuclear Regulatory Commission, Washington, DC 20555-0001
28. W. L. Gamble, Professor of Civil Engineering, University of Illinois, 3122 Newmark, Civil Engineering Laboratory, 205 N. Mathews, Urbana, IL 61801
29–37. H. L. Graves III, RES/DET/ERAB/MSE, Mail 10 D20, U.S. Nuclear Regulatory Commission, Washington, DC 20555-0001
38. F. E. Gregor, LCM Engineering, PLLC, 2103 Otter Court, Tarpon Springs, FL 34689
39. W. Heep, NOK AG—Engineering, Parkstrasse 23, 5401 Baden AG, Switzerland
40. W. G. Imbro, NRR/ADPT/DE/EMEB, Mail 9 D3, U.S. Nuclear Regulatory Commission, Washington, DC 20555-0001
41. D. C. Jeng, NRR/ADES/DE/EGCB, Mail 9 D3, U.S. Nuclear Regulatory Commission, Washington, DC 20555-0001

42. P-T. Kuo, NRR/DRIP/RLEP, Mail 11 F1, U.S. Nuclear Regulatory Commission, Washington, DC 20555-0001
43. H. Kwun, Southwest Research Institute, 6220 Culebra Road, P.O. Drawer 28510, San Antonio, TX 78228-0510
44. K. Manoly, NRR/ADES/DE/EEMB, Mail 9 D3, U.S. Nuclear Regulatory Commission, Washington, DC 20555-0001
45. H. W. Massie, Defense Nuclear Facilities Safety Board, 625 Indiana Ave., NW, Suite 700, Washington, DC 20004
46. T. McNulty, Nuclear Safety Directorate, Health and Safety Executive, ONIT 2F, Room 402, St. Peters House, Balliol Road, Bootle, Merseyside L20 3LZ, United Kingdom
47. H. Müller, Universität Karlsruhe, Institut für Massivbau und, Baustofftechnologie, Abt. Baustofftechnologie, D-76128 Karlsruhe
48. W. E. Norris, RES/DET/MEB/AITS, Mail 10 E10, U.S. Nuclear Regulatory Commission, Washington, DC 20555-0001
49. J. Philip, RES/DSARE/RPERWM, Mail 9 C34, U.S. Nuclear Regulatory Commission, Washington, DC 20555-0001
50. V. Schmitz, Head of Department Quantitative NDE, Fraunhofer IzfP, Universität, Geb 37, D-66123 Saarbruecken, Germany
51. S. P. Shah, Center for ACBM, Northwestern University, 1800 Ridge Avenue, Evanston, IL 60208-4400
52. R. E. Shewmaker, NMSS/SFPO/TRD/SM, Mail 13 D13, U.S. Nuclear Regulatory Commission, Washington, DC 20555-0001
53. J. Staffiera. Firstenergy Corp., 10 Center Road (A170), Perry, OH 44081-9514
54. H. Stephens, EPRI NDE Center, 1300W, Harris Boulevard, Charlotte, NC 28262
55. J. P. Vora, RES/DET/MEB/AITS, Mail 10 D20, U.S. Nuclear Regulatory Commission, Washington, DC 20555-0001
56. H. Wiggenhauser, Bundesanstalt für Materialforschung und Prüfung, Division IV.4 Non-Destructive Damage Assessment and Environmental Assessment Methods, Unter den Eichen 87, D-12205 Berlin, Germany